The phylogeny, physiology, and evolution of salinity tolerance in Cyanobacteria

by

Jennifer Lee Reeve

B.Sc., Haverford College, 2014

M.Sc., University of Victoria, 2016

A thesis submitted to the

Faculty of the Graduate School of the

University of Colorado in partial fulfillment

of the requirement for the degree of

Doctor of Philosophy

Department of Geological Sciences

2023

Committee Members:

Assoc. Prof. Boswell Wing

Assis. Prof. Carl Simpson

Assis. Prof. Sebastian Kopf

Assis. Prof. Jeffrey Cameron

Prof. Shelley Copley

Abstract

Reeve, Jennifer Lee (Ph.D., Geological Sciences)

The phylogeny, physiology, and evolution of salinity tolerance in Cyanobacteria

Thesis advised by Associate Professor Boswell A. Wing

The evolution of oxygenic photosynthesis in the cyanobacterial phylum led to the irreversible oxidation of the Earth's atmosphere at the Great Oxidation Event (GOE), ~2.5 – 2.0 billion years ago. While the GOE provides a minimum age for the evolution of oxygenic photosynthesis, there is evidence that oxygenic photosynthesis evolved significantly before the GOE. If this is the case, the oxygenation of the Earth's atmosphere, and by extension cyanobacterial evolution, must have been delayed by some biotic or abiotic factor(s). My dissertation addresses the hypothesis that early cyanobacteria were restricted to terrestrial environments due to salinity intolerance, and their expansion into the marine environment was the trigger for enhanced global oxygenic photosynthesis and the GOE.

My dissertation evaluates this hypothesis across multiple timescales. The first chapter investigates how phylogenetic methods reconstruct microbial traits versus environmental history in deep time. The second chapter focuses on the physiological timescale to empirically investigate the plasticity of salinity tolerance within multiple taxa of modern cyanobacteria. And the third chapter uses experimental evolution to observe the impacts of salinity selection on the salinity response of cyanobacteria.

To test the implications of ancestral state reconstruction (ASR) methods, I produced simulated trait distributions of salinity optima via two models of evolution. These simulated "modern" distributions were used as the data for testing ASR predictions. I established the range of

evolutionary rates that allow for salinity to be reconstructed across the cyanobacterial tree, which are slow in comparison with published estimates of rates from fossil and experimental macroevolution data.

I collated data from scientific papers published over the last 70 years reporting cyanobacterial growth responses to changes in salinity. Upon standardizing this historical dataset, I evaluated differences in responses to salinities across the phylum. Over half of the strains isolated from "terrestrial" habitats grew at salinities above the thresholds (0.5 - 5 ppt) typically used to distinguish between terrestrial and marine environments. They are, however, rationalized in terms of a mechanistic model that relates growth rate to maintenance of osmotic homeostasis.

To evaluate how these responses change on evolutionary timescales, I grew sixteen experimental lineages of the model euryhaline cyanobacterium *Synechococcus* sp. PCC 7002, inoculated from a genetically homogenous ancestor into 4 treatments, ranging from 10% marine salinity to 100% marine salinity, and serially transferred twice a week. I then evaluated these evolved lineages for changes in their general fitness, as well as changes in their plastic response to varying salinities.

My data on both the physiological and evolutionary response of cyanobacteria to changes in salinity suggests that we need to reevaluate how we consider salinity tolerance as a trait in phylogenetic reconstructions. Salinity does not appear to behave as a discrete trait, and salinity tolerance does not appear to be a trait maintained only by strains regularly exposed to higher salinities. These eco-evolutionary results indicate that our perspective of geobiological records of cyanobacterial evolution and the Great Oxidation Event needs to shift from a focus on salinity tolerance of individual organisms toward consideration of the relative environmental niches (marine versus terrestrial) available on the Archean Earth. While phylogenetics can inform our

understanding of the evolutionary trajectories of early life, we must address the challenge of considering not just the modern distribution of traits, but also the variance of those traits over ecological and evolutionary timescales.

Dedication

To the younger me, may this serve as the definitive proof you never needed that you were always capable and always worth believing in. Thank you for your bravery and determination, I am so grateful for the life we've had and the person we've become.

Acknowledgements

I have gratitude beyond measure for the family, all chosen one way or another, who have supported, encouraged, and believed in me throughout my PhD, and throughout my life. There are too many individuals to thank you all, but I am so grateful to have your support and friendship.

A few special thanks:

To my Aharon. For being my partner for nearly a decade, and never doubting me. And for finding my ramblings about science bemusing rather than annoying. You have made space for me to grow and change as a person throughout my PhD and that will always mean the world to me.

To Boz. For being the advisor I needed and wanted, even if we both probably thought I had drifted a bit too far off course a few times over my PhD.

Table of Contents

Table of Tables

Table of Figures

Chapter 1: Introduction

Background

Cyanobacteria and Earth history

Cyanobacteria are one of the most widespread phyla on the planet, regularly occurring in habitats ranging from sea ice to hot springs, acidic bogs to alkaline seas, desert soil crusts to the open ocean (Dvořák et al., 2017; Whitton and Potts, 2012). In addition to their ecological contributions as the source of eukaryotic photosynthetic abilities, free-living cyanobacteria conduct a significant portion of modern photosynthesis, with just the marine *Prochlorococcus* and *Synechococcus* strains thought to drive nearly a quarter of marine primary production (Flombaum et al., 2013; Sánchez-Baracaldo et al., 2021). While some strains of Cyanobacteria are considered laboratory models, and extremely well-studied (Cameron et al., 2015; Gordon et al., 2016; Markley et al., 2015; Mehdizadeh Allaf and Peerhossaini, 2022), new strains and new habitats are discovered regularly (Jasser et al., 2022; Panou and Gkelis, 2022; Puente-Sánchez et al., 2018; Rasouli-Dogaheh et al., 2022).

Cyanobacteria are often described as one of the most important phyla in Earth history due to their role in the oxygenation of the Earth's atmosphere (Dvořák et al., 2017; Hamilton et al., 2016; Hammerschmidt et al., 2021; Sánchez-Baracaldo et al., 2021; Sánchez-Baracaldo and Cardona, 2020; Schirrmeister et al., 2016, 2015; Whitton and Potts, 2012). Oxygenic photosynthesis evolved in the ancestors of modern cyanobacteria, although exactly when this metabolism emerged remains uncertain (Shih et al., 2017). In the absence of alternative sources of free O_2, oxygenic photosynthesis is thought to be responsible for the accumulation of O_2 known as the Great Oxidation Event (GOE, ~2.5-2.0 Gyr) (Gumsley et al., 2017; Lyons et al., 2014). The timing of the GOE thus provides a minimum age for the cyanobacterial ancestor.

However, attempts to determine the history of the phylum Cyanobacteria prior to this time are divergent.

There are two broad hypotheses about the early history of Cyanobacteria. The first posits that stem group cyanobacteria capable of oxygenic photosynthesis arose close in time to the appearance of molecular O_2 in the atmosphere (Shih et al., 2017; Ward et al., 2016). This 'origination' scenario contrasts with the 'ecological' alternative, which posits that oxygenic Cyanobacteria existed prior to the rise in atmospheric O_2, but environmental constraints made them a localized and ineffective biogeochemical agent (Hammerschmidt et al., 2021; Lalonde and Konhauser, 2015; Sánchez-Baracaldo et al., 2005; Sánchez-Baracaldo et al., 2017b; Sánchez-Baracaldo and Cardona, 2020; Swanner et al., 2015).

While this hypothesis is supported by a preponderance of evidence relative to the 'origination' hypothesis (Czaja et al., 2012; Lalonde and Konhauser, 2015; Planavsky et al., 2014; Ward et al., 2016), most of this evidence can be traced back to studies that rely on modern cyanobacterial traits and physiology to determine the character of the most recent common cyanobacterial ancestor, at least 2.5 billion years ago (Cardona et al., 2015; Hammerschmidt et al., 2021; Oliver et al., 2021; Sánchez-Baracaldo et al., 2005; Sánchez-Baracaldo and Cardona, 2020).

One of the key environmental constraints proposed by the 'ecological' hypothesis is salinity, as trait reconstructions in cyanobacteria often suggest a freshwater ancestor (Hammerschmidt et al., 2021; Sánchez-Baracaldo et al., 2005; Sánchez-Baracaldo et al., 2014; Sánchez-Baracaldo, 2015; Sánchez-Baracaldo et al., 2017b; Sánchez-Baracaldo and Cardona, 2020; Uyeda et al., 2016). Not only have trait reconstructions often indicated a freshwater ancestor, but the geochemical evidence for 'whiffs' of oxygen prior to the GOE is mostly from

lacustrine systems (Lalonde and Konhauser, 2015; Wilmeth et al., 2019). Thus the 'ecological' hypothesis suggests that salinity was a factor in preventing cyanobacteria from moving into the global oceans and producing significant amounts of O_2.

Cyanobacteria and salinity

While cyanobacteria can be found across the entire range of salinities present on Earth's surface (Oren, 2015; Whitton, 2012), we lack consistent and clear language surrounding the preferred and tolerated salinities of different strains. In most of the literature, the salinity tolerance or preference of a strain is indicated by a habitat label, typically simply derived from the approximate isolation environment. These habitats are not clearly defined as shown in Table 1, with highly variable category boundaries. Additionally, there is often a conflation of freshwater and terrestrial habitats, which lumps strains isolated from soils with those isolated from freshwater aquatic environments, despite significant differences in the salinities experienced in these environments (Chen et al., 2021; Hu et al., 2012). When studies have separated terrestrial from freshwater and marine strains in phylum level analyses, they have found distinct differences between each category (Chen et al., 2021). As with our classification of the thermal preferences and tolerances of microbes, it is beneficial to adopt language of tolerance versus preference (halotolerant versus halophilic) (Golubic, 1980). Additionally, if we wish to use oligo-/meso-/hyper-saline categories, we must decide on consistent boundaries between these categories.

Table 1: Definitions of the salinity of habitats from assorted literature. "Not included" indicates that the source paper did not evaluate the category, "Not defined" indicates that the source paper evaluated the category but did not provide a definition.

Fresh	Brackish	Marine	Hypersaline	Source
Not included	Not included	Not included	> 70 ppt	(Oren, 2012)
0 – 0.5 ppt	0.5 – 30 ppt	30 – 50 ppt	Not included	(Sánchez-Baracaldo et al., 2017b)
Not defined	Not defined	1.5 – 50 ppt	50 – 200 ppt	(Sánchez-Baracaldo et al., 2005)
Not defined	Not defined	20 – 40 ppt	> 40 ppt	(Blank, 2013)
< 5 ppt	Not included	30 – 50 ppt	Not included	(Uyeda et al., 2016)
1 ppt	16 ppt	30 ppt	Not included	(Herrmann and Gehringer, 2019)
0 – 3 ppt	5 – 8 ppt	10 – 31 ppt	Not included	(Herlemann et al., 2011)
0 – 3 ppt	3 – 6 ppt	Not included	Not included	(Brutemark et al., 2015)
0.5 ppt	12 ppt	38 ppt	Not included	(Dittami et al., 2017)
< 1 ppt	1 – 35 ppt	> 35 ppt	Not included	(Li et al., 2021)
Not defined	Not defined	Not defined	Not defined	(Rippka et al., 1979; Stanier and Cohen-Bazire, 1977)

Research into salinity tolerance is further confounded by the need to distinguish between osmotic stress and salt stress. Osmotic stress is caused by significant differences in the osmolarity of the external environment relative to the intracellular environment (Galinski, 1995). Higher osmolarity inside the cell results in the osmotic pressure driving water into the cell, and higher osmolarity in the environment draws water out of the cell (Galinski, 1995). These differences in osmolarity can be caused by both salt ions and non-ionic solutes (Galinski, 1995). Salt stress is the unique combination of both osmotic stress and ionic stress, and does not necessarily match the stress response of the same organism to similar osmolarities caused by non-ionic solutes (Allakhverdiev et al., 2000; Fernandes et al., 1993; Kanesaki et al., 2002). Additionally, ionic stress can be induced by changes in the contributions of different ions without changes to the net ionic balance (Beer et al., 2014; Billini et al., 2008; Mikkat et al., 2000; So et al., 1998).

My dissertation focuses on the salinity tolerance of Cyanobacteria, which means that I am interested in the combination of osmotic and ionic stresses and am trying to utilize quantitative measures of salinity rather than broad categories. When terms such as freshwater/terrestrial/brackish/marine/hypersaline are used, they are used to communicate the habitat of isolation as best known, and to allow for connection to existing literature. Additionally, salinity lacks a consistent scale due to differences in measurement techniques. I have opted to use units of parts per thousand (ppt) as it is a common and easily convertible unit of measurement. For reference, modern marine salinities range from 30 to 35 ppt and NaCl is soluble in water up to 357 ppt at 25°C (Lee et al., 2018; Oren, 2012).

Cyanobacterial salinity tolerance mechanisms

All domains of life, including Cyanobacteria, are known to have an assortment of mechanisms by which they maintain osmotic homeostasis (Avonce et al., 2006; Csonka and Hanson, 1991; Empadinhas and da Costa, 2011; Galinski, 1995; Hagemann, 2013, 2011; Klähn et al., 2021; Oren, 2016, 2011, 2002; Singh et al., 2022). In addition to the broad need to maintain homeostasis, there are some unique aspects of salinity tolerance in cyanobacteria, due to the role of Na^+ in photosynthesis and other key processes (Billini et al., 2008; Brown et al., 1990; Espie et al., 1988; Mikkat et al., 2000; Ritchie, 1992; So et al., 1998; Wang et al., 2002). Below I outline osmoregulation mechanisms in cyanobacteria. This summary is necessarily deficient but acts to provide sufficient information for further discussion throughout my dissertation.

Ion transport

The simplest set of osmoregulation mechanisms is the transport of salt ions into and out of the cell (Table 2). While salt ions can diffuse through cell membranes, there are also multiple types of transporters known to move salt ions into and out of the cell. These include ATP-dependent transporters as well as proton antiporter systems (Hagemann, 2011).

Transport of Na^+ both into and out of cyanobacterial cells is well established (Billini et al., 2008; Blumwald et al., 1984; Elanskaya et al., 2002; Hagemann, 2011; Inaba et al., 2001; Mikkat et al., 2000; Tsunekawa et al., 2009; Waditee et al., 2001; Wutipraditkul et al., 2005). Several cyanobacterial genomes are known to have multiple genes for Na^+/H^+ antiporters which can be used to both import and export Na^+ from the cell (Billini et al., 2008; Bualuang et al., 2010; Elanskaya et al., 2002; Hagemann, 2011; Inaba et al., 2001; Mikkat et al., 2000; Tsunekawa et al., 2009; Wang et al., 2002). Knockout studies of these genes suggest that most

are in fact redundant, however in *Synechocystis* sp. PCC 6803 but not *Aphanothece halophytica*, the NhaS3 gene was essential for cell function (Billini et al., 2008; Elanskaya et al., 2002; Inaba et al., 2001; Tsunekawa et al., 2009; Wang et al., 2002; Wutipraditkul et al., 2005). There is evidence for the localization of the NhaS3 antiporter in the thylakoid membrane, suggesting that in cyanobacteria it is directly involved in the maintenance of Na^+ concentrations specifically around the photosynthetic electron transport chain and allowing for inactivation of the production of active oxygen species when cells are under Na^+ stress (Tsunekawa et al., 2009). Additionally, the NhaS3 Na^+/H^+ antiporter appears to be the most highly conserved Na^+/H^+ antiporter amongst cyanobacteria (Wang et al., 2002).

While other Na^+/H^+ antiporters are not essential for cell function in most conditions, knockout studies have shown NhaS2 to cause low Na^+ sensitivity (Wang et al., 2002). The NhaS2 antiporter also appears to be absent from some marine cyanobacterial genomes, further supporting its role in maintaining Na^+ concentrations at low salinities (Wang et al., 2002).

In the halotolerant strain *Aphanothece halophytica*, research has shown that some Na^+/H^+ antiporters, including NhaP and NapA, can also use other cations to exchange with H^+, including Li^+, K^+, and Ca^{2+}, however the ATPase-based Na^+ uniporter is Na^+-specific (Bualuang et al., 2010; Hamada et al., 2001; Soontharapirakkul and Incharoensakdi, 2010; Waditee et al., 2006, 2001). Genetic studies have shown that expression of Na^+/H^+ antiporters from halophilic cyanobacteria including *Aphanothece halophytica* improves the salinity tolerance of non-halophilic strains including *Synechococcus* sp. PCC 7942 (Waditee et al., 2002; Wutipraditkul et al., 2005).

Research on both *Synechocystis* sp. PCC 6803 and *Aphanothece halophytica* has shown that the NhaP Na^+/H^+ antiporter is largely homologous to eukaryotic NhaP antiporters, however

there is a significant lack of homology in the C-terminal tails which are significantly longer in the cyanobacterial variants (Hamada et al., 2001; Waditee et al., 2006, 2001). The C-terminus of Na^+/H^+ antiporters is cytoplasmic and believed to be involved in regulation while the N-terminus contains transmembrane portions involved in the ion exchange (Hamada et al., 2001; Padan et al., 2004; Waditee et al., 2006, 2001). Truncation of the cyanobacterial NhaP C-terminal tail results in altered ion specificity, reducing the ability of the *Synechocystis* sp. PCC 6803 NhaP to transport Li^+ in addition to Na^+ and the ability of the *Aphanothece halophytica* NhaP to transport Ca^+ in addition to Na^+ (Hamada et al., 2001; Waditee et al., 2006, 2001).

Cyanobacterial K^+ transport is similarly complex (Ballal et al., 2007; Hagemann, 2011). There are three primary K^+ uptake transporter families in prokaryotes: Ktr/Trk/HKT (Na^+/K^+ symport), Kup/HAK/KT, and Kdp (K^+-transport ATPase) (Berry et al., 2003; Nanatani et al., 2015). There are two K^+ transporter pathways, Ktr and Kdp, that have been identified in Cyanobacteria (Berry et al., 2003; Nanatani et al., 2015). In *Synechocystis* sp. PCC 6803 the *kdp* transport system appears to primarily be used for maintenance of intracellular K^+ concentrations in K^+ limiting environments, while the *ktr* system is used to rapidly transport K^+ at higher environmental concentrations (Berry et al., 2003; Nanatani et al., 2015). While many cyanobacterial strains contain a version of the common prokaryotic high-affinity K^+ transport system *kdp*, this version is unique with a truncated KdpD lacking membrane-spanning domains and no KdpE (Alahari et al., 2001; Ballal et al., 2007; Berry et al., 2003). Additionally, there seems to be a difference in unicellular versus filamentous K^+ transport, as unicellular cyanobacterial strains have at most one *kdp* system, while filamentous strains have at least two *kdp* systems (Ballal et al., 2007). Regulation of the *kdp* system also appears to be distinct in

cyanobacteria, responding to environmental K^+ concentrations but not to osmotic stress as seen in *Escherichia coli* (Alahari et al., 2001; Ballal and Apte, 2005).

Cl^- transport in cyanobacteria is significantly less well characterized (Hagemann, 2011). A handful of putative Cl^- transport genes have been identified, including ion efflux pumps (Kobayashi et al., 2006). Despite the lack of specific proteins involved in Cl^- transport, it has been repeatedly shown that export of Cl^- is essential for Photosystem II function (Allakhverdiev and Murata, 2008; Inoue-Kashino et al., 2005; Katoh et al., 2001; Kobayashi et al., 2006; Popelková and Yocum, 2007; Shen et al., 1998).

Table 2: Cyanobacterial transport systems associated with salt ions and compatible solutes.

Solute	**Gene/Protein**	**Strains**	**Source**
Na^+	NhaS/P	PCC 6803, *Aphanothece halophytica*	(Tsunekawa et al., 2009; Waditee et al., 2001)
Na^+	Mrp	PCC 7120, *Aphanothece halophytica*	(Blanco-Rivero et al., 2009, 2005; Fukaya et al., 2009)
Na^+	NapA	*Aphanothece halophytica*	(Wutipraditkul et al., 2005)
K^+	Ktr	*Synechocystis* sp. PCC 6803, *Anabaena* sp. PCC 7120	(Nanatani et al., 2015)
K^+	Kdp	*Synechocystis* sp. PCC 6803, *Anabaena* sp. PCC 7120, *Anabaena* sp. L-31, *Anabaena torulosa*, *Nostoc punctiforme*, *Nodularia spumigena* CCY9414, *Gloeobacter violaceous*	(Alahari et al., 2001; Ballal et al., 2007; Ballal and Apte, 2005; Nanatani et al., 2015)
Cl^-	*sll1864* (putative gene) or Slr0753	*Synechocystis* sp. PCC 6803, *Thermosynechococcus elongatus*, *Thermosynechococcus vulcanus*	(Inoue-Kashino et al., 2005; Katoh et al., 2001; Kobayashi et al., 2006; Shen et al., 1998)

Sucrose/trehalose/ glucosyglyercol	Ggt	*Synechocystis* sp. PCC 6803, *Synechoccocus* sp. PCC 7002, *Synechococcus* sp. PCC 6301, marine *Synechoccocus* and *Prochlorococcus* strains	(M. Hagemann et al., 1997; Mikkat et al., 1996, 1997; Mikkat and Hagemann, 2000; Scanlan et al., 2009)
Glycine betaine	BetT	*Aphanothece halophytica*, marine *Synechococcus* and *Prochlorococcus* strains	(Laloknam et al., 2006; Scanlan et al., 2009)
Glycine betaine/choline	ProU	"terrestrial" strains, *Nodularia spumigena* CCY9414	(Chen et al., 2021; Voß et al., 2013)
Glycine betaine/proline	*nsp6940*/*nsp6950*	*Nodularia spumigena* CCY9414	(Voß et al., 2013)

There are only a handful of studies on the transport of other ions by cyanobacteria, but it is believed that Ca^{2+}, Mg^{2+}, and Li^{+} all have import and export mechanisms maintained in cyanobacteria (Koropatkin et al., 2007; Lockau and Pfeffer, 1983; Pandey et al., 1996; Pohland and Schneider, 2019; Wever et al., 2019).

Compatible solutes

There are five common organic osmolytes synthesized by cyanobacteria: sucrose, trehalose, glucosylglycerol (GG), glucosylglycerate (GGA), and glycine betaine (GB) (Bianchini, 2022; Blank, 2013; Hagemann, 2013, 2011). The general understanding is that terrestrial strains use sucrose and trehalose, the sugar osmolytes, while marine strains use GG and halophilic strains use GB (Klaehn et al., 2021; Klähn et al., 2021). However, this rule of thumb is known to have exceptions (Klähn et al., 2010; Pade et al., 2016, 2012).

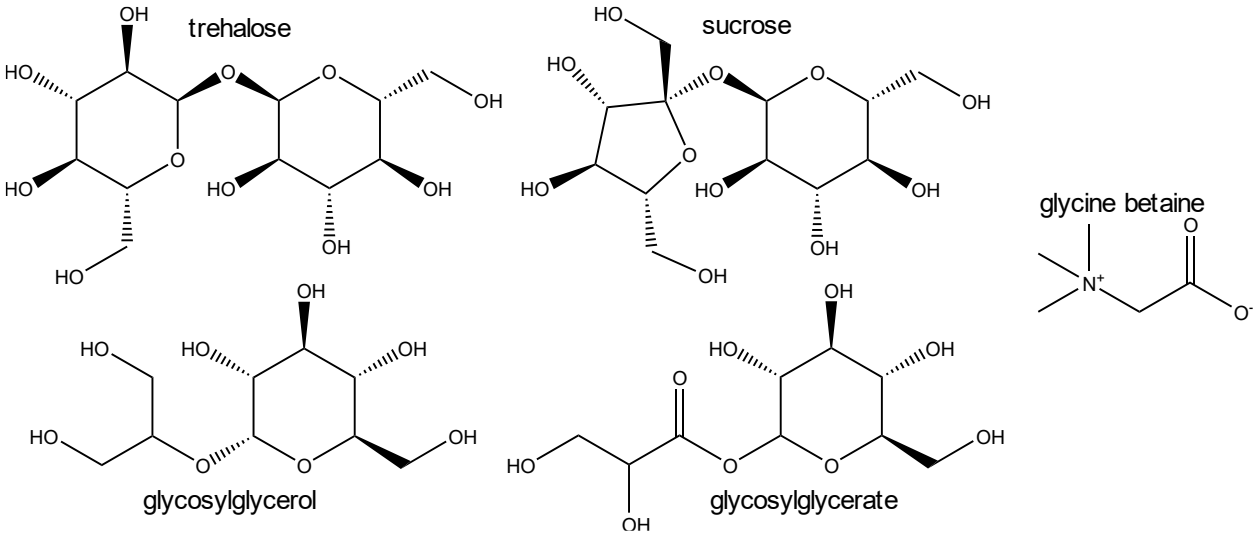

Figure 1: Structures of common compatible solutes used by cyanobacteria.

Sucrose is the most widespread osmolyte biosynthesized within the cyanobacterial phylum, likely due to its role in photoautotrophic carbon metabolism (Hagemann, 2013; Kolman et al., 2015, 2012; Porchia and Salerno, 1996). Accumulation of sucrose as an osmoprotectant

occurs predominantly within the heterocystous, N_2-fixing *Nostocales* clade (Ehira et al., 2014; Hagemann, 2013), however several non-*Nostocales* strains of cyanobacteria have been shown to induce sucrose biosynthesis under salt stress conditions (Cumino et al., 2010; Curatti et al., 1998; Hagemann, 2013; Hagemann and Marin, 1999; Lunn, 2002). Sucrose biosynthesis for osmotic regulation purposes requires two enzymes: sucrose-phosphate synthase (Sps) and sucrose-phosphate phosphatase (Spp) (Cumino et al., 2010; Curatti et al., 1998; Ehira et al., 2014; Hagemann, 2013; Hagemann and Marin, 1999; Kirsch et al., 2019; Kolman et al., 2015, 2012; Lunn, 2002; Porchia and Salerno, 1996).

$$UDP - glucose \ + \ fructose\ 6 - phosphate \xrightarrow{Sps} sucrose - phosphate \ + \ UDP$$

$$Sucrose - phosphate \xrightarrow{Spp} sucrose \ + \ P_i$$

Also relevant for the balance of intracellular sucrose concentrations are several additional enzymes involved in sucrose degradation: sucrose synthase (Sus), amylosucrase (AMS), and invertase or sucrase (Hagemann, 2013; Kirsch et al., 2019; Perez-Cenci and Salerno, 2014).

$$Sucrose \ + \ UDP \xleftrightarrow{Sus} UDP - glucose \ + \ fructose$$

$$Sucrose \xrightarrow{invertase} fructose \ + \ glucose$$

$$Sucrose \xrightarrow{AMS} fructose \ + \ glucose$$

In at least the laboratory model cyanobacterium *Synechococcus* sp. PCC 7002, sucrose synthesis genes have been shown to occur in the gene cluster with amylosucrase and downstream fructose activation genes (Perez-Cenci and Salerno, 2014). This is notable as the coordination of sucrose biosynthesis genes in oxygenic phototrophs was previously established for the first time in *Synechococcus* sp. PCC 7002 (Cumino et al., 2010).

The studies of the evolution of Sps/Spp sucrose biosynthesis suggest that the pathway is modular (Lunn, 2002; Martínez-Noël et al., 2013; Roy, 1999; Snel and Huynen, 2004). It has been hypothesized that the enzymes were originally domains in a single bidomain enzyme with both glucosyltransferase (GTD) and phosphohydrolase (PHD) catalytic domains (Lunn, 2002; Martínez-Noël et al., 2013). In one cyanobacterial strain, *Synechococcus elongatus* PCC 7942, there is evidence for a bidomainal SPS enzyme containing active sites with both GTD and PHD activity (Martínez-Noël et al., 2013). It has also been shown that in several cyanobacterial species (*Synechoccocus* sp. PCC 7002, *Synechocystis* sp. PCC 6803, and *Anabaena* sp. PCC 7120), the *spsA* gene produces a bidomainal SPS with a functioning GTD and a non-functional PHD; these strains each have an additional SPP protein with a catalytic PHD domain (Martínez-Noël et al., 2013).

The primary trehalose biosynthesis pathway in bacteria is the OtsAB pathway, using trehalose-phosphate synthase (OtsA) and trehalose-phosphate phosphatase (OtsB) (Hagemann, 2013).

$$UDP - glucose \ + \ glucose\,6 - phosphate \xrightarrow{OtsA} trehalose - phosphate \ + \ UDP$$

$$Trehalose - phosphate \xrightarrow{OtsB} trehalose \ + \ P_i$$

Alternate pathways include the TreYZ pathway (Avonce et al., 2006; Hagemann, 2013):

$$\alpha - 1{,}4 - polyglucose \xrightarrow{TreY} \alpha - 1{,}1 - maltooligosyltrehalose$$

$$\alpha - 1{,}1 - maltooligosyltrehalose \xrightarrow{TreZ} trehalose \ + \ \alpha - 1{,}4\ polyglucose\ (n-2)$$

TreS pathway (Avonce et al., 2006):

$$maltose \xrightarrow{TreS} trehalose$$

TreP pathway (Avonce et al., 2006):

$$glucose\ 1-phosphate\ +\ glucose \overset{TreP}{\longleftrightarrow} trehalose\ +\ P_i$$

and TreT pathway(Avonce et al., 2006):

$$ADP-glucose\ +\ glucose \overset{TreT}{\longleftrightarrow} trehalose\ +\ ADP$$

Trehalose as the primary compatible solute seems to primarily occur in filamentous cyanobacteria, as well as more dessication tolerant strains (Azua-Bustos et al., 2014; Fagliarone et al., 2020; Hagemann, 2013, 2011; Hershkovitz et al., 1991; Heyer et al., 1989; Kothari et al., 2013; Murik et al., 2017; Page-Sharp et al., 1999; Sakamoto et al., 2011; Shang et al., 2019; Shimura et al., 2015; Starkenburg et al., 2011; Xu et al., 2021). The TreYZ pathway appears to be the primary trehalose synthesis pathway in cyanobacteria (Asthana et al., 2008; Fagliarone et al., 2020; Hagemann, 2013; Higo et al., 2006; Meeks et al., 2001; Ohmori et al., 2009; Page-Sharp et al., 1999; Sakamoto et al., 2009; Shang et al., 2019; Starkenburg et al., 2011; Voß et al., 2013; Wu et al., 2011; Yoshida and Sakamoto, 2009), although the OtsAB pathway is thought to have been laterally transferred into *Crocosphaera watsonii* WH 8501 (Pade et al., 2012). The non-filamentous/N_2 fixing strains with the TreYZ pathway are thermophiles and may use trehalose as a thermoprotectant rather than an osmoprotectant (Furuki, 2009; Hagemann, 2013). The TreS pathway has been identified via *in silico* analyses in several dessication tolerant strains including *Chroococcidiopsis* sp. CCMEE 029, *Gloeocapsopsis* sp. UTEX B3054, *Leptolyngbya ohadii*, *Leptolyngbya boryana* PCC 6306, *Leptolyngbya* sp. NIES-2104, and *Microcoleus vaginatus* FGP-2 (Fagliarone et al., 2020; Hershkovitz et al., 1991; Murik et al., 2017; Shimura et al., 2015; Starkenburg et al., 2011; Urrejola et al., 2019). The *in silico* analyses on *Leptolyngbya ohadii* also suggested the strain may have genes in the TreP and OtsAB pathways as well (Murik et al., 2017).

The TreYZ pathway often appears in an operon containing TreH, a trehalase, however TreH does not seem to be associated as closely with TreYZ in some cyanobacteria (Fagliarone et al., 2020; Higo et al., 2006; Murik et al., 2017; Shimura et al., 2015). Of the marine picocyanobacteria, only *Prochlorococcus* sp. MED4 possesses TreH (Scanlan et al., 2009).

Glucosylglycerol (GG) is generally considered an indication of moderate halotolerance and strains which accumulate GG are often capable of growth in both freshwater and marine media (Engelbrecht et al., 1999; Hagemann, 2013; Marin et al., 1998). GG biosynthesis is a two-step process using GG-phosphate synthase (GgpS) and GG-phosphate phosphatase (GgpP/StpA) (Engelbrecht et al., 1999; Hagemann, 2013; M Hagemann et al., 1997).

$$ADP - glucose \ + \ glycerol\ 3 - phosphate \xrightarrow{GgpS} glucosylglycerol - phosphate \ + \ ADP$$

$$Glucosylglycerol - phosphate \xrightarrow{GgpP} glucosylglycerol \ + \ P_i$$

In at least *Synechocystis* sp. PCC 6803, while sucrose and trehalose biosynthesis can use UDP- or ADP-glucose, GG was strictly dependent on ADP-glucose (Hagemann and Erdmann, 1994; Miao et al., 2003). GG synthesis seems to be specific to salt stress rather than osmotic stress (Hagemann et al., 2001; Hagemann and Erdmann, 1994; Marin et al., 2006; Stirnberg et al., 2007).

Cyanobacterial GgpS genes form two closely related clades, those from picoplanktic cyanobacteria and those from other cyanobacteria, and these clades are separate from heterotrophic GgpS genes phylogenetically (Hagemann, 2011). While heterotrophic GgpS and GgpP are typically a fused protein, they appear to be separate proteins in cyanobacterial genomes (Hagemann et al., 2008). Additionally, while the *ggpS* and *ggpP* genes are often found adjacent in marine picoplanktic *Synechoccocus* strains, they are never found in an operon-like configuration in the beta-cyanobacteria (Hagemann, 2013; Scanlan et al., 2009). In

Synechococcus sp. RCC307 the putative GG-transport system is also linked to the *ggpS*/*ggpP* genes (Scanlan et al., 2009).

GG accumulation is common in marine cyanobacteria, however while *ggpS* is nearly universal within the marine picoplanktic *Synechococcus* strains, it is absent from the marine picoplanktic *Procholorococcus* strains (Klähn et al., 2010; Scanlan et al., 2009). However, marine *Prochlorococcus* strains do have the *ggpP* gene present; this is thought to be due to the loss of the *ggpS* gene from *Prochlorococcus* strains after divergence from the marine *Synechococcus*/*Prochlorococcus* common ancestor (Scanlan et al., 2009).

Comparison of the regulation of *ggpS* in *Synechococcus* sp. PCC 7002 and *Synechocystis* sp. PCC 6803 indicates that while PCC 7002 uses transcriptional control, PCC 6803 uses posttranslational control (Engelbrecht et al., 1999; Stirnberg et al., 2007).

Glucosylglycerate (GGA) biosynthesis occurs via a nearly identical pathway to GG biosynthesis using GGA-phosphate synthase (GpgS) and GGA-phosphate phosphatase (GpgP) (Hagemann, 2013).

$$NDP - glucose \; + \; glycerate\,3 - phosphate \xrightarrow{GpgS} GGA - phosphate \; + \; NDP$$

$$GGA - phosphate \xrightarrow{GpgP} GGA \; + \; P_i$$

gpgS genes are typically found in an operon with *gpgP* and a gene encoding GGA hydrolase (Hagemann, 2013). Unlike most compatible solutes, GGA is a charged molecule (Klähn et al., 2010). While GGA biosynthesis has been detected in many cyanobacterial strains, it seems to be primarily used by marine picoplanktic *Synechococcus* and *Prochlorococcus* strains, and is upregulated under nitrogen limiting conditions (Hagemann, 2013; Klähn et al., 2010). Using a charged compatible solute may allow the cells to use GGA as both a compatible

solute and a charged counter to inorganic anions, replacing the more commonly used glutamate, a nitrogen-containing molecule (Klähn et al., 2010).

Glycine betaine biosynthesis in most organisms occurs through a two-step oxidative pathway starting with choline and using a choline dehydrogenase (CDH) followed by a betaine aldehyde dehydrogenase (BADH), however while this pathway has been suggested to be present in some cyanobacteria, its activity has not been confirmed (Hagemann, 2013; Incharoensakdi and Wutipraditkul, 1999; Waditee et al., 2003). All glycine betaine accumulating cyanobacteria use a direct methylation biosynthesis pathway which occurs in three steps through two enzymes which both use S-adenosyl-methionine (SAM) as the methyl-donor: glycine/sarcosine-N-methyltransferase (GSMT) and dimethylglycine-N-methyltransferase (DMT) (Hagemann, 2013; Waditee et al., 2003).

$$Glycine + SAM \xrightarrow{GSMT} \mathrm{N-methylglycine\ (sarcosine)} + \mathrm{SAH}$$

$$Sarcosine + SAM \xrightarrow{GSMT} N,N-dimethylglycine + SAH$$

$$N,N-dimethylglycine + SAM \xrightarrow{DMT} N,N,N-trimethylglycine\ (glycine\ betaine) + SAH$$

Glycine betaine is often associated with halophily, however it has been found in cyanobacterial strains with only moderate salinity tolerance (Hagemann, 2011; Lu et al., 2006; Mackay et al., 1984; Yang et al., 2020). There has been some phylogenetic evidence for glycine betaine synthesis early in the cyanobacterial phylogeny (Bianchini, 2022; Lu et al., 2006).

The regulation of compatible solute biosynthesis is an active area of research (Ehira et al., 2014; Liang et al., 2020). Transcriptional regulators, including *orrA*, *sigB2* and *sigJ*, have been identified as associated with salt induction of genes including compatible solute synthesis genes in multiple cyanobacterial strains (Ehira et al., 2014; Higo et al., 2006; Nikkinen et al., 2012;

Schwartz et al., 1998; Yoshimura et al., 2007). There is also evidence for post-translational regulation of SpsA in *Anabaena* sp. PCC 7120 (Ehira et al., 2014). It has also been established that salt stress and osmotic stress do not induce the same sets of genes and same physiological responses, indicating that these two related processes need to be studied with a careful eye towards separating the effects of each (Allakhverdiev et al., 2000; Liang et al., 2020).

In addition to biosynthesis of these compatible solutes, many organisms actively transport compatible solutes into and out of the cell. While import of compatible solutes is a primary response to salt stress in heterotrophic bacteria, in cyanobacteria it seems to mostly be used to counteract the diffusion of synthesized compatible solutes out of the cell (Hagemann, 2011). However, compatible solute transporters have been identified in cyanobacteria (Chen et al., 2021; Hagemann, 2011; M. Hagemann et al., 1997; Laloknam et al., 2006; Mikkat et al., 1997, 1996; Mikkat and Hagemann, 2000; Scanlan et al., 2009) and are included in Table 2.

In addition to mechanisms described above, there are potential salinity tolerance mechanisms which have yet to be thoroughly investigated including: lipid membrane composition changes and hydrocarbon production (Allakhverdiev et al., 2001, 1999, 1998), export of phosphatase/phosphodiesterase (Kageyama et al., 2011), synthesis of proline/glutamate betaine/oligosaccharides/mycosporin-like amino acids as compatible solutes (Chaneva et al., 2011; Hagemann, 2011; Lin and Wu, 2014; Mackay et al., 1984; Pontis et al., 2007; Salerno et al., 2004; Yadav et al., 2021), and chaperone proteins induced in salt stress conditions (Hibino et al., 1999; Lee et al., 1997; Waditee et al., 2002).

Given the complex array of molecular mechanisms by which cyanobacteria manage salt stress, trying to understand salt stress across the entire cyanobacterial phylum is a task for a generation of scientists. Instead of trying to understand the individual mechanisms used by

cyanobacteria, I am approaching the study of cyanobacterial salinity tolerance from a high-level viewpoint. My dissertation attempts to understand broad patterns in cyanobacterial salinity tolerance, in cyanobacterial phylogeny, physiology, and evolution. While this work does not target specific molecular mechanisms, it works to provide broad understanding, and provoke questions which can be asked of any salinity tolerance mechanism.

Overview

The overarching approach to my dissertation is illustrated in Figure 2, each chapter addresses a different timescale, from macroevolution in Chapter 2 to physiology in Chapter 3 and adaptation in Chapter 4.

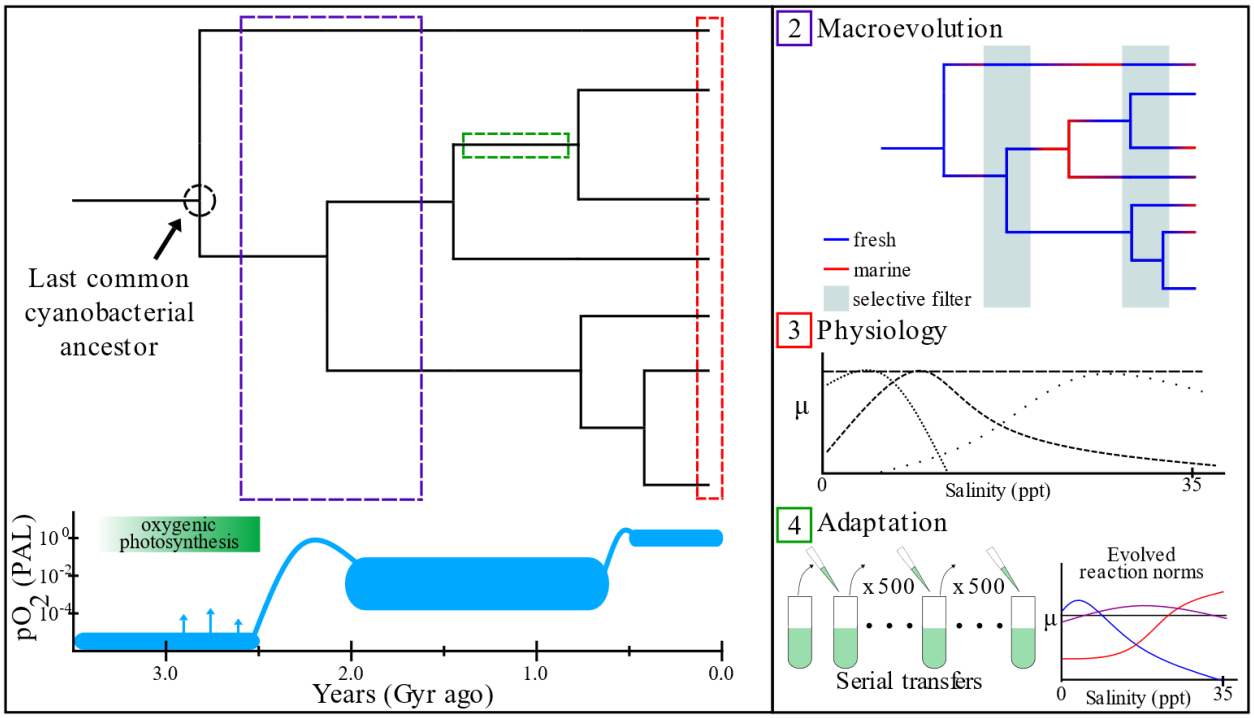

Figure 2: Diagram highlighting the approaches of each chapter of the dissertation.

In Chapter 2: Simulating cyanobacterial trait evolution: influences of deep time and global events, I assess the impact of deep time on our ability to reconstruct microbial traits. Ancestral state reconstructions (ASR) combine our knowledge of modern traits with phylogenies

to predict the likely trait of ancestral species. ASR methods were developed on eukaryotic species with fossil records which could verify not only the phylogeny, but the trait value at specific ancestral nodes. Given our inability to determine specifics of species or traits from microfossils, we rely on eukaryotic methods to predict ancient microbial traits.

Given the extremely deep roots of the cyanobacterial phylogeny, I wondered how environmental change would impact ASR of microbial traits. I approach this from a computational perspective, simulating trait evolution under different evolutionary scenarios and evaluating the ability of ASR methods to predict the 'true' ancestral state.

In Chapter 3: Reevaluating the plastic response of extant cyanobacteria to changes in salinity, I assess two related questions: is salinity a discrete or continuous trait? And does the habitat from which a cyanobacterium was isolated predict its salinity tolerance?

There is evidence in the literature that salinity tolerance is in fact a continuous trait, with some cyanobacterial strains having salinity optima which do not match their habitat of isolation (Bano and Siddiqui, 2004; Batterton and Van Baalen, 1971; Brand, 1984; Duval et al., 2018; Fu and Bell, 2003; Herrmann and Gehringer, 2019; Khatoon et al., 2010; Melero-Jiménez et al., 2019; Stam and Holleman, 1979, 1975; Stulp and Stam, 1984). Additionally, as with temperature tolerance, there is evidence that salinity tolerance should not be constricted simply to its optimum but rather described via a reaction norm (Bano and Siddiqui, 2004; Duval et al., 2018; Herrmann and Gehringer, 2019; Melero-Jiménez et al., 2019). I hypothesized that salinity tolerance in cyanobacteria is both a continuous trait and not restricted to an optimum, thus providing evolutionary potential for cyanobacteria to relatively easily move between environments with varying salinities.

To assess these questions, I curated a database of cyanobacterial responses to changes in salinity from the literature. My database contains reaction norms from over 70 strains, from dozens of papers across more than 6 decades. Using this database, I assess how we classify salinity tolerance and provide a mechanistic model to allow for quantitative assessment of cyanobacterial salinity tolerances.

In Chapter 4: Experimental evolution of salinity tolerance in a laboratory model cyanobacterium, I assess the stability of the response of a cyanobacterium to changes in salinity under selective pressure.

For phylogenetic trait reconstructions to be applied to the cyanobacterial ancestor, the trait must be conserved enough that the modern trait distribution retains information about the ancestral state. However, salinities of isolation are rarely monophyletic within the phylum (Hagemann, 2011). Additionally, there is experimental evidence from eukaryotic oxygenic phototrophs that adaptation to a different salinity can occur within hundreds to thousands of generations (Lachapelle et al., 2015; Perrineau et al., 2014). If salinity tolerance in Cyanobacteria is not conserved relative to the age of the phylum, the modern distribution of salinity tolerance on the cyanobacterial tree cannot independently determine the salinity tolerance of the cyanobacterial ancestor.

I evolved 16 lineages of the laboratory model cyanobacterium *Synechococcus* sp. PCC 7002 for over 750 generations in 4 different salinity conditions via serial transfer. Over the course of the experiment, I assessed the changes in the general fitness of the evolved lineages as well as changes in the response of the evolved lineages to changes in salinity.

Together these three chapters assess key assumptions underlying our understanding of cyanobacterial salinity tolerance and the early history of Cyanobacteria. By looking across

timescales, and providing quantitative assessment of these assumptions, I provide a key foundation on which to move our understanding of cyanobacterial salinity tolerance forward and develop a more comprehensive model for future research.

Chapter 2: Simulating cyanobacterial trait evolution: influences of deep time and global events

Introduction

Cyanobacteria have long been a focal phylum in geobiological research due to their dominant role in Earth history and in modern biogeochemical cycling. Additionally, the evolution of cyanobacteria is deeply interconnected with that of Earth systems and of interest from both evolutionary biology and Earth history perspectives. Beyond their pivotal role in the initial oxidation of the Earth's atmosphere at the Great Oxidation Event (GOE), they were the primary endosymbiont in the evolution of eukaryotic phototrophs, and their physiological evolution likely played a significant role in both the low primary productivity that characterized the Proterozoic as well as the Neoproterozoic Oxidation Event and Cryogenian glaciations (Hamilton et al., 2016; Hammerschmidt et al., 2021; Hurley et al., 2021; Sánchez-Baracaldo et al., 2021, 2014). The Earth system dominance of Cyanobacteria persists today, as the phylum is directly responsible for a significant portion of modern primary productivity (Flombaum et al., 2013).

Given their history, the evolution of Cyanobacteria has been researched extensively from physiological, ecological, and macroevolutionary perspectives. The application of these tools to cyanobacterial evolution has been discussed in previous literature (Schirrmeister et al., 2016, 2015). Despite the long history and multidisciplinary nature of these approaches, there is still uncertainty about when the last common ancestor of modern Cyanobacteria originated, as well as its primordial habitat and the ecological and environmental constraints on subsequent evolutionary radiation. Estimates for the evolution of oxygenic photosynthesis range from the origin of life to 3.7 Gyr to 2.5 Gyr (Cardona et al., 2019; Lalonde and Konhauser, 2015;

Planavsky et al., 2014; Rosing and Frei, 2004; Sánchez-Baracaldo and Cardona, 2020; Schirrmeister et al., 2015; Shih et al., 2017). These estimates broadly fall into two categories: those based on molecular clock reconstructions of the Cyanobacteria phylum or key enzymes for oxygenic photosynthesis (Cardona et al., 2019; Sánchez-Baracaldo and Cardona, 2020; Schirrmeister et al., 2015; Shih et al., 2017), and those based on geochemical signatures of oxidation in the rock record (Lalonde and Konhauser, 2015; Planavsky et al., 2014; Rosing and Frei, 2004). Central to the wide range in estimates in both categories is the lack of any clear and definitive signatures of oxygenic photosynthesis or oxygenic photosynthesizers in the rock record prior to the GOE (Hamilton, 2019). Unlike the evolutionary history of animal diversification, the majority of the history of Cyanobacteria lacks any fossils on which to anchor key innovations (Schirrmeister et al., 2016; Schopf, 2011).

Ancestral state reconstructions (ASR) can be used to predict the evolutionary history of DNA and protein sequences, geographical range, and phenotypes based on a provided model of evolution (Joy et al., 2016). Typically, the model for evolution underlying ASR is a stochastic process; either Markov chain for discrete traits, or Brownian Motion or Ornstein-Uhlenbeck processes for continuous traits (Joy et al., 2016). Evaluation of trait reconstruction typically occurs through either maximum likelihood (ML) or Bayesian inference methods (Joy et al., 2016). ASR typically relies on the fossil record to provide constraints and calibration points for the reconstruction, and it has been repeatedly shown that reconstructions without fossil data are significantly less reliable (Slater et al., 2012). ASR has been applied to Cyanobacteria with regard to the history of specific traits, as well as with regard to the evolution of key enzymes (Blank and Sánchez-Baracaldo, 2010; Cardona et al., 2019; Hammerschmidt et al., 2021; Kacar et al., 2017; Sánchez-Baracaldo, 2015; Sánchez-Baracaldo et al., 2017b; Uyeda et al., 2016).

While traditionally ASR is thought of as reconstructing the evolutionary history of traits within a lineage, we must consider that in deep time ASRs on microbial lineages may instead reconstruct the history of the Earth environment.

Salinity tolerance, often based on the habitat of isolation, is a regular target of ASR in Cyanobacteria. Due to results from both ASR and geochemical studies, ancestral salinity tolerance has been central to hypotheses surrounding the timing of the evolution of Cyanobacteria and the GOE (Hammerschmidt et al., 2021; Lalonde and Konhauser, 2015; Sánchez-Baracaldo et al., 2017b). Given its role in models of early biogeochemistry, and its frequent evaluation in ASR, we utilize it here as the trait of interest. Additionally, existing literature suggests that salinity tolerance may be a continuous trait (Duval et al., 2018; Hagemann, 2011; Herrmann and Gehringer, 2019; Reed et al., 1986, 1985; Reed and Stewart, 1985), and here we consider both continuous and discrete representations of salinity tolerance as a character trait. In addition to its use in investigations of cyanobacterial evolutionary history, salinity tolerance is a complex trait known to be influenced by multiple genetic mechanisms, including compatible solute synthesis and transport, ion pumps, and water movements (Hagemann, 2011). Investigations of compatible solute synthesis genes on the cyanobacterial species tree have shown that different compatible solute genes have different evolutionary histories on the cyanobacterial phylogeny (Bianchini, 2022; Blank, 2013). While this paper focuses on a specific evolutionary scenario, the results are applicable to other geobiological contexts.

Here I aim to specifically address the application of phylogenetic trait reconstruction tools and the influence of deep time on the underlying assumptions of these methods. As shown in Figure 3, I utilize two models of trait evolution, Brownian Motion and Ornstein-Uhlenbeck

processes, to produce simulated "modern" traits on previously published cyanobacterial phylogenies. Within each trait evolution model, I evaluate across a wide range of both evolutionary variabilities and selective pressures as well as running each scenario on multiple phylogenetic topologies. I evaluate these simulated trait datasets from multiple perspectives, including the distributions of traits, phylogenetic significance of traits both before and after discretization, evolutionary rates predicted from the scenarios, and finally for accuracy of ASR models. By using datasets with a "true" answer, I can assess how ASR functions in different evolutionary scenarios without fossil constraints.

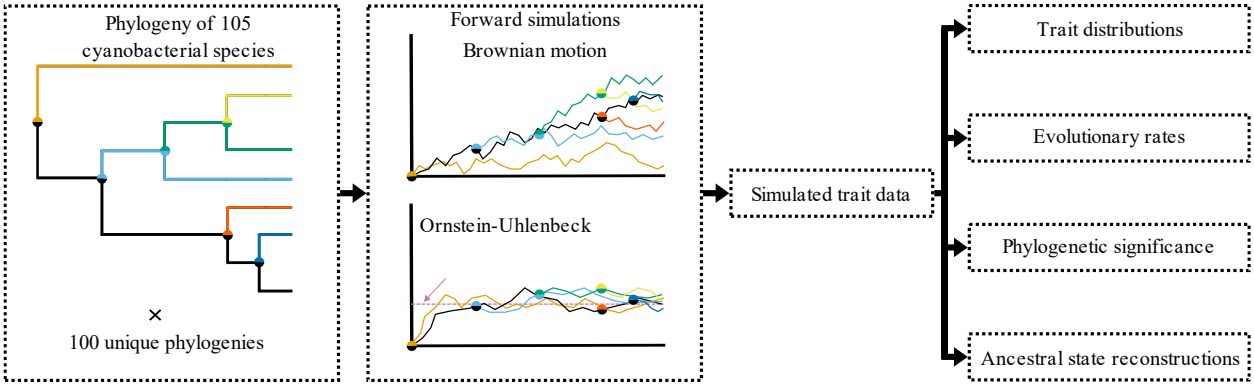

Figure 3: Workflow diagram for simulating trait data on cyanobacterial phylogenies and downstream analyses

Methods

Phylogenies

To ensure that the phylogenies used as the basis for my simulations were realistic, I utilized published cyanobacterial phylogenies based on Bayesian analyses on concatenated amino acid and ribosomal RNA sequences (Uyeda et al., 2016). I chose to use phylogenies identified as lacking long branch attraction and utilized the phylogenies with 105 species included, for a total of 100 phylogenies. I also generated a maximum clade credibility phylogeny

from this set of phylogenies using the maxCladeCred function from the phangorn R package (Schliep, 2011).

Forward simulations

Forward simulations were run using two models for trait evolution. The first model is Brownian Motion (BM) which represents a 2D random walk as: $\delta X(t) = \sigma * \delta\beta(t),\ X(0) = X_0$. Under Brownian evolution, lineages evolve through time via variations determined by random selection from a Gaussian distribution with a mean of 0 and variance of δt and magnified by the value of σ, the evolutionary variance.

The second model for trait evolution is the Ornstein-Uhlenbeck (OU) expansion on Brownian motion: $\delta X(t) = \alpha(\theta - X(t))\delta t + \sigma\,\delta\beta(t)$. This model adds an adaptive optimum (θ) and a rate of movement towards said optimum (α). While this model can allow for movement of the optimum through time and is typically written as $\theta(t)$, in this study the optimum is set at the same value across the entire timespan of each simulation.

To implement these models, I utilized the OUwie R package which allowed for setting and changing evolutionary regimes across the trees. I modified the OUwie.sim function to include upper and lower bounds on the possible trait values. The boundaries set for these simulations were 0 ppt and 357 ppt, to avoid negative salinities or salinities higher than the saturation point of sodium chloride. Cyanobacteria have been observed growing at both extremes of this range, so utilizing physical restrictions is an appropriate choice for boundaries (Oren, 2011). The datasets presented here use boundaries that reflect the trait value back across the boundary. For example, if a trait value reaches 362, it is converted to 352 (now 5 below the bound as it was 5 above the bound) and the simulation continues. I also evaluated the use of

boundaries which take any value which exceeds a boundary and modifies to be at the boundary, and comparisons between these boundary types can be found in Appendix A.

For each model I tested a range of values for the controlling parameters (σ for both BM and OU, and α for OU). The parameter choices for the various simulations are shown in Table 1. For the OU model, I tested each pairing of σ and α values to evaluate how the changes in each parameter affect the trait evolution independently and in conjunction with each other. For both models and all parameter sets tested, I ran a simulation on each of the 100 phylogenies described above, providing a total set of simulations for each model that is 100 times the number of parameter options evaluated. This allows me to investigate potential effects of phylogenetic topology on the results, as well as providing a sampling of the evolutionary space generated by the random variation underlying both models.

Analysis of simulated trait values

To allow for comparison with the evaluations of the history of the habitat salinity of cyanobacteria in the existing literature, I discretized the simulated trait data using a published discretization cutoff where salinities below 5 ppt were designated as *fresh* and those above 5 ppt were designated as *marine* (Uyeda et al., 2016).

To compare the rates of evolution observed in my simulated datasets with evolutionary rates measured empirically and in the fossil record, I calculate the rate of evolution for each simulated trait value. Given the lack of population data, I utilize the calculation for evolutionary rates in darwins: $r_{evo} = \frac{\ln\frac{X}{X_0}}{\delta t}$ (Haldane, 1949). The evolutionary rate, r_{evo}, is determined by the difference in the natural logarithm of the trait value (X) and the natural logarithm of the ancestral trait value (X_0), normalized to the time over which this evolutionary change occurred (δt).

To investigate the phylogenetic significance of the data I generate, I utilize Pagel's λ (Pagel, 1999). I evaluated the signal on both the continuous trait data generated by the simulations, as well as on the discretized datasets and compared the predicted λ values and model fits with those conducted on a phylogeny in which all extant species are equally distant from a single common ancestor. I utilized the fitContinuous and fitDiscrete functions from the geiger R package for each respective dataset and used the lambda transform option to produce the λ values for comparison (Pennell et al., 2014).

Ancestral state reconstructions

Discretized simulation datasets were analyzed using the make.simmap function in the phytools R package (Revell, 2012). Reconstructions were conducted using both the equal-rates (ER) and the all-rates-differ (ARD) models of trait transitions. Transition matrices were derived via Markov chain Monte Carlo sampling of the posterior probability distribution. Reconstructions were sampled every 100 simulations after burn-in to generate a dataset of 100 reconstructions. The reported likelihood of a freshwater ancestor is the percent of the 100 sampled reconstructions which had a root node with the fresh trait.

Table 3: Parameters for simulated datasets

Simulation	σ	α	θ	X_0	Total simulated datasets
Brownian Motion (BM)	10^{-5} to 10^{0} (n = 100)	10^{-16} (n = 1)	NA	0	10^{4}
Ornstein-Uhlenbeck (OU)	10^{-5} to 10^{0} (n = 10)	10^{-5} to 10^{0} (n = 10)	35	0	10^{4}

Results

Forward simulations

The trait distributions derived from the Brownian motion forward simulations are primarily controlled by the σ value of the simulation (Figure 4A). As σ increases, the width of the distribution increases, and the mean trait value slowly follows. The maximum trait value only surpasses 35 ppt (modern marine salinity) at $\sigma > 1e^{-2}$, but given the threshold for being discretized as *marine* (> 5 ppt), approximately 50% of tips are considered *marine* by this point (Figure 4B).

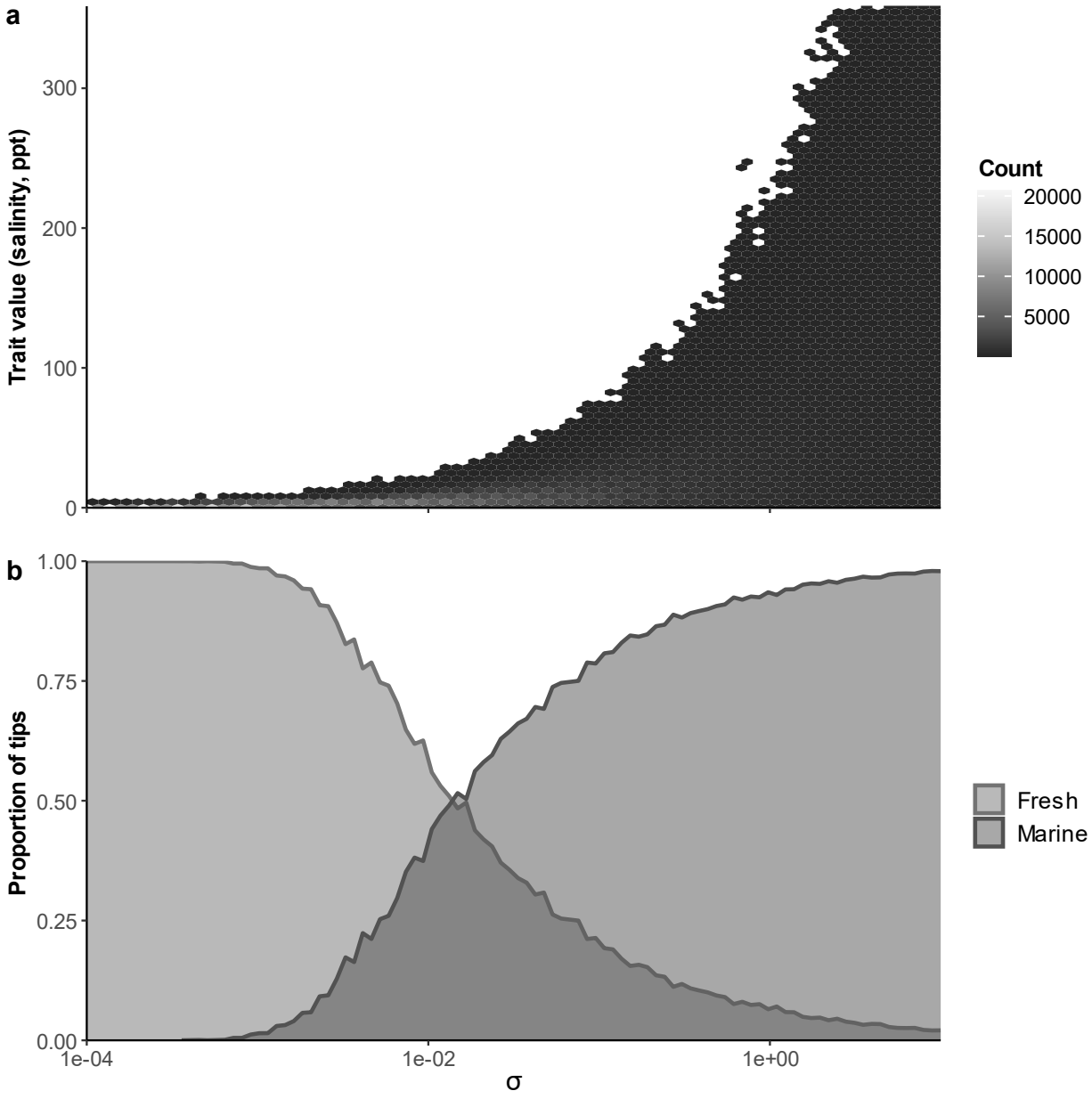

Figure 4: Simulated trait data from the Brownian Motion forward simulations. In a is the number of tips with a given salinity across the simulations. In b is the proportion of tips which are discretized as fresh versus marine.

The Ornstein-Uhlenbeck (OU) forward simulations have two controlling parameters for the trait distributions: σ and α. Generally, whichever parameter is greater is the one driving the trait distribution. As with the BM data, the trait distribution is very narrow until σ values are

greater than $1e^{-2}$, but this threshold also increase with α, until the distribution is very narrow across the full range of σ values (Figure 5).

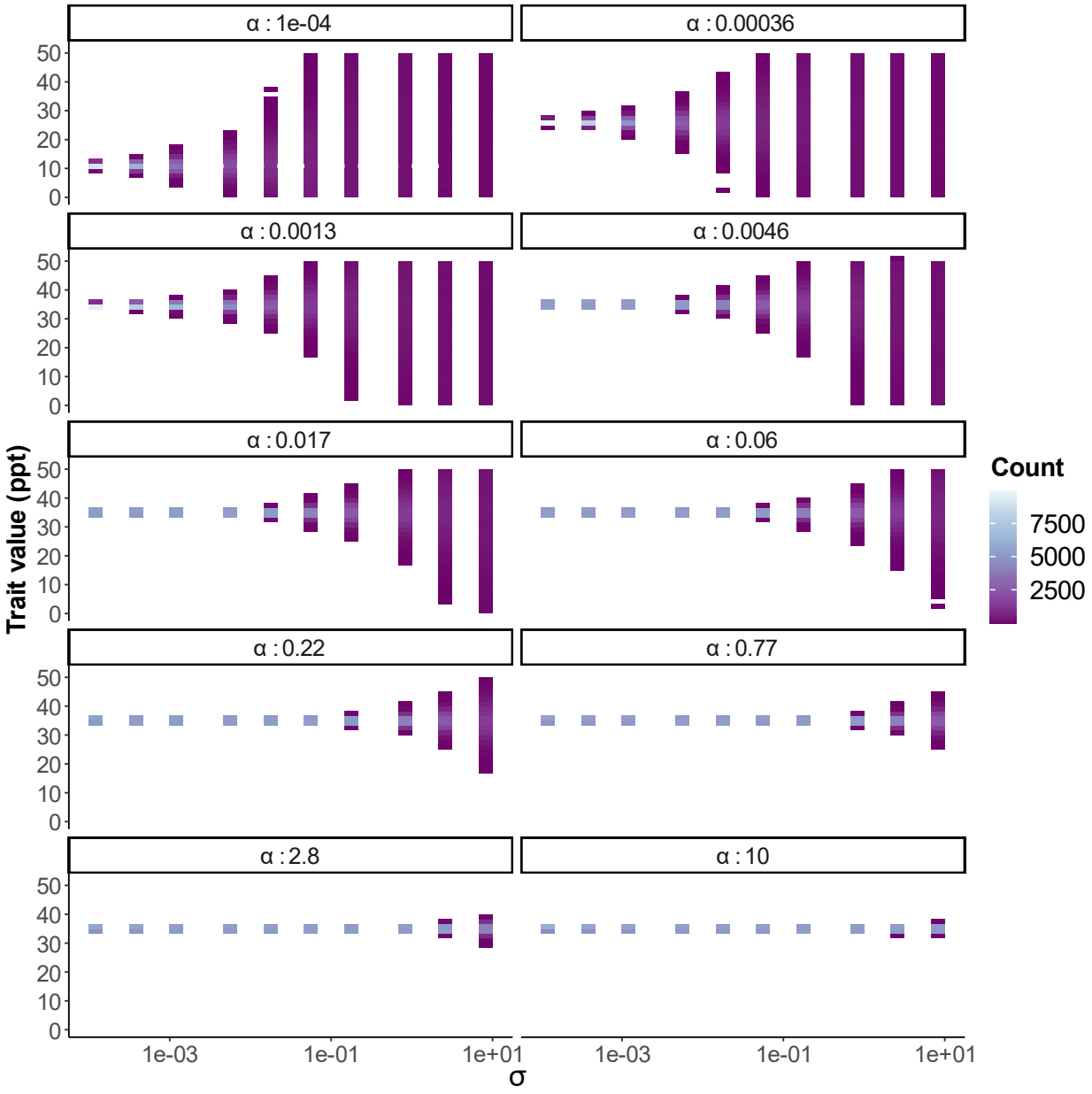

Figure 5: Simulated trait data from the Ornstein-Uhlenbeck forward simulations. Each panel has a different α value. The y-axis has been restricted to a range of 0 - 50 ppt.

Unlike the BM simulations, the mean trait value shifts considerably, primarily controlled by α. As α increases to $1e^{-3}$, the mean shifts from approximately 10 ppt to 35 ppt, the defined

optimum, and then remains constant at the optimum for all higher values of α (Figure 5). As a result, there are no OU simulations where more than 25% of the tips are discretized as fresh.

When the simulated data are used to estimate evolutionary rates, the rates obtained are small ($3.6 * 10^{-9}$ to 0.0038). I calculated rates using three potential timespans over which the salinity of cyanobacteria evolved:

- over the entire cyanobacterial phylogeny dating back to 3.5 billion years ago
- over the entire cyanobacterial phylogeny dating back to the Great Oxidation Event 2.5 billion years ago
- since the most recent Neoproterozoic Snowball Earth period, 635 million years ago

Regardless of the length of evolution, the general trend is that increasing sigma results in increasing rates. Generally, the OU simulated data has lower rates than the BM simulated data, likely due to the constraint provided by the optima.

On the continuous data produced in BM forward simulations, the median value across all σ values for Pagel's λ is 0.98, with a minimum median λ of 0.97 at a σ value of 10 and a maximum median λ of 0.99 at a σ value of 0.34. The continuous OU data exclusively produces Pagel's λ values of 1.

For the BM forward simulations, the calculated Pagel's λ after discretization covers the full range of values (0 to 1). Using both equal rates and all-rates-differ transition matrices, the highest phylogenetic significance is observed around σ values of approximately 0.01, which coincides with the crossover point where more tips are discretized as marine than fresh. Outside of this region, λ values range from 0 to 1, but are generally weighted towards higher values.

For the OU forward simulations where tips were not entirely discretized as marine ($\sigma > 1e^{-2}$ and $\alpha < 0.06$), calculated λ values again ranged from 0 to 1, with the highest densities of values at either 0 or 1.

Ancestral state reconstructions

For the datasets from BM simulations, a freshwater ancestor was predicted nearly 100% of the time at σ values below 0.001 regardless of model choice (Figure 6 A and C). At $\sigma > 0.001$, the equal-rates model rapidly shifts from 100% likelihood of fresh ancestor to 0% likelihood of fresh ancestor by σ values of 0.1 (Figure 6A). In contrast, the all-rates-differ model consistently produces a 50% likelihood of fresh ancestry at σ values above 0.001 (Figure 6C).

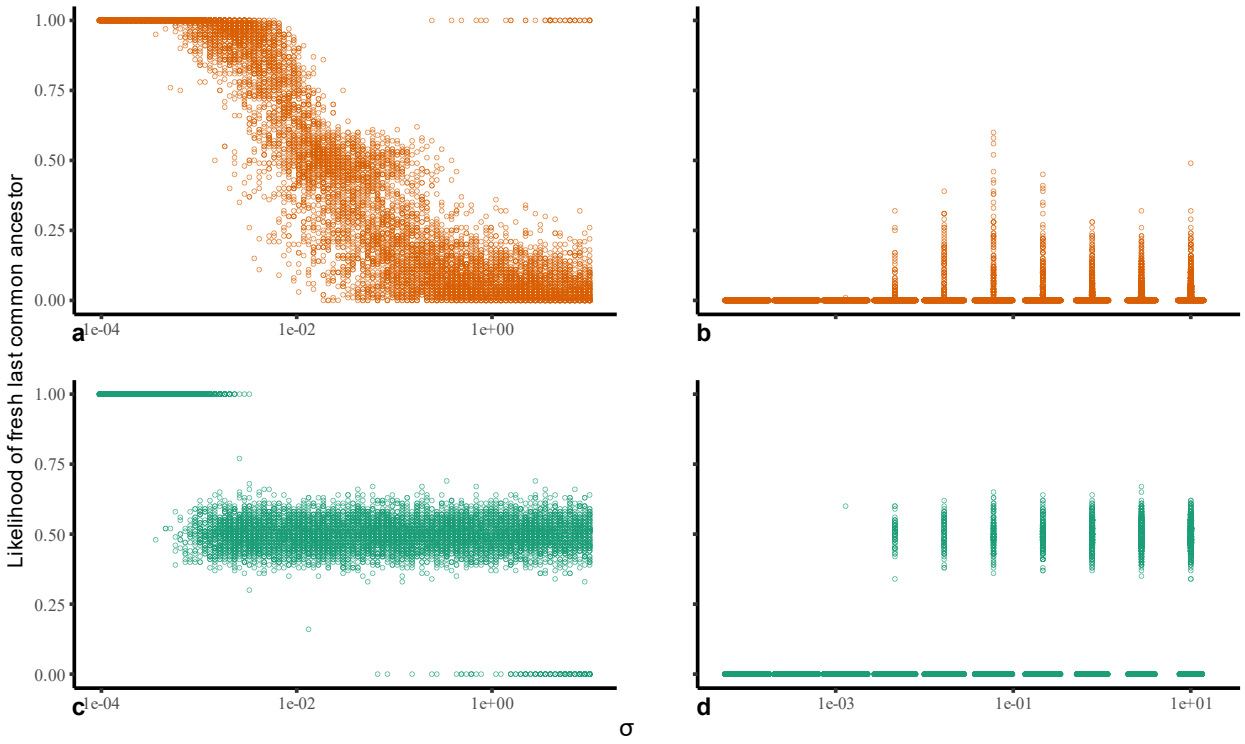

Figure 6: Likelihood of reconstruction of freshwater habitat for the last common ancestor given the value of sigma used to produce the simulated trait data. a and b show reconstructions using the equal-rates (ER) model for the Brownian Motion and Ornstein-Uhlenbeck simulations respectively. C and D show reconstructions using the all-rates-differ (ARD) model for the Brownian Motion and Ornstein-Uhlenbeck simulations respectively. For the Ornstein-Uhlenbeck reconstructions (B and D), all α values tested for each σ are shown. Breakouts of the impact of α on the likelihoods can be seen in the supplemental materials (Figure 32).

For the OU simulation datasets, any likelihood of a fresh ancestor only occurs at α values less than 0.02, and the maximum likelihood of a fresh ancestor is 67% (Figure 6 B and D). While the equal-rates model has likelihoods that taper off as α increases at each σ (Figure 6B), the all-rates-differ model produces likelihoods of 0.0 or 0.5 in almost all cases (Figure 6D).

Discussion

General implications

Model choice has a large impact on reconstructed ancestral states when transition rates are not constrained (Nakov et al., 2017; Sánchez-Baracaldo et al., 2017b, 2017a). Using only the simulated trait distributions, it is clear that as a phylum, Cyanobacteria only require very low evolutionary variance in order to sample the entire trait space for salinity. This is supported by the observation of the "blunderbuss pattern" in which the bounds of evolutionary divergences expand dramatically over timescales greater than one million years (Uyeda et al., 2011).

Rates of change of salinity tolerance in cyanobacteria need to be orders-of-magnitude lower than natural rates for reliable reconstruction of ancestral habitats. If we consider only the σ space over which BM models have a greater than 50% chance of reconstructing a freshwater ancestor ($\sigma < 0.001$), the evolutionary rates predicted by the trait data range from $3.6 * 10^{-9}$ to 0.0038 darwins given an ancestor at the GOE. In comparison, a survey of evolutionary rates in the literature provided magnitudes of rates ranging from 0 to over 8,000 darwins for fossil studies, and from 0 to over 2,000,000 darwins for field studies (Uyeda et al., 2011). These simulated rates likely do not reflect evolutionary reality as salinity tolerance is a complex multivariate trait that we represent as the mode of a salinity reaction norm. However, even when the timescale over which these rates is reduced dramatically, from the Great Oxidation Event to the Neoproterozoic Oxidation Event, the rates for simulations which can reconstruct the ancestral state are only $1.4 * 10^{-8}$ to 0.015 darwins. Additionally, generational timescales in natural populations of cyanobacteria may vary by orders-of-magnitude, which will potentially lead to a biased sharpening up of the rate distributions estimate here.

Geobiological implications

Over geologic timescales, even extremely weak selective pressures can lead to significant adaptive change. This has previously been established when surveying evolutionary rates from microevolutionary, historical, and paleontological datasets, where less than 10^7 generations are required to show significant response to even very weak selection (Estes and Arnold, 2007). As such, when microbial evolution occurs in the presence of a selective regime, as modeled in the OU simulations, ASR reconstructs the regime, not the ancestral state. While I do not consider rate shifts that may be associated with rapid environmental changes or lineage-specific evolutionary regimes and instead apply a global selective regime, the approach presented here can be modified to take such processes into account.

Moving forward as geobiologists, we must take care to acknowledge the limitations of our methods, both geological and biological, and consider whether the assumptions underlying these methods remain reasonable as we utilize them in new contexts. Additionally, we must evaluate whether methods validated on macrofossils can be applied to microbial evolutionary history when fossil constraints are significantly less available. ASR remains a useful and informative tool for interrogating the appearance of traits in evolutionary history, and its applications to the cyanobacterial phylogeny continue to provide new hypotheses to investigate surrounding their role in the evolution of our planet.

The ensemble of phenotypic traits in cyanobacterial populations may reflect the tempo, mode, and variation of environmental change on Earth rather than the evolutionary history of cyanobacterial lineages themselves. This is due largely to the fact that the timescales over which microbes evolve to selective regimes are many orders of magnitude smaller than the timescales

over which we apply ASR. We must consider the possibility that we are observing the impact of strong fluctuating selection rather than evolutionary stasis.

This study suggests several important lessons moving forward in the use of ASR to study the evolution of microbes in deep time. While we rarely, if ever, have fossils which can be tied to a specific branch of a microbial tree as well as a specific trait, our results suggest that accounting for broader scale changes in the environment may provide a better understanding of the evolution of microbial traits alongside environmental change. There may be space to connect our knowledge of major climatic shifts to microbial phylogenies to ask new questions using ASR. The results also suggest that we should focus on developing clearer understandings of the complexities of traits to better understand how trait complexity interplays with adaptation in microbial populations.

Chapter 3: Reevaluating the plastic response of extant cyanobacteria to changes in salinity

Introduction

Cyanobacteria are the only phylum to have independently evolved the ability to perform oxygenic photosynthesis (Blankenship and Hartman, 1998; Cardona, 2016; Nisbet et al., 2007; Sánchez-Baracaldo et al., 2021; Sánchez-Baracaldo and Cardona, 2020; Soo et al., 2017). Not only did a cyanobacterium become the primary chloroplast driving eukaryotic photosynthesis, but the evolution of oxygenic photosynthesis in Cyanobacteria is believed to be the primary driver in the oxidation of the Earth's atmosphere 2.5 – 2.0 billion years ago at the Great Oxidation Event (GOE) (Blank and Sánchez-Baracaldo, 2010; Sánchez-Baracaldo et al., 2021; Sánchez-Baracaldo and Cardona, 2020; Schirrmeister et al., 2016; Soo et al., 2017; Ward et al., 2016). In addition to their historical importance, cyanobacteria remain dominant primary producers in modern ecosystems and perform a significant portion of global oxygen production (Dvořák et al., 2014; Falkowski et al., 2008; Flombaum et al., 2013).

One environmental parameter of interest in the study of cyanobacteria is salinity. Salinity is a primary controlling factor in microbial biodiversity, and transitions between freshwater and marine environments are uncommon across many domains of life (Cabello-Yeves and Rodriguez-Valera, 2019; Dittami et al., 2017; Logares et al., 2009; Paver et al., 2018; Vermeij and Dudley, 2000; Whittle et al., 2021). However, in research on the phylum, salinity tolerance is typically classified as based on the habitat the strain was isolated from, and rarely direct measures of tolerance (Bianchini, 2022; Blank, 2013; Sánchez-Baracaldo et al., 2017b; Uyeda et al., 2016).

Salinity, or more broadly osmolarity, is known to impact growth rates due to the stresses it can place on a cell to retain or exclude solutes. It has been theorized that the relationship

between salinity and growth rate is caused by the impact of salinity on the macromolecular packing density of the cell (Dill et al., 2011; Ghosh et al., 2016). There are varying mechanisms by which cells can control their internal osmolarity, including transport of salt ions and the production and transport of small organic molecules (Hagemann, 2011).

In this chapter, I will present a meta-analysis of cyanobacterial responses to salinity. Through this dataset I will answer two questions: Does habitat of isolation predict salinity tolerance? And is salinity tolerance a discrete trait? Upon establishing an observational perspective on cyanobacterial salinity tolerance, I will provide an updated framework for understanding salinity tolerance based on biophysical constraints. This framework provides both a conceptual and quantitative framework by which we can move forward in our understanding of salinity tolerance.

Rather than developing a fine-grained model to precisely fit a well-constrained system, my conceptual model takes a coarse-grained approach. Using this approach, the model predicts the phenotypic response of cyanobacteria to changes in salinity, rather than considering the specific mechanisms. Given the complex array of osmoregulatory mechanisms, this provides a model useful outside of laboratory model systems. Additionally, this approach does not focus on the molecular specifics, but rather on the downstream effects of those specifics.

Methods

Literature data

I extracted data from figures using WebPlotDigitizer if data was not reported in a table or supplemental file. Where available, I used growth rates reported in the original paper.
If only growth curve data was available, I extracted this data and performed a simple realized growth rate calculation in which the growth rate (μ) was simply the change in the cell growth

metric (x) over time (t): $\mu = \frac{x_f - x_0}{t_f - t_0}$. Where possible, the strains used in each paper were matched with their NCBI Taxonomy ID to assist in downstream analyses and avoid errors due to strain naming histories. Raw data extracted from these papers is available on request.

Laboratory data

For strains newly characterized for this paper, growth measurements were made based on the optical density determined from the absorbance at 730nm measured on a ThermoScientific Genesys 30 visible spectrophotometer. Cultures were grown in 10 mL of medium in aerobic culturing vials, shaking under continuous LED 5300K white light illumination. The salinity gradient was created by mixing BG-11 (a freshwater medium) with AASW (an artificial seawater medium). All raw optical density data is available on request. Growth rates were determined from the realized growth of each strain in each condition.

Normalization

Growth rates were normalized to the maximum growth rate observed for each specific experiment and strain. Strains that were measured repeatedly in a single paper or across multiple papers were normalized separately for each set of measurements. All processing scripts are available on request.

The salinity of optimal growth was identified as the salinity at which the normalized growth rate was equal to 1. The maximum salinity of growth was determined to be the highest salinity at which the normalized growth rate was > 0.1.

K-means clustering

I assessed the ability to categorize cyanobacterial strains by their salinity tolerance by conducting k-means clustering analyses based on the salinity of optimal growth and maximum

salinity of growth for each strain. I compared results of clustering with 2 to 5 categories utilizing the total within-cluster sum of squares.

Results

Salinity of optimum growth

The range of salinities at which the optimal growth occurred in all strains was 0 to 40 ppt. Only 3 strains, all isolated from marine habitats, had optimal salinities above 35 ppt. One terrestrially isolated strain had an optimal salinity of 35 ppt. The lack of a significant relationship between habitat of isolation and the optimal salinity of growth was confirmed via a one-way analysis of means which failed to reject the null hypothesis that the mean optimal salinity of growth was equal in different habitats of isolation ($p = 0.074$).

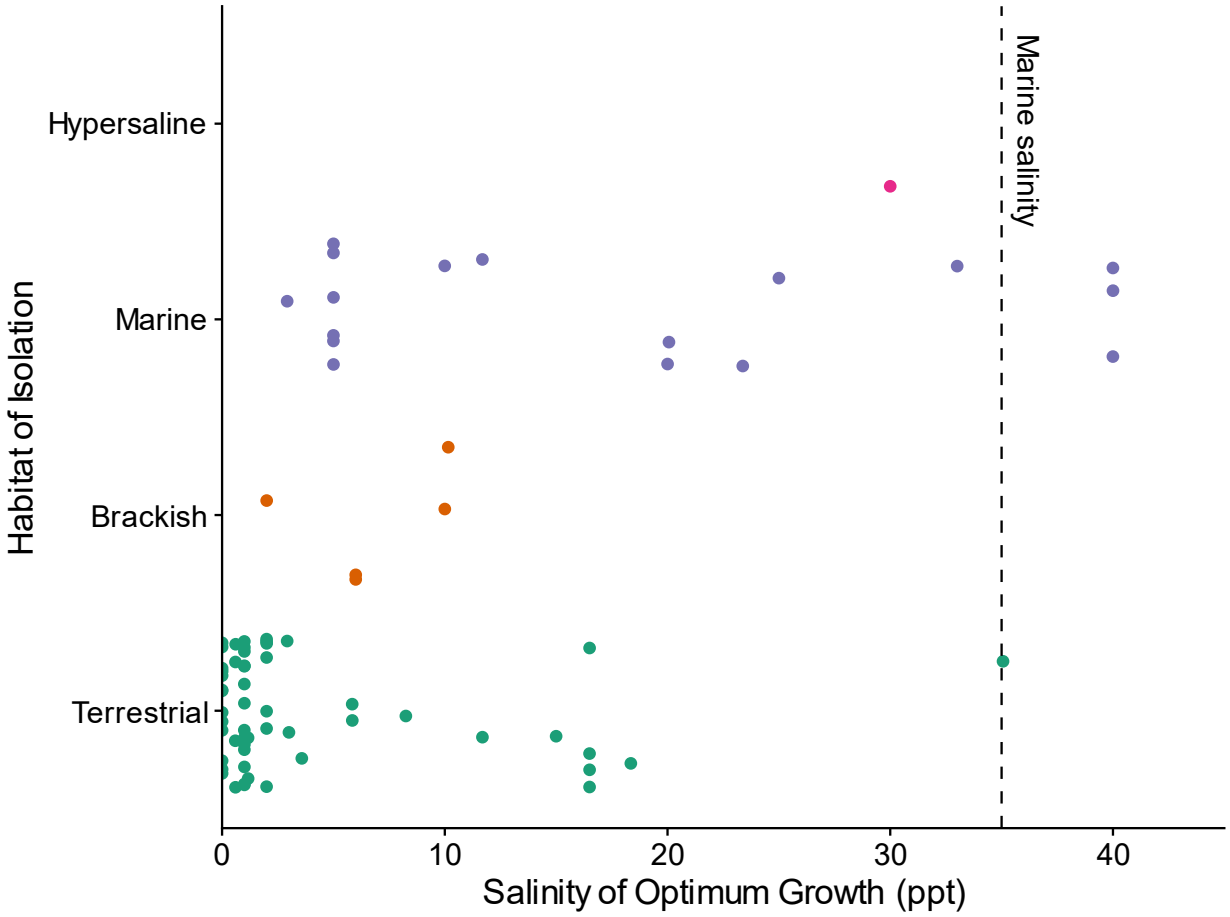

Figure 7: Salinity in parts per thousand (ppt) at which the optimal growth rate was observed for each strain. Strains are categorized by their habitat of isolation. The dashed vertical line indicates modern marine salinity at 35 ppt.

Maximum salinity of growth

The range of maximum salinities of growth was 1.5 to 240 ppt. The highest maximum salinity of growth occurred in a terrestrial strain. Oddly, several strains identified as having been isolated from marine habitats had maximum salinities of growth significantly less than 35 ppt. All strains isolated from hypersaline environments had maximum salinities of growth above marine salinities. The lack of a significant relationship between habitat of isolation and the maximal salinity of growth was confirmed via a one-way analysis of means which failed to reject

the null hypothesis that the mean maximal salinity of growth was equal in different habitats of isolation ($p = 0.086$).

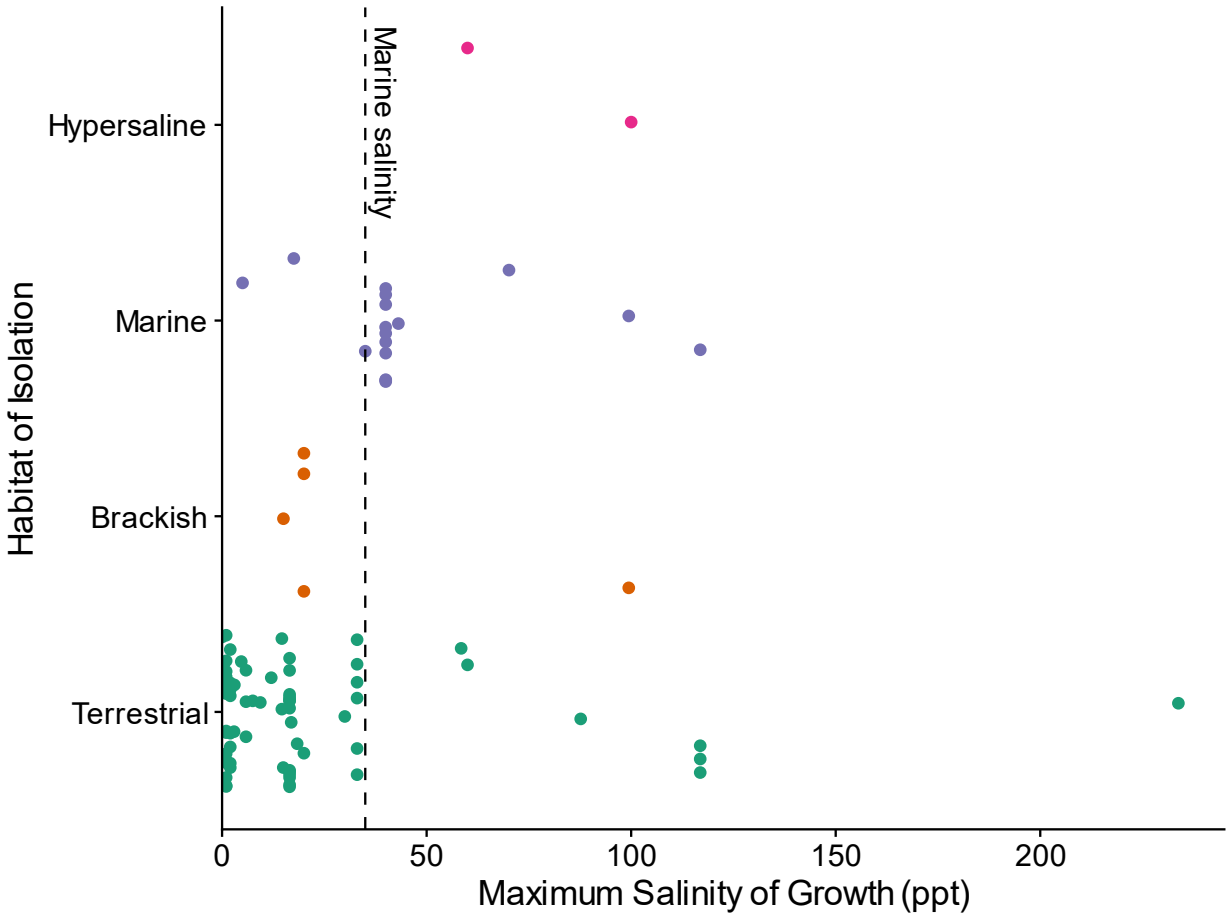

Figure 8: Maximum salinity in parts per thousand (ppt) at which growth was observed in each strain. Strains are categorized according to their habitat of isolation. The vertical dashed line indicates modern marine salinity at 35 ppt.

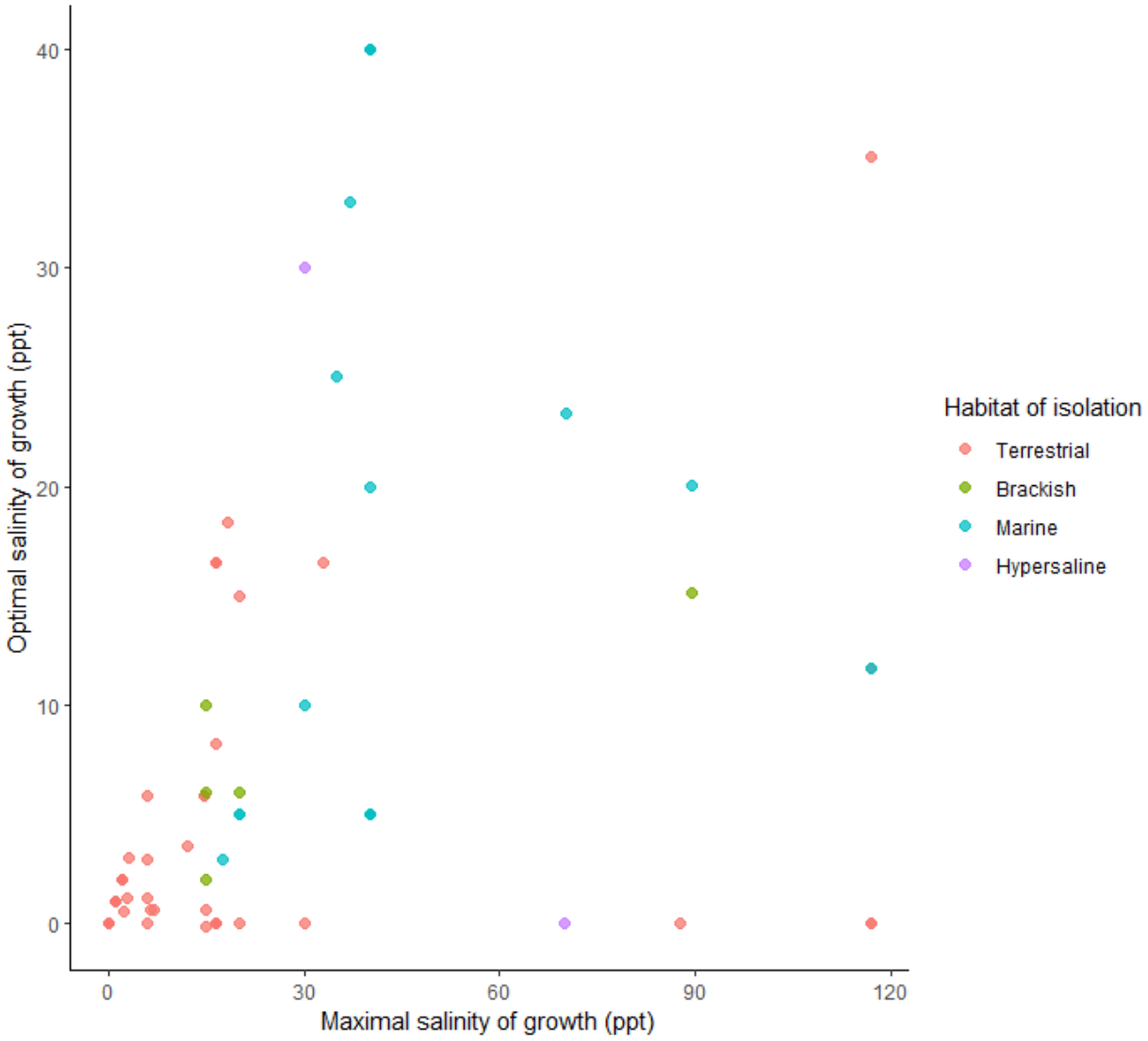

Figure 9: The optimal salinity of growth against the maximal salinity of growth for each strain. Color indicates the habitat of isolation for each strain.

Reaction norms

Individual reaction norms for each strain can be found in Appendix B.

K-means clustering

The results of each clustering analysis are shown in Figure 10. The comparison on the total within-cluster sum of squares for different numbers of clusters is shown in Figure 34. These results suggest that grouping strains into four salinity tolerance clusters is ideal, however, the

divisions are primarily based on the maximum salinity of growth, rather than the optimal salinity of growth.

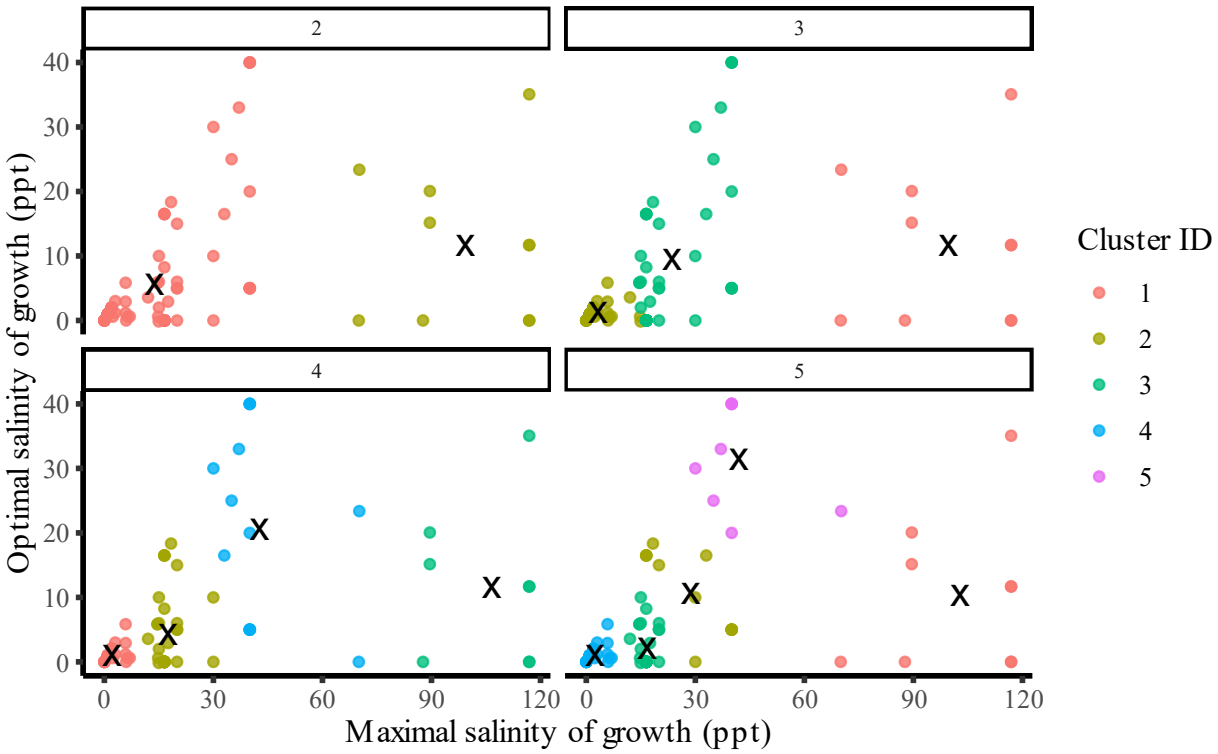

Figure 10: Each subplot shows the same data plotted with the optimal salinity of growth against the salinity of maximum growth. The Xs indicate the center of each cluster. Each subplot shows the result of clustering with a different number of clusters, from 2-5.

Biophysics-informed conceptual model of salinity tolerance

Based on the varied response shapes of the different strains to salinity, I developed a conceptual model of mechanisms of osmoregulation and the impact of salinity on growth rate based on biophysics. The growth rate of a cell is strongly correlated with the volume fraction of proteins within the cell, or the macromolecular packing density (Dill et al., 2011; Ghosh et al., 2016). This packing density controls the diffusion rate of proteins within the cell, too low of a packing density will cause interactions between proteins to occur only rarely, too high of a packing density and the crowding will slow diffusion (Dill et al., 2011). The bacterial salt growth law supposes that the growth rate of a cell is proportional to the collision rate between proteins

within the cell caused by protein diffusional transport (Ghosh et al., 2016). Modeling and experimental work has suggested that this protein diffusion-based growth law is driven by the impact of diffusion on protein translation through the change in diffusion of the tRNA complexes which bring amino acids to the ribosome (Ghosh et al., 2016; Klumpp et al., 2013). Thus the intracellular packing density is a tightly controlled parameter which directly impacts cell growth and fitness (Dill et al., 2011).

As illustrated in Figure 11, the packing density, ϕ, has a proportional impact on the rate of diffusion-limited reactions in cells, r_d, which can be defined as: $r_d \sim \phi \left(1 - \frac{\phi}{\phi_c}\right)^2$ (Dill et al., 2011; Ghosh et al., 2016; Schmit et al., 2009). ϕ_c is the macromolecular packing density at which the glass transition occurs and diffusion stops ($\phi_c = 0.58$) (Weeks et al., 2000). This glass transition density has been proposed to be a mechanism for inducing cell dormancy under extreme osmotic stress (Mourão et al., 2014). The packing density at which the diffusion-limited reaction rate, and thus growth, is optimized is $\phi_{opt} = \frac{\phi_c}{3} = 0.19$ (Dill et al., 2011; Schmit et al., 2009). This is reflected in the fact that cell protein densities are typically around 20% (Dill et al., 2011; Ellis, 2001; Zimmerman and Trach, 1991).

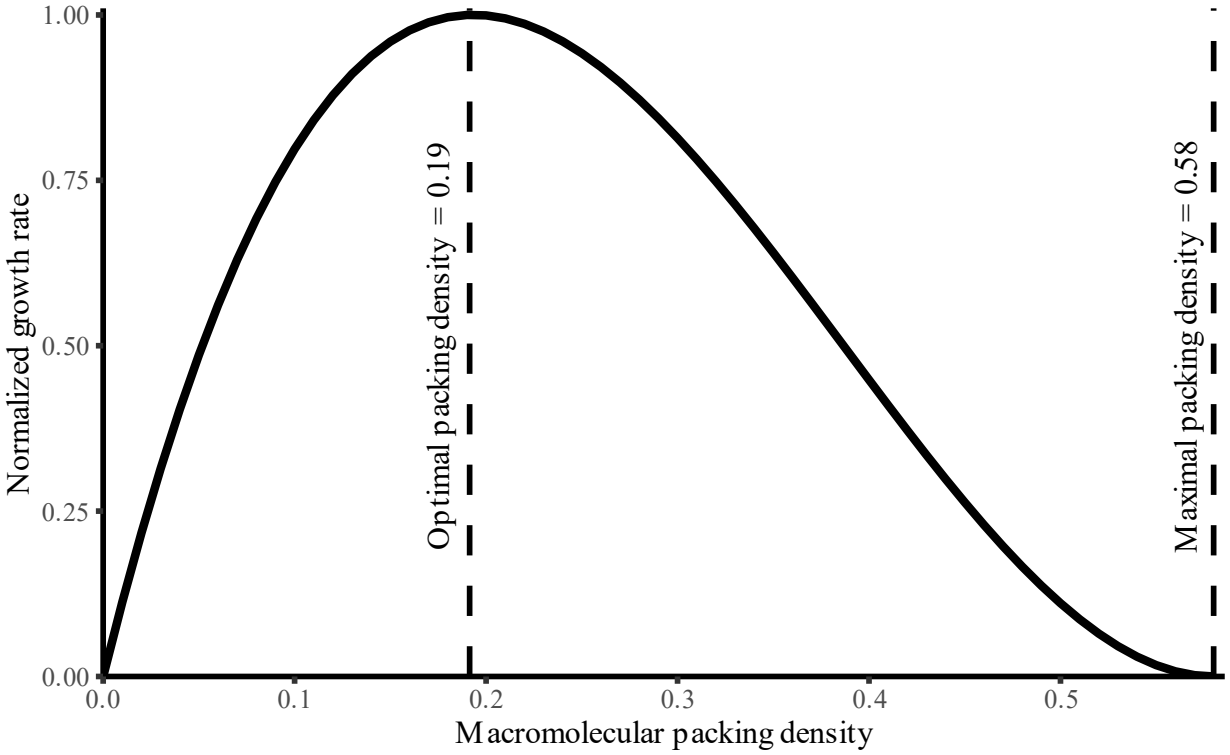

Figure 11: Relationship between normalized growth rate and packing density.

Osmotic stress is associated with the movement of water into or out of the cell, causing changes in the cell volume and its macromolecular packing density. Thus, the ability of a strain to maintain its macromolecular packing density across a range of salinities directly leads to the ability to maintain its growth rate across a range of salinities. When environmental salinity increases, the cell volume decreases as water is lost to the environment, this results in the macromolecular packing density increasing and diffusion rates slowing. Conversely, when the environmental salinity decreases, the cell volume increases due to the rush of water into the cell, this results in a decrease in macromolecular packing density and interactions between macromolecules. While macromolecular packing density is an important physiological variable, it is significantly impacted by environmental osmolarity and salinity.

The normalized growth rate response of a specific strain to a change in salinity can thus be considered the result of its ability to control how the environmental salinity changes the

macromolecular packing density, or the cell's ability to osmoregulate. This is illustrated in Figure 12 showing how various levels of osmoregulation impact the response of the macromolecular packing density to changes in environmental salinity. No osmoregulation results in a simple linear relationship between the macromolecular packing density and the environmental salinity as increased environmental salinity leads to decreased cell volume and increased macromolecular packing density. In contrast, perfect osmoregulation would result in a constant optimal packing density across the full range of salinities, allowing for a cell to maintain its optimal macromolecular packing density regardless of environmental salinity. While neither of these endmember cases are likely in living cells, they begin to allow us to consider how different methods of maintaining homeostasis impact this relationship.

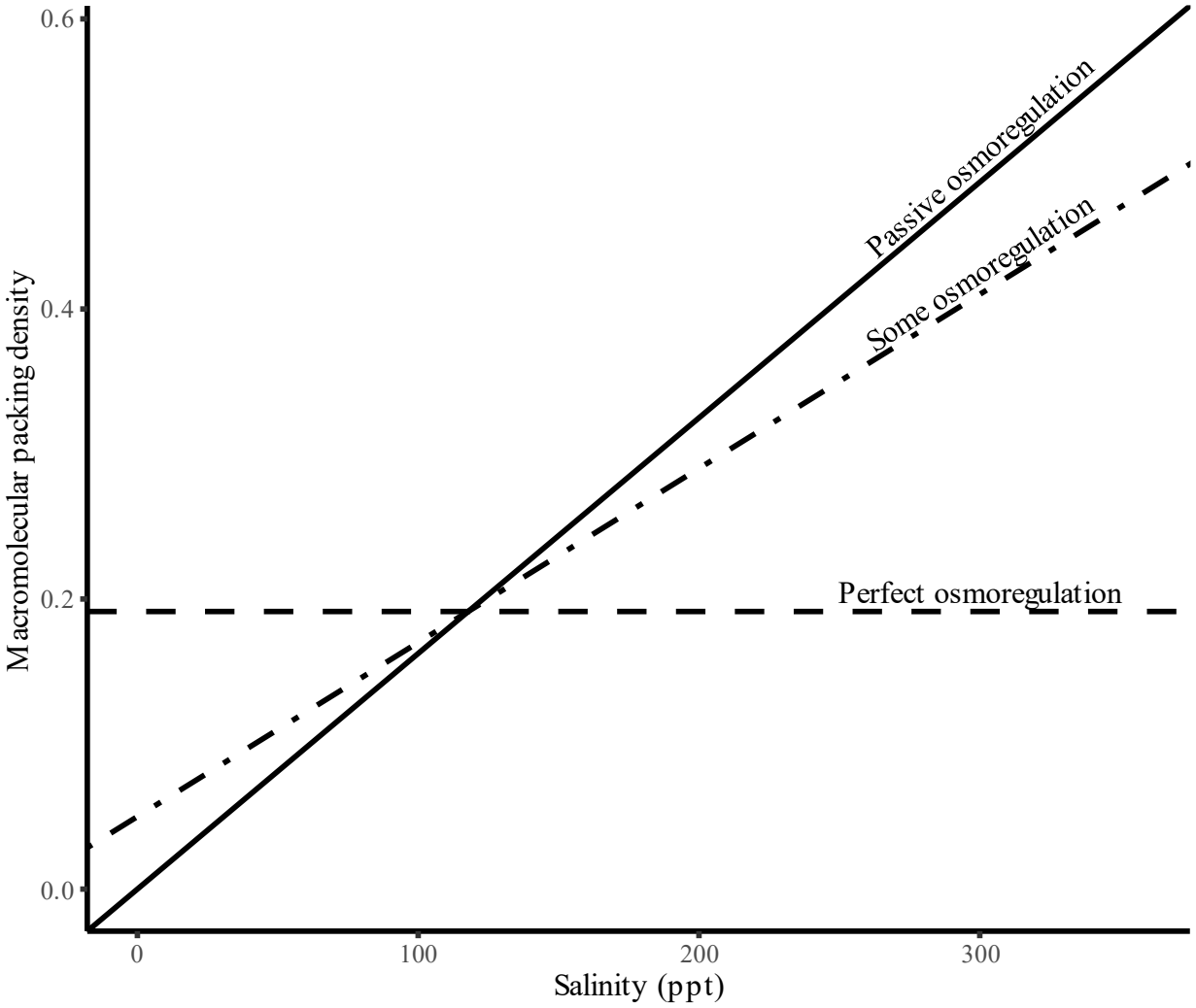

Figure 12: Impacts of various levels of osmoregulation on intracellular packing density across a range of environmental salinities

At simplest this can be considered a change in the slope of the relationship between packing density and external salinity. However, this simply results in a change of the salinity of optimal growth and does not fundamentally change the shape of the response curve. For strains to have response curves which maintain near optimal growth rates across a range of salinities they must be able to stabilize their intracellular packing densities near the optimal packing density across that range. This suggests that the response of intracellular packing density to

external salinity must be considered a piecewise function, where the slope of the packing density versus salinity relationship changes at different salinity ranges.

I assessed four theoretical models of osmoregulation for the relationship between environmental salinity and macromolecular packing densities. These relationships are shown in Figure 13.

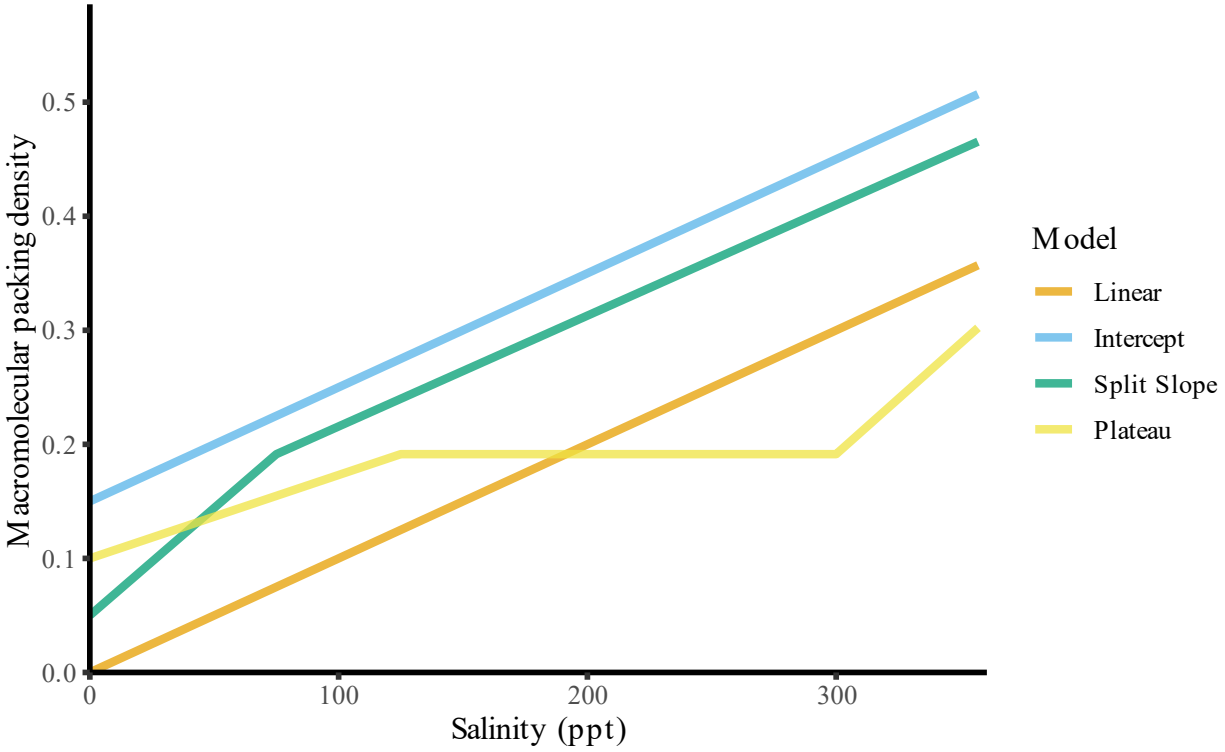

Figure 13: Macromolecular packing density and salinity relationships of the four theoretical models.

The simplest model (Linear) has only one parameter, the slope of the relationship between the salinity and the packing density (k_1), and a set y-intercept of 0:

$$\varphi = k_1 \times S$$

In this model, cell growth rates in fully fresh conditions are always 0 and increase to an optimum at the packing density of maximum growth ($\varphi = 0.19$) based on the slope of the relationship between the packing density and the salinity (k_1). As shown in Figure 14, the higher

the slope (k_1), the faster the packing density of maximum growth is reached. However, because the slope of the packing density-salinity relationship is constant, the faster the packing density of maximum growth is reached, the faster the glass transition packing density is reached. For a strain to have a high growth rate at low salinities, it must then also reach its maximum salinity of growth, at the glass transition, at low salinities. This restricts all strains with high initial growth rates to a limited range of salinities.

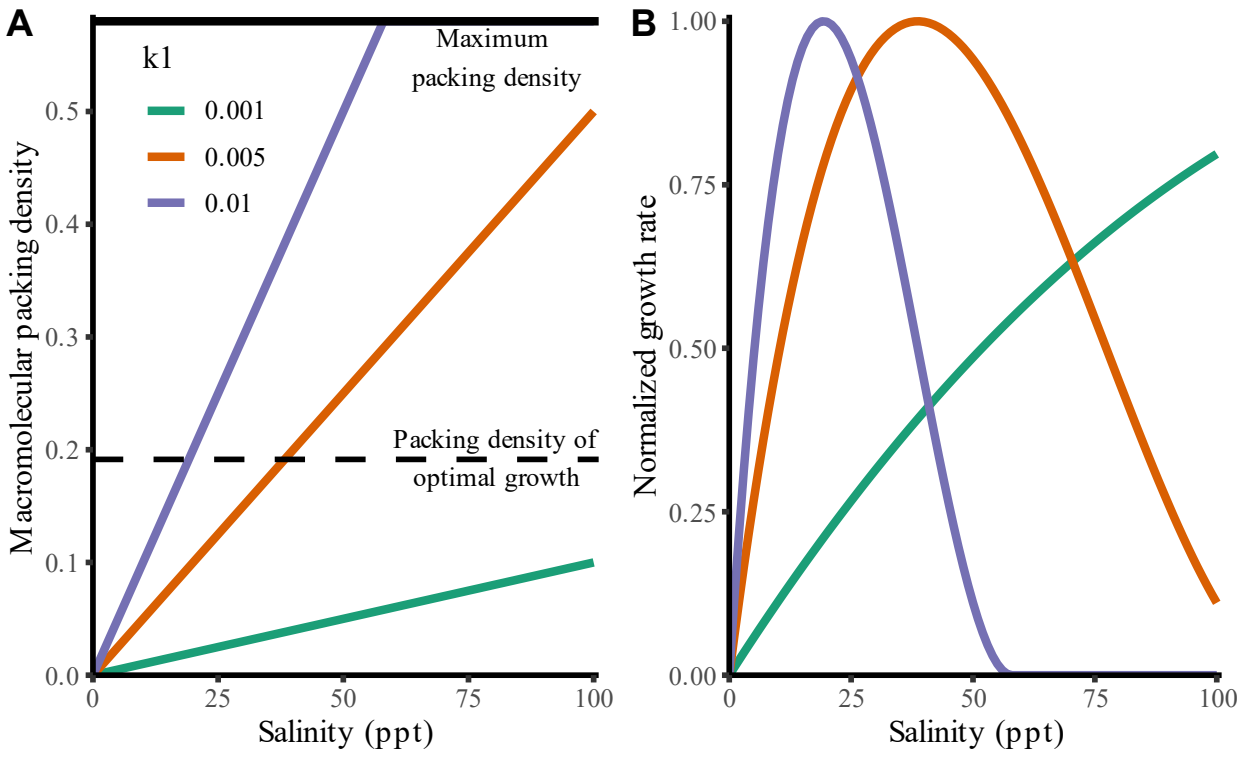

Figure 14: Impact of varying k_1 in the Linear model on the packing density versus salinity relationship (A) and the normalized growth rate versus salinity relationship (B). Each colored line represents a different value for the slope in the packing density versus salinity relationship. The resulting growth rate for each of these packing density-salinity slopes is shown in B as the relationship between the normalized growth rate and the salinity. As k_1 increases, the packing density of maximal growth is reached faster, and thus the maximum growth rate occurs at a lower salinity.

Figure 15 shows the next model for the packing density-salinity relationship (Intercept) which adds only a single additional free parameter, the value of the y-intercept (b):

$$\varphi = k_1 \times S + b$$

When b is 0, this model simply recapitulates the Linear model. When b is increased without any change to the slope, the growth rate curve is shifted towards lower salinities. Increasing b indicates the ability of the cell to maintain sufficient macromolecular packing density even in low salinities. This allows for strains to have maximum growth rates at lower salinities while having a slower increase in the macromolecular packing density with salinity (k_1). This means that strains with low optimal salinities are able to continue growing across a wider range of salinities than possible in the Linear model.

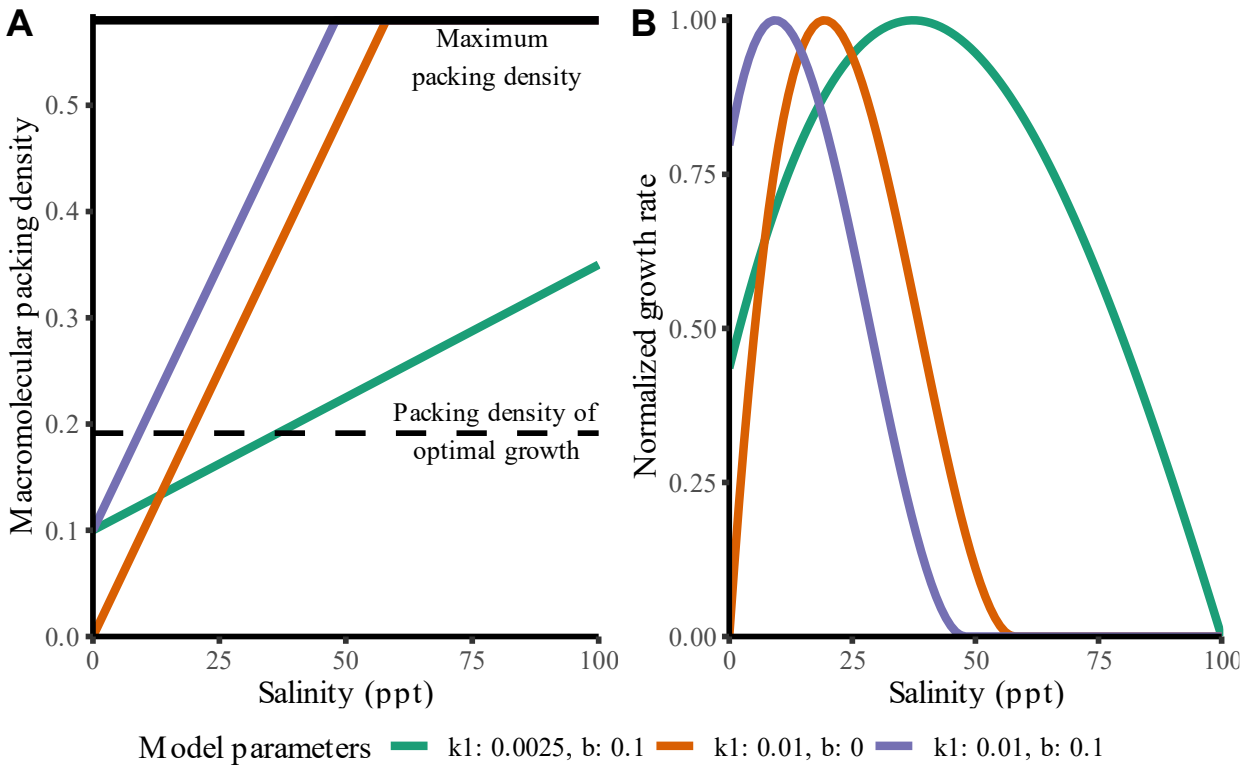

Figure 15: Impact of varying k1 and b in the Intercept model on the packing density versus salinity relationship (A) and the normalized growth rate versus salinity relationship (B) Each colored line represents a different combination for the slope (k_1) and intercept (b) in the packing density versus salinity relationship. The resulting growth rate for each of these packing density-salinity relationships is shown in B as the relationship between the normalized growth rate and the salinity. Increases in b results in a decrease of the salinity of optimum growth at the same k_1.

The third model (Split Slope), shown in Figure 16, allows for a change in the slope of the relationship between the packing density and the salinity, with one slope before and one slope

after the salinity of maximum growth rate in addition to the y-intercept (b) remaining a free parameter. The slopes are calculated based on the salinity of optimal growth (x_{opt}) and the salinity of maximum growth (x_{max}), where the slope before the packing density of maximum growth is defined as $k = \frac{\varphi_{opt} - b}{x_{opt}}$ and the slope after the packing density of maximum growth is defined as $k = \frac{\varphi_c - \varphi_{opt}}{x_{max} - x_{opt}}$. The packing density-salinity relationship is defined as two functions, one for below x_{opt}:

$$\varphi = \frac{\varphi_{opt} - b}{x_{opt}} \times S + b$$

And one for above x_{opt}:

$$\varphi = \frac{\varphi_c - \varphi_{opt}}{x_{max} - x_{opt}} \times S + \varphi_{opt}$$

This divides osmoregulation abilities of a strain between osmoregulation below the optimal salinity of growth and osmoregulation above the optimal salinity of growth. This reflects the reality that osmoregulatory mechanisms do not function equally well across all salinities.

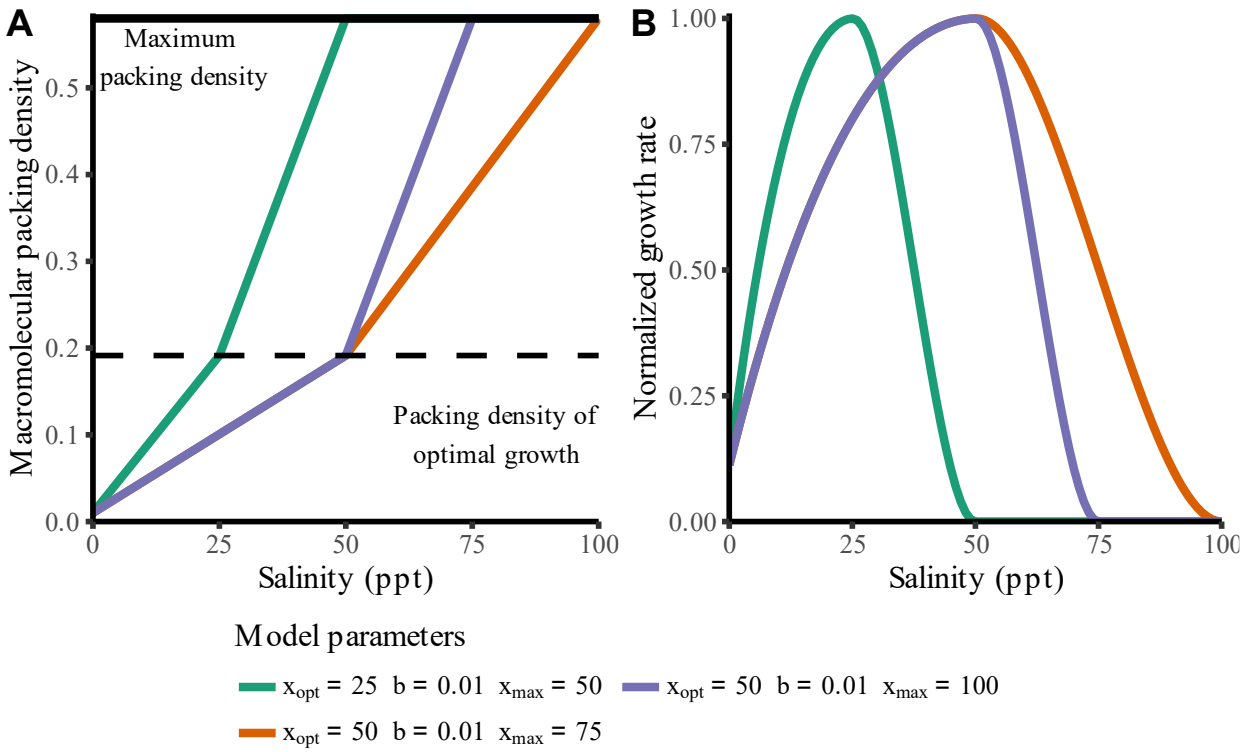

Figure 16: Impact of varying the optimal and maximal salinities and b in the Split Slope model on the packing density versus salinity relationship (A) and the normalized growth rate versus salinity relationship (B) Each colored line represents a different combination of the intercept (b) and the slopes in the packing density-salinity relationship determined by x_{opt} and x_{max} as described in the text. The resulting growth rate for each of these parameter combinations is shown in B as the relationship between the normalized growth rate and the salinity. Higher values of x_{opt} result in maximum growth rates at higher salinities, while higher values of x_{max} result in higher maximum salinities of growth.

The final model (Plateau), shown in Figure 17, adds a region of salinity over which the strain is able to maintain a constant packing density. This allows for an extension of the range at which the growth rate is near optimal, while still allowing for rapid declines in growth rate on either side of this plateau. As with the Split Slope model, this results in different functions for the packing density-salinity relationship based on the salinity. Below x_{opt} it is defined as:

$$\varphi = \frac{\varphi_{opt} - b}{x_{opt}} \times S + b$$

Along the length of the plateau (from x_{opt} to x_{opt} plus the length of the plateau) it is defined as:

$$\varphi = \varphi_{opt}$$

And above the plateau it is defined as:

$$\varphi = \frac{\varphi_c - \varphi_{opt}}{x_{max} - x_{opt} + plateau} \times S + \varphi_{opt}$$

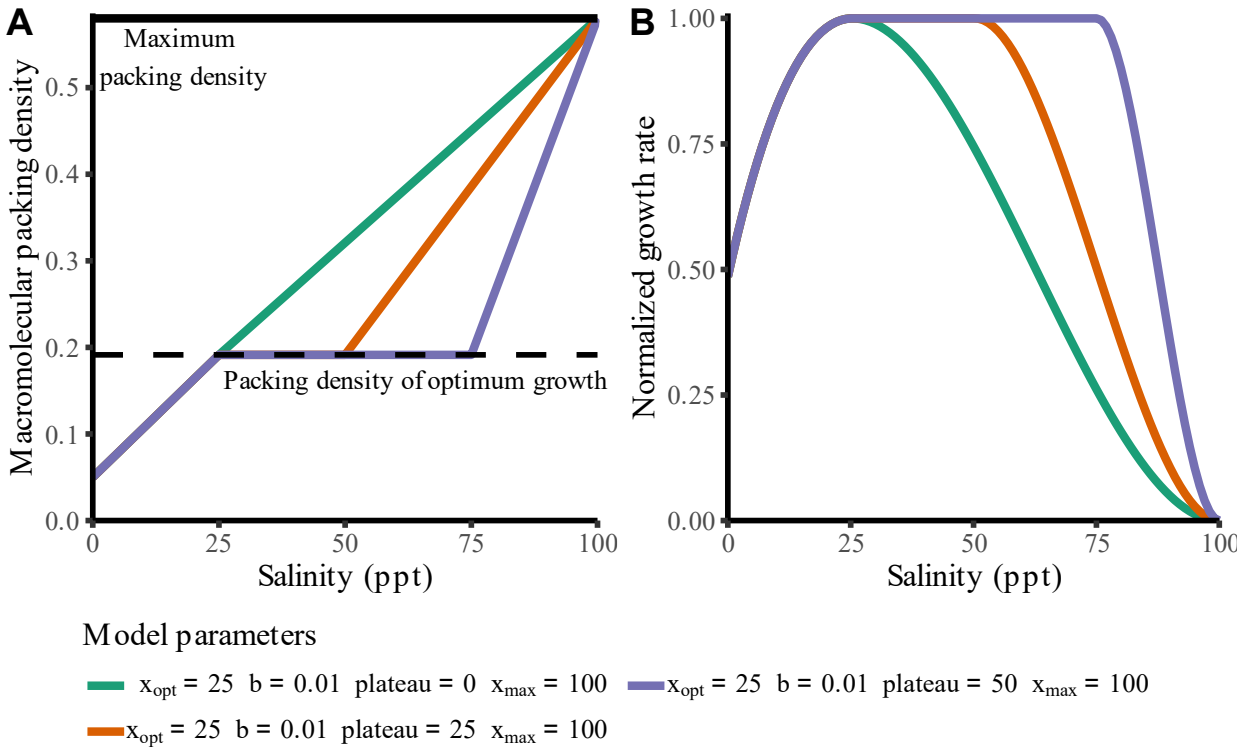

Figure 17: Impact of varying the optimal and maximal salinities, plateau length, and b in the Plateau model on the packing density versus salinity relationship (A) and the normalized growth rate versus salinity relationship (B) Each colored line represents a different combination of the intercept (b), plateau length and the slopes in the packing density-salinity relationship determined by x_{opt} and x_{max} as described in the text. The resulting growth rate for each of these parameter combinations is shown in B as the relationship between the normalized growth rate and the salinity. Increasing plateau length results in an increase of the range of salinities at which the maximum growth rate is maintained.

The y-intercept parameter, b, can be interpreted as a measure of the ability of a strain to maintain the necessary intracellular osmolarity when in environments with low osmolarities. Strains which struggle to maintain sufficient intracellular osmolarity or concentrations of specific ions needed for metabolic processes will have lower b values than those which are adapted to obtaining and maintaining intracellular ion concentrations in ion-poor environments.

The slope of the packing density-salinity relationship at any given point in time reflects how quickly the strain gains or loses its ability to osmoregulate with changes in salinity. Strains

tolerant to wider ranges of salinities will have lower slopes. In the Split Slope and Plateau models, this slope is not required to be constant over the entire range of salinities.

Model fitting results

I fit these theoretical models to the reaction norm datasets I collected from the literature to assess how well they could be used to interpret experimental data. To ensure the best use of the datasets available, each dataset was fit to any model for which the dataset had one more datapoint than free parameters (Table 4). Figures showing the predicted packing densities and growth rates relative to salinity for each dataset are shown in Appendix B.

Table 4: Number of free parameters and datasets fit for each model.

Model	**Free parameters**	**Datasets with at least n+1 datapoints**
Linear	1	93
Intercept	2	88
Split Slope	3	42
Plateau	4	25

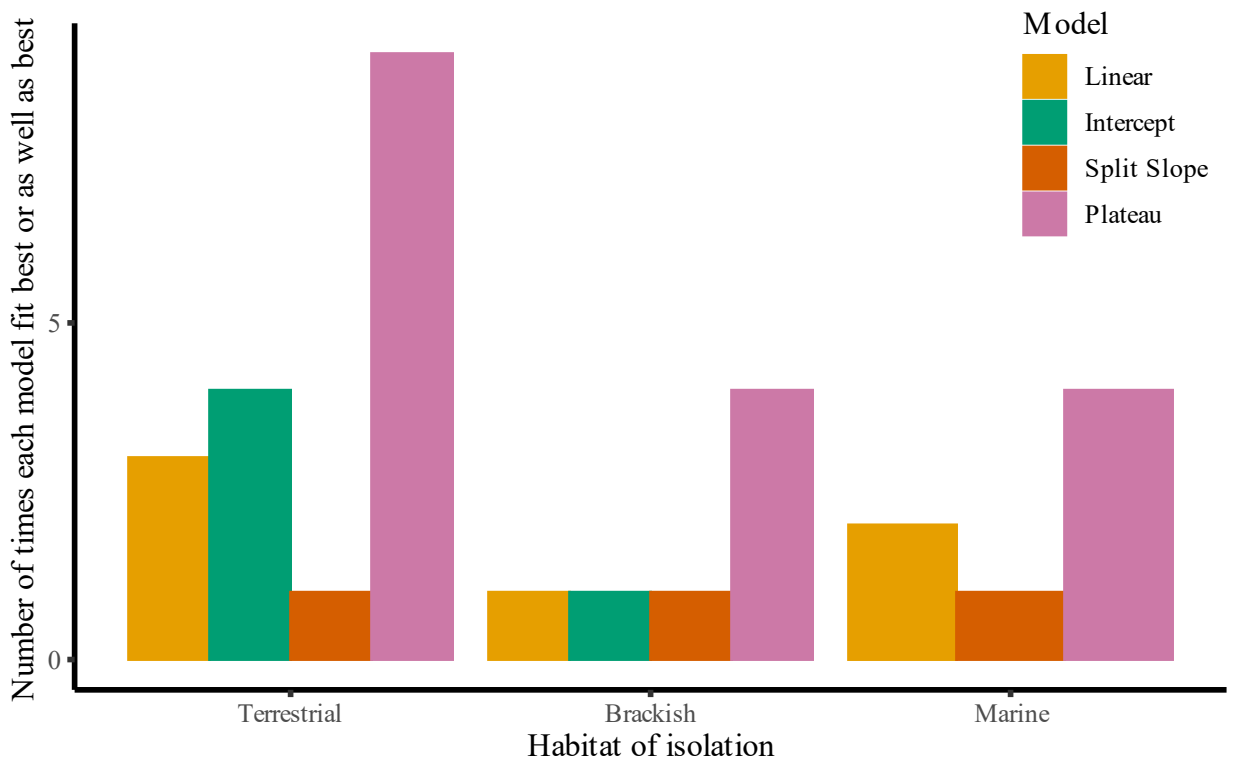

Figure 18: Distribution of best fitting or equally good fitting models by habitat of isolation. Only results for models with $n \geq 5$ are shown.

Figure 18 shows the differences in which theoretical model best fit the measured data for a strain based on its habitat of isolation. The relative fit of models was determined by the Akaike information criterion (AIC), which penalizes models with additional parameters. Despite requiring additional parameters, the Plateau model is the most commonly best fitting model for datasets from terrestrial and marine habitats of isolation.

Comparing the results of fitting both of the Linear and Intercept models, it is clear that providing b as a free parameter allows for a much wider range of slopes controlling the relationship between the salinity and the packing density (Figure 19). Given that higher values of k_1 mean steeper slopes and lower optimal salinities, the distribution of k_1 values being wider for strains isolated from terrestrial habitats makes sense.

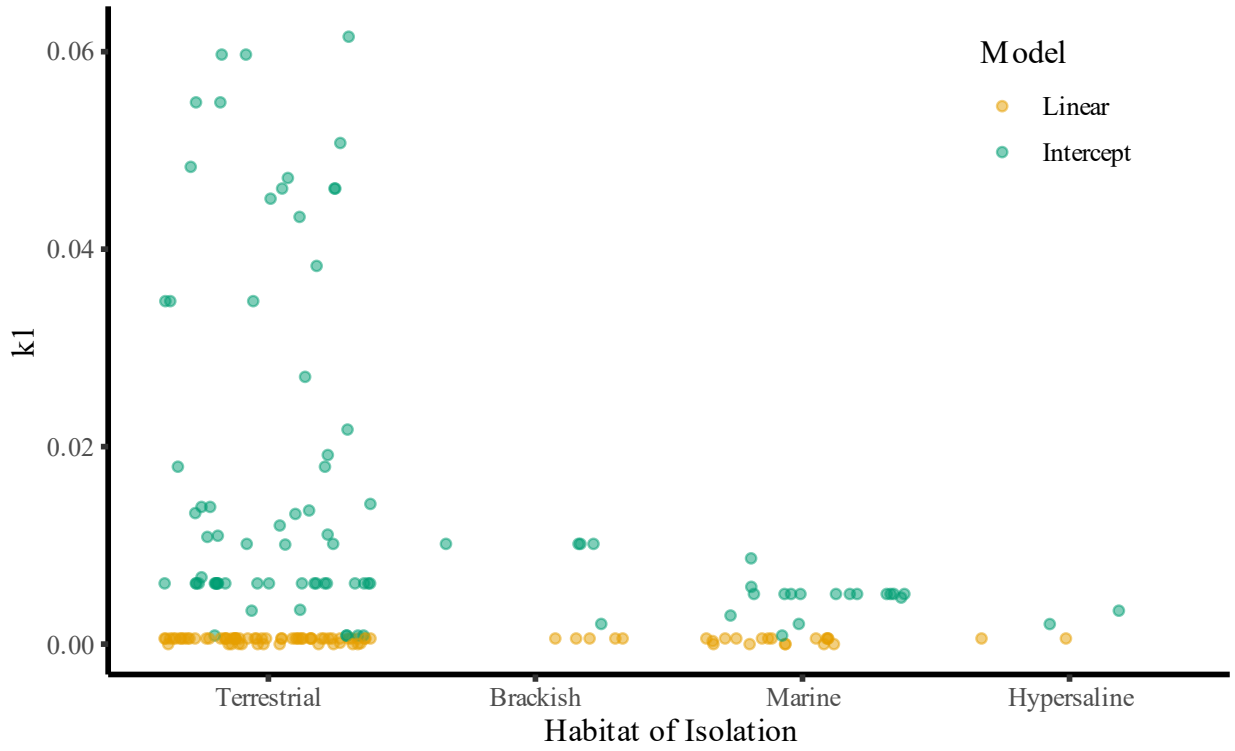

Figure 19: Values of k_1 from fitting data with the Linear and Intercept models. Only results from datasets with $n \geq 3$ are shown here.

The high frequency of low b values in strains isolated from terrestrial environments is surprising (Figure 20), but likely reflects the wide range of salinities that comprise "freshwater" environments.

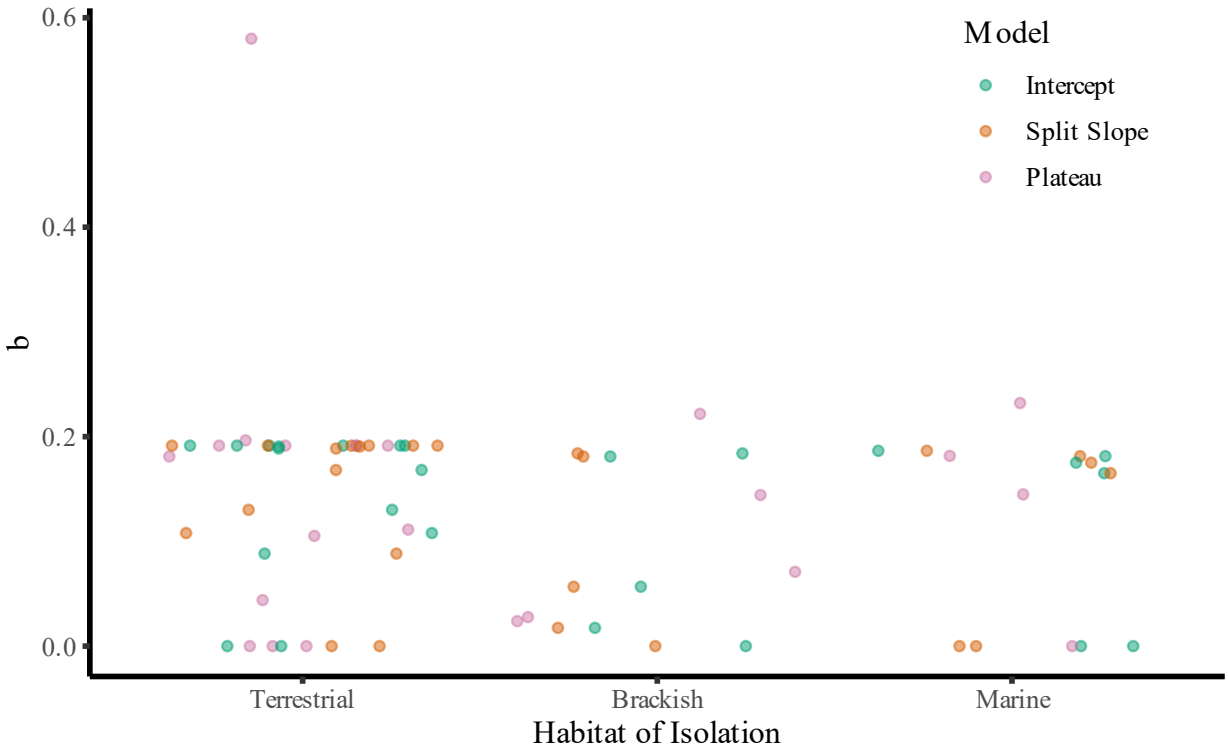

Figure 20: Values of b from fitting data with the Intercept, Split Slope and Plateau models

The Plateau model has two unique features to the parameter values it predicts relative to the Split Slope model. The Plateau model has b values higher than the optimal packing density while the Split Slope model never does (Figure 20), and the Plateau model has x_{opt} values below 0 while the Split Slope model never does (Figure 21).

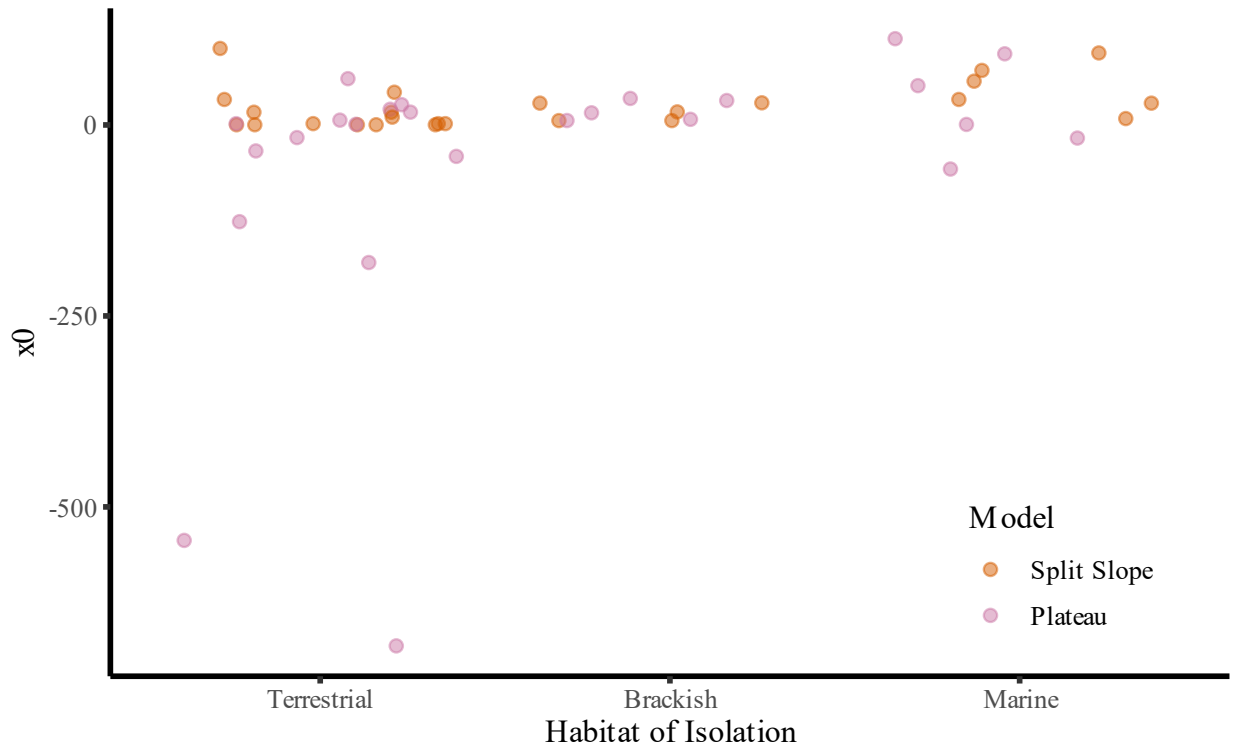

Figure 21: Values of x_0 from fitting data with the Split Slope and Plateau models

Discussion

Does habitat predict salinity tolerance?

The habitat of isolation, at least on the coarse terrestrial/brackish/marine/hypersaline scale, does not provide the ability to estimate either the optimal salinity of growth or the maximal salinity of growth. More specific information about the habitat of isolation might allow for improved ability to estimate the maximal salinity of growth, particularly if the terrestrial category is divided into aquatic and soil dwelling categories, potentially with information about the aridity of the local climate given the impact of desiccation cycles on soil salinity (Hu et al., 2012). However, the optimal salinity of growth seems to vary only slightly across all species surveyed here, falling below modern marine salinity in all but four strains (Figure 7).

This disconnect between the habitat of isolation and the salinity tolerance of a strain makes clear that they should not be considered synonymous. While salinity varies between environments, cyanobacteria do not have salinity tolerances exclusive to their current habitat, meaning that salinity is likely not the primary factor in the distribution of strains. There is considerable literature investigating the apparent lack of transitions between habitats of differing salinities (Cabello-Yeves and Rodriguez-Valera, 2019; Logares et al., 2009; Paver et al., 2018), however salinity tolerance itself may play only a minor role in this phenomenon. We need to consider the roles of competition and community ecology in investigating transitions between terrestrial and marine habitats.

In cases where the salinity tolerance of a strain is a primary focus, these data highlight the need to empirically evaluate the salinity tolerance of a strain rather than assuming it based on the habitat it was isolated from.

Is salinity tolerance a discrete trait?

I made an initial effort to test the ability to consider salinity tolerance as a discrete trait by evaluating the ability to cluster strains by their optimal and maximal salinities of growth using k-means clustering. However, this method divided the strains by their maximal salinity of growth, which still requires the establishment of boundaries for categorization.

Additionally, in evaluating the reaction norms, even strains with similar maximal salinities of growth displayed highly varied responses across the range of salinities at which they could grow. Some strains showed a clear optimal salinity of growth, with rapidly declining normalized growth rates away from this salinity; others had growth rates which were constant across salinity ranges of over 100 ppt.

Given the continuous nature of salinity tolerance, ancestral state reconstructions should be adjusted to consider salinity and salinity tolerance as a continuous trait. While in some cases this may be well served by considering the salinity of optimum growth for strains, it is also an opportunity to explore new methods in phylogenetics which consider reaction norms and function-valued traits (Goolsby, 2015; Griswold et al., 2008; Kingsolver et al., 2014; Knies et al., 2009, 2006; Stinchcombe and Kirkpatrick, 2012; The Functional Phylogenies Group, 2012; Tittes et al., 2019).

Conceptual model

The conceptual model outlined above provides a unique ability to develop an understanding of the physiological impacts of changes in environmental salinity. It is easy to use the fit of these models to predict strains with minimum NaCl concentration requirements, and what those requirements may be, based on the value of b predicted by the model fitting.

As our knowledge of the reaction norms of strains improves and can be connected to genomic data, the ability to understand the ranges over which specific compatible solutes are able to act as osmoprotectants will be helpful, both in understanding the specifics of their use, and developing the ability to predict salinity tolerances from genomes. Connecting the compatible solutes synthesized by a strain to the length or maximum value of the growth plateau will allow us to move beyond generally categorizing compatible solutes as those used in low or high salinity environments.

The results of fitting the models make it clear that while some strains of cyanobacteria have very restricted salinity ranges, and clear optimization for a specific salinity, others have extremely wide ranges. Some of these strains with very large salinity ranges still show a distinct optimal salinity of growth and show significant growth rate decreases away from this optimum,

but others are clearly able to osmoregulate to their ideal packing densities at a wide range of salinities. This is particularly interesting because it diverges significantly from thermal adaptation curves which typically show an increase to a maximum growth rate followed by a sharp decline in growth after the maximum (Izem and Kingsolver, 2005; Knies et al., 2009, 2006; Stinchcombe and Kirkpatrick, 2012). Much of the existing research on function-value trait evolution has focused on thermal adaptation curves, and the impact of the broad plateaus and slow declines in growth rate seen in the salinity reaction norms may provide insight into changes need to generalize function-value trait methods for non-thermal adaptation curves (Goolsby, 2015; Izem and Kingsolver, 2005).

A common issue I faced while working with these datasets is that not all experiments attempted to find the full range of salinities at which any given strain could grow, this means there are many datasets where the maximum salinity measured is not the maximal salinity of growth. While this can make the use of function-value trait methods more difficult (Izem and Kingsolver, 2005), my models provide the ability to extrapolate these reaction norms.

In addition to providing a new framework for understanding cyanobacterial responses to changes in salinity, this model provides predictions about subcellular physiology from a simple set of growth rate experiments. Future research into the molecular mechanisms of osmoregulation can now use this model to predict macromolecular packing density based on growth rate, and evaluate how a specific molecular mechanism impacts the reaction norm of the strain.

I am not the first to attempt to model osmoregulation in bacteria, however my model framework provides a uniquely simple method for interpreting osmoregulation. Previous models of bacterial osmoregulation have used substrate-inhibition models to predict the salinity

dependence of growth rates (Dötsch et al., 2008). These substrate-inhibition models were then used to develop a model of the synthesis and transport of compatible solutes and ions in response to changes in salinity in a continuous growth culture setup (Dötsch et al., 2008). This model is highly specific to the study organism, as it relies on specific compatible solute synthesis and transport pathways in addition to K^+ transport (Dötsch et al., 2008).

Chapter 4: Experimental evolution of salinity tolerance in a laboratory model cyanobacterium

Introduction

Experimental evolution is a useful tool for interrogating questions of evolution via an empirical framework (McDonald, 2019). As a tool, experimental evolution has answered questions about the interactions of history, chance and adaptation (Travisano et al., 1995), the evolution of multicellularity (Boyd et al., 2018; Herron et al., 2018; Ratcliff et al., 2015, 2012), the role of predation on diversification (Bohannan and Lenski, 2000; Boyd et al., 2018; Chao et al., 1977; Koskella and Brockhurst, 2014), evolutionary trade-offs (Wenger et al., 2011), genetic mechanisms of evolution (Brown et al., 1998; Dunham et al., 2002; Kroll et al., 2013; Nilsson et al., 2005; Piotrowski et al., 2012), the impact of changing environments (Baym et al., 2016; Bell, 2010; Cesar et al., 2020; Hughes et al., 2007; Kellermann et al., 2015; Ketola and Hiltunen, 2014; Kim et al., 2014; Manenti et al., 2015; Skoracka et al., 2022), evolution in communities (Chao et al., 1977; Hansen et al., 2007; Koskella and Brockhurst, 2014), and evolution of symbioses ranging from mutualisms to endosymbiosis (Hillesland and Stahl, 2010; Hosoda et al., 2014; Marchetti et al., 2017, 2014, 2010; Nilsson et al., 2005).

Salinity tolerance has been a target of selection experiments across organisms in all three domains of life (Table 5) (Beer et al., 2014; Bell and Gonzalez, 2009; Cesar et al., 2020; Delpech, 2009; Dhar et al., 2011; Gonzalez and Bell, 2013; Gostinčar et al., 2021; He et al., 2010; Ketola and Hiltunen, 2014; Lachapelle et al., 2017, 2015; Lachapelle and Bell, 2012; Samani and Bell, 2010; Zhou et al., 2017, 2015, 2013). But there have been relatively few salinity selection experiments in Cyanobacteria, and these have primarily focused on relatively short-term (<100 generations) adaptation (Georges des Aulnois et al., 2019; Lu and Vonshak,

1999; Melero-Jiménez et al., 2022, 2020; Melero-Jiménez et al., 2019). We lack empirical examination of the rates of gain and loss of salinity tolerance, and thus rely on observational patterns of species distributions and diversity to estimate its conservation (Cabello-Yeves and Rodriguez-Valera, 2019; Dittami et al., 2017; Logares et al., 2009; Paver et al., 2018).

Table 5: Summary of salinity selection experiments from the literature. Bolded species are in the cyanobacterial phylum.

Domain	Species	Generations	Type of stress	Results	Source
Bacteria	*Escherichia coli*	250	Proline, sorbitol, sucrose, glycine betaine, NaCl	Adaptations can be broadly applicable to different osmolytes or specific to the osmolyte, observed some trade-offs, different sets of mutations in populations adapted in different osmolytes	(Cesar et al., 2020)
	Desulfovibrio vulgaris Hildenborough	<20 generations	NaCl	Transcriptional changes and accumulation of glutamate and alanine	(He et al., 2010)
		1200	NaCl	Increased organic solutes, decreased cell motility, PFLA saturation changes	(Zhou et al., 2017, 2015, 2013)
		5000	NaCl	Increased organic solutes, increased cell motility, PFLA saturation changes	(Zhou et al., 2017)

	Serratia marcescens	300	NaCl	observed biggest changes in salt tolerance in highest constant stress levels	(Ketola and Hiltunen, 2014)
	Spirulina platensis	<100	NaCl	PSII changes	(Lu and Vonshak, 1999)
	***Microcystis aeruginosa* MaAVc**	<100	NaCl	Higher initial stress led to higher final tolerance	(Melero-Jiménez et al., 2019)
	***Microcystis aeruginosa* Ma1Vc, Ma5Vc, and MaAVc**	~25	NaCl	More populations reached lethal levels when change was slow, strains responded differently	(Melero-Jiménez et al., 2020)
	***Microcystis aeruginosa* Ma5Vc**	<100	NaCl	Increased dispersal and prior stress exposure increased ability to survive exposure to lethal stress	(Melero-Jiménez et al., 2022)

	***Microcystis aeruginosa* PCC 7820 and PCC 7806**	~50	Artificial seawater	Acclimation increases salt tolerance, differences in compatible solutes accumulated between strains	(Georges des Aulnois et al., 2019)
Archaea	*Halobacterium salinarum* NRC-1	~50 years lab culturing	Total salinity, Na:K, MgSO4	retention of peaks in complex fitness landscape after growth in constant environment as lab model strain, best growth across a range of salinity variables matched with conditions found in ancestral environment not lab environment	(Beer et al., 2014)
Eukaryotes	*Chlamydomonas reinhardtii*	300	NaCl	Differences caused by population size and sexual/asexual reproduction in adaptation to increasing salt, bigger population and sexual reproduction led to faster adaptation/better evolutionary rescue	(Lachapelle and Bell, 2012)

		<500	NaCl	Exposure to increasing salt concentrations showed both an acclimation response and an adaptation response	(Lachapelle et al., 2015)
		500	NaCl	Impact of history of selection on extinction risk, more stressful history increased extinction risk	(Lachapelle et al., 2017)
	Saccharomyces cerevisiae	25	NaCl	evolutionary rescue in yeast is possible and occurs quickly, but requires a large enough initial population size	(Bell and Gonzalez, 2009)
	Saccharomyces paradoxus	~50	NaCl	Yeast exposure to increasing salt concentrations, stress can't increase too much, and population size has to be big enough	(Samani and Bell, 2010)
	Saccharomyces cerevisiae and	100	NaCl	yeast exposed to sublethal stress before exposure to lethal stress, success in lethal stress found in either large populations that	(Gonzalez and Bell, 2013)

	Saccharomyces paradoxus			had experience minimal stress or highly stressed small populations, but significant differences seen in the two species of yeast used.	
	Saccharomyces cerevisiae	300	NaCl	saw increased genome size and expression changes, only one SNP that conferred increased tolerance	(Dhar et al., 2011)
	Hortaea werneckii	800	NaCl	evolution in stressful but not lethal levels of salt, saw phenotypic changes but not with regards to salt tolerance or growth rate	(Gostinčar et al., 2021)

Given the spectrum of reaction norms observed in Chapter 3, a particular question of interest for this chapter is: How do reaction norms change during evolution? Reaction norms are defined as the function describing the phenotypes expressed by a given genotype over different environmental parameters (Kirkpatrick and Heckman, 1989). There is existing literature on the evolution of thermal response curves that use template modes of variation to quantifiably identify different types of evolution (Izem and Kingsolver, 2005). Template mode of variation is a method in which variation in a response curve can be quantifiably separated into predetermined modes of variation. Typically, these modes are vertical shift, horizontal shift, and generalist-specialist shift (Izem and Kingsolver, 2005; Kingsolver et al., 2014; Knies et al., 2009, 2006). Vertical shifts indicate an increase in the average fitness observed (parameterized as h). Horizontal shifts indicate a change in the location of the maximum fitness along the environmental variable (parameterized as w). And finally, generalist-specialist shifts indicate changes in the range of conditions tolerated. For a shift towards generalist, even if the average fitness (h) and location (m) of the optimum condition are constant, the area under the response curve is larger, and vice versa for specialist shifts. Using these three modes of evolution, thermal adaptation could decomposed and more directly assessed (Izem and Kingsolver, 2005; Latimer et al., 2011). One aim of this experiment was to begin to evaluate if similar modes of evolution could be applied to the evolution of salinity tolerance reaction norms.

The experiment described here acts to provide a framework for further evaluation of the evolution of cyanobacterial salinity tolerance. This experiment was conducted on the laboratory model cyanobacterial strain *Synechococcus* sp. PCC 7002, which is generally considered to be a euryhaline strain (Batterton and Van Baalen, 1971; Ludwig and Bryant, 2012).

Methods

General culturing conditions

Cultures were maintained and assayed in 20mL borosilicate glass tubes with plain ends and polypropylene caps. They were grown at 30°C under continuous LED 5300K white light illumination with constant shaking and exposure to atmospheric gas concentrations.

Salinity gradients, for both reaction norms and selection conditions, were produced by mixing a freshwater medium (BG-11) with a saltwater medium (AASW). Recipes for each individual medium can be found in Appendix C. While BG-11 is a standard freshwater growth medium for cyanobacteria, AASW is an amendment of the standard ASW medium for marine cyanobacteria with additional salts to increase the salinity from ~18 ppt (ASW) to ~35 ppt (AASW).

Establishing isogenic founder population

The initial inoculation for the selection experiment came from a dilution series to produce an isogenic founder population. This population was maintained in a 50:50 mix of the two media for 3 transfers before the individual lineages were established.

Serial transfer parameters

Four lineages were maintained in each of four treatment conditions: 100% AASW, the medium in which the ancestor had been cultured in our laboratory, 90% AASW, 50% AASW and 10% AASW (Table 6). 10% AASW was the freshest treatment condition because it was the lowest percentage of AASW that had consistent growth. 90% AASW was included as a mirror to the 10% AASW mix, a mostly marine condition with a mixture of the two media types. This was included so that differences due to minor components (e.g., iron provided by chelated iron versus

ferric ammonium citrate) of each of the media could be accounted for even in a highly saline condition.

Table 6: Treatment conditions for each lineage in the selection experiment.

Treatment condition	Lineages
10% AASW	A, B, C, D
50% AASW	E, F, G, H
90% AASW	I, J, K, L
100% AASW	M, N, O, P

Transfers were conducted twice a week, with slightly unequal gaps in the duration of growth of 3 and 4 days. As with transfers for assays, cultures were inoculated with 100µL of the previous culture into 10mL of the fresh medium. After being used as inoculants, the previous transfer was maintained until the next transfer timepoint for further growth characterization and to maintain a viable stock of each lineage in case of any issues with growth.

Freezing protocols

After ~50, 100, 200, 400, 600, 775 generations, freezer stocks of the lineages experiment were grown in 50 or 100mL batches, centrifuged and preserved with 4% DMSO for storage in an ULT freezer set at -70°C.

Resurrection protocols

Frozen stocks were resurrected from the freezer by thawing at room temperature. After thawing, samples were microcentrifuged at 3000rpm for 5 minutes to pellet the cells. The supernatant was then discarded, and the cells resuspended in 2mL of the standard growth medium for the strain (100% AASW for the ancestor and the treatment medium for the evolved

lineages). The resuspended cells were then centrifuged again, and the supernatant discarded. The rinsed cell pellet was then resuspended in 1mL of the standard growth medium for the strain and transferred into a culture tube containing 10mL of growth medium.

Growth characterization

Growth of each culture was measured via optical density at 730nm using a ThermoScientific Genesys 30 visible spectrophotometer. These measurements were then converted to cells per mL using a calibration curve of optical densities against cell concentrations measured on a Beckman Coulter Multisizer 4e.

Due to cell shading, phototrophic cultures experience a short period of exponential growth followed by a linear growth period (Sinetova et al., 2012; Zavřel et al., 2021). Given this linear growth rate for most of the growth of the cultures, growth rates were calculated as realized growth rates, which is the change in cell concentration over the period of growth. Growth rates measured during the serial transfer experiment were based on the growth until the culture was used to inoculate the next culture, rather than the final measurement taken.

Salinity tolerance assays

Measurements of the change in growth rate in different salinity conditions (salinity reaction norm) of the ancestor and evolved lineages were conducted in the same light, temperature and atmospheric conditions as the serial transfers. Each test condition was inoculated in triplicate. During the serial transfer experiment coarse-grained reaction norms were measured at only the treatment condition salinities (10% AASW, 50% AASW, 90% AASW, 100% AASW) as well as 0% AASW. After the serial transfer experiment, the salinity response curves of the ancestor and the lineages evolved in 10% AASW were tested at higher resolution after resurrection from the freezer and three passages in their standard growth medium (100%

AASW for the ancestor, 10% AASW for the evolved lineages). These lineages were selected as they experienced the strongest selective pressure. The high-resolution reaction norms were conducted at 11 different salinity levels, increasing from 0 to 100% AASW with 10% step sizes.

During salinity assays, lack of growth was determined after there was no change in absorbance was detected for two weeks.

Results

Growth rate changes

As shown in Figure 22 and Table 7, there was an increase in the realized growth at the time of transfer across the lineages grown in their respective selection conditions. ANOVA comparisons of the measured growth rates in the first 50 generations (0 – 50 generations) with the measured growth rates in the last 50 generations (677 – 727 generations) showed that the growth rate in the last 50 generations was significantly higher in all but one lineage (lineage L, Table 7).

Table 7: Realized growth at transfer point for the first and last 50 generations by lineage. p values from ANOVA (not always assuming equal variance) test

Lineage	μ_{init} ($\Delta OD/\Delta t$)	μ_{final} ($\Delta OD/\Delta t$)	p
A	$3.77 \pm 0.63 * 10^{-3}$	$4.45 \pm 0.41 * 10^{-3}$	**0.0317**
B	$3.45 \pm 0.68 * 10^{-3}$	$5.85 \pm 2.47 * 10^{-3}$	**0.0290**
C	$3.12 \pm 0.85 * 10^{-3}$	$5.51 \pm 1.57 * 10^{-3}$	**0.0041**
D	$3.41 \pm 0.70 * 10^{-3}$	$4.95 \pm 0.47 * 10^{-3}$	**0.0004**
E	$3.52 \pm 0.45 * 10^{-3}$	$5.87 \pm 1.80 * 10^{-3}$	**0.0064**
F	$3.68 \pm 0.46 * 10^{-3}$	$5.49 \pm 0.65 * 10^{-3}$	$\mathbf{5.85 * 10^{-5}}$
G	$3.45 \pm 0.47 * 10^{-3}$	$5.54 \pm 0.25 * 10^{-3}$	$\mathbf{2.25 * 10^{-7}}$
H	$3.72 \pm 0.48 * 10^{-3}$	$5.18 \pm 0.29 * 10^{-3}$	$\mathbf{4.47 * 10^{-5}}$
I	$3.63 \pm 0.73 * 10^{-3}$	$5.51 \pm 1.43 * 10^{-3}$	**0.0092**
J	$3.42 \pm 0.40 * 10^{-3}$	$5.46 \pm 0.21 * 10^{-3}$	$\mathbf{2.19 * 10^{-7}}$
K	$4.09 \pm 0.51 * 10^{-3}$	$5.85 \pm 1.11 * 10^{-3}$	**0.0025**
L	$4.24 \pm 1.50 * 10^{-3}$	$5.12 \pm 0.72 * 10^{-3}$	0.2178
M	$3.84 \pm 0.65 * 10^{-3}$	$6.24 \pm 0.88 * 10^{-3}$	$\mathbf{8.61 * 10^{-5}}$
N	$3.44 \pm 0.41 * 10^{-3}$	$5.30 \pm 0.50 * 10^{-3}$	$\mathbf{5.86 * 10^{-6}}$
O	$3.36 \pm 0.34 * 10^{-3}$	$5.72 \pm 0.42 * 10^{-3}$	$\mathbf{7.52 * 10^{-8}}$
P	$2.87 \pm 0.44 * 10^{-3}$	$7.42 \pm 1.74 * 10^{-3}$	$\mathbf{2.17 * 10^{-5}}$

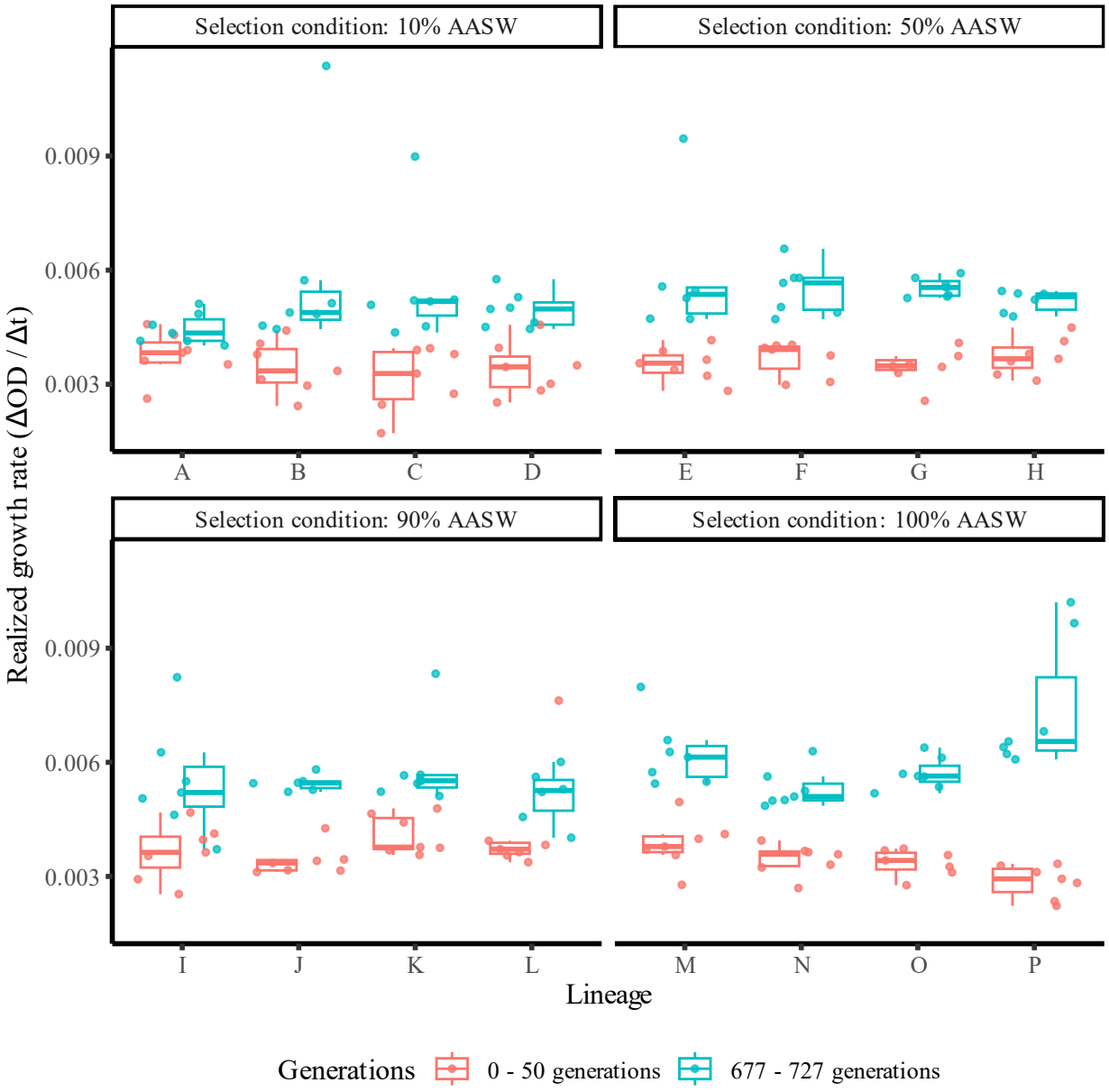

Figure 22: Realized growth rate at transfer time point for each lineage in the first (pink) and last (blue) 50 generations.

To compare the adaptation observed to other microbial evolution experiments, particularly the Long Term Evolution Experiment conducted for more than 50,000 generations in *Escherichia coli* (LTEE) (Lenski, 2017; Lenski et al., 2015; Lenski and Travisano, 1994; Wiser et al., 2013), I used relative growth rate as a proxy for fitness. I fit the fitness versus generations relationship with both hyperbolic and power law models as used to interpret fitness gains in other

evolution experiments (Lenski and Travisano, 1994; Wiser et al., 2013). Using the fitness (w) and number of generations (t), the hyperbolic model is defined as: $w = 1 + \frac{a \times t}{t+b}$. The power law model is defined as: $w = (bt + 1)^a$. The offsets of +1 constrain the ancestral fitness to be 1. While both models have decelerating trajectories, the hyperbolic model approaches an asymptote, but the power law model has no upper limit, allowing for continuously increasing fitness. The difference between the hyperbolic and power law models was only observable in the LTEE after approximately 20,000 generations, significantly longer than the duration of this experiment. The model fits are shown with the relative growth rates in Figure 23. The model fits were assessed using Akaike information criterion (AIC) which has a lower value for a better fitting model but penalizes models which overfit the data with too many parameters. No lineage had a difference in AIC between the models of more than 6, the difference threshold which indicates statistically significant differences in the model fits.

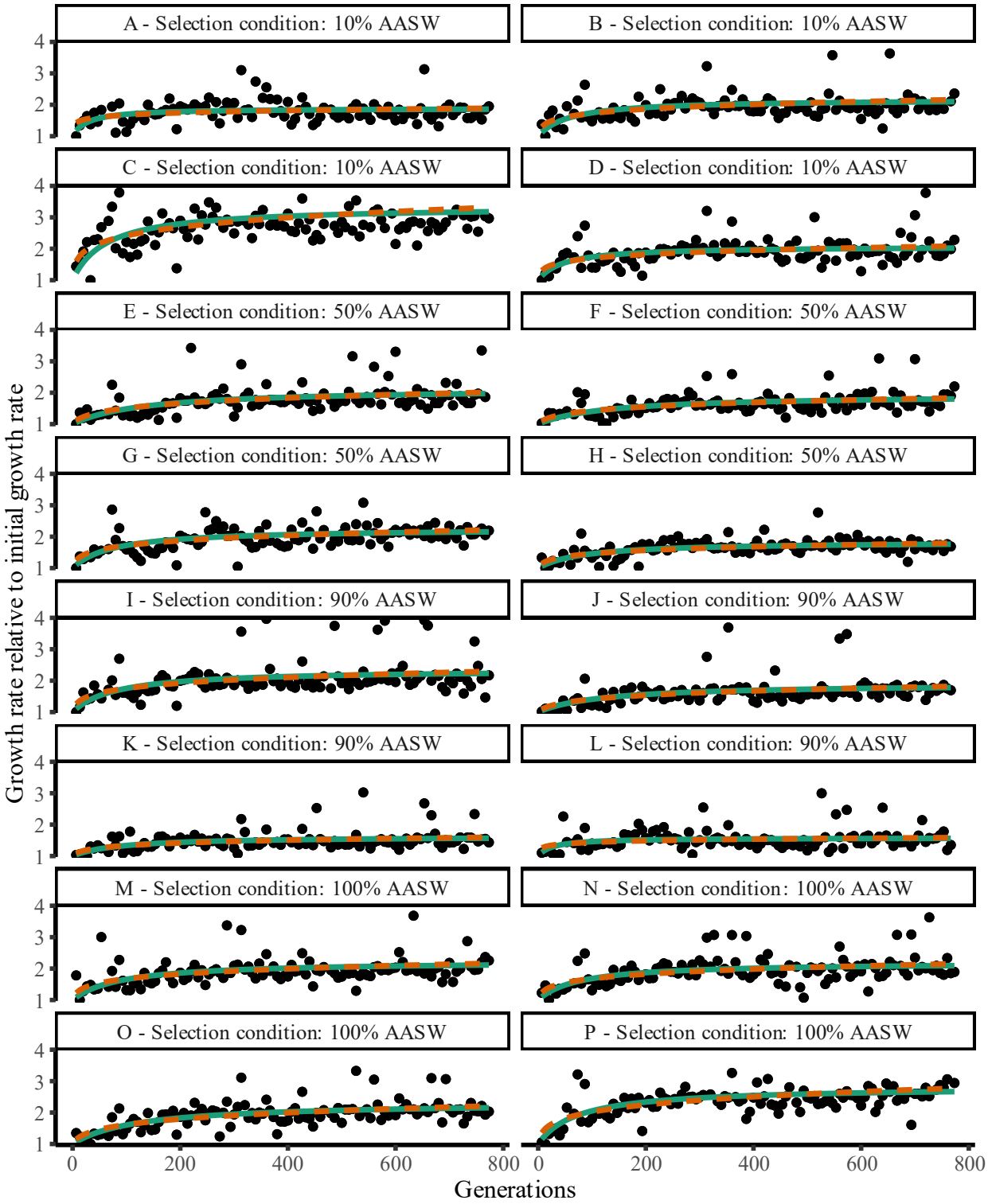

Figure 23: Hyperbolic and power law model fits to the realized growth rate versus generations relationship for each evolved lineage. Measured data points are shown in solid black while the growth rates predicted by the hyperbolic and power law models are shown in the solid and dashed lines respectively.

In order to increase the statistical power of these analyses, I pooled the growth rates within each treatment condition and calculated the fitness for each treatment condition. Upon refitting the hyperbolic and power law models I found that the treatment fitness improvement still could not distinguish between the models (Figure 24).

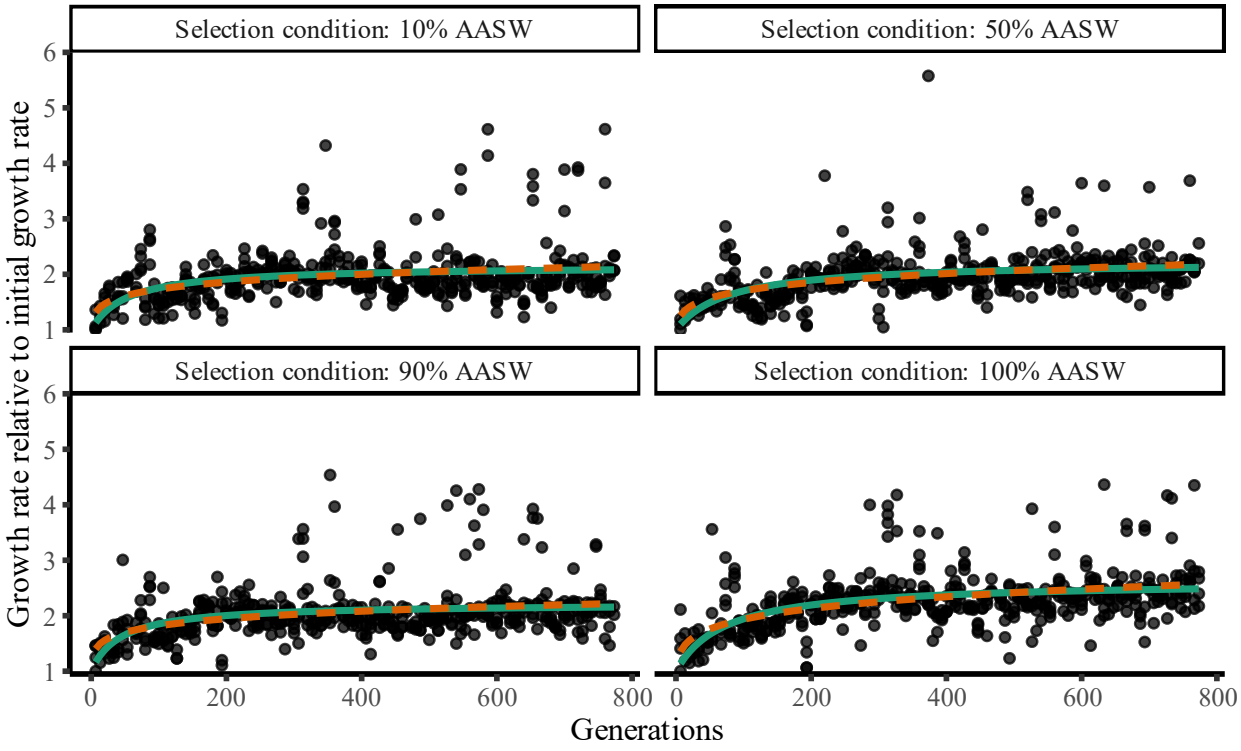

Figure 24: Hyperbolic and power law model fits to the relative growth rate versus generations relationship pooled by selection condition. Measured data points are shown in solid black while the growth rates predicted by the hyperbolic and power law models are shown in the solid and dashed lines respectively.

Finally, I fit the models to the pooled data for the entire experiment. While treatment differences were ignored for this analysis, it allowed further interrogation of the potential for continued long term improvements in fitness. For the experiment-wide fitness, the hyperbolic model was a significantly better fit than the power law model (AIC_{hyper} - AIC_{power} = -8.86, Figure 25). Over the course of my selection experiment, I was not able to observe the improved fitting of the power law model in long term evolution experiments.

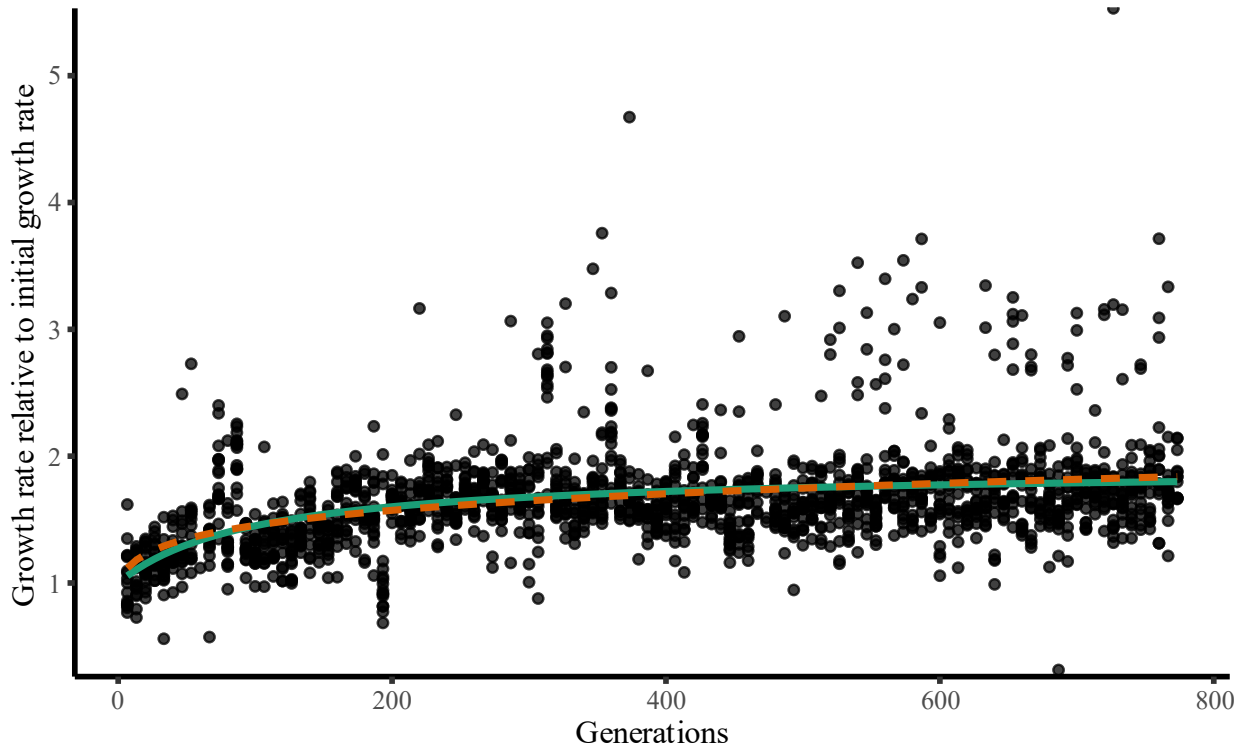

Figure 25: Hyperbolic and power law model fits to the relative growth rate versus generations relationship on the pooled evolved lineages. Measured data points are shown in solid black while the growth rates predicted by the hyperbolic and power law models are shown in the solid and dashed lines respectively.

Coarse-grained salinity response curves

I conducted coarse-grained salinity tolerance responses during the serial transfer experiment after approximately 600 generations (Figure 26). The primary feature seen in all the salinity responses is poor, but variable, growth in the 0% AASW condition, and a significant improvement in growth at 10% AASW. Every condition but the 0% AASW has relatively similar growth rates. However, many of the lineages have variable growth in 0% AASW, with some replicates failing to grow and others growing near the growth rates of the rest of the salinities tested. Two lineages (J and N) had growth in all replicates at 0% AASW, and the growth rates observed were only slightly lower than those at the higher salinities.

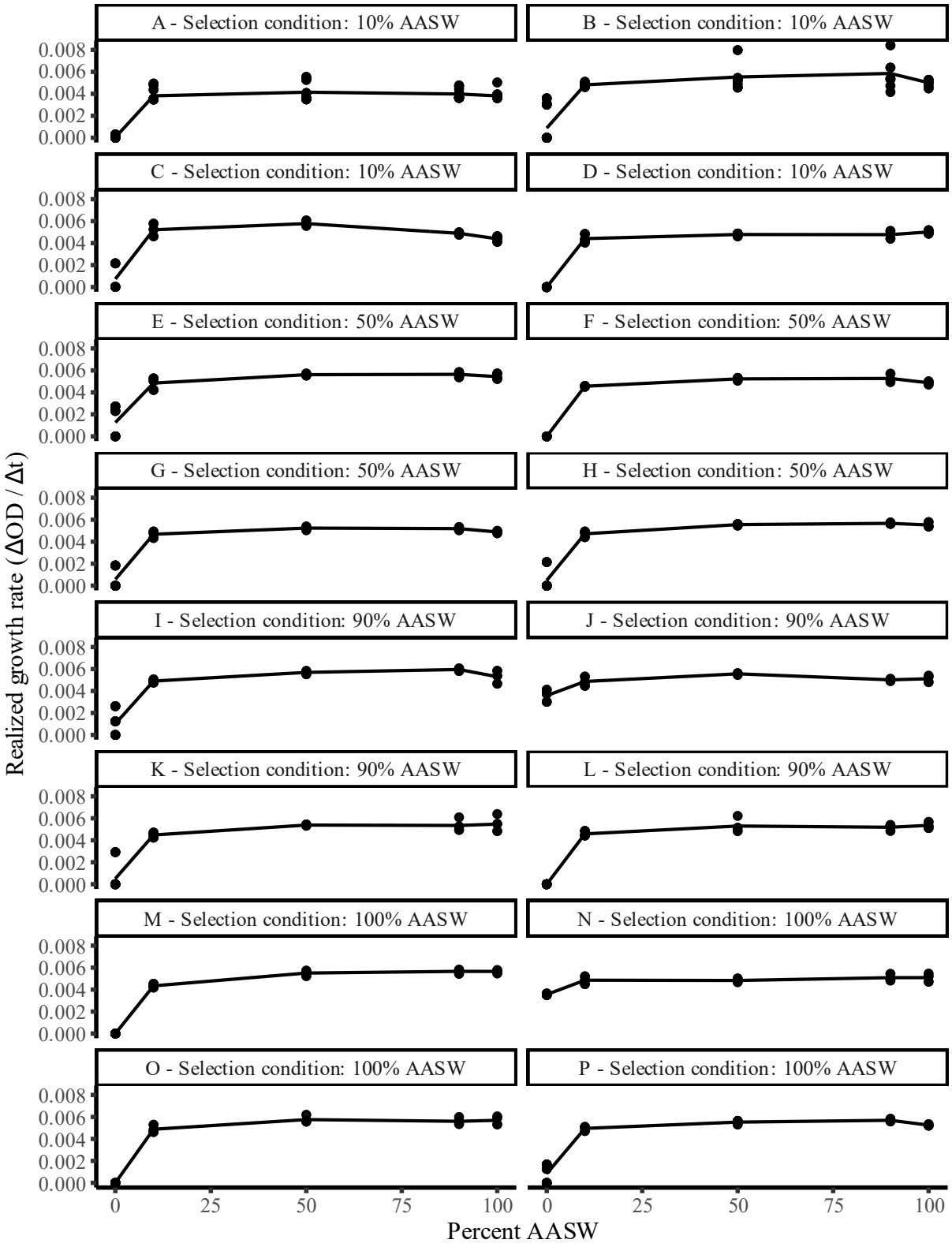

Figure 26: Realized growth rate at 0% AASW as well as the treatment conditions for the evolved lineages after > 600 generations. The line in each subplot represents the mean growth rate for that lineage at that salinity.

Fine-grained salinity response curves

After the serial transfer experiment, I resurrected frozen stocks of the ancestor as well as stocks from the final timepoint for the lineages selected in 10% AASW. I conducted fine-grained salinity response curves on these samples, with salinity increases of 10% across the range of 0 to 100% AASW (Figure 27). These lineages were selected for more detailed analysis because they experienced selection in the condition most different from the ancestral condition.

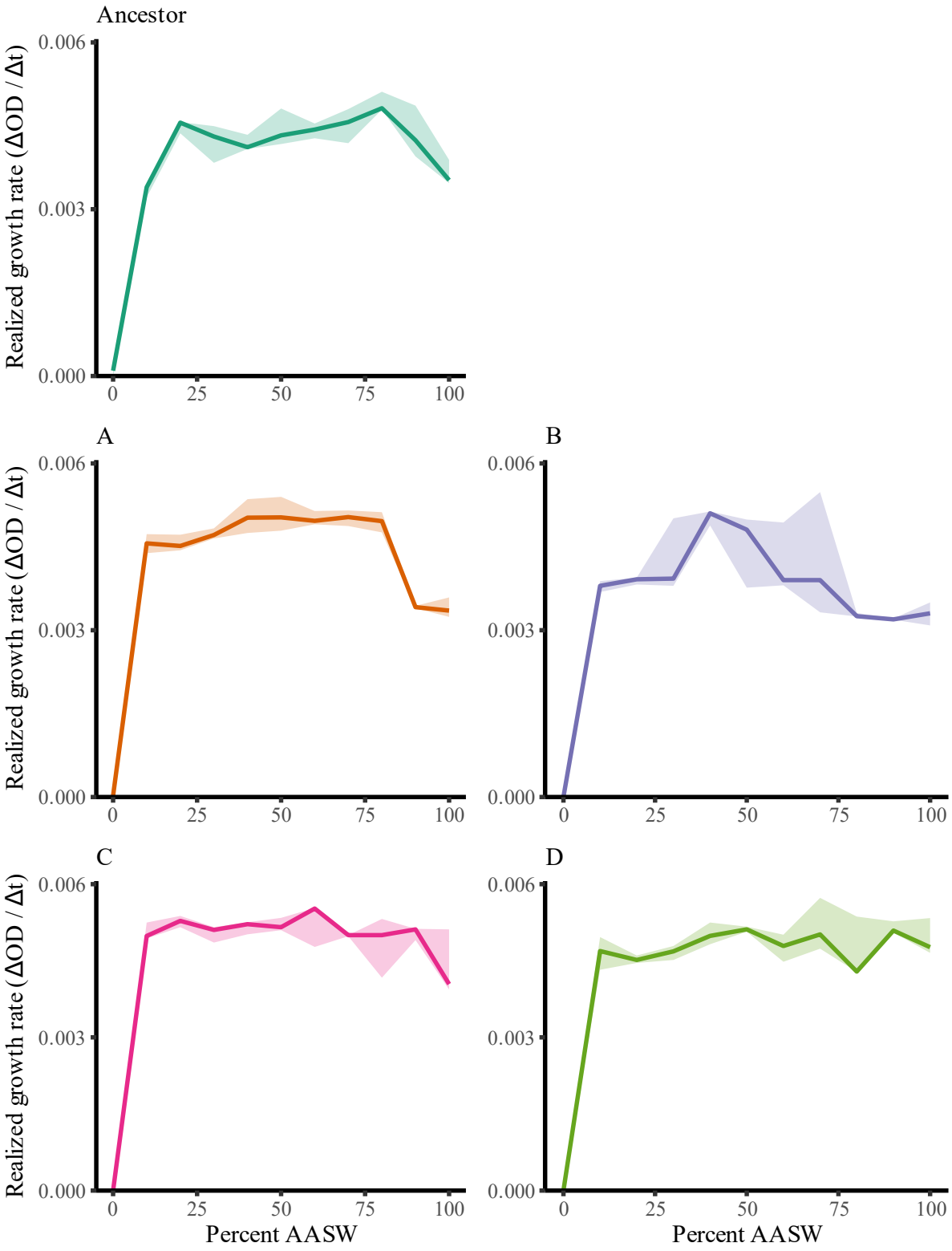

Figure 27: Fine-grained salinity response curves for the ancestor and lineages evolved in 10% AASW. Solid lines indicate the median growth rate for each condition while the shading indicates the full range of growth rates observed for each condition.

An analysis of variance (ANOVA) in the growth rates at different salinities within each lineage showed that all had significant variation in growth rate with salinity (Ancestor: $p = 5.38e^{-15}$, A: $p = 1.49e^{-19}$, B: $p = 2.74e^{-9}$, C: $p = 1.71e^{-14}$, D: $p = 3.00e^{-14}$). I performed post-hoc Tukey tests to identify where the variation occurred in the response of each lineage. The ancestor grew uniformly across the salinity conditions from 20 – 100% AASW. There were statistical improvements in growth from the 0% to 10% AASW conditions ($p = 5.7e^{-14}$) and 10% to 20% AASW conditions ($p = 0.0027$). Lineage A showed a slight, but significant, decrease in growth in the 90 and 100% AASW conditions relative to growth in the 10 – 80% AASW range ($p <= 0.031$). Lineage B showed a more complex salinity tolerance response. Growth at 40% AASW was significantly higher than growth in 10 – 20% AASW or 80 – 100% AASW ($p <= 0.029$) and growth at 50% AASW was significantly higher than growth in 80 – 100% AASW ($p <=0.010$). Lineages C and D both had uniform growth rates from 10% AASW to 100% AASW, showing only a minor improvement in the relative growth rates at 10% AASW relative to the higher salinities than the ancestral salinity tolerance response. Neither lineage C nor D lost salinity tolerance in the range tested.

The salinity tolerance response of the ancestor was compared with that of the lineages evolved in 10% AASW (A, B, C, D). ANOVA tests of the variance in growth rate at each salinity tested by lineage showed that there were significant differences in growth at 10, 20, 40, 60, 80, 90, and 100% AASW caused by the lineage (Table 8). At 0% AASW, both the ancestor and all the evolved lineages failed to grow (Figure 27). In 10% AASW, the condition that the evolved lineages were grown in for the entire experiment, lineages A, C, and D were all grew statistically faster than the ancestor ($p < 0.05$). The growth of lineage B in 10% AASW was statistically slower than lineage C ($p = 0.0057$), but not statistically different than the ancestor or

lineages A and D ($p > 0.05$). In AASW, the growth of the ancestor and lineages A, B and C could not be distinguished ($p > 0.05$), but lineage D grew significantly faster than the ancestor ($p = 0.004$).

When the salinity response curves of the ancestor and lineages evolved in 10% AASW were fit with the models outlined in Chapter 3, all were best fit by the Plateau model (Figure 28). Comparisons of the Plateau model fits for the ancestor and 10% AASW evolved lineages are shown in Figure 29. For the Plateau model, lineage B had a predicted plateau length of 0, but a lower salinity of optimum growth predicted by the Plateau model than the Split Slope model. Lineages C and D had lower predicted salinities of optimum growth and larger plateau lengths than either the ancestor or lineage A.

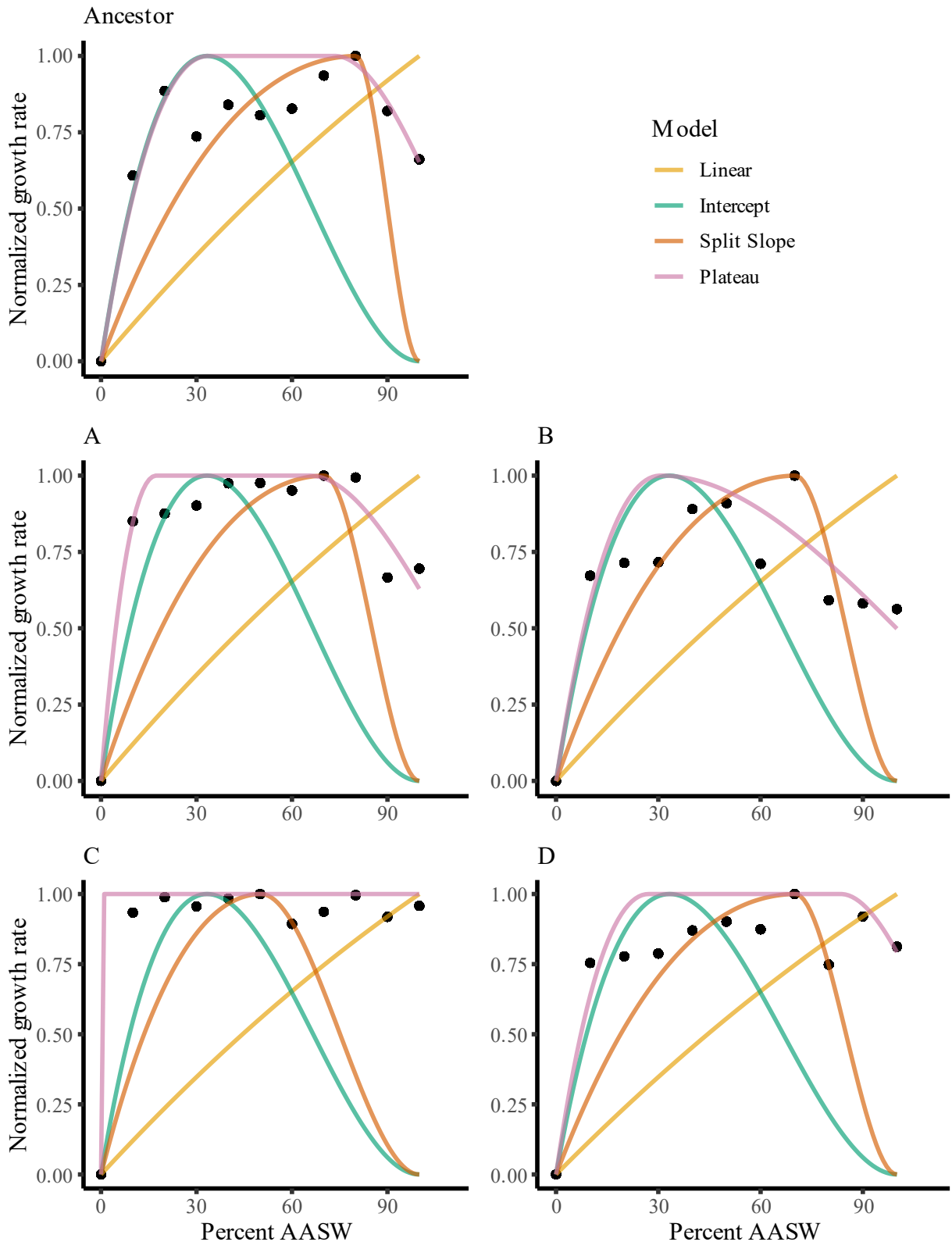

Figure 28: Salinity tolerance model fits to the response curves of the ancestor and lineages evolved in 10% AASW.

I used the fits of the Plateau model to evaluate the changes in the salinity response curves seen in the evolved lineages (Figure 29). The Plateau model highlights the improvement in growth of the evolved lineages in their treatment condition (10% AASW). Additionally, the differences in how the response of the different lineages are clear, with lineages C and D having the best growth across the entire range of salinities, and lineage B having decreasing growth rates with increasing salinities. The plateau length increased for lineages A, C and D relative to the ancestor, while the plateau length for lineage B went to 0. The beginning of the plateau also decreased for all the evolved lineages relative to the ancestor.

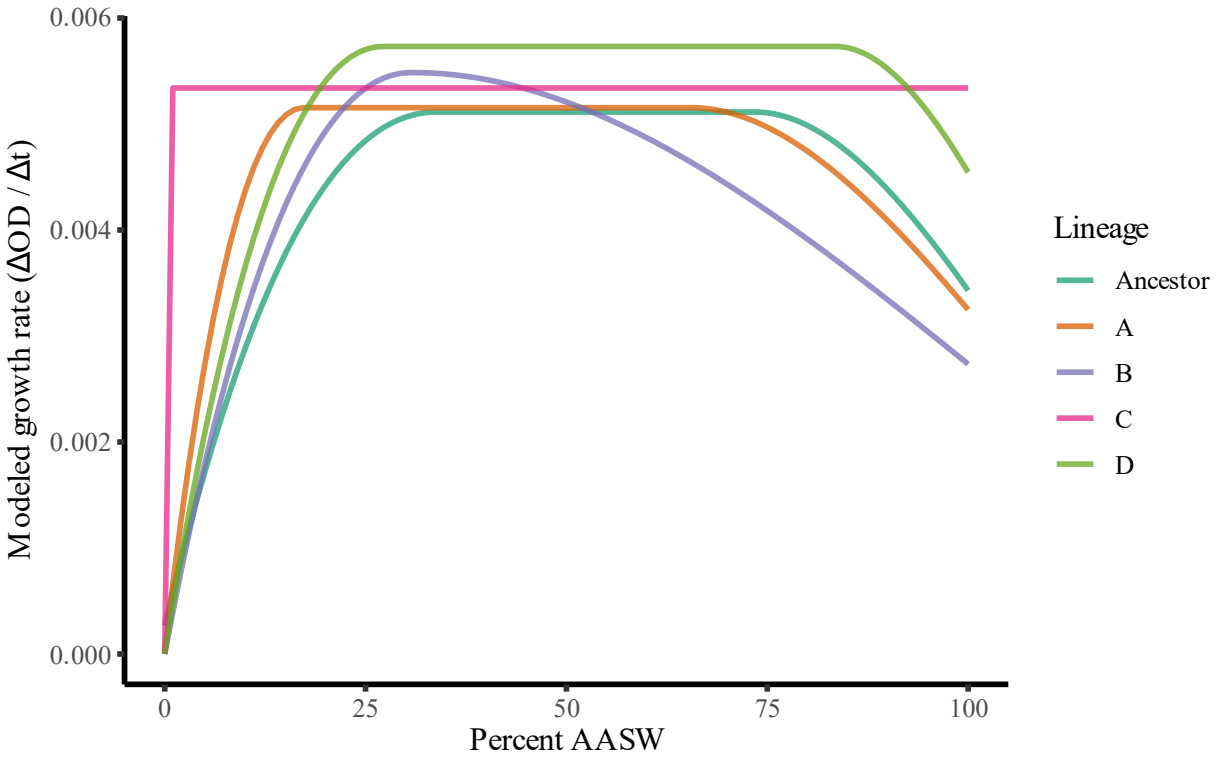

Figure 29: Comparison of the predicted growth rates from the Plateau model fits for each lineage.

Discussion

Potential for long-term fitness improvements

Previous evolution experiments have shown that fitness improvements lack an upper bound. The LTEE showed that over more than 20,000 generations, *Escherichia coli* fitness was better fit by a power law model than a hyperbolic model, implying that there was no upper limit to the fitness improvements (Wiser et al., 2013). Based on the hyperbolic model fit for the entire pooled dataset, the evolved strains had essentially reached their maximum fitness levels (~1.9) by 800 generations, with approximately 10% further improvement possible. In the absence of competition, the experimental evolved lineages maximized their fitness in the different salinity conditions, highlighting the speed of microbial evolution and how rapidly the physiology of a microbe reflects its environment.

Evolution of salinity responses

When the salinity tolerance response of the lineages evolved in the lowest salinity treatment (10% AASW, A – D) was assessed, there was improvement seen in the ability of the evolved lineages to grown in 10% AASW relative to the ancestor. However, the lineages showed differences in their responses at high salinities (100% AASW). Two lineages showed no decrease in growth at the highest salinity, while two showed decreased growth at the highest salinity. Additionally, none of the evolved lineages gained the ability to grow in purely fresh conditions (0% AASW).

These different changes in the salinity tolerance responses of the evolved lineages can be associated with the modes of evolution used to assess evolution of thermal response curves (Izem and Kingsolver, 2005). When I apply these standard template modes of variation to the evolved lineages I observe a predominantly horizontal mode shift in Lineage A, a predominantly vertical

mode shift in B, and C and D predominantly generalist/specialist mode shifts. These mode shifts can also be seen in the changes in the Plateau model parameters predicted for each lineage. Lineage A has a lower optimum salinity, with a similar plateau length to the ancestor, while lineages C and D have both lower optimum salinities and longer plateau lengths. The vertical shift in lineage B is less well captured given the normalization of the growth rate data in the model fits, however the significant decrease in the plateau length does highlight the near optimum growth rates at a narrower range of salinities than seen in the ancestor.

Given the consistent discovery that acclimation to increasing salinities results in high salinity tolerances, it is likely that evolved responses will expand on this capacity (Georges des Aulnois et al., 2019; Ketola and Hiltunen, 2014; Melero-Jiménez et al., 2022; Melero-Jiménez et al., 2019). This acclimation response suggests that salinity tolerance adaptation will likely proceed largely through regulation-based changes (Lachapelle et al., 2015), and supports significant broadening of the salinity tolerance as a primary mode of adaptation.

The relative stability of the salinity response curves of the 10% AASW evolved lineages at 100% AASW, with half the lineages showing no loss of tolerance, highlights how salinity tolerance does not appear to be susceptible to rapid loss (Beer et al., 2014). While salinity selection experiments have observed significant increases in the salinity tolerance after evolution, the lack of a loss of tolerance to the ancestral condition has been observed previously (Melero-Jiménez et al., 2019). This suggests that it may be easier to gain salinity tolerance than lose it.

Every lineage evolved at the lowest salinities had improvements in growth in the low salinity conditions relative to the ancestor. However, their responses to higher salinities were varied. The experiment supports the importance of investigating the evolution of salinity

tolerance as a function-valued trait. This evidence supports the rapid adjustment of salinity tolerance to new environments, without consistent loss of tolerance to the ancestral salinity condition.

Chapter 5: Conclusions

The results from each of my chapters suggest that salinity tolerance, while variable, is not the primary factor driving the environments in which specific cyanobacterial strains live. This suggests that we should consider the role of competition and ecology in the apparent lack of transitions between habitats of differing salinities (Logares et al., 2009).

While salinity tolerance is often considered a complex trait due to the numerous mechanisms and underlying genotypes associated with maintenance of osmotic homeostasis (Hagemann, 2011; Martiny et al., 2015), it may be useful to consider it a complex *converged* trait, where organisms can combine different sets of individually simple mechanisms to create similar phenotypes.

In Chapter 2, I used simulations of evolution to evaluate what rates of evolution allow for the reconstruction of salinity as a trait on the cyanobacterial phylogeny. This dataset showed that to reconstruct the trait history of salinity cyanobacteria must have evolved very slowly. With the evaluation of the impacts of applying selective pressure on their evolution, I showed that the apparent salinity trait history could instead reflect the environmental history. While these results do not provide the ability to definitively say that reconstruction of the trait history of salinity tolerance is not possible across the cyanobacterial phylogeny, it does provide some bounds on the evolutionary rates that would allow such reconstruction.

In Chapter 3 I evaluated the currently available data on how cyanobacterial species respond to changes in salinity. I used data from the literature to assess how we currently classify salinity as a trait in cyanobacteria and established that while the current classification can provide information for some strains, it fails to capture the diversity of salinity responses. I then used the dataset to quantitatively evaluate a new framework for understanding salinity tolerance

based on our understanding of the biophysical limits of cells. My model provides the ability to evaluate salinity tolerance quantitatively, compare tolerance between strains, and evaluate the trait without requiring consistent molecular mechanisms of osmoregulation. By taking a population level measurement of growth and producing a subcellular prediction of macromolecular packing density, I provide a simple quantitative method for evaluating how different molecular mechanisms impact salinity tolerance.

In Chapter 4 I evaluated the salinity tolerance of a laboratory model strain of cyanobacteria, *Synechococcus* sp. PCC 7002, and used experimental evolution to understand if and how salinity tolerance changes for strains with broad tolerances. Over the course of 750 generations, the apparent upper limit of fitness improvements was more than 90% reached. Simultaneously, the lineages evolved in the most different, and freshest, condition showed consistent gains in their fitness at lower salinities but did not all have decreases in fitness in the ancestral condition.

The results from Chapter 4 allow me to revisit the conclusions from Chapter 2 and emphasize the role of the environment in cyanobacterial salinity tolerance history. The rapid fitness changes observed via experimental evolution confirm that extremely slow rates of evolution are unlikely to have existed over the entire cyanobacterial phylogeny.

Moving forward, my dissertation provides a new framework for evaluating salinity tolerance in cyanobacteria as well as understanding how different molecular mechanisms impact salinity tolerance. This framework is useful across many scales of research, from providing quantitative measures of salinity tolerance, to making predictions of the impact of environmental salinity on cell physiology and intracellular dynamics. Combined with the tools of experimental evolution, it provides a method for understanding the broad pathways over which salinity

tolerance evolves without needing strains to use similar methods of osmoregulation to be compared to one another.

References

Alahari, A., Ballal, A., Apte, S.K., 2001. Regulation of Potassium-Dependent Kdp-ATPase Expression in the Nitrogen-Fixing Cyanobacterium Anabaena torulosa. J. Bacteriol. 183, 5778–5781. https://doi.org/10.1128/JB.183.19.5778-5781.2001

Allakhverdiev, S.I., Kinoshita, M., Inaba, M., Suzuki, I., Murata, N., 2001. Unsaturated fatty acids in membrane lipids protect the photosynthetic machinery against salt-induced damage in Synechococcus. Plant Physiol. 125, 1842–1853. https://doi.org/10.1104/pp.125.4.1842

Allakhverdiev, S.I., Murata, N., 2008. Salt stress inhibits photosystems II and I in cyanobacteria. Photosynth. Res. https://doi.org/10.1007/s11120-008-9334-x

Allakhverdiev, S.I., Nishiyama, Y., Suzuki, I., Tasaka, Y., Murata, N., 1999. Genetic engineering of the unsaturation of fatty acids in membrane lipids alters the tolerance of Synechocystis to salt stress. Proc. Natl. Acad. Sci. U. S. A. 96, 5862–5867. https://doi.org/10.1073/pnas.96.10.5862

Allakhverdiev, S.I., Nishiyama, Y., Suzuki, I., Tasaka, Y., Murata, N., 1998. Fatty Acids Unsaturation of Membrane Lipids is Involved in the Tolerance to Salt Stress. https://doi.org/10.1007/978-94-011-3953-3_424

Allakhverdiev, S.I., Sakamoto, A., Nishiyama, Y., Inaba, M., Murata, N., 2000. Ionic and Osmotic Effects of NaCl-Induced Inactivation of Photosystems I and II in Synechococcus sp.1. Plant Physiol. 123, 1047–1056. https://doi.org/10.1104/pp.123.3.1047

Asthana, R.K., Nigam, S., Maurya, A., Kayastha, A.M., Singh, S.P., 2008. Trehalose-Producing Enzymes MTSase and MTHase in Anabaena 7120 Under NaCl Stress. Curr. Microbiol. 56, 429–435. https://doi.org/10.1007/s00284-008-9121-0

Avonce, N., Mendoza-Vargas, A., Morett, E., Iturriaga, G., 2006. Insights on the evolution of trehalose biosynthesis. BMC Evol. Biol. 6, 109. https://doi.org/10.1186/1471-2148-6-109

Azua-Bustos, A., Zúñiga, J., Arenas-Fajardo, C., Orellana, M., Salas, L., Rafael, V., 2014. Gloeocapsopsis AAB1, an extremely desiccation-tolerant cyanobacterium isolated from the Atacama Desert. Extremophiles 18, 61–74. https://doi.org/10.1007/s00792-013-0592-y

Ballal, A., Apte, S.K., 2005. Differential Expression of the Two kdp Operons in the Nitrogen-Fixing Cyanobacterium Anabaena sp. Strain L-31. Appl. Environ. Microbiol. 71, 5297–5303. https://doi.org/10.1128/AEM.71.9.5297-5303.2005

Ballal, A., Basu, B., Apte, S.K., 2007. The Kdp-ATPase system and its regulation. J. Biosci. 32, 559–568. https://doi.org/10.1007/s12038-007-0055-7

Bano, A., Siddiqui, P.J.A., 2004. Characterization of five marine cyanobacterial species with respect to their pH and salinity requirements. Pak. J. Bot. 36, 133–143.

Batterton, J.C., Van Baalen, C., 1971. Growth responses of blue-green algae to sodium chloride concentration. Arch. Für Mikrobiol. 76, 151–165. https://doi.org/10.1007/BF00411789

Baym, M., Lieberman, T.D., Kelsic, E.D., Chait, R., Gross, R., Yelin, I., Kishony, R., 2016. Spatiotemporal microbial evolution on antibiotic landscapes. Science 353, 1147–1151. https://doi.org/10.1126/science.aag0822

Beer, K.D., Wurtmann, E.J., Pinel, N., Baliga, N.S., 2014. Model Organisms Retain an "Ecological Memory" of Complex Ecologically Relevant Environmental Variation. Appl. Environ. Microbiol. 80, 1821–1831. https://doi.org/10.1128/AEM.03280-13

Bell, G., 2010. Fluctuating selection: the perpetual renewal of adaptation in variable environments. Philos. Trans. R. Soc. B Biol. Sci. 365, 87–97. https://doi.org/10.1098/rstb.2009.0150

Bell, G., Gonzalez, A., 2009. Evolutionary rescue can prevent extinction following environmental change. Ecol. Lett. 12, 942–948. https://doi.org/10.1111/j.1461-0248.2009.01350.x

Bemal, S., Anil, A.C., 2018. Effects of salinity on cellular growth and exopolysaccharide production of freshwater Synechococcus strain CCAP1405. J. Plankton Res. 40, 46–58. https://doi.org/10.1093/plankt/fbx064

Berry, S., Esper, B., Karandashova, I., Teuber, M., Elanskaya, I.V., Rögner, M., Hagemann, M., 2003. Potassium uptake in the unicellular cyanobacterium Synechocystis sp. strain PCC 6803 mainly depends on a Ktr-like system encoded by slr1509 (ntpJ). FEBS Lett. 548, 53–58. https://doi.org/10.1016/s0014-5793(03)00729-4

Bianchini, G., 2022. Bayesian methods using genomic data to gain insights into the history of photosynthesis. University of Bristol.

Billini, M., Stamatakis, K., Sophianopoulou, V., 2008. Two Members of a Network of Putative Na+/H+ Antiporters Are Involved in Salt and pH Tolerance of the Freshwater Cyanobacterium Synechococcus elongatus. J. Bacteriol. 190, 6318–6329. https://doi.org/10.1128/JB.00696-08

Blanco-Rivero, A., Leganés, F., Fernández-Valiente, E., Calle, P., Fernández-Piñas, F., 2005. mrpA, a gene with roles in resistance to Na+ and adaptation to alkaline pH in the cyanobacterium Anabaena sp. PCC7120. Microbiology 151, 1671–1682. https://doi.org/10.1099/mic.0.27848-0

Blanco-Rivero, A., Leganés, F., Fernández-Valiente, E., Fernández-Piñas, F., 2009. mrpA (all1838), a gene involved in alkali and Na+ sensitivity, may also have a role in energy metabolism in the cyanobacterium Anabaena sp. strain PCC 7120. J. Plant Physiol. 166, 1488–1496. https://doi.org/10.1016/j.jplph.2009.03.007

Blank, C.E., 2013. Phylogenetic distribution of compatible solute synthesis genes support a freshwater origin for cyanobacteria. J. Phycol. https://doi.org/10.1111/jpy.12098

Blank, C.E., Sánchez-Baracaldo, P., 2010. Timing of morphological and ecological innovations in the cyanobacteria – a key to understanding the rise in atmospheric oxygen. Geobiology. https://doi.org/10.1111/j.1472-4669.2009.00220.x

Blankenship, R.E., Hartman, H., 1998. The origin and evolution of oxygenic photosynthesis. Trends Biochem. Sci. https://doi.org/10.1016/s0968-0004(98)01186-4

Blumwald, E., Wolosin, J.M., Packer, L., 1984. Na+/H+ exchange in the cyanobacterium Synechococcus 6311. Biochem. Biophys. Res. Commun. 122, 452–459. https://doi.org/10.1016/0006-291x(84)90497-2

Bohannan, B.J.M., Lenski, R.E., 2000. The Relative Importance of Competition and Predation Varies with Productivity in a Model Community. Am. Nat. 156, 329–340. https://doi.org/10.1086/303393

Boyd, M., Rosenzweig, F., Herron, M.D., 2018. Analysis of motility in multicellular Chlamydomonas reinhardtii evolved under predation. PLOS ONE 13, e0192184. https://doi.org/10.1371/journal.pone.0192184

Brand, L.E., 1984. The salinity tolerance of forty-six marine phytoplankton isolates. Estuar. Coast. Shelf Sci. 18, 543–556. https://doi.org/10.1016/0272-7714(84)90089-1

Brown, C.J., Todd, K.M., Rosenzweig, R.F., 1998. Multiple duplications of yeast hexose transport genes in response to selection in a glucose-limited environment. Mol. Biol. Evol. 15, 931–942. https://doi.org/10.1093/oxfordjournals.molbev.a026009

Brown, I.I., Fadeyev, S.I., Kirik, I.I., Severina, I.I., Skulachev, V.P., 1990. Light-dependent Δ\smNa-generation and utilization in the marine cyanobacterium Oscillatoria brevis. FEBS Lett. 270, 203–206. https://doi.org/10.1016/0014-5793(90)81268-S

Brutemark, A., Vandelannoote, A., Engström-Öst, J., Suikkanen, S., 2015. A Less Saline Baltic Sea Promotes Cyanobacterial Growth, Hampers Intracellular Microcystin Production, and Leads to Strain-Specific Differences in Allelopathy. PLOS ONE 10, e0128904. https://doi.org/10.1371/journal.pone.0128904

Bualuang, A., Soontharapirakkul, K., Incharoensakdi, A., 2010. Na + /H + exchange activity in the alkaliphile halotolerant cyanobacterium Aphanothece halophytica. J. Appl. Phycol. 22, 123–129. https://doi.org/10.1007/s10811-009-9431-z

Cabello-Yeves, P.J., Rodriguez-Valera, F., 2019. Marine-freshwater prokaryotic transitions require extensive changes in the predicted proteome. Microbiome 7, 117. https://doi.org/10.1186/s40168-019-0731-5

Cameron, J.C., Gordon, G.C., Pfleger, B.F., 2015. Genetic and genomic analysis of RNases in model cyanobacteria. Photosynth. Res. 126, 171–183. https://doi.org/10.1007/s11120-015-0076-2

Cardona, T., 2016. Reconstructing the Origin of Oxygenic Photosynthesis: Do Assembly and Photoactivation Recapitulate Evolution? Front. Plant Sci. https://doi.org/10.3389/fpls.2016.00257

Cardona, T., Murray, J.W., Rutherford, A.W., 2015. Origin and Evolution of Water Oxidation before the Last Common Ancestor of the Cyanobacteria. Mol. Biol. Evol. 32, 1310–1328. https://doi.org/10.1093/molbev/msv024

Cardona, T., Sánchez-Baracaldo, P., Rutherford, A.W., Larkum, A.W., 2019. Early Archean origin of Photosystem II. Geobiology 17, 127–150. https://doi.org/10.1111/gbi.12322

Cesar, S., Anjur-Dietrich, M., Yu, B., Li, E., Rojas, E., Neff, N., Cooper, T.F., Huang, K.C., 2020. Bacterial Evolution in High-Osmolarity Environments. mBio 11, e01191-20. https://doi.org/10.1128/mBio.01191-20

Chaneva, G., Pilarski, P., Petrova, D.H., 2011. Changes of proline content in a cyanobacterium under oxidative stress. Oxid. Commun. 34, 439–445.

Chao, L., Levin, B.R., Stewart, F.M., 1977. A Complex Community in a Simple Habitat: An Experimental Study with Bacteria and Phage. Ecology 58, 369–378. https://doi.org/10.2307/1935611

Chen, M.-Y., Teng, W.-K., Zhao, L., Hu, C.-X., Zhou, Y.-K., Han, B.-P., Song, L.-R., Shu, W.-S., 2021. Comparative genomics reveals insights into cyanobacterial evolution and habitat adaptation. ISME J. 15, 211–227. https://doi.org/10.1038/s41396-020-00775-z

Csonka, L.N., Hanson, A.D., 1991. PROKARYOTIC OSMOREGULATION: Genetics and Physiology. Annu. Rev. Microbiol. 45, 569–606. https://doi.org/10.1146/annurev.mi.45.100191.003033

Cumino, A.C., Perez-Cenci, M., Giarrocco, L.E., Salerno, G.L., 2010. The proteins involved in sucrose synthesis in the marine cyanobacterium Synechococcus sp. PCC 7002 are encoded by two genes transcribed from a gene cluster. FEBS Lett. 584, 4655–4660. https://doi.org/10.1016/j.febslet.2010.10.040

Curatti, L., Folco, E., Desplats, P., Abratti, G., Limones, V., Herrera-Estrella, L., Salerno, G., 1998. Sucrose-phosphate synthase from Synechocystis sp. strain PCC 6803: identification of the spsA gene and characterization of the enzyme expressed in Escherichia coli. J. Bacteriol. 180, 6776–6779. https://doi.org/10.1128/JB.180.24.6776-6779.1998

Czaja, A.D., Johnson, C.M., Roden, E.E., Beard, B.L., Voegelin, A.R., Thomas F. Nägler, Nicolas J. Beukes, Martin Wille, 2012. Evidence for free oxygen in the Neoarchean ocean based on coupled iron-molybdenum isotope fractionation. Geochim. Cosmochim. Acta. https://doi.org/10.1016/j.gca.2012.03.007

Dhar, R., Sägesser, R., Weikert, C., Yuan, J., Wagner, A., 2011. Adaptation of Saccharomyces cerevisiae to saline stress through laboratory evolution. J. Evol. Biol. 24, 1135–1153. https://doi.org/10.1111/j.1420-9101.2011.02249.x

Dill, K.A., Ghosh, K., Schmit, J.D., 2011. Physical limits of cells and proteomes. Proc. Natl. Acad. Sci. 108, 17876–17882. https://doi.org/10.1073/pnas.1114477108

Dittami, S.M., Heesch, S., Olsen, J.L., Collén, J., 2017. Transitions between marine and freshwater environments provide new clues about the origins of multicellular plants and algae. J. Phycol. 53, 731–745. https://doi.org/10.1111/jpy.12547

Dötsch, A., Severin, J., Alt, W., Galinski, E.A., Kreft, J.-U., 2008. A mathematical model for growth and osmoregulation in halophilic bacteria. Microbiology 154, 2956–2969. https://doi.org/10.1099/mic.0.2007/012237-0

Dunham, M.J., Badrane, H., Ferea, T., Adams, J., Brown, P.O., Rosenzweig, F., Botstein, D., 2002. Characteristic genome rearrangements in experimental evolution of Saccharomyces cerevisiae. Proc. Natl. Acad. Sci. 99, 16144–16149. https://doi.org/10.1073/pnas.242624799

Duval, C., Thomazeau, S., Drelin, Y., Yéprémian, C., Bouvy, M., Couloux, A., Troussellier, M., Rousseau, F., Bernard, C., 2018. Phylogeny and salt-tolerance of freshwater Nostocales strains: Contribution to their systematics and evolution. Harmful Algae 73, 58–71. https://doi.org/10.1016/j.hal.2018.01.008

Dvořák, P., Casamatta, D.A., Hašler, P., Jahodářová, E., Norwich, A.R., Poulíčková, A., 2017. Diversity of the Cyanobacteria, in: Hallenbeck, P.C. (Ed.), Modern Topics in the Phototrophic Prokaryotes: Environmental and Applied Aspects. Springer International Publishing, Cham, pp. 3–46. https://doi.org/10.1007/978-3-319-46261-5_1

Dvořák, P., Casamatta, D.A., Poulíčková, A., Hašler, P., Ondřej, V., Sanges, R., 2014. Synechococcus: 3 billion years of global dominance. Mol. Ecol. 23, 5538–5551. https://doi.org/10.1111/mec.12948

Ehira, S., Kimura, S., Miyazaki, S., Ohmori, M., 2014. Sucrose Synthesis in the Nitrogen-Fixing Cyanobacterium Anabaena sp. Strain PCC 7120 Is Controlled by the Two-Component Response Regulator OrrA. Appl. Environ. Microbiol. 80, 5672–5679. https://doi.org/10.1128/AEM.01501-14

Elanskaya, I.V., Karandashova, I.V., Bogachev, A.V., Hagemann, M., 2002. Functional Analysis of the Na+/H+ Antiporter Encoding Genes of the Cyanobacterium Synechocystis PCC 6803. Biochem. Mosc. 67, 432–440. https://doi.org/10.1023/A:1015281906254

Ellis, R.J., 2001. Macromolecular crowding: obvious but underappreciated. Trends Biochem. Sci. 26, 597–604. https://doi.org/10.1016/S0968-0004(01)01938-7

Empadinhas, N., da Costa, M.S., 2011. Diversity, biological roles and biosynthetic pathways for sugar-glycerate containing compatible solutes in bacteria and archaea. Environ. Microbiol. 13, 2056–2077. https://doi.org/10.1111/j.1462-2920.2010.02390.x

Engelbrecht, F., Marin, K., Hagemann, M., 1999. Expression of the ggpS Gene, Involved in Osmolyte Synthesis in the Marine CyanobacteriumSynechococcus sp. Strain PCC 7002, Revealed Regulatory Differences between This Strain and the Freshwater StrainSynechocystis sp. Strain PCC 6803. Appl. Environ. Microbiol. 65, 4822–4829. https://doi.org/10.1128/AEM.65.11.4822-4829.1999

Espie, G.S., Miller, A.G., Canvin, D.T., 1988. Characterization of the Na+-Requirement in Cyanobacterial Photosynthesis 1. Plant Physiol. 88, 757–763. https://doi.org/10.1104/pp.88.3.757

Estes, S., Arnold, S.J., 2007. Resolving the Paradox of Stasis: Models with Stabilizing Selection Explain Evolutionary Divergence on All Timescales. Am. Nat. 169, 227–244. https://doi.org/10.1086/510633

Fagliarone, C., Napoli, A., Chiavarini, S., Baqué, M., de Vera, J.-P., Billi, D., 2020. Biomarker Preservation and Survivability Under Extreme Dryness and Mars-Like UV Flux of a Desert Cyanobacterium Capable of Trehalose and Sucrose Accumulation. Front. Astron. Space Sci. 7.

Falkowski, P.G., Fenchel, T., Delong, E.F., 2008. The Microbial Engines That Drive Earth's Biogeochemical Cycles. Science 320, 1034–1039. https://doi.org/10.1126/science.1153213

Fernandes, T.A., Iyer, V., Apte, S.K., 1993. Differential Responses of Nitrogen-Fixing Cyanobacteria to Salinity and Osmotic Stresses. Appl. Environ. Microbiol. 59, 899–904. https://doi.org/10.1128/aem.59.3.899-904.1993

Flombaum, P., Gallegos, J.L., Gordillo, R.A., Rincón, J., Zabala, L.L., Jiao, N., Karl, D.M., Li, W.K.W., Lomas, M.W., Veneziano, D., Vera, C.S., Vrugt, J.A., Martiny, A.C., 2013. Present and future global distributions of the marine Cyanobacteria Prochlorococcus and Synechococcus. Proc. Natl. Acad. Sci. 110, 9824–9829. https://doi.org/10.1073/pnas.1307701110

Fu, F.-X., Bell, P.R.F., 2003. Effect of salinity on growth, pigmentation, N2 fixation and alkaline phosphatase activity of cultured Trichodesmium sp. Mar. Ecol. Prog. Ser. 257, 69–76. https://doi.org/10.3354/meps257069

Fukaya, F., Promden, W., Hibino, T., Tanaka, Y., Nakamura, T., Takabe, T., 2009. An Mrp-Like Cluster in the Halotolerant Cyanobacterium Aphanothece halophytica Functions as a Na+/H+ Antiporter. Appl. Environ. Microbiol. 75, 6626–6629. https://doi.org/10.1128/AEM.01387-09

Furuki, T., 2009. Thermodynamic, hydration and structural characteristics of alpha,alpha-trehalose. Front. Biosci. Volume, 3523. https://doi.org/10.2741/3468

Galinski, E.A., 1995. Osmoadaptation in Bacteria. Adv. Microb. Physiol. https://doi.org/10.1016/s0065-2911(08)60148-4

Georges des Aulnois, M., Roux, P., Caruana, A., Réveillon, D., Briand, E., Hervé, F., Savar, V., Bormans, M., Amzil, Z., 2019. Physiological and Metabolic Responses of Freshwater and Brackish-Water Strains of Microcystis aeruginosa Acclimated to a Salinity Gradient: Insight into Salt Tolerance. Appl. Environ. Microbiol. 85, e01614-19. https://doi.org/10.1128/AEM.01614-19

Ghosh, K., de Graff, A.M.R., Sawle, L., Dill, K.A., 2016. Role of Proteome Physical Chemistry in Cell Behavior. J. Phys. Chem. B 120, 9549–9563. https://doi.org/10.1021/acs.jpcb.6b04886

Golubic, S., 1980. Halophily and Halotolerance in Cyanophytes, in: Ponnamperuma, C., Margulis, L. (Eds.), Limits of Life, Limits of Life. Springer Netherlands, Dordrecht, pp. 69–83. https://doi.org/10.1007/978-94-009-9085-2_7

Gonzalez, A., Bell, G., 2013. Evolutionary rescue and adaptation to abrupt environmental change depends upon the history of stress. Philos. Trans. R. Soc. B 368, 20120079–20120079. https://doi.org/10.1098/rstb.2012.0079

Goolsby, E.W., 2015. Phylogenetic Comparative Methods for Evaluating the Evolutionary History of Function-Valued Traits. Syst. Biol. 64, 568–578. https://doi.org/10.1093/sysbio/syv012

Gordon, G.C., Korosh, T.C., Cameron, J.C., Markley, A.L., Begemann, M.B., Pfleger, B.F., 2016. CRISPR interference as a titratable, trans-acting regulatory tool for metabolic engineering in the cyanobacterium Synechococcus sp. strain PCC 7002. Metab. Eng. 38, 170–179. https://doi.org/10.1016/j.ymben.2016.07.007

Gostinčar, C., Stajich, J.E., Kejžar, A., Sinha, S., Nislow, C., Lenassi, M., Gunde-Cimerman, N., 2021. Seven Years at High Salinity-Experimental Evolution of the Extremely Halotolerant Black Yeast Hortaea werneckii. J. Fungi 7, 723–723. https://doi.org/10.3390/jof7090723

Griswold, C.K., Gomulkiewicz, R., Heckman, N., 2008. Hypothesis testing in comparative and experimental studies of function-valued traits. Evol. Int. J. Org. Evol. 62, 1229–1242. https://doi.org/10.1111/j.1558-5646.2008.00340.x

Gumsley, A.P., Chamberlain, K.R., Bleeker, W., Söderlund, U., Kock, M.O. de, Larsson, E.R., Bekker, A., 2017. Timing and tempo of the Great Oxidation Event. Proc. Natl. Acad. Sci. 114, 1811–1816. https://doi.org/10.1073/pnas.1608824114

Hagemann, M., 2013. Genomics of Salt Acclimation: Synthesis of Compatible Solutes among Cyanobacteria. Adv. Bot. Res. https://doi.org/10.1016/b978-0-12-394313-2.00002-0

Hagemann, M., 2011. Molecular biology of cyanobacterial salt acclimation. FEMS Microbiol. Rev. 35, 87–123. https://doi.org/10.1111/j.1574-6976.2010.00234.x

Hagemann, M., Effmert, U., Kerstan, T., Schoor, A., Erdmann, N., 2001. Biochemical characterization of glucosylglycerol-phosphate synthase of Synechocystis sp. strain PCC 6803: comparison of crude, purified, and recombinant enzymes. Curr. Microbiol. 43, 278–283. https://doi.org/10.1007/s002840010301

Hagemann, M., Erdmann, N., 1994. Activation and pathway of glucosylglycerol synthesis in the cyanobacterium Synechocystis sp. PCC 6803. Microbiology 140, 1427–1431. https://doi.org/10.1099/00221287-140-6-1427

Hagemann, M., Erdmann, N., Wittenburg, E., 1987. Synthesis of glueosylglycerol in salt-stressed cells of the cyanobacterium Microcystisfivma.

Hagemann, M., Marin, K., 1999. Salt-induced Sucrose Accumulation is Mediated by Sucrose-phosphate-synthase in Cyanobacteria. J. Plant Physiol. https://doi.org/10.1016/s0176-1617(99)80126-6

Hagemann, M., Ribbeck-Busch, K., Klähn, S., Hasse, D., Steinbruch, R., Berg, G., 2008. The Plant-Associated Bacterium Stenotrophomonas rhizophila Expresses a New Enzyme for the Synthesis of the Compatible Solute Glucosylglycerol. J. Bacteriol. 190, 5898–5906. https://doi.org/10.1128/JB.00643-08

Hagemann, M., Richter, S., Mikkat, S., 1997. The ggtA gene encodes a subunit of the transport system for the osmoprotective compound glucosylglycerol in Synechocystis sp. strain PCC 6803. J. Bacteriol. 179, 714–720. https://doi.org/10.1128/jb.179.3.714-720.1997

Hagemann, M, Schoor, A., Jeanjean, R., Zuther, E., Joset, F., 1997. The stpA gene form Synechocystis sp. strain PCC 6803 encodes the glucosylglycerol-phosphate phosphatase involved in cyanobacterial osmotic response to salt shock. J. Bacteriol. 179, 1727–1733. https://doi.org/10.1128/jb.179.5.1727-1733.1997

Haldane, J.B.S., 1949. Suggestions as to Quantitative Measurement of Rates of Evolution. Evolution 3, 51–56. https://doi.org/10.1111/j.1558-5646.1949.tb00004.x

Hamada, A., Hibino, T., Nakamura, T., Takabe, T., 2001. Na+/H+ Antiporter from Synechocystis Species PCC 6803, Homologous to SOS1, Contains an Aspartic Residue and Long C-Terminal Tail Important for the Carrier Activity. Plant Physiol. 125, 437–446. https://doi.org/10.1104/pp.125.1.437

Hamilton, T.L., 2019. The trouble with oxygen: The ecophysiology of extant phototrophs and implications for the evolution of oxygenic photosynthesis. Free Radic. Biol. Med. https://doi.org/10.1016/j.freeradbiomed.2019.05.003

Hamilton, T.L., Bryant, D.A., Macalady, J.L., 2016. The role of biology in planetary evolution: cyanobacterial primary production in low-oxygen Proterozoic oceans. Environ. Microbiol. 18, 325–340. https://doi.org/10.1111/1462-2920.13118

Hammerschmidt, K., Landan, G., Domingues Kümmel Tria, F., Alcorta, J., Dagan, T., 2021. The Order of Trait Emergence in the Evolution of Cyanobacterial Multicellularity. Genome Biol. Evol. 13, evaa249. https://doi.org/10.1093/gbe/evaa249

Hansen, S.K., Rainey, P.B., Haagensen, J.A.J., Molin, S., 2007. Evolution of species interactions in a biofilm community. Nature 445, 533–536. https://doi.org/10.1038/nature05514

He, Z., Zhou, A., Baidoo, E.E.K., He, Q., Qiang He, Joachimiak, M.P., Benke, P.I., Phan, R., Mukhopadhyay, A., Hemme, C.L., Huang, K.H., Alm, E.J., Fields, M.W., Wall, J.D., Stahl, D.A., Stahl, D.A., David A. Stahl, Hazen, T.C., Keasling, J.D., Arkin, A.P., Zhou, J., 2010. Global Transcriptional, Physiological, and Metabolite Analyses of the Responses of Desulfovibrio vulgaris Hildenborough to Salt Adaptation. Appl. Environ. Microbiol. 76, 1574–1586. https://doi.org/10.1128/aem.02141-09

Herlemann, D.P., Labrenz, M., Jürgens, K., Bertilsson, S., Waniek, J.J., Andersson, A.F., 2011. Transitions in bacterial communities along the 2000 km salinity gradient of the Baltic Sea. ISME J. 5, 1571–1579. https://doi.org/10.1038/ismej.2011.41

Herrmann, A.J., Gehringer, M.M., 2019. An investigation into the effects of increasing salinity on photosynthesis in freshwater unicellular cyanobacteria during the late Archaean. Geobiology 17, 343–359. https://doi.org/10.1111/gbi.12339

Herron, M.D., Ratcliff, W.C., Boswell, J., Rosenzweig, F., 2018. Genetics of a de novo origin of undifferentiated multicellularity. R. Soc. Open Sci. 5, 180912. https://doi.org/10.1098/rsos.180912

Hershkovitz, N., Oren, A., Cohen, Y., 1991. Accumulation of Trehalose and Sucrose in Cyanobacteria Exposed to Matric Water Stress. Appl. Environ. Microbiol. 57, 645–648. https://doi.org/10.1128/aem.57.3.645-648.1991

Heyer, H., Stal, L., Krumbein, W.E., 1989. Simultaneous heterolactic and acetate fermentation in the marine cyanobacterium Oscillatoria limosa incubated anaerobically in the dark. Arch. Microbiol. 151, 558–564. https://doi.org/10.1007/BF00454875

Hibino, T., Kaku, N., Yoshikawa, H., Takabe, T., Takabe, T., 1999. Molecular characterization of DnaK from the halotolerant cyanobacterium Aphanothece halophytica for ATPase, protein folding, and copper binding under various salinity conditions. Plant Mol. Biol. 40, 409–418. https://doi.org/10.1023/a:1006273124726

Higo, A., Katoh, H., Ohmori, K., Ikeuchi, M., Ohmori, M., 2006. The role of a gene cluster for trehalose metabolism in dehydration tolerance of the filamentous cyanobacterium Anabaena sp. PCC 7120. Microbiology 152, 979–987. https://doi.org/10.1099/mic.0.28583-0

Hillesland, K.L., Stahl, D.A., 2010. Rapid evolution of stability and productivity at the origin of a microbial mutualism. Proc. Natl. Acad. Sci. 107, 2124–2129. https://doi.org/10.1073/pnas.0908456107

Hosoda, K., Habuchi, M., Suzuki, S., Miyazaki, M., Takikawa, G., Sakurai, T., Kashiwagi, A., Sueyoshi, M., Matsumoto, Y., Kiuchi, A., Mori, K., Yomo, T., 2014. Adaptation of a Cyanobacterium to a Biochemically Rich Environment in Experimental Evolution as an Initial Step toward a Chloroplast-Like State. PLOS ONE 9, e98337. https://doi.org/10.1371/journal.pone.0098337

Hu, C., Gao, K., Whitton, B.A., 2012. Semi-arid Regions and Deserts, in: Whitton, B.A. (Ed.), Ecology of Cyanobacteria II: Their Diversity in Space and Time. Springer Netherlands, Dordrecht, pp. 345–363. https://doi.org/10.1007/978-94-007-3855-3

Hughes, B.S., Cullum, A.J., Bennett, A.F., 2007. An Experimental Evolutionary Study on Adaptation to Temporally Fluctuating pH in Escherichia coli. Physiol. Biochem. Zool. 80, 406–421. https://doi.org/10.1086/518353

Hurley, S.J., Wing, B.A., Jasper, C.E., Hill, N.C., Cameron, J.C., 2021. Carbon isotope evidence for the global physiology of Proterozoic cyanobacteria. Sci. Adv. 7, eabc8998. https://doi.org/10.1126/sciadv.abc8998

Inaba, M., Sakamoto, A., Murata, N., 2001. Functional Expression in Escherichia coli of Low-Affinity and High-Affinity Na+(Li+)/H+ Antiporters of Synechocystis. J. Bacteriol. 183, 1376–1384. https://doi.org/10.1128/JB.183.4.1376-1384.2001

Incharoensakdi, A., Wutipraditkul, N., 1999. Accumulation of glycinebetaine and its synthesis from radioactive precursors under salt-stress in the cyanobacterium Aphanothece halophytica. J. Appl. Phycol. 11, 515–523. https://doi.org/10.1023/A:1008186309006

Inoue-Kashino, N., Kashino, Y., Satoh, K., Terashima, I., Pakrasi, H.B., 2005. PsbU Provides a Stable Architecture for the Oxygen-Evolving System in Cyanobacterial Photosystem II. Biochemistry 44, 12214–12228. https://doi.org/10.1021/bi047539k

Izem, R., Kingsolver, J.G., 2005. Variation in Continuous Reaction Norms: Quantifying Directions of Biological Interest. Am. Nat. 166, 277–289. https://doi.org/10.1086/431314

Jasser, I., Panou, M., Khomutovska, N., Sandzewicz, M., Panteris, E., Niyatbekov, T., Łach, Ł., Kwiatowski, J., Kokociński, M., Gkelis, S., 2022. Cyanobacteria in hot pursuit: Characterization of cyanobacteria strains, including novel taxa, isolated from geothermal habitats from different ecoregions of the world. Mol. Phylogenet. Evol. 170, 107454. https://doi.org/10.1016/j.ympev.2022.107454

Jha, M.N., Venkataraman, G.S., Kaushik, B.D., 1987. Response ofWestiellopsis prolifica andAnabaena sp. to salt stress. MIRCEN J. Appl. Microbiol. Biotechnol. 3, 307–317. https://doi.org/10.1007/BF00933584

Joy, J.B., Liang, R.H., McCloskey, R.M., Nguyen, T., Poon, A.F.Y., 2016. Ancestral Reconstruction. PLOS Comput. Biol. 12, e1004763. https://doi.org/10.1371/journal.pcbi.1004763

Kacar, B., Hanson-Smith, V., Adam, Z.R., Boekelheide, N., 2017. Constraining the timing of the Great Oxidation Event within the Rubisco phylogenetic tree. Geobiology 15, 628–640. https://doi.org/10.1111/gbi.12243

Kageyama, H., Tripathi, K., Rai, A.K., Cha-um, S., Waditee-Sirisattha, R., Takabe, T., 2011. An Alkaline Phosphatase/Phosphodiesterase, PhoD, Induced by Salt Stress and Secreted Out of the Cells of Aphanothece halophytica, a Halotolerant Cyanobacterium. Appl. Environ. Microbiol. 77, 5178–5183. https://doi.org/10.1128/AEM.00667-11

Kanesaki, Y., Suzuki, I., Allakhverdiev, S.I., Mikami, K., Murata, N., 2002. Salt Stress and Hyperosmotic Stress Regulate the Expression of Different Sets of Genes in Synechocystis sp. PCC 6803. Biochem. Biophys. Res. Commun. 290, 339–348. https://doi.org/10.1006/bbrc.2001.6201

Katoh, H., Itoh, S., Shen, J.-R., Ikeuchi, M., 2001. Functional Analysis of psbV and a Novel c-type Cytochrome Gene psbV2 of the Thermophilic Cyanobacterium Thermosynechococcuselongatus Strain BP-1. Plant Cell Physiol. 42, 599–607. https://doi.org/10.1093/pcp/pce074

Kellermann, V., Hoffmann, A.A., Kristensen, T.N., Moghadam, N.N., Loeschcke, V., 2015. Experimental Evolution under Fluctuating Thermal Conditions Does Not Reproduce Patterns of Adaptive Clinal Differentiation in Drosophila melanogaster. Am. Nat. 186, 582–593. https://doi.org/10.1086/683252

Ketola, T., Hiltunen, T., 2014. Rapid evolutionary adaptation to elevated salt concentrations in pathogenic freshwater bacteria Serratia marcescens. Ecol. Evol. 4, 3901–3908. https://doi.org/10.1002/ece3.1253

Khatoon, H., Banerjee, S., Yusoff, F.M., Shariff, M., 2010. Effects of salinity on the growth and proximate composition of selected tropical marine periphytic diatoms and cyanobacteria. Aquac. Res. 41, 1348–1355. https://doi.org/10.1111/j.1365-2109.2009.02423.x

Kim, S., Lieberman, T.D., Kishony, R., 2014. Alternating antibiotic treatments constrain evolutionary paths to multidrug resistance. Proc. Natl. Acad. Sci. 111, 14494–14499. https://doi.org/10.1073/pnas.1409800111

Kingsolver, J., Diamond, S., Gomulkiewicz, R., 2014. Curve-Thinking: Understanding Reaction Norms and Developmental Trajectories as Traits, in: Integrative Organismal Biology. John Wiley & Sons, Ltd, pp. 39–53. https://doi.org/10.1002/9781118398814.ch3

Kirkpatrick, M., Heckman, N., 1989. A quantitative genetic model for growth, shape, reaction norms, and other infinite-dimensional characters. J. Math. Biol. 27, 429–450. https://doi.org/10.1007/BF00290638

Kirsch, F., Klähn, S., Hagemann, M., 2019. Salt-Regulated Accumulation of the Compatible Solutes Sucrose and Glucosylglycerol in Cyanobacteria and Its Biotechnological Potential. Front. Microbiol. https://doi.org/10.3389/fmicb.2019.02139

Klaehn, S., Mikkat, S., Riediger, M., Riediger, M., Georg, J., Hess, W.R., Hagemann, M., 2021. Integrative analysis of the salt stress response in cyanobacteria. bioRxiv. https://doi.org/10.1101/2021.07.28.454097

Klähn, S., Mikkat, S., Riediger, M., Georg, J., Hess, W.R., Hagemann, M., 2021. Integrative analysis of the salt stress response in cyanobacteria. Biol. Direct 16, 26. https://doi.org/10.1186/s13062-021-00316-4

Klähn, S., Steglich, C., Hess, W.R., Hagemann, M., 2010. Glucosylglycerate: a secondary compatible solute common to marine cyanobacteria from nitrogen-poor environments. Environ. Microbiol. 12, 83–94. https://doi.org/10.1111/j.1462-2920.2009.02045.x

Klumpp, S., Scott, M., Pedersen, S., Hwa, T., 2013. Molecular crowding limits translation and cell growth. Proc. Natl. Acad. Sci. 110, 16754–16759. https://doi.org/10.1073/pnas.1310377110

Knies, J.L., Izem, R., Supler, K.L., Kingsolver, J.G., Burch, C.L., 2006. The Genetic Basis of Thermal Reaction Norm Evolution in Lab and Natural Phage Populations. PLOS Biol. 4, e201. https://doi.org/10.1371/journal.pbio.0040201

Knies, J.L., Kingsolver, J.G., Burch, C.L., 2009. Hotter Is Better and Broader: Thermal Sensitivity of Fitness in a Population of Bacteriophages. Am. Nat. 173, 419–430. https://doi.org/10.1086/597224

Kobayashi, M., Katoh, H., Ikeuchi, M., 2006. Mutations in a putative chloride efflux transporter gene suppress the chloride requirement of photosystem II in the cytochrome c550-deficient mutant. Plant Cell Physiol. 47, 799–804. https://doi.org/10.1093/pcp/pcj052

Kolman, M. de L.A., Nishi, C.N., Perez-Cenci, M., Graciela L. Salerno, 2015. Sucrose in Cyanobacteria: From a Salt-Response Molecule to Play a Key Role in Nitrogen Fixation. Life. https://doi.org/10.3390/life5010102

Kolman, M. de L.A., Torres, L.L., Martín, M.L., Salerno, G.L., 2012. Sucrose synthase in unicellular cyanobacteria and its relationship with salt and hypoxic stress. Planta. https://doi.org/10.1007/s00425-011-1542-5

Koropatkin, N.M., Koppenaal, D.W., Pakrasi, H.B., Smith, T.J., 2007. The Structure of a Cyanobacterial Bicarbonate Transport Protein, CmpA *. J. Biol. Chem. 282, 2606–2614. https://doi.org/10.1074/jbc.M610222200

Koskella, B., Brockhurst, M.A., 2014. Bacteria–phage coevolution as a driver of ecological and evolutionary processes in microbial communities. FEMS Microbiol. Rev. 38, 916–931. https://doi.org/10.1111/1574-6976.12072

Kothari, A., Vaughn, M., Garcia-Pichel, F., 2013. Comparative genomic analyses of the cyanobacterium, Lyngbya aestuarii BL J, a powerful hydrogen producer. Front. Microbiol. 4.

Kroll, E., Coyle, S., Dunn, B., Koniges, G., Aragon, A., Edwards, J., Rosenzweig, F., 2013. Starvation-Associated Genome Restructuring Can Lead to Reproductive Isolation in Yeast. PLOS ONE 8, e66414. https://doi.org/10.1371/journal.pone.0066414

Lachapelle, J., Bell, G., 2012. Evolutionary rescue of sexual and asexual populations in a deteriorating environment. Evol. Int. J. Org. Evol. 66, 3508–3518. https://doi.org/10.1111/j.1558-5646.2012.01697.x

Lachapelle, J., Bell, G., Colegrave, N., 2015. Experimental adaptation to marine conditions by a freshwater alga. Evolution 69, 2662–2675. https://doi.org/10.1111/evo.12760

Lachapelle, J., Colegrave, N., Bell, G., 2017. The effect of selection history on extinction risk during severe environmental change. J. Evol. Biol. 30, 1872–1883. https://doi.org/10.1111/jeb.13147

Laloknam, S., Tanaka, K., Buaboocha, T., Waditee, R., Incharoensakdi, A., Hibino, T., Tanaka, Y., Takabe, T., 2006. Halotolerant Cyanobacterium Aphanothece halophytica Contains a Betaine Transporter Active at Alkaline pH and High Salinity. Appl. Environ. Microbiol. 72, 6018–6026. https://doi.org/10.1128/AEM.00733-06

Lalonde, S.V., Konhauser, K.O., 2015. Benthic perspective on Earth's oldest evidence for oxygenic photosynthesis. Proc. Natl. Acad. Sci. 112, 995–1000. https://doi.org/10.1073/pnas.1415718112

Latimer, C. a. L., Wilson, R.S., Chenoweth, S.F., 2011. Quantitative genetic variation for thermal performance curves within and among natural populations of Drosophila serrata. J. Evol. Biol. 24, 965–975. https://doi.org/10.1111/j.1420-9101.2011.02227.x

Lee, B.H., Hibino, T., Jo, J., Viale, A.M., Takabe, T., 1997. Isolation and characterization of a dnaK genomic locus in a halotolerant cyanobacterium Aphanothece halophytica. Plant Mol. Biol. 35, 763–775. https://doi.org/10.1023/A:1005867420619

Lee, C.J.D., McMullan, P.E., O'Kane, C.J., Stevenson, A., Santos, I.C., Roy, C., Ghosh, W., Mancinelli, R.L., Mormile, M.R., McMullan, G., Banciu, H.L., Fares, M.A., Benison, K.C., Oren, A., Dyall-Smith, M.L., Hallsworth, J.E., 2018. NaCl-saturated brines are thermodynamically moderate, rather than extreme, microbial habitats. FEMS Microbiol. Rev. 42, 672–693. https://doi.org/10.1093/femsre/fuy026

Lee, Hwanhui, Noh, Y., Hong, S.-J., Lee, Hookeun, Kim, D.-M., Cho, B.-K., Lee, C.-G., Choi, H.-K., 2021. Photosynthetic pigment production and metabolic and lipidomic alterations in the marine cyanobacteria Synechocystis sp. PCC 7338 under various salinity conditions. J. Appl. Phycol. 33, 197–209. https://doi.org/10.1007/s10811-020-02273-3

Lenski, R.E., 2017. Experimental evolution and the dynamics of adaptation and genome evolution in microbial populations. ISME J. 11, 2181–2194. https://doi.org/10.1038/ismej.2017.69

Lenski, R.E., Travisano, M., 1994. Dynamics of adaptation and diversification: a 10,000-generation experiment with bacterial populations. Proc. Natl. Acad. Sci. 91, 6808–6814. https://doi.org/10.1073/pnas.91.15.6808

Lenski, R.E., Wiser, M.J., Ribeck, N., Blount, Z.D., Nahum, J.R., Morris, J.J., Zaman, L., Turner, C.B., Wade, B.D., Maddamsetti, R., Burmeister, A.R., Baird, E.J., Bundy, J., Grant, N.A., Card, K.J., Rowles, M., Weatherspoon, K., Papoulis, S.E., Sullivan, R., Clark, C., Mulka, J.S., Haiela, N., 2015. Sustained fitness gains and variability in fitness trajectories in the long-term evolution experiment with Escherichia coli. Proc. R. Soc. B 282. https://doi.org/10.1098/rspb.2015.2292

Li, Z., Gao, Y., Wang, S., Lu, Y., Sun, K., Jia, J., Wang, Y., 2021. Phytoplankton community response to nutrients along lake salinity and altitude gradients on the Qinghai-Tibet Plateau. Ecol. Indic. 128, 107848. https://doi.org/10.1016/j.ecolind.2021.107848

Liang, Y., Zhang, M., Wang, M., Zhang, W., Qiao, C., Luo, Q., Lu, X., 2020. Freshwater Cyanobacterium Synechococcus elongatus PCC 7942 Adapts to an Environment with Salt Stress via Ion-Induced Enzymatic Balance of Compatible Solutes. Appl. Environ. Microbiol. 86, e02904-19. https://doi.org/10.1128/AEM.02904-19

Lin, C.-S., Wu, J.-T., 2014. Tolerance of soil algae and cyanobacteria to drought stress. J. Phycol. 50, 131–139. https://doi.org/10.1111/jpy.12141

Lockau, W., Pfeffer, S., 1983. ATP-dependent calcium transport in membrane vesicles of the cyanobacterium, Anabaena variabilis. Biochim. Biophys. Acta BBA - Biomembr. 733, 124–132. https://doi.org/10.1016/0005-2736(83)90098-6

Logares, R., Bråte, J., Bertilsson, S., Clasen, J.L., Shalchian-Tabrizi, K., Rengefors, K., 2009. Infrequent marine–freshwater transitions in the microbial world. Trends Microbiol. 17, 414–422. https://doi.org/10.1016/j.tim.2009.05.010

Lu, C., Vonshak, A., 1999. Characterization of PSII photochemistry in salt-adapted cells of cyanobacterium Spirulina platensis. New Phytol. 141, 231–239. https://doi.org/10.1046/j.1469-8137.1999.00340.x

Lu, W.-D., Chi, Z.-M., Su, C.-D., 2006. Identification of glycine betaine as compatible solute in Synechococcus sp. WH8102 and characterization of its N-methyltransferase genes involved in betaine synthesis. Arch. Microbiol. 186, 495–506. https://doi.org/10.1007/s00203-006-0167-8

Ludwig, M., Bryant, D.A., 2012. Synechococcus sp. Strain PCC 7002 Transcriptome: Acclimation to Temperature, Salinity, Oxidative Stress, and Mixotrophic Growth Conditions. Front. Microbiol. 3. https://doi.org/10.3389/fmicb.2012.00354

Lunn, J.E., 2002. Evolution of sucrose synthesis. Plant Physiol. 128, 1490–1500. https://doi.org/10.1104/pp.010898

Lyons, T.W., Reinhard, C.T., Planavsky, N.J., 2014. The rise of oxygen in Earth's early ocean and atmosphere. Nature 506, 307–315. https://doi.org/10.1038/nature13068

Mackay, M.A., Norton, R.S., Borowitzka, L.J., 1984. Organic Osmoregulatory Solutes in Cyanobacteria. Microbiology. https://doi.org/10.1099/00221287-130-9-2177

Manenti, T., Loeschcke, V., Moghadam, N.N., Sørensen, J.G., 2015. Phenotypic plasticity is not affected by experimental evolution in constant, predictable or unpredictable fluctuating thermal environments. J. Evol. Biol. 28, 2078–2087. https://doi.org/10.1111/jeb.12735

Marchetti, M., Capela, D., Glew, M., Cruveiller, S., Chane-Woon-Ming, B., Gris, C., Timmers, T., Poinsot, V., Gilbert, L.B., Heeb, P., Médigue, C., Batut, J., Masson-Boivin, C., 2010. Experimental Evolution of a Plant Pathogen into a Legume Symbiont. PLOS Biol. 8, e1000280. https://doi.org/10.1371/journal.pbio.1000280

Marchetti, M., Clerissi, C., Yousfi, Y., Gris, C., Bouchez, O., Rocha, E., Cruveiller, S., Jauneau, A., Capela, D., Masson-Boivin, C., 2017. Experimental evolution of rhizobia may lead to either extra- or intracellular symbiotic adaptation depending on the selection regime. Mol. Ecol. 26, 1818–1831. https://doi.org/10.1111/mec.13895

Marchetti, M., Jauneau, A., Capela, D., Remigi, P., Gris, C., Batut, J., Masson-Boivin, C., 2014. Shaping Bacterial Symbiosis With Legumes by Experimental Evolution. Mol. Plant-Microbe Interactions® 27, 956–964. https://doi.org/10.1094/MPMI-03-14-0083-R

Marin, K., Stirnberg, M., Eisenhut, M., Krämer, R., Hagemann, M., 2006. Osmotic stress in Synechocystis sp. PCC 6803: low tolerance towards nonionic osmotic stress results from lacking activation of glucosylglycerol accumulation. Microbiology 152, 2023–2030. https://doi.org/10.1099/mic.0.28771-0

Marin, K., Zuther, E., Kerstan, T., Kunert, A., Hagemann, M., 1998. The ggpS Gene from Synechocystis sp. Strain PCC 6803 Encoding Glucosyl-Glycerol-Phosphate Synthase Is Involved in Osmolyte Synthesis. J. Bacteriol. 180, 4843–4849. https://doi.org/10.1128/JB.180.18.4843-4849.1998

Markley, A.L., Begemann, M.B., Clarke, R.E., Gordon, G.C., Pfleger, B.F., 2015. Synthetic Biology Toolbox for Controlling Gene Expression in the Cyanobacterium Synechococcus sp. strain PCC 7002. ACS Synth. Biol. 4, 595–603. https://doi.org/10.1021/sb500260k

Martínez-Noël, G.M.A., Cumino, A.C., de los Angeles Kolman, M., Salerno, G.L., 2013. First evidence of sucrose biosynthesis by single cyanobacterial bimodular proteins. FEBS Lett. 587, 1669–1674. https://doi.org/10.1016/j.febslet.2013.04.012

Martiny, J.B.H., Jones, S.E., Lennon, J.T., Martiny, A.C., 2015. Microbiomes in light of traits: A phylogenetic perspective. Science 350, aac9323. https://doi.org/10.1126/science.aac9323

McDonald, M.J., 2019. Microbial Experimental Evolution – a proving ground for evolutionary theory and a tool for discovery. EMBO Rep. 20, e46992. https://doi.org/10.15252/embr.201846992

Meeks, J.C., Elhai, J., Thiel, T., Potts, M., Larimer, F., Lamerdin, J., Predki, P., Atlas, R., 2001. An overview of the genome of Nostoc punctiforme, a multicellular, symbiotic cyanobacterium. Photosynth. Res. 70, 85–106. https://doi.org/10.1023/A:1013840025518

Mehdizadeh Allaf, M., Peerhossaini, H., 2022. Cyanobacteria: Model Microorganisms and Beyond. Microorganisms 10, 696. https://doi.org/10.3390/microorganisms10040696

Melero-Jiménez, I.J., Martín-Clemente, E., García-Sánchez, M.J., Bañares-España, E., Flores-Moya, A., 2020. The limit of resistance to salinity in the freshwater cyanobacterium Microcystis aeruginosa is modulated by the rate of salinity increase. Ecol. Evol. 10, 5045–5055. https://doi.org/10.1002/ece3.6257

Melero-Jiménez, I.J., Martín-Clemente, E., García-Sánchez, M.J., Flores-Moya, A., Bañares-España, E., 2019. Adaptation of the toxic freshwater cyanobacterium Microcystis aeruginosa to salinity is achieved by the selection of spontaneous mutants. Phycol. Res. 67, 192–201. https://doi.org/10.1111/pre.12370

Melero-Jiménez, I.J., Martín-Clemente, E., Reul, A., García-Sánchez, M.J., Flores-Moya, A., Bañares-España, E., 2022. Dispersal of populations and environmental deterioration rate influence evolutionary rescue under selection by salinity in the freshwater cyanobacterium Microcystis aeruginosa. Eur. J. Phycol. 57, 96–106. https://doi.org/10.1080/09670262.2021.1896787

Miao, X., Wu, Q., Wu, G., Zhao, N., 2003. Sucrose accumulation in salt-stressed cells of agp gene deletion-mutant in cyanobacterium Synechocystis sp. PCC 6803. FEMS Microbiol. Lett. 218, 71–77. https://doi.org/10.1111/j.1574-6968.2003.tb11500.x

Mikkat, S., Effmert, U., Hagemann, M., 1997. Uptake and use of the osmoprotective compounds trehalose, glucosylglycerol, and sucrose by the cyanobacterium Synechocystis sp. PCC6803. Arch. Microbiol. https://doi.org/10.1007/s002030050423

Mikkat, S., Hagemann, M., 2000. Molecular analysis of the ggtBCD gene cluster of Synechocystis sp. strain PCC6803 encoding subunits of an ABC transporter for osmoprotective compounds. Arch. Microbiol. 174, 273–282. https://doi.org/10.1007/s002030000201

Mikkat, S., Hagemann, M., Schoor, A., 1996. Active transport of glucosylglycerol is involved in salt adaptation of the cyanobacterium Synechocystis sp. strain PCC 6803. Microbiology 142, 1725–1732. https://doi.org/10.1099/13500872-142-7-1725

Mikkat, S., Milkowski, C., Hagemann, M., 2000. The gene sll0273 of the cyanobacterium Synechocystis sp. strain PCC6803 encodes a protein essential for growth at low Na+/K+ ratios. Plant Cell Environ. 23, 549–559. https://doi.org/10.1046/j.1365-3040.2000.00565.x

Moisander, P.H., McClinton, E., Paerl, H.W., 2002. Salinity Effects on Growth, Photosynthetic Parameters, and Nitrogenase Activity in Estuarine Planktonic Cyanobacteria. Microb. Ecol. 43, 432–442. https://doi.org/10.1007/s00248-001-1044-2

Moore, D.J., Reed, R.H., Stewart, W.D.P., 1985. Responses of Cyanobacteria to Low Level Osmotic Stress: Implications for the Use of Buffers. Microbiology 131, 1267–1272. https://doi.org/10.1099/00221287-131-6-1267

Mourão, M.A., Hakim, J.B., Schnell, S., 2014. Connecting the Dots: The Effects of Macromolecular Crowding on Cell Physiology. Biophys. J. 107, 2761–2766. https://doi.org/10.1016/j.bpj.2014.10.051

Murik, O., Oren, N., Shotland, Y., Raanan, H., Treves, H., Kedem, I., Keren, N., Hagemann, M., Pade, N., Kaplan, A., 2017. What distinguishes cyanobacteria able to revive after desiccation from those that cannot: the genome aspect. Environ. Microbiol. 19, 535–550. https://doi.org/10.1111/1462-2920.13486

Nakov, T., Boyko, J.D., Alverson, A.J., Beaulieu, J.M., 2017. Models with unequal transition rates favor marine origins of Cyanobacteria and photosynthetic eukaryotes. Proc. Natl. Acad. Sci. 114, E10606–E10607. https://doi.org/10.1073/pnas.1716692114

Nanatani, K., Shijuku, T., Takano, Y., Zulkifli, L., Yamazaki, T., Tominaga, A., Souma, S., Onai, K., Morishita, M., Ishiura, M., Hagemann, M., Suzuki, I., Maruyama, H., Arai, F., Uozumi, N., 2015. Comparative Analysis of kdp and ktr Mutants Reveals Distinct Roles of the Potassium Transporters in the Model Cyanobacterium Synechocystis sp. Strain PCC 6803. J. Bacteriol. 197, 676–687. https://doi.org/10.1128/JB.02276-14

Nikkinen, H.-L., Hakkila, K., Gunnelius, L., Huokko, T., Pollari, M., Tyystjärvi, T., 2012. The SigB σ Factor Regulates Multiple Salt Acclimation Responses of the Cyanobacterium Synechocystis sp. PCC 6803. Plant Physiol. 158, 514–523. https://doi.org/10.1104/pp.111.190058

Nilsson, A.I., Koskiniemi, S., Eriksson, S., Kugelberg, E., Hinton, J.C.D., Andersson, D.I., 2005. Bacterial genome size reduction by experimental evolution. Proc. Natl. Acad. Sci. 102, 12112–12116. https://doi.org/10.1073/pnas.0503654102

Nisbet, E.G., Grassineau, N., Howe, C.J., Abell, P., Regelous, M., Regelous, Marcel, Nisbet, R.E.R., Nisbet, R.E.R., 2007. The age of Rubisco: the evolution of oxygenic photosynthesis. Geobiology. https://doi.org/10.1111/j.1472-4669.2007.00127.x

Ohmori, K., Ehira, S., Kimura, S., Ohmori, M., 2009. Changes in the Amount of Cellular Trehalose, the Activity of Maltooligosyl Trehalose Hydrolase, and the Expression of Its Gene in Response to Salt Stress in the Cyanobacterium *Spirulina platensis*. Microbes Environ. 24, 52–56. https://doi.org/10.1264/jsme2.ME08537

Oliver, T.H., Sánchez-Baracaldo, P., Larkum, A.W.D., Rutherford, A.W., Cardona, T., 2021. time resolved comparative molecular evolution of oxygenic photosynthesis. Biochim. Biophys. Acta. https://doi.org/10.1016/j.bbabio.2021.148400

Oren, A., 2016. Life in Hypersaline Environments. https://doi.org/10.1007/978-3-319-28071-4_8

Oren, A., 2015. Cyanobacteria in hypersaline environments: biodiversity and physiological properties. Biodivers. Conserv. https://doi.org/10.1007/s10531-015-0882-z

Oren, A., 2012. Salts and Brines, in: Whitton, B.A. (Ed.), Ecology of Cyanobacteria II: Their Diversity in Space and Time. Springer Netherlands, Dordrecht, pp. 401–426. https://doi.org/10.1007/978-94-007-3855-3_15

Oren, A., 2011. Thermodynamic limits to microbial life at high salt concentrations. Environ. Microbiol. 13, 1908–1923. https://doi.org/10.1111/j.1462-2920.2010.02365.x

Oren, A., 2002. Diversity of halophilic microorganisms: Environments, phylogeny, physiology, and applications. J. Ind. Microbiol. Biotechnol. 28, 56–63.

Padan, E., Tzubery, T., Herz, K., Kozachkov, L., Rimon, A., Galili, L., 2004. NhaA of Escherichia coli, as a model of a pH-regulated Na+/H+ antiporter. Biochim. Biophys. Acta BBA - Bioenerg., EBEC 2004 1658, 2–13. https://doi.org/10.1016/j.bbabio.2004.04.018

Pade, N., Compaoré, J., Klähn, S., Stal, L.J., Hagemann, M., 2012. The marine cyanobacterium Crocosphaera watsonii WH8501 synthesizes the compatible solute trehalose by a laterally acquired OtsAB fusion protein. Environ. Microbiol. 14, 1261–1271. https://doi.org/10.1111/j.1462-2920.2012.02709.x

Pade, N., Michalik, D., Ruth, W., Belkin, N., Hess, W.R., Berman-Frank, I., Hagemann, M., 2016. Trimethylated homoserine functions as the major compatible solute in the globally significant oceanic cyanobacterium Trichodesmium. Proc. Natl. Acad. Sci. 113, 13191–13196. https://doi.org/10.1073/pnas.1611666113

Pagel, M., 1999. Inferring the historical patterns of biological evolution. Nature 401, 877–884. https://doi.org/10.1038/44766

Page-Sharp, M., Behm, C.A., Smith, G.D., 1999. Involvement of the compatible solutes trehalose and sucrose in the response to salt stress of a cyanobacterial Scytonema species isolated from desert soils. Biochim. Biophys. Acta BBA - Gen. Subj. 1472, 519–528. https://doi.org/10.1016/S0304-4165(99)00155-5

Pandey, P.K., Singh, B.B., Mishra, R., Bisen, P.S., 1996. Ca2+ Uptake and Its Regulation in the Cyanobacterium Nostoc MAC. Curr. Microbiol. 32, 332–335. https://doi.org/10.1007/s002849900059

Pandey, U., Chatterjee, C., 1999. Response of two strains of Nostoc muscorum to metal stress and salinity. Ann. Appl. Biol. 134, 259–263. https://doi.org/10.1111/j.1744-7348.1999.tb05262.x

Pandhal, J., Ow, S.Y., Wright, P.C., Biggs, C.A., 2009. Comparative Proteomics Study of Salt Tolerance between a Nonsequenced Extremely Halotolerant Cyanobacterium and Its Mildly Halotolerant Relative Using in vivo Metabolic Labeling and in vitro Isobaric Labeling. J. Proteome Res. 8, 818–828. https://doi.org/10.1021/pr800283q

Panou, M., Gkelis, S., 2022. Unravelling unknown cyanobacteria diversity linked with HCN production. Mol. Phylogenet. Evol. 166, 107322. https://doi.org/10.1016/j.ympev.2021.107322

Paver, S.F., Muratore, D., Newton, R.J., Coleman, M.L., 2018. Reevaluating the Salty Divide: Phylogenetic Specificity of Transitions between Marine and Freshwater Systems. mSystems 3, e00232-18. https://doi.org/10.1128/mSystems.00232-18

Pennell, M.W., Eastman, J.M., Slater, G.J., Brown, J.W., Uyeda, J.C., FitzJohn, R.G., Alfaro, M.E., Harmon, L.J., 2014. geiger v2.0: an expanded suite of methods for fitting macroevolutionary models to phylogenetic trees. Bioinformatics 30, 2216–2218. https://doi.org/10.1093/bioinformatics/btu181

Perez-Cenci, M., Salerno, G.L., 2014. Functional characterization of Synechococcus amylosucrase and fructokinase encoding genes discovers two novel actors on the stage of cyanobacterial sucrose metabolism. Plant Sci. 224, 95–102. https://doi.org/10.1016/j.plantsci.2014.04.003

Perrineau, M.-M., Zelzion, E., Gross, J., Price, D.C., Boyd, J., Bhattacharya, D., 2014. Evolution of salt tolerance in a laboratory reared population of Chlamydomonas reinhardtii. Environ. Microbiol. 16, 1755–1766. https://doi.org/10.1111/1462-2920.12372

Piotrowski, J.S., Nagarajan, S., Kroll, E., Stanbery, A., Chiotti, K.E., Kruckeberg, A.L., Dunn, B., Sherlock, G., Rosenzweig, F., 2012. Different selective pressures lead to different genomic outcomes as newly-formed hybrid yeasts evolve. BMC Evol. Biol. 12, 46. https://doi.org/10.1186/1471-2148-12-46

Planavsky, N.J., Asael, D., Hofmann, A., Reinhard, C.T., Lalonde, S.V., Andrew Knudsen, Xiangli Wang, Frantz Ossa Ossa, Ernesto Pecoits, Albertus J.B. Smith, Nicolas J. Beukes, Andrey Bekker, Thomas Martin Johnson, Kurt O. Konhauser, Timothy W. Lyons, Olivier Rouxel, 2014. Evidence for oxygenic photosynthesis half a billion years before the Great Oxidation Event. Nat. Geosci. https://doi.org/10.1038/ngeo2122

Pohland, A.-C., Schneider, D., 2019. Mg2+ homeostasis and transport in cyanobacteria – at the crossroads of bacterial and chloroplast Mg2+ import. Biol. Chem. 400, 1289–1301. https://doi.org/10.1515/hsz-2018-0476

Pontis, H.G., Vargas, W.A., Salerno, G.L., 2007. Structural characterization of the members of a polymer series, compatible solutes in Anabaena cells exposed to salt stress. Plant Sci. 172, 29–35. https://doi.org/10.1016/j.plantsci.2006.07.007

Popelková, H., Yocum, C.F., 2007. Current status of the role of Cl− ion in the oxygen-evolving complex. Photosynth. Res. 93, 111–121. https://doi.org/10.1007/s11120-006-9121-5

Porchia, A.C., Salerno, G.L., 1996. Sucrose biosynthesis in a prokaryotic organism: Presence of two sucrose-phosphate synthases in Anabaena with remarkable differences compared with the plant enzymes. Proc. Natl. Acad. Sci. U. S. A. https://doi.org/10.1073/pnas.93.24.13600

Potts, M., Friedmann, E.I., 1981. Effects of water stress on cryptoendolithic cyanobacteria from hot desert rocks. Arch. Microbiol. 130, 267–271. https://doi.org/10.1007/BF00425938

Puente-Sánchez, F., Arce-Rodríguez, A., Oggerin, M., García-Villadangos, M., Moreno-Paz, M., Blanco, Y., Rodríguez, N., Bird, L., Lincoln, S.A., Tornos, F., Prieto-Ballesteros, O., Freeman, K.H., Pieper, D.H., Timmis, K.N., Amils, R., Parro, V., 2018. Viable cyanobacteria in the deep continental subsurface. Proc. Natl. Acad. Sci. 115, 10702–10707. https://doi.org/10.1073/pnas.1808176115

Rasouli-Dogaheh, S., Komárek, J., Chatchawan, T., Hauer, T., 2022. Thainema gen. nov. (Leptolyngbyaceae, Synechococcales): A new genus of simple trichal cyanobacteria isolated from a solar saltern environment in Thailand. PLOS ONE 17, e0261682. https://doi.org/10.1371/journal.pone.0261682

Ratcliff, W.C., Denison, R.F., Borrello, M., Travisano, M., 2012. Experimental evolution of multicellularity. Proc. Natl. Acad. Sci. 109, 1595–1600. https://doi.org/10.1073/pnas.1115323109

Ratcliff, W.C., Fankhauser, J.D., Rogers, D.W., Greig, D., Travisano, M., 2015. Origins of multicellular evolvability in snowflake yeast. Nat. Commun. 6, 6102. https://doi.org/10.1038/ncomms7102

Reed, R.H., Stewart, W.D.P., 1985. Osmotic adjustment and organic solute accumulation in unicellular cyanobacteria from freshwater and marine habitats. Mar. Biol. https://doi.org/10.1007/bf00393037

Reed, R.H., Warr, S.R.C., Kerby, N.W., Stewart, W.D.P., 1986. Osmotic shock-induced release of low molecular weight metabolites from free-living and immobilized cyanobacteria. Enzyme Microb. Technol. https://doi.org/10.1016/0141-0229(86)90080-3

Reed, R.H., Warr, S.R.C., Richardson, D.L., Moore, D.J., Stewart, W.D.P., 1985. Multiphasic osmotic adjustment in a euryhaline cyanobacterium. Fems Microbiol. Lett. https://doi.org/10.1111/j.1574-6968.1985.tb00796.x

Revell, L.J., 2012. phytools: an R package for phylogenetic comparative biology (and other things). Methods Ecol. Evol. 3. https://doi.org/10.1111/j.2041-210X.2011.00169.x

Rezayian, M., Niknam, V., Faramarzi, M.A., 2019. Antioxidative responses of Nostoc ellipsosporum and Nostoc piscinale to salt stress. J. Appl. Phycol. 31, 157–169. https://doi.org/10.1007/s10811-018-1506-2

Rezayian, M., Niknam, V., Faramarzi, M.A., 2017. Effect of salinity on some physiological and biochemical responses in the cyanobacterium Synechococcus elongatus. Prog. Biol. Sci. 7, 67–77. https://doi.org/10.22059/pbs.2018.230997.1260

Rippka, R., Deruelles, J., Waterbury, J.B., Herdman, M., Stanier, R.Y., 1979. Generic Assignments, Strain Histories and Properties of Pure Cultures of Cyanobacteria. Microbiology, 111, 1–61. https://doi.org/10.1099/00221287-111-1-1

Ritchie, R.J., 1992. Sodium Transport and the Origin of the Membrane Potential in the Cyanobacterium Synechococcus R-2 (Anacystis Nidulans) PCC 7942. J. Plant Physiol. 139, 320–330. https://doi.org/10.1016/S0176-1617(11)80345-7

Rosales, N., Ortega, J., Mora, R., Morales, E., 2005. Influence of salinity on the growth and biochemical composition of the cyanobacterium Synechococcus sp. Cienc. Mar. 31, 349–355. https://doi.org/10.7773/cm.v31i2.59

Rosing, M.T., Frei, R., 2004. U-rich Archaean sea-floor sediments from Greenland - indications of >3700 Ma oxygenic photosynthesis. Earth Planet. Sci. Lett. https://doi.org/10.1016/s0012-821x(03)00609-5

Roy, S., 1999. Multifunctional enzymes and evolution of biosynthetic pathways: Retro-evolution by jumps. Proteins Struct. Funct. Bioinforma. 37, 303–309. https://doi.org/10.1002/(SICI)1097-0134(19991101)37:2<303::AID-PROT15>3.0.CO;2-6

Ruangsomboon, S., 2014. Effect of Media and Salinity on Lipid Content of Cyanobacterium Hapalosiphon sp. Chiang Mai J Sci 41, 9.

Sakamoto, T., Kumihashi, K., Kunita, S., Masaura, T., Inoue-Sakamoto, K., Yamaguchi, M., 2011. The extracellular-matrix-retaining cyanobacterium Nostoc verrucosum accumulates trehalose, but is sensitive to desiccation. FEMS Microbiol. Ecol. 77, 385–394. https://doi.org/10.1111/j.1574-6941.2011.01114.x

Sakamoto, T., Yoshida, T., Arima, H., Hatanaka, Y., Takani, Y., Tamaru, Y., 2009. Accumulation of trehalose in response to desiccation and salt stress in the terrestrial cyanobacterium Nostoc commune. Phycol. Res. 57, 66–73. https://doi.org/10.1111/j.1440-1835.2008.00522.x

Salerno, G.L., Porchia, A.C., Vargas, W.A., Abdian, P.L., 2004. Fructose-containing oligosaccharides: novel compatible solutes in Anabaena cells exposed to salt stress. Plant Sci. 167, 1003–1008. https://doi.org/10.1016/j.plantsci.2004.05.029

Samani, P., Bell, G., 2010. Adaptation of experimental yeast populations to stressful conditions in relation to population size. J. Evol. Biol. 23, 791–796. https://doi.org/10.1111/j.1420-9101.2010.01945.x

Sánchez-Baracaldo, P., 2015. Origin of marine planktonic cyanobacteria. Sci. Rep. 5, 1–10. https://doi.org/10.1038/srep17418

Sánchez-Baracaldo, P., Bianchini, G., Huelsenbeck, J.P., Raven, J.A., Pisani, D., Knoll, A.H., 2017a. Reply to Nakov et al.: Model choice requires biological insight when studying the ancestral habitat of photosynthetic eukaryotes. Proc. Natl. Acad. Sci. 114, E10608–E10609. https://doi.org/10.1073/pnas.1717417114

Sánchez-Baracaldo, P., Bianchini, G., Wilson, J.D., Knoll, A.H., 2021. Cyanobacteria and biogeochemical cycles through Earth history. Trends Microbiol. 0. https://doi.org/10.1016/j.tim.2021.05.008

Sánchez-Baracaldo, P., Cardona, T., 2020. On the origin of oxygenic photosynthesis and Cyanobacteria. New Phytol. 225, 1440–1446. https://doi.org/10.1111/nph.16249

Sánchez-Baracaldo, P., Hayes, P.K., Blank, C.E., 2005. Morphological and habitat evolution in the Cyanobacteria using a compartmentalization approach. Geobiology 3, 145–165. https://doi.org/10.1111/j.1472-4669.2005.00050.x

Sánchez-Baracaldo, P., Raven, J.A., Pisani, D., Knoll, A.H., 2017b. Early photosynthetic eukaryotes inhabited low-salinity habitats. Proc. Natl. Acad. Sci. 114, E7737–E7745. https://doi.org/10.1073/pnas.1620089114

Sánchez-Baracaldo, P., Ridgwell, A., Raven, J.A., 2014. A Neoproterozoic Transition in the Marine Nitrogen Cycle. Curr. Biol. 24, 652–657. https://doi.org/10.1016/j.cub.2014.01.041

Scanlan, D.J., Ostrowski, M., Mazard, S., Dufresne, A., Garczarek, L., Hess, W.R., Post, A.F., Hagemann, M., Paulsen, I., Partensky, F., 2009. Ecological Genomics of Marine Picocyanobacteria. Microbiol. Mol. Biol. Rev. 73, 249–299. https://doi.org/10.1128/MMBR.00035-08

Schirrmeister, B.E., Gugger, M., Donoghue, P.C.J., 2015. Cyanobacteria and the Great Oxidation Event: evidence from genes and fossils. Palaeontology 58, 769–785. https://doi.org/10.1111/pala.12178

Schirrmeister, B.E., Sanchez-Baracaldo, P., Wacey, D., 2016. Cyanobacterial evolution during the Precambrian. Int. J. Astrobiol. 15, 187–204. https://doi.org/10.1017/S1473550415000579

Schliep, K.P., 2011. phangorn: phylogenetic analysis in R. Bioinformatics 27, 592–593. https://doi.org/10.1093/bioinformatics/btq706

Schmit, J.D., Kamber, E., Kondev, J., 2009. Lattice Model of Diffusion-Limited Bimolecular Chemical Reactions in Confined Environments. Phys. Rev. Lett. 102, 218302. https://doi.org/10.1103/PhysRevLett.102.218302

Schopf, J.W., 2011. The paleobiological record of photosynthesis. Photosynth. Res. 107, 87–101. https://doi.org/10.1007/s11120-010-9577-1

Schubert, H., Hagemann, M., 1990. Salt effects on 77K fluorescence and photosynthesis in the cyanobacterium Synechocystis sp. PCC 6803. FEMS Microbiol. Lett. 71, 169–172. https://doi.org/10.1111/j.1574-6968.1990.tb03817.x

Schwartz, S.H., Black, T.A., Jäger, K., Panoff, J.-M., Wolk, C.P., 1998. Regulation of an Osmoticum-Responsive Gene in Anabaena sp. Strain PCC 7120. J. Bacteriol. 180, 6332–6337.

Shang, J.-L., Chen, M., Hou, S., Li, T., Yang, Y.-W., Li, Q., Jiang, H.-B., Dai, G.-Z., Zhang, Z.-C., Hess, W.R., Qiu, B.-S., 2019. Genomic and transcriptomic insights into the survival of the subaerial cyanobacterium Nostoc flagelliforme in arid and exposed habitats. Environ. Microbiol. 21, 845–863. https://doi.org/10.1111/1462-2920.14521

Shen, J.-R., Qian, M., Inoue, Y., Burnap, R.L., 1998. Functional Characterization of Synechocystis sp. PCC 6803 ΔpsbU and ΔpsbV Mutants Reveals Important Roles of Cytochrome c-550 in Cyanobacterial Oxygen Evolution. Biochemistry 37, 1551–1558. https://doi.org/10.1021/bi971676i

Shih, P.M., Hemp, J., Ward, L.M., Matzke, N.J., Fischer, W.W., 2017. Crown group Oxyphotobacteria postdate the rise of oxygen. Geobiology 15, 19–29. https://doi.org/10.1111/gbi.12200

Shimura, Y., Hirose, Y., Misawa, N., Osana, Y., Katoh, H., Yamaguchi, H., Kawachi, M., 2015. Comparison of the terrestrial cyanobacterium Leptolyngbya sp. NIES-2104 and the freshwater Leptolyngbya boryana PCC 6306 genomes. DNA Res. 22, 403–412. https://doi.org/10.1093/dnares/dsv022

Sinetova, M.A., Červený, J., Zavřel, T., Nedbal, L., 2012. On the dynamics and constraints of batch culture growth of the cyanobacterium Cyanothece sp. ATCC 51142. J. Biotechnol., Photosynthetic microorganisms for bio-fuel production from sun light 162, 148–155. https://doi.org/10.1016/j.jbiotec.2012.04.009

Singh, D.P., Kshatriya, K., 2002. Characterization of Salinity-Tolerant Mutant of Anabaena doliolum Exhibiting Multiple Stress Tolerance. Curr. Microbiol. 45, 165–170. https://doi.org/10.1007/s00284-001-0112-7

Singh, R.P., Yadav, P., Kujur, R., Pandey, K.D., Gupta, R., 2022. Cyanobacteria and salinity stress tolerance. https://doi.org/10.1016/b978-0-323-90634-0.00003-2

Skoracka, A., Laska, A., Radwan, J., Konczal, M., Lewandowski, M., Puchalska, E., Karpicka-Ignatowska, K., Przychodzka, A., Raubic, J., Kuczyński, L., 2022. Effective specialist or jack of all trades? Experimental evolution of a crop pest in fluctuating and stable environments. Evol. Appl. 15, 1639–1652. https://doi.org/10.1111/eva.13360

Slater, G.J., Harmon, L.J., Alfaro, M.E., 2012. Integrating Fossils with Molecular Phylogenies Improves Inference of Trait Evolution. Evolution 66, 3931–3944. https://doi.org/10.1111/j.1558-5646.2012.01723.x

Snel, B., Huynen, M.A., 2004. Quantifying Modularity in the Evolution of Biomolecular Systems. Genome Res. 14, 391–397. https://doi.org/10.1101/gr.1969504

So, A.K., Kassam, A., Espie, G.S., 1998. Na+-dependent HCO3- transport in the cyanobacterium Synechocystis PCC6803. Can. J. Bot. 76, 1084–1091. https://doi.org/10.1139/b98-071

Soo, R.M., Hemp, J., Parks, D.H., Fischer, W.W., Hugenholtz, P., 2017. On the origins of oxygenic photosynthesis and aerobic respiration in Cyanobacteria. Science. https://doi.org/10.1126/science.aal3794

Soontharapirakkul, K., Incharoensakdi, A., 2010. Na+-stimulated ATPase of alkaliphilic halotolerant cyanobacterium Aphanothece halophytica translocates Na+ into proteoliposomes via Na+ uniport mechanism. BMC Biochem. 11, 30–30. https://doi.org/10.1186/1471-2091-11-30

Stam, W.T., Holleman, H.C., 1979. Cultures of Phormidium, Plectonema, Lyngbya and Synechococcus (Cyanophyceae) Under Different Conditions: Their Growth and Morphological Variability. Acta Bot. Neerlandica 28, 45–66. https://doi.org/10.1111/j.1438-8677.1979.tb01155.x

Stam, W.T., Holleman, H.C., 1975. The Influence of Different Salinities on Growth and Morphological Variability of a Number of Phormidium Strains (Cyanophyceae) in Culture. Acta Bot. Neerlandica 24, 379–390. https://doi.org/10.1111/j.1438-8677.1975.tb01028.x

Stanier, R.Y., Cohen-Bazire, G., 1977. Phototrophic Prokaryotes: The Cyanobacteria. Annu. Rev. Microbiol. 31, 225–274. https://doi.org/10.1146/annurev.mi.31.100177.001301

Starkenburg, S.R., Reitenga, K.G., Freitas, T., Johnson, S., Chain, P.S.G., Garcia-Pichel, F., Kuske, C.R., 2011. Genome of the Cyanobacterium Microcoleus vaginatusFGP-2, a Photosynthetic Ecosystem Engineer of Arid Land Soil Biocrusts Worldwide. J. Bacteriol. 193, 4569–4570. https://doi.org/10.1128/JB.05138-11

Stinchcombe, J.R., Kirkpatrick, M., 2012. Genetics and evolution of function-valued traits: understanding environmentally responsive phenotypes. Trends Ecol. Evol. 27, 637–647. https://doi.org/10.1016/j.tree.2012.07.002

Stirnberg, M., Fulda, S., Huckauf, J., Hagemann, M., Krämer, R., Marin, K., 2007. A membrane-bound FtsH protease is involved in osmoregulation in Synechocystis sp. PCC 6803: the compatible solute synthesizing enzyme GgpS is one of the targets for proteolysis. Mol. Microbiol. 63, 86–102. https://doi.org/10.1111/j.1365-2958.2006.05495.x

Stulp, B.K., Stam, W.T., 1984. Growth and morphology of Anabaena strains (Cyanophyceae, Cyanobacteria) in cultures under different salinities. Br. Phycol. J. 19, 281–286. https://doi.org/10.1080/00071618400650301

Swanner, E.D., Mloszewska, A.M., Cirpka, O.A., Schoenberg, R., Konhauser, K.O., Kappler, A., 2015. Modulation of oxygen production in Archaean oceans by episodes of Fe(II) toxicity. Nat. Geosci. 8, 126–130. https://doi.org/10.1038/ngeo2327

The Functional Phylogenies Group, 2012. Phylogenetic inference for function-valued traits: speech sound evolution. Trends Ecol. Evol. 27, 160–166. https://doi.org/10.1016/j.tree.2011.10.001

Tittes, S.B., Walker, J.F., Torres-Martínez, L., Emery, N.C., 2019. Grow Where You Thrive, or Where Only You Can Survive? An Analysis of Performance Curve Evolution in a Clade with Diverse Habitat Affinities. Am. Nat. 193. https://doi.org/10.1086/701827

Tonk, L., Bosch, K., Visser, P., Huisman, J., 2007. Salt tolerance of the harmful cyanobacterium Microcystis aeruginosa. Aquat. Microb. Ecol. 46, 117–123. https://doi.org/10.3354/ame046117

Travisano, M., Mongold, J.A., Bennett, A.F., Lenski, R.E., 1995. Experimental Tests of the Roles of Adaptation, Chance, and History in Evolution. Science 267, 87–90. https://doi.org/10.1126/science.7809610

Tsunekawa, K., Shijuku, T., Hayashimoto, M., Kojima, Y., Onai, K., Morishita, M., Ishiura, M., Kuroda, T., Nakamura, T., Kobayashi, H., Sato, M., Toyooka, K., Matsuoka, K., Omata, T., Uozumi, N., 2009. Identification and Characterization of the Na+/H+ Antiporter NhaS3 from the Thylakoid Membrane of Synechocystis sp. PCC 6803 *. J. Biol. Chem. 284, 16513–16521. https://doi.org/10.1074/jbc.M109.001875

Urrejola, C., Alcorta, J., Salas, L., Vásquez, M., Polz, M.F., Vicuña, R., Díez, B., 2019. Genomic Features for Desiccation Tolerance and Sugar Biosynthesis in the Extremophile Gloeocapsopsis sp. UTEX B3054. Front. Microbiol. 10.

Uyeda, J.C., Hansen, T.F., Arnold, S.J., Pienaar, J., 2011. The million-year wait for macroevolutionary bursts. Proc. Natl. Acad. Sci. 108, 15908–15913. https://doi.org/10.1073/pnas.1014503108

Uyeda, J.C., Harmon, L.J., Blank, C.E., 2016. A Comprehensive Study of Cyanobacterial Morphological and Ecological Evolutionary Dynamics through Deep Geologic Time. PLOS ONE 11, e0162539. https://doi.org/10.1371/journal.pone.0162539

Vermeij, G.J., Dudley, R., 2000. Why are there so few evolutionary transitions between aquatic and terrestrial ecosystems? Biol. J. Linn. Soc. 70, 541–554. https://doi.org/10.1111/j.1095-8312.2000.tb00216.x

Voß, B., Bolhuis, H., Fewer, D.P., Kopf, M., Möke, F., Haas, F., El-Shehawy, R., Hayes, P., Bergman, B., Sivonen, K., Dittmann, E., Scanlan, D.J., Hagemann, M., Stal, L.J., Hess, W.R., 2013. Insights into the Physiology and Ecology of the Brackish-Water-Adapted Cyanobacterium Nodularia spumigena CCY9414 Based on a Genome-Transcriptome Analysis. PLOS ONE 8, e60224. https://doi.org/10.1371/journal.pone.0060224

Waditee, R., Buaboocha, T., Kato, M., Hibino, T., Suzuki, S., Shigetoshi Suzuki, Nakamura, T., Takabe, T., 2006. Carboxyl-terminal hydrophilic tail of a NhaP type Na+/H+ antiporter from cyanobacteria is involved in the apparent affinity for Na+ and pH sensitivity. Arch. Biochem. Biophys. 450, 113–121. https://doi.org/10.1016/j.abb.2006.02.013

Waditee, R., Hibino, T., Nakamura, T., Incharoensakdi, A., Takabe, T., 2002. Overexpression of a Na+/H+ antiporter confers salt tolerance on a freshwater cyanobacterium, making it capable of growth in sea water. Proc. Natl. Acad. Sci. 99, 4109–4114. https://doi.org/10.1073/pnas.052576899

Waditee, R., Hibino, T., Tanaka, Y., Nakamura, T., Incharoensakdi, A., Takabe, T., 2001. Halotolerant cyanobacterium Aphanothece halophytica contains an Na(+)/H(+) antiporter, homologous to eukaryotic ones, with novel ion specificity affected by C-terminal tail. J. Biol. Chem. 276, 36931–36938. https://doi.org/10.1074/jbc.M103650200

Waditee, R., Tanaka, Y., Aoki, K., Hibino, T., Jikuya, H., Takano, J., Takabe, Tetsuko, Takabe, Teruhiro, 2003. Isolation and functional characterization of N-methyltransferases that catalyze betaine synthesis from glycine in a halotolerant photosynthetic organism Aphanothece halophytica. J. Biol. Chem. 278, 4932–4942. https://doi.org/10.1074/jbc.M210970200

Wang, H.-L., Postier, B.L., Burnap, R.L., 2002. Polymerase chain reaction-based mutageneses identify key transporters belonging to multigene families involved in Na+ and pH homeostasis of Synechocystis sp. PCC 6803. Mol. Microbiol. 44, 1493–1506. https://doi.org/10.1046/j.1365-2958.2002.02983.x

Ward, L.M., Kirschvink, J.L., Fischer, W.W., 2016. Timescales of Oxygenation Following the Evolution of Oxygenic Photosynthesis. Orig. Life Evol. Biospheres. https://doi.org/10.1007/s11084-015-9460-3

Weeks, E.R., Crocker, J.C., Levitt, A.C., Schofield, A., Weitz, D.A., 2000. Three-Dimensional Direct Imaging of Structural Relaxation Near the Colloidal Glass Transition. Science 287, 627–631. https://doi.org/10.1126/science.287.5453.627

Wenger, J.W., Piotrowski, J., Nagarajan, S., Chiotti, K., Sherlock, G., Rosenzweig, F., 2011. Hunger Artists: Yeast Adapted to Carbon Limitation Show Trade-Offs under Carbon Sufficiency. PLOS Genet. 7, e1002202. https://doi.org/10.1371/journal.pgen.1002202

Wever, A.D., Benzerara, K., Coutaud, M., Caumes, G., Poinsot, M., Skouri-Panet, F., Laurent, T., Duprat, E., Gugger, M., 2019. Evidence of high Ca uptake by cyanobacteria forming intracellular CaCO3 and impact on their growth. Geobiology 17, 676–690. https://doi.org/10.1111/gbi.12358

Whittle, A., Barnett, R.L., Charman, D.J., Gallego-Sala, A.V., 2021. Low-salinity transitions drive abrupt microbial response to sea-level change. Ecol. Lett. n/a. https://doi.org/10.1111/ele.13893

Whitton, B.A. (Ed.), 2012. Ecology of Cyanobacteria II: Their Diversity in Space and Time. Springer Netherlands, Dordrecht. https://doi.org/10.1007/978-94-007-3855-3

Whitton, B.A., Potts, M., 2012. Introduction to the Cyanobacteria, in: Whitton, B.A. (Ed.), Ecology of Cyanobacteria II: Their Diversity in Space and Time. Springer Netherlands, Dordrecht. https://doi.org/10.1007/978-94-007-3855-3

Wilmeth, D.T., Corsetti, F.A., Beukes, N.J., Awramik, S.M., Petryshyn, V., Spear, J.R., Celestian, A.J., 2019. Neoarchean (2.7 Ga) lacustrine stromatolite deposits in the Hartbeesfontein Basin, Ventersdorp Supergroup, South Africa: Implications for oxygen oases. Precambrian Res. 320, 291–302. https://doi.org/10.1016/j.precamres.2018.11.009

Wiser, M.J., Ribeck, N., Lenski, R.E., 2013. Long-Term Dynamics of Adaptation in Asexual Populations. Science 342, 1364–1367. https://doi.org/10.1126/science.1243357

Wu, S., He, L., Shen, R., Zhang, X., Wang, Q., 2011. Molecular Cloning of Maltooligosyltrehalose Trehalohydrolase Gene from Nostoc flagelliforme and Trehalose-Related Response to Stresses. J. Microbiol. Biotechnol. 21, 830–837. https://doi.org/10.4014/jmb.1101.10068

Wutipraditkul, N., Waditee, R., Incharoensakdi, A., Hibino, T., Tanaka, Y., Nakamura, T., Shikata, M., Takabe, Tetsuko, Takabe, Teruhiro, 2005. Halotolerant Cyanobacterium Aphanothece halophytica Contains NapA-Type Na+/H+ Antiporters with Novel Ion Specificity That Are Involved in Salt Tolerance at Alkaline pH. Appl. Environ. Microbiol. 71, 4176–4184. https://doi.org/10.1128/AEM.71.8.4176-4184.2005

Xu, H.-F., Raanan, H., Dai, G.-Z., Oren, N., Berkowicz, S., Murik, O., Kaplan, A., Qiu, B.-S., 2021. Reading and surviving the harsh conditions in desert biological soil crust: the cyanobacterial viewpoint. FEMS Microbiol. Rev. 45, fuab036. https://doi.org/10.1093/femsre/fuab036

Yadav, R.K., Tripathi, K., Varghese, E., Abraham, G., 2021. Physiological and Proteomic Studies of the Cyanobacterium Anabaena sp. Acclimated to Desiccation Stress. Curr. Microbiol. 78, 2429–2439. https://doi.org/10.1007/s00284-021-02504-x

Yang, H.W., Song, J.Y., Cho, S.M., Kwon, H.C., Kwon, H.C., Pan, C.-H., Park, Y.-I., 2020. Genomic Survey of Salt Acclimation-Related Genes in the Halophilic Cyanobacterium Euhalothece sp. Z-M001. Sci. Rep. https://doi.org/10.1038/s41598-020-57546-1

Yoshida, T., Sakamoto, T., 2009. Water-stress induced trehalose accumulation and control of trehalase in the cyanobacterium <I>Nostoc punctiforme </I>IAM M-15. J. Gen. Appl. Microbiol. 55, 135–145. https://doi.org/10.2323/jgam.55.135

Yoshimura, H., Okamoto, S., Tsumuraya, Y., Ohmori, M., 2007. Group 3 sigma factor gene, sigJ, a key regulator of desiccation tolerance, regulates the synthesis of extracellular polysaccharide in cyanobacterium Anabaena sp. strain PCC 7120. DNA Res. 14, 13–24. https://doi.org/10.1093/dnares/dsm003

Zavřel, T., Schoffman, H., Lukeš, M., Fedorko, J., Keren, N., Červený, J., 2021. Monitoring fitness and productivity in cyanobacteria batch cultures. Algal Res. 56, 102328. https://doi.org/10.1016/j.algal.2021.102328

Zhou, A., Baidoo, E., He, Z., Mukhopadhyay, A., Baumohl, J.K., Benke, P., Joachimiak, M.P., Xie, M., Song, R., Arkin, A.P., Hazen, T.C., Keasling, J.D., Wall, J.D., Stahl, D.A., Zhou, J., 2013. Characterization of NaCl tolerance in Desulfovibrio vulgaris

Hildenborough through experimental evolution. ISME J. 7, 1790–1802. https://doi.org/10.1038/ismej.2013.60

Zhou, A., Hillesland, K.L., He, Z., Schackwitz, W., Tu, Q., Zane, G.M., Ma, Q., Qu, Y., Stahl, D.A., Wall, J.D., Hazen, T.C., Fields, M.W., Arkin, A.P., Zhou, J., 2015. Rapid selective sweep of pre-existing polymorphisms and slow fixation of new mutations in experimental evolution of Desulfovibrio vulgaris. ISME J. 9, 2360–2372. https://doi.org/10.1038/ismej.2015.45

Zhou, A., Lau, R., Baran, R., Ma, J., Netzer, F. von, Shi, W., Gorman-Lewis, D., Kempher, M.L., He, Z., Qin, Y., Shi, Z., Zane, G.M., Wu, L., Bowen, B.P., Northen, T.R., Hillesland, K.L., Stahl, D.A., Wall, J.D., Arkin, A.P., Zhou, J., 2017. Key Metabolites and Mechanistic Changes for Salt Tolerance in an Experimentally Evolved Sulfate-Reducing Bacterium, Desulfovibrio vulgaris. mBio 8. https://doi.org/10.1128/mBio.01780-17

Zimmerman, S.B., Trach, S.O., 1991. Estimation of macromolecule concentrations and excluded volume effects for the cytoplasm of Escherichia coli. J. Mol. Biol. 222, 599–620. https://doi.org/10.1016/0022-2836(91)90499-V

Appendices

Appendix A

Supplemental Methods

Boundary method testing: To test the effects of the different boundary methods we implemented, we conducted BM and OU simulations across the maximum clade credibility tree using both boundary methods. The absorbing method took any trait value that exceeded the boundaries and set the value at that node to be the boundary limit that it had exceeded. The reflecting method took any trait value that exceeded the boundaries and set the value to be equally far from the boundary in the opposite direction. Comparisons of the simulations using each method can be seen in Supplemental Figures 1 and 2 for the BM and OU simulations respectively.

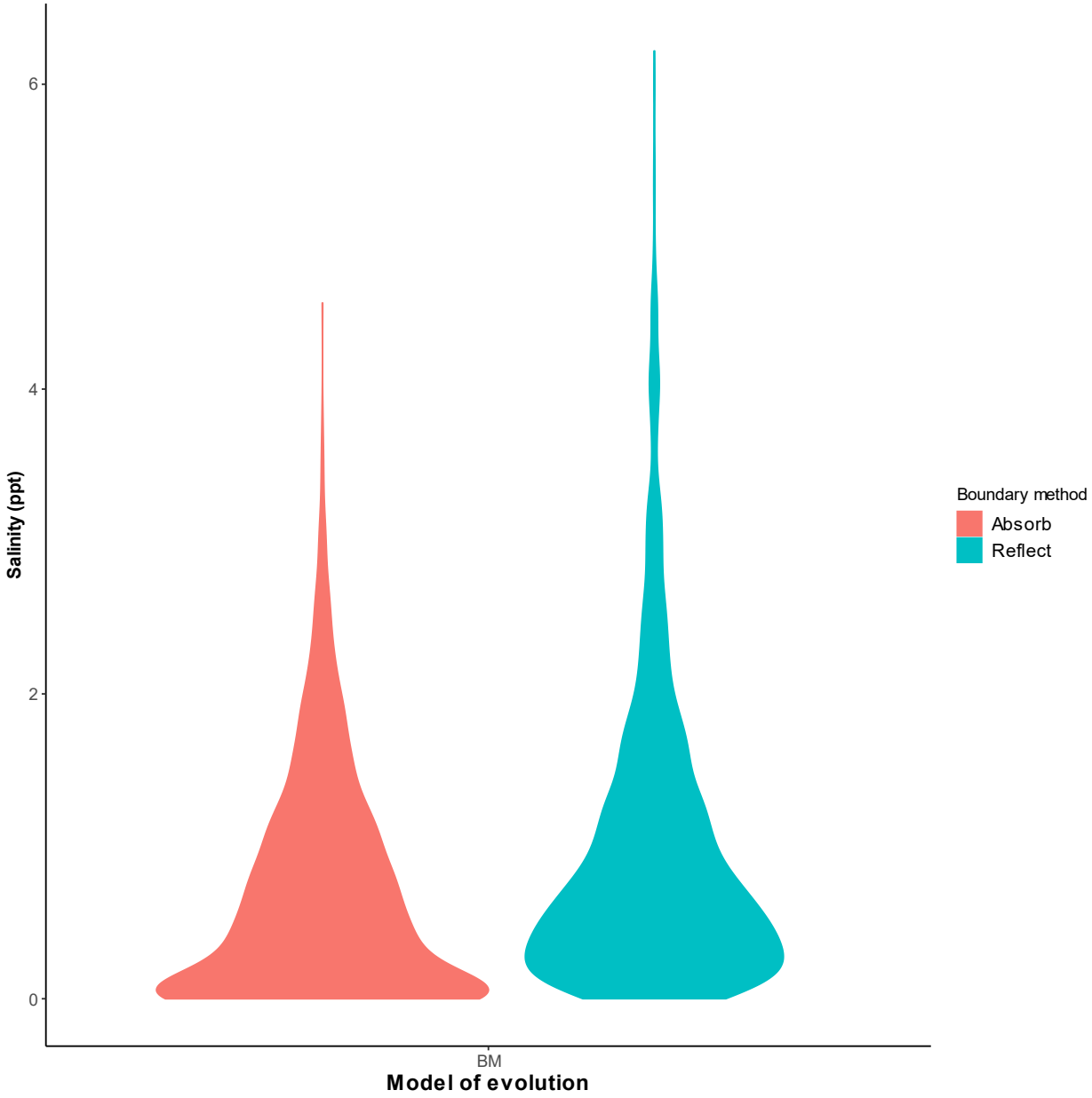

Figure 30: Distribution of salinities at the tips of Brownian Motion simulations ($0.001 < \sigma < 0.01$) using absorbing versus reflecting boundaries.

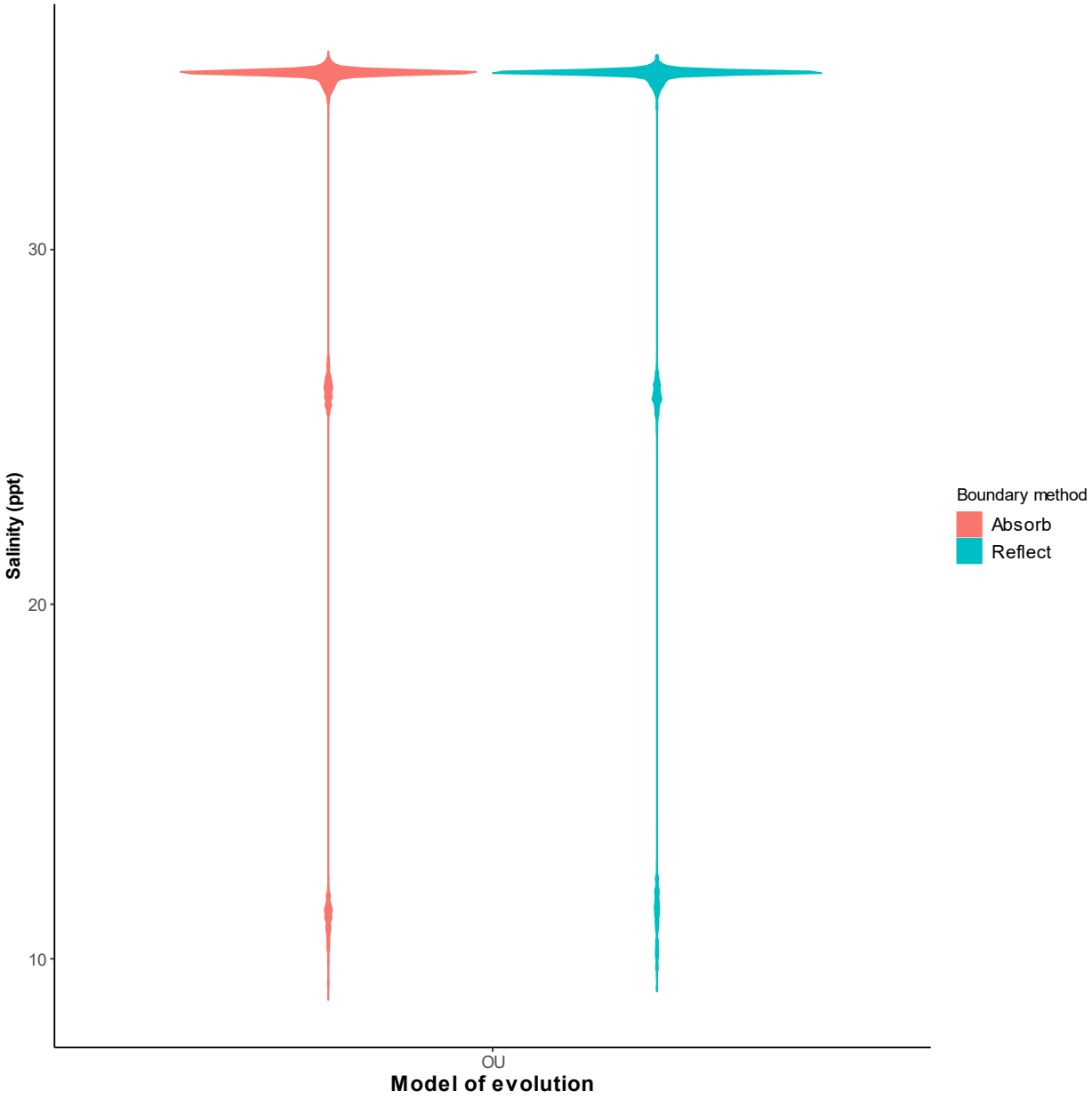

Figure 31: Distribution of salinities at the tips of Ornstein-Uhlenbeck simulations ($0.001 < \sigma < 0.01$) using absorbing versus reflecting boundaries.

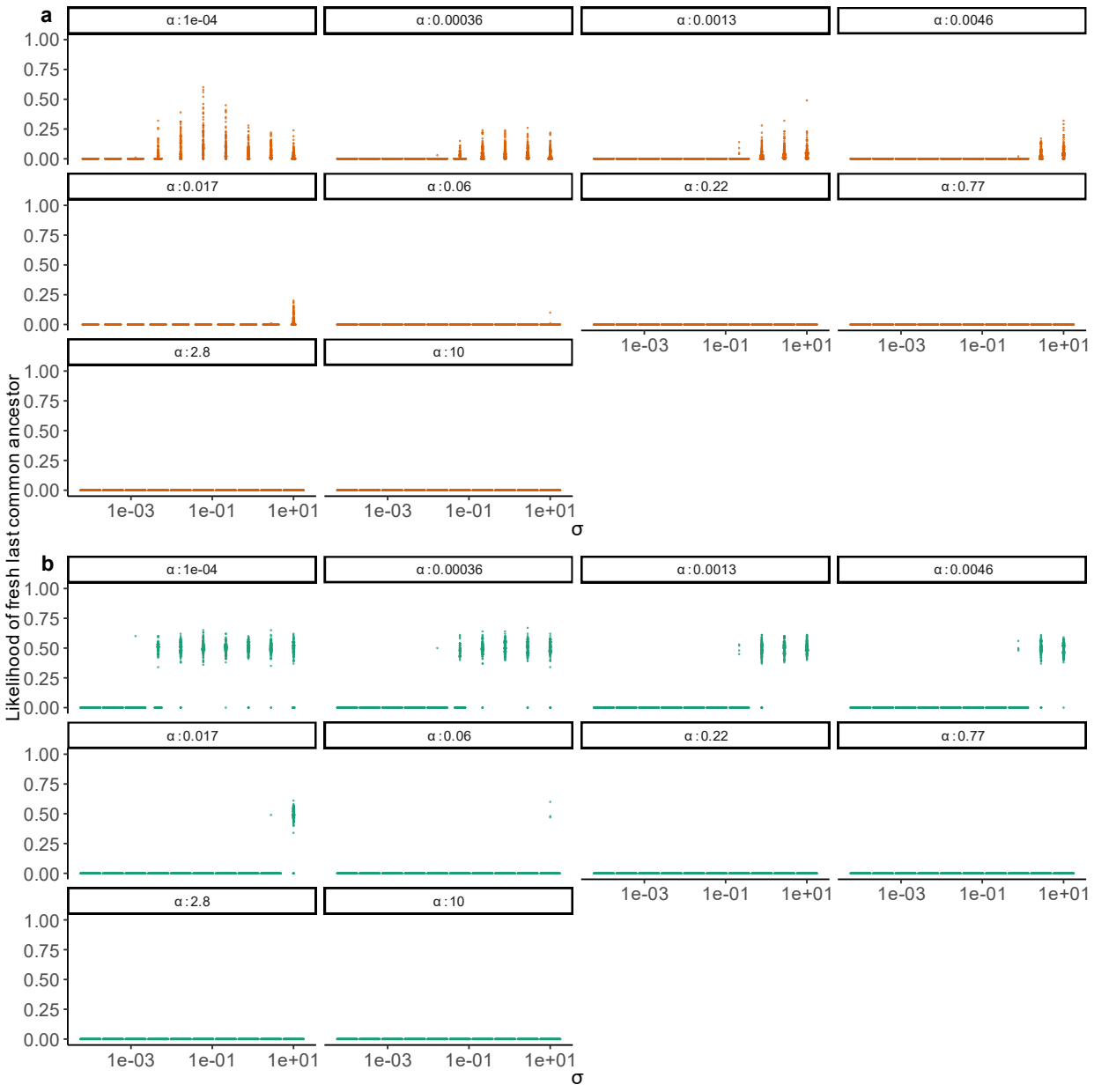

Figure 32: Likelihood of reconstructing a fresh ancestor for Ornstein-Uhlenbeck simulations using the equal-rates model (a) and all-rates-differ model (b). Each subpanel has a constant α value and shows the likelihood across the range of σ values tested.

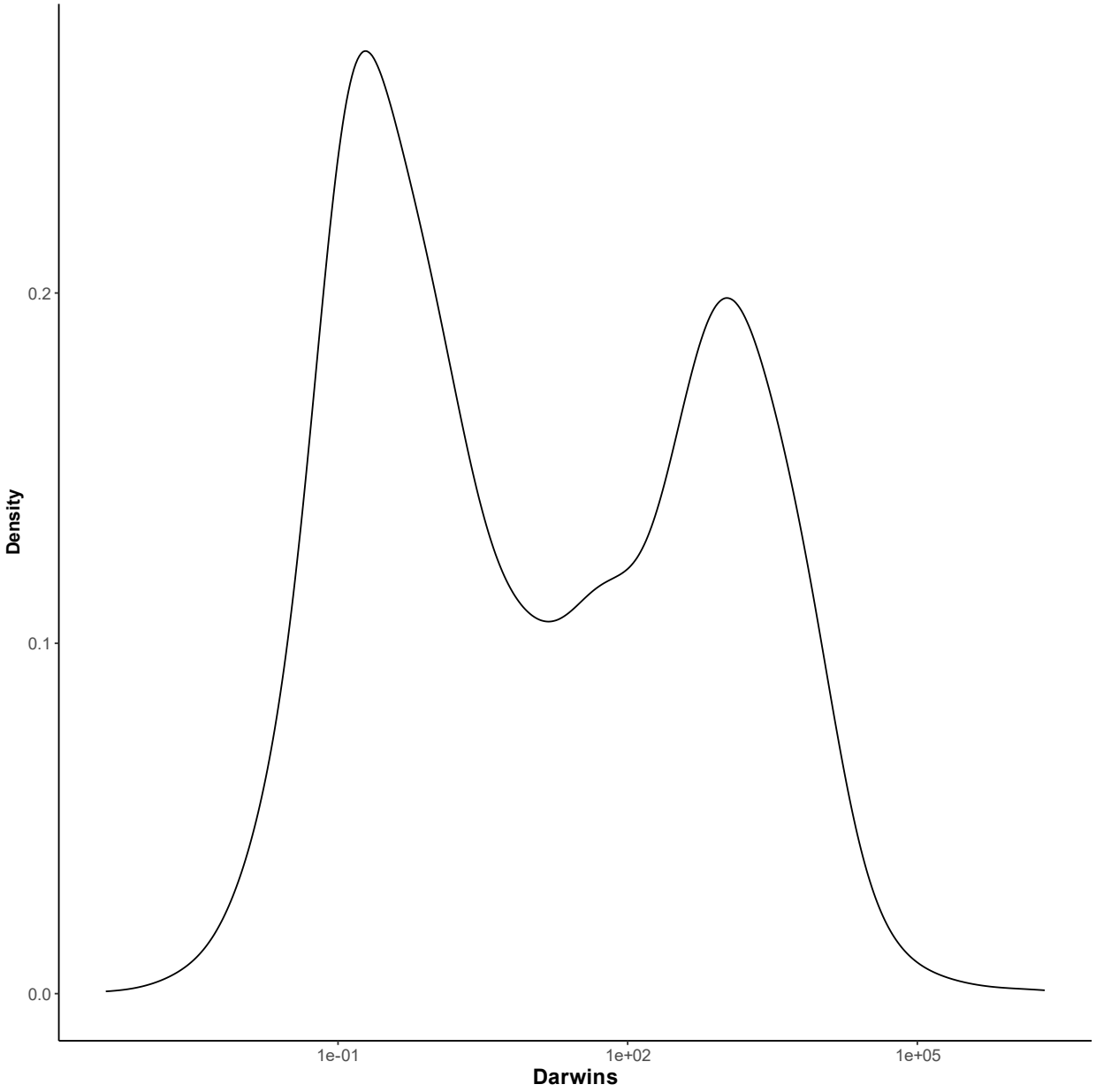

Figure 33: Distribution of evolutionary rates in darwins from dataset provided by (Uyeda et al., 2011).

Appendix B

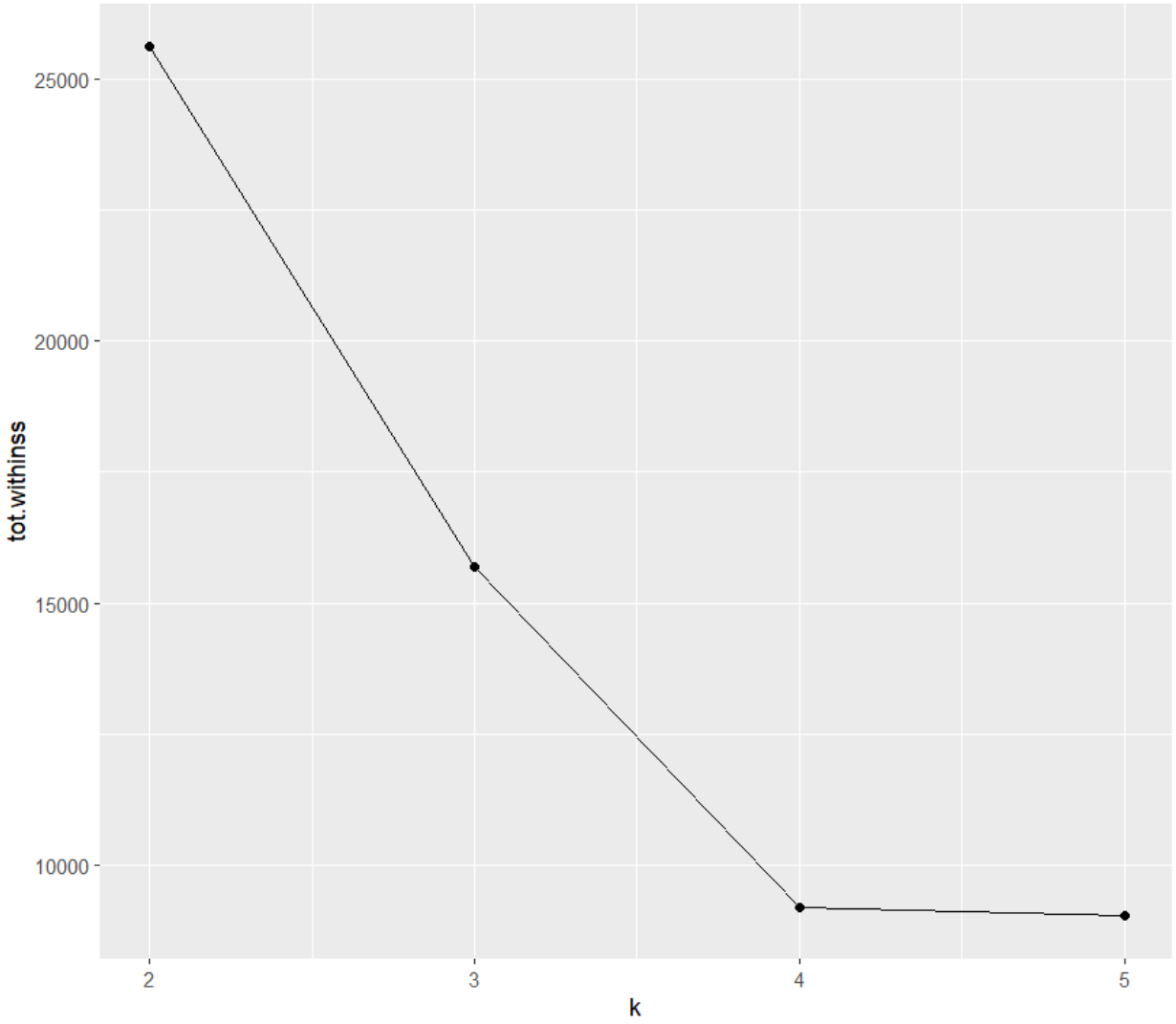

Figure 34: The total within-cluster sum of squares against the number of clusters in the analysis.

Reaction norms and model fits

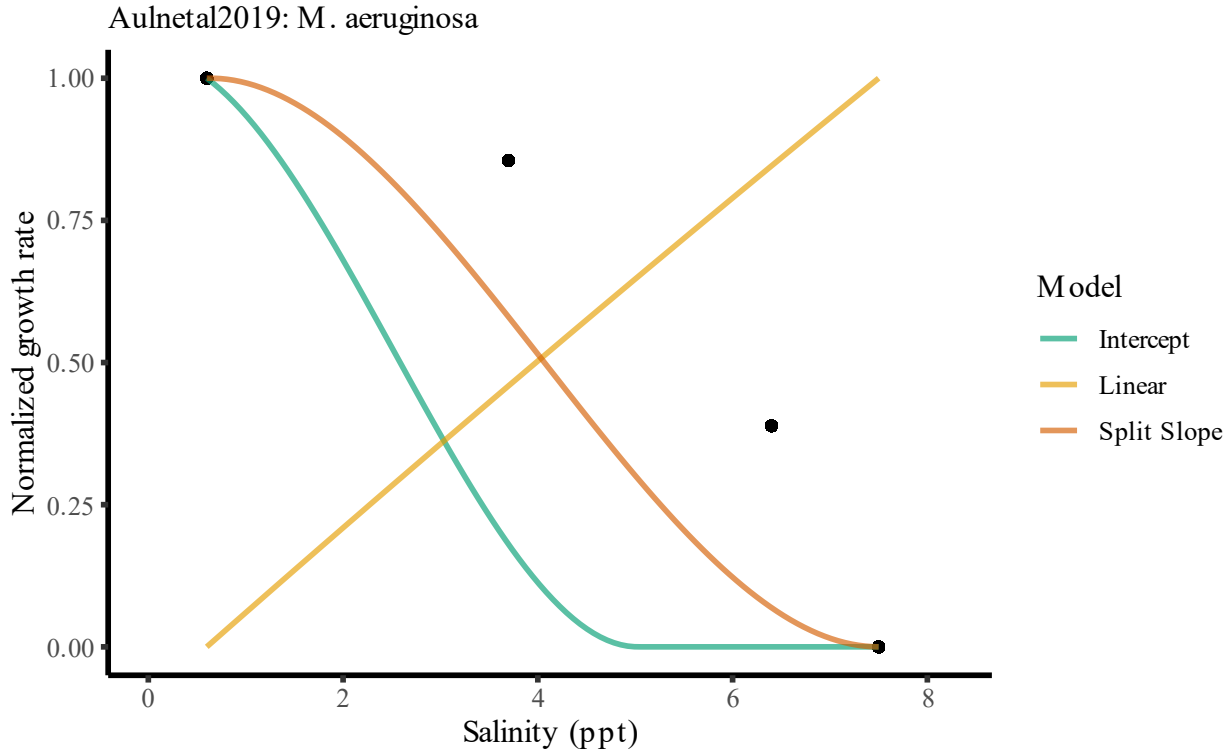

Figure 35: Reaction norm and model fits for Microcystis aeruginosa from (Georges des Aulnois et al., 2019)

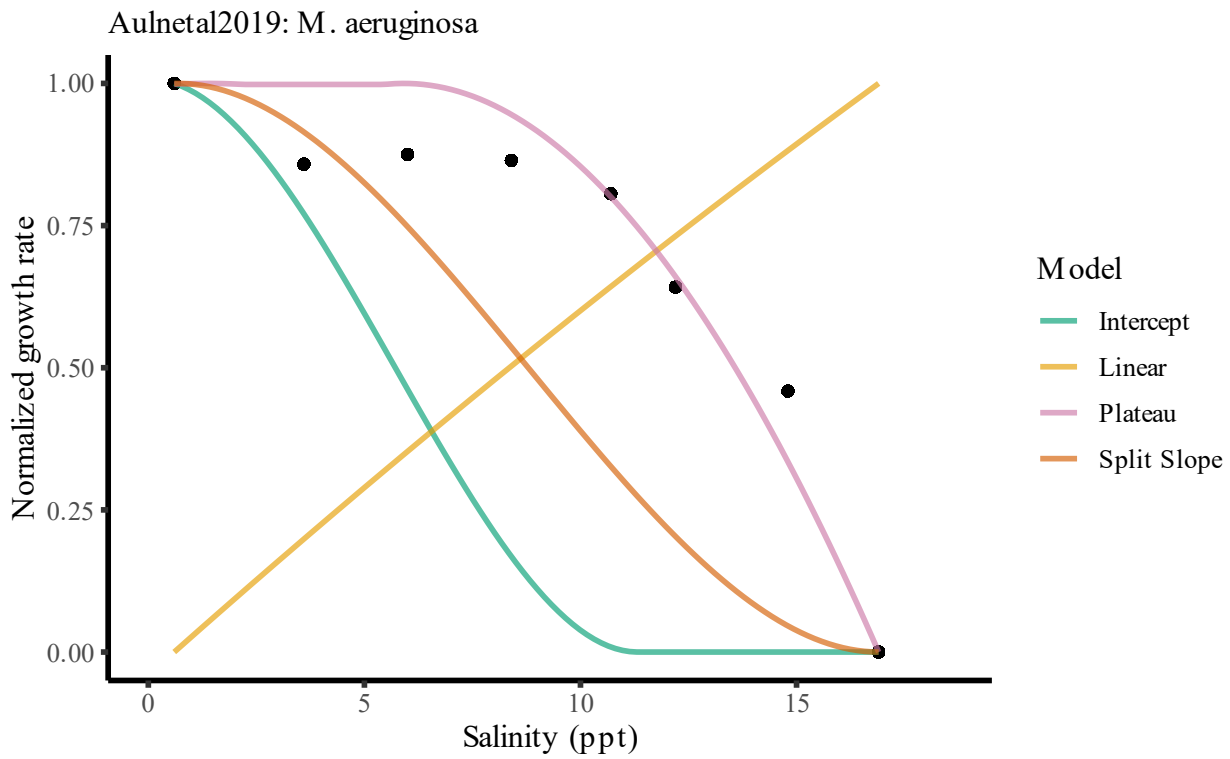

Figure 36: Reaction norm and model fits for Microcystis aeruginosa from (Georges des Aulnois et al., 2019)

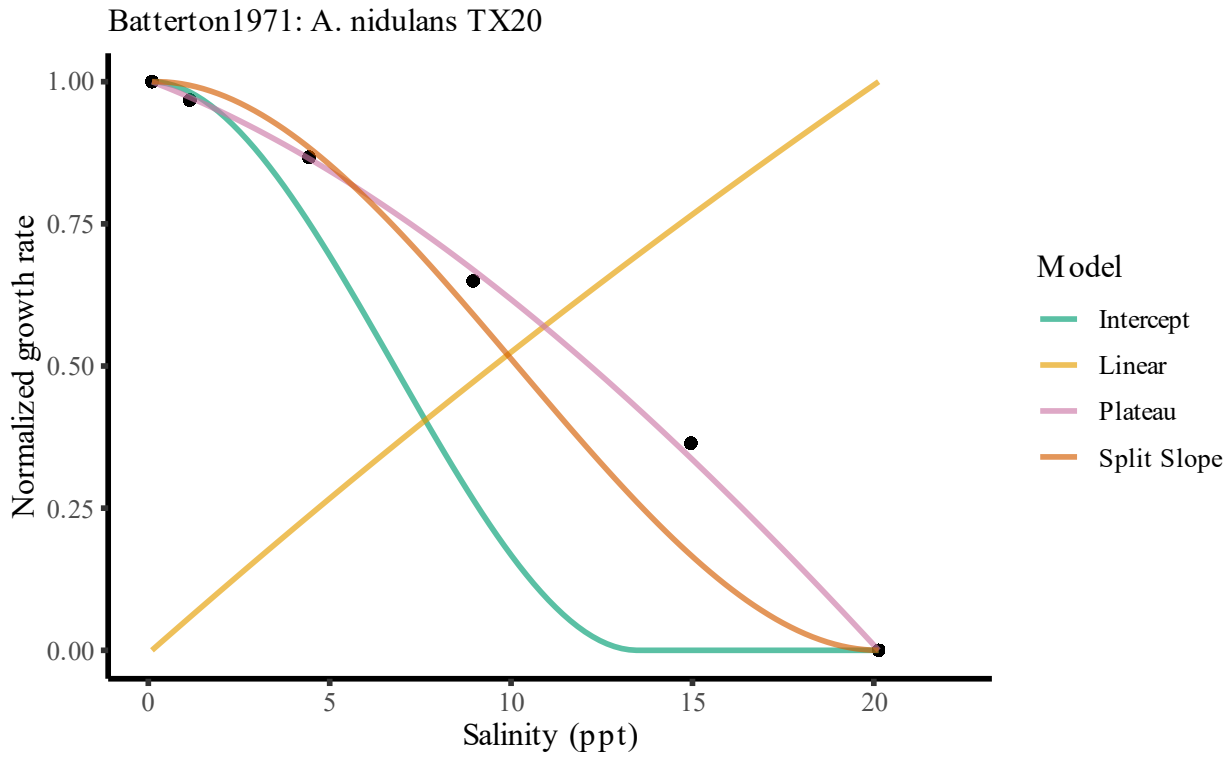

Figure 37: Reaction norm and model fits for Anacystis nidulans TX20 from (Batterton and Van Baalen, 1971)

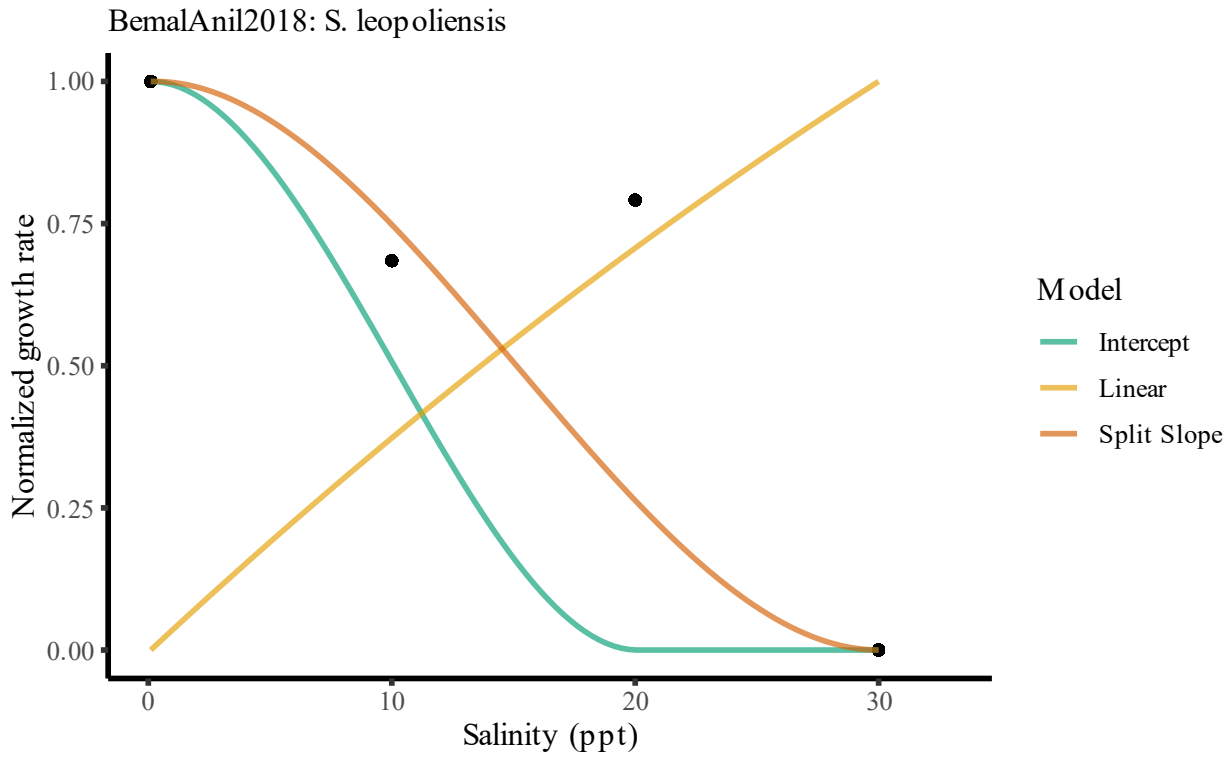

Figure 38: Reaction norm and model fits for Synechococcus leopoliensis from (Bemal and Anil, 2018)

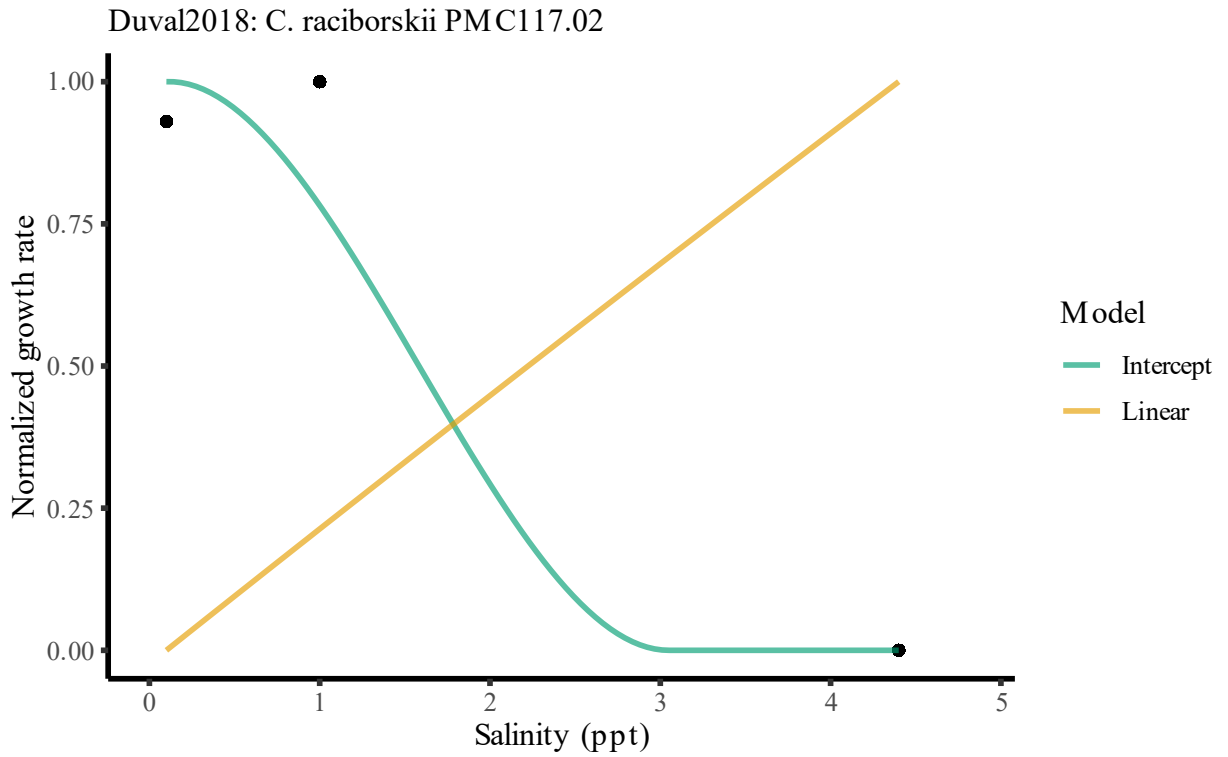

Figure 39: Reaction norm and model fits for Cylindrospermopsis raciborskii PMC117.02 from (Duval et al., 2018)

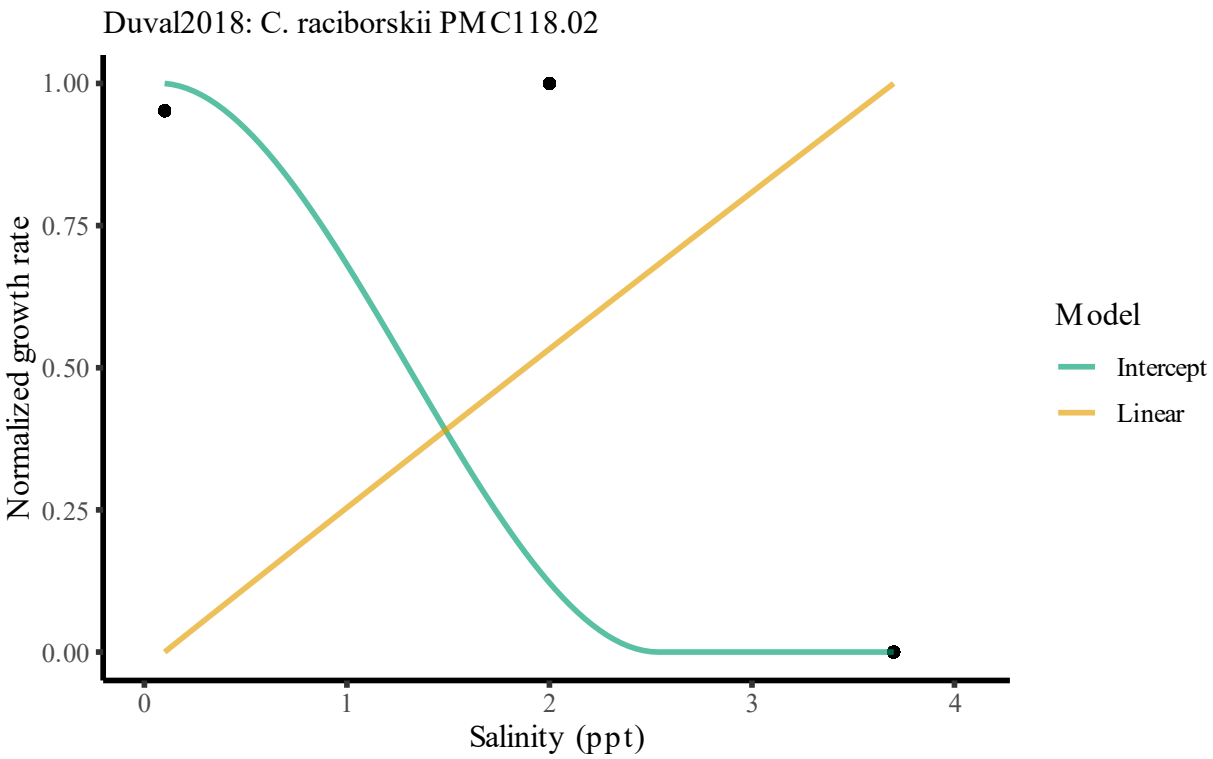

Figure 40: Reaction norm and model fits for Cylindrospermopsis raciborskii PMC118.02 from (Duval et al., 2018)

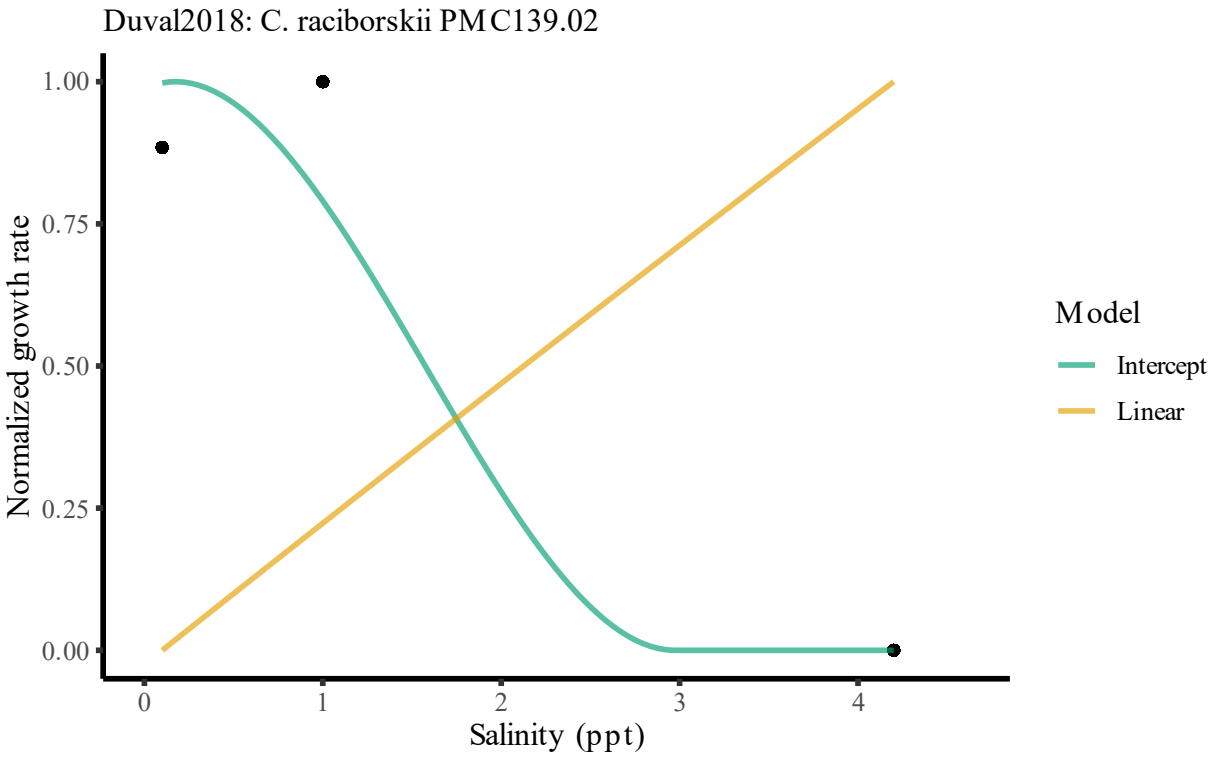

Figure 41: Reaction norm and model fits for Cylindrospermopsis raciborskii PMC139.02 from (Duval et al., 2018)

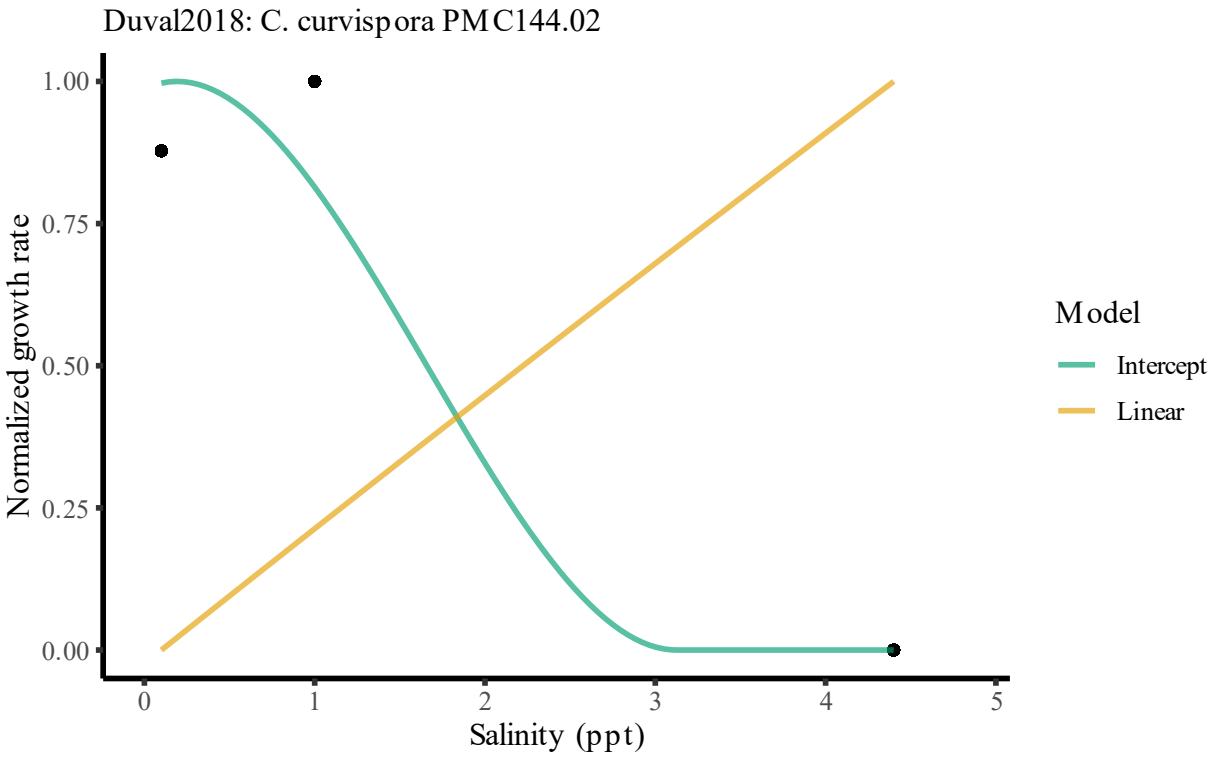

Figure 42: Reaction norm and model fits for Cylindrospermopsis curvispora PMC144.02 from (Duval et al., 2018)

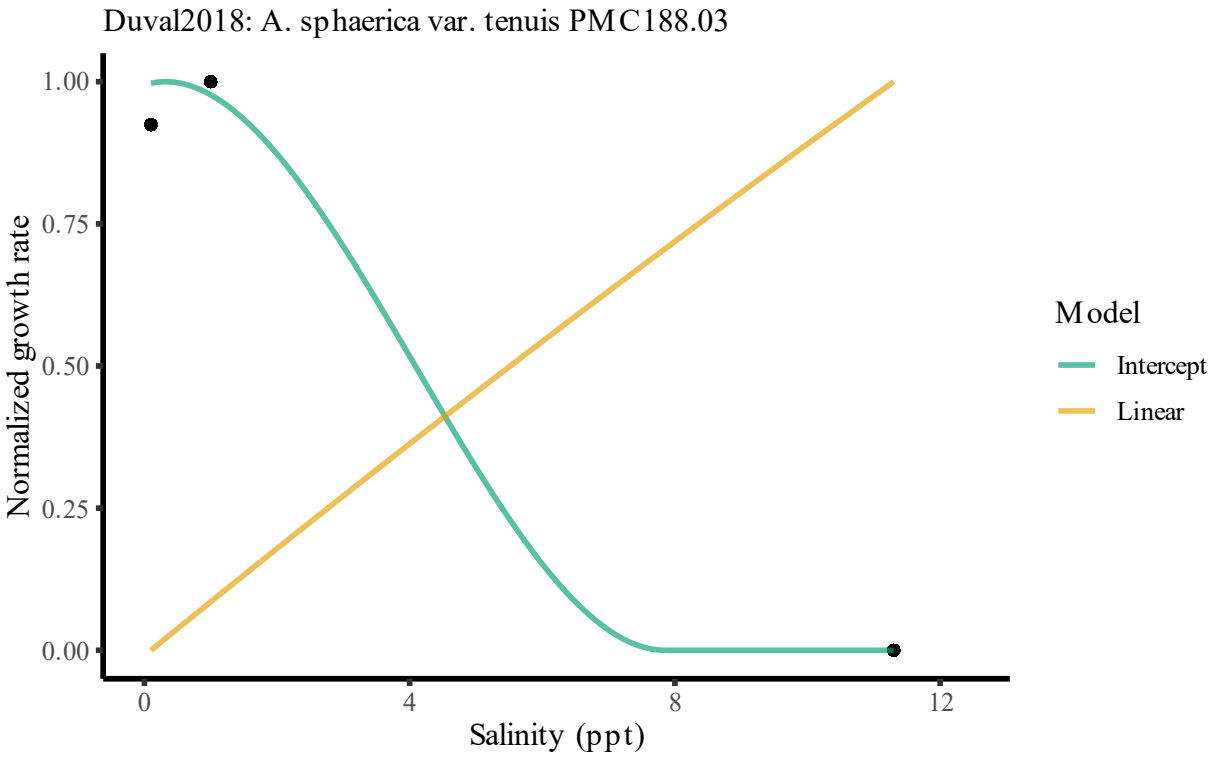

Figure 43: Reaction norm and model fits for Anabaena sphaerica var. tenuis PMC188.03 from (Duval et al., 2018)

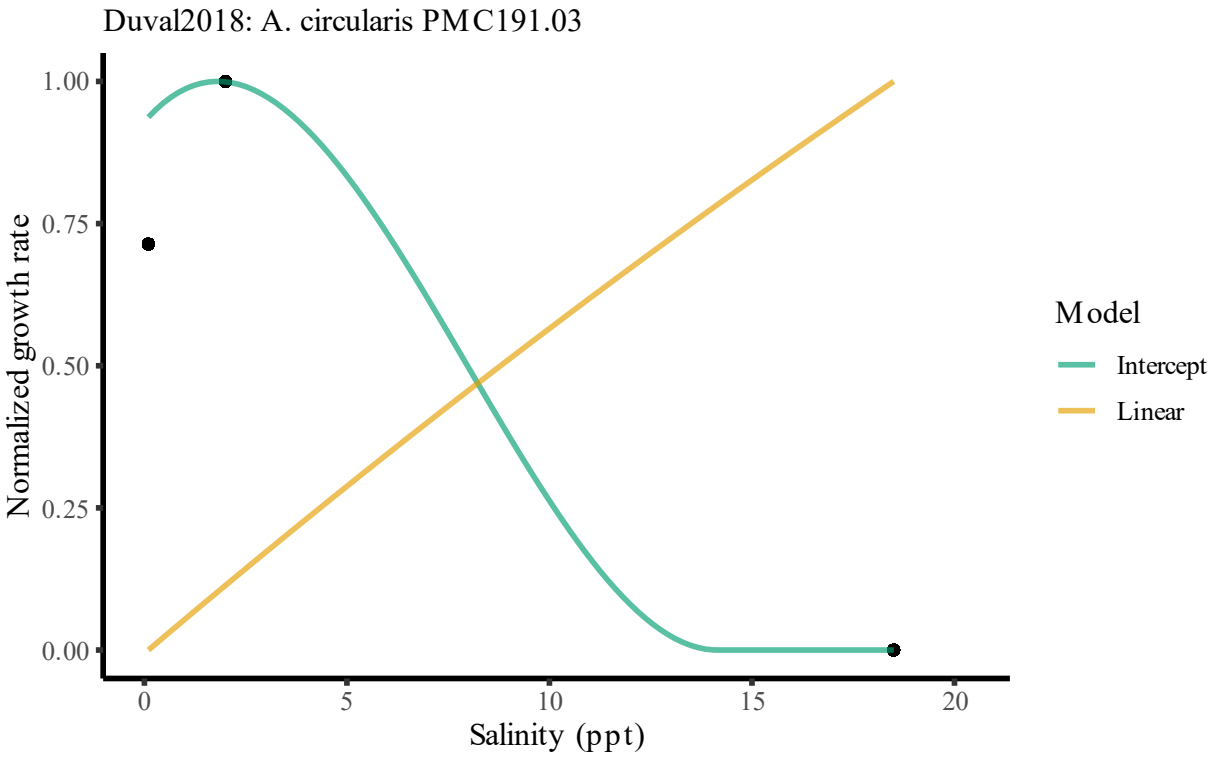

Figure 44: Reaction norm and model fits for Anabaenopsis circularis PMC191.03 from (Duval et al., 2018)

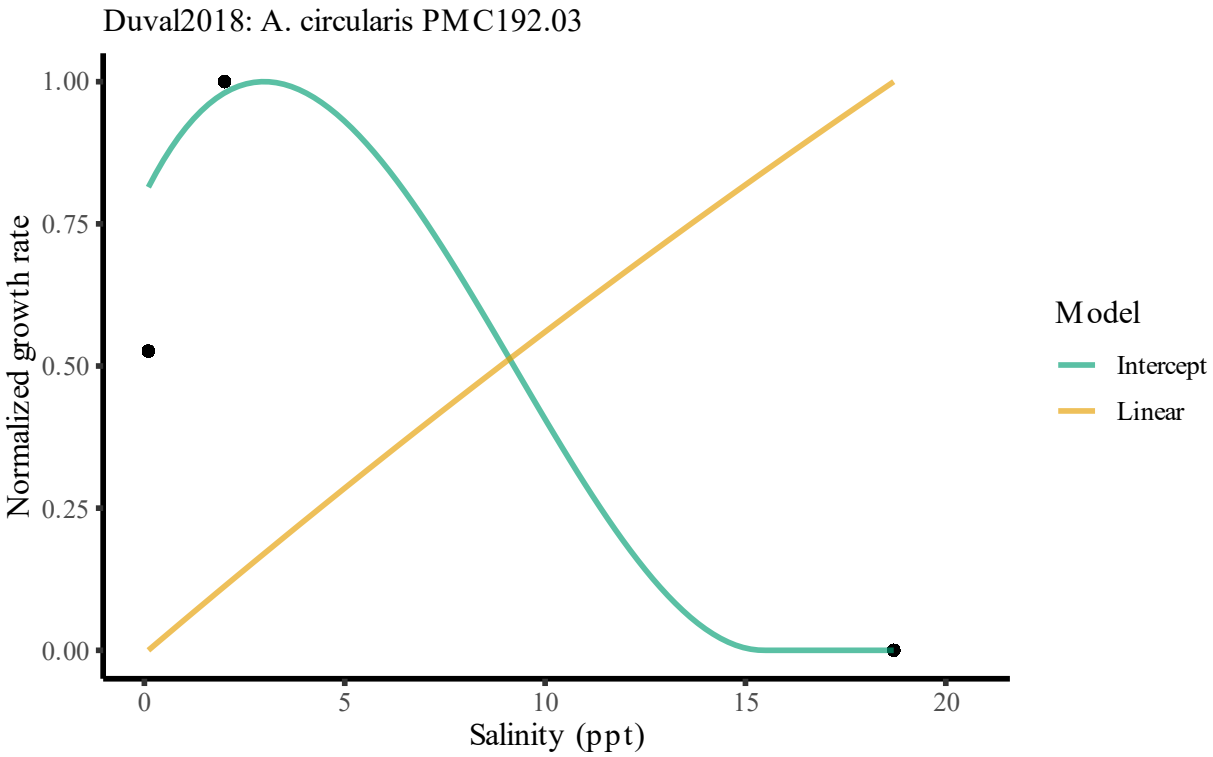

Figure 45: Reaction norm and model fits for Anabaenopsis circularis PMC192.03 from (Duval et al., 2018)

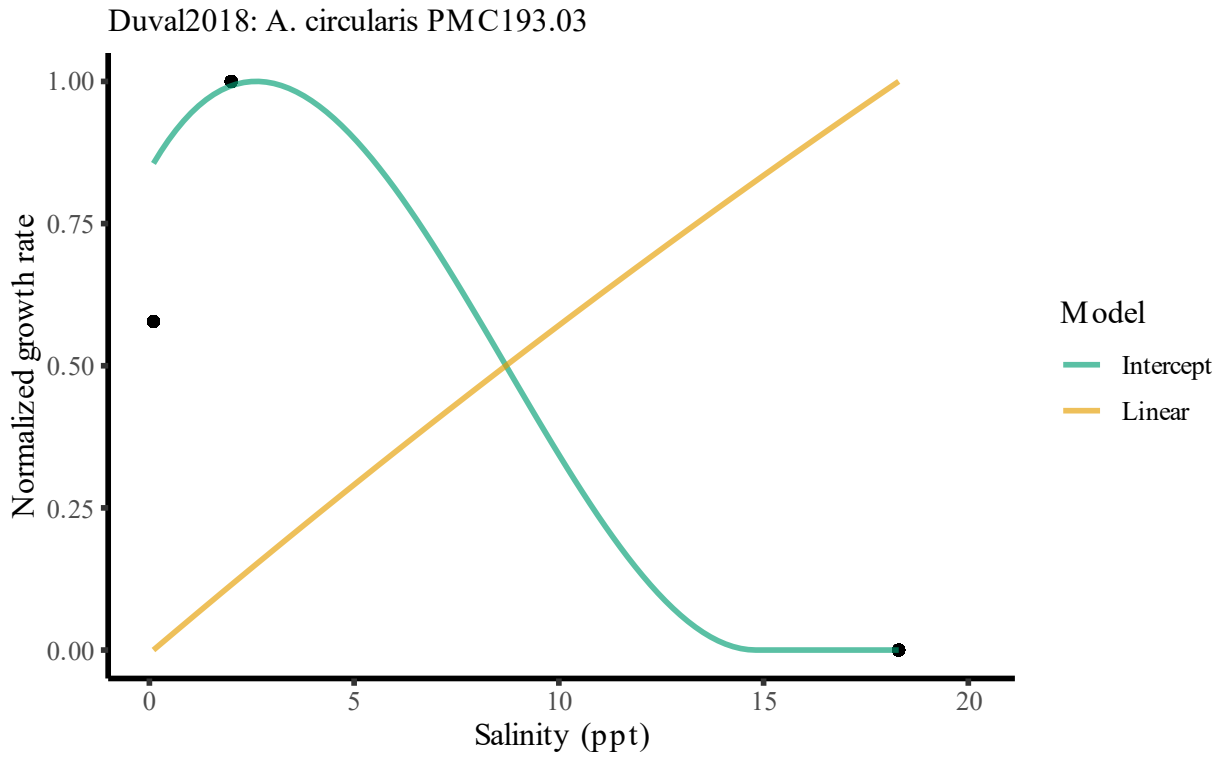

Figure 46: Reaction norm and model fits for Anabaenopsis circularis PMC193.03 from (Duval et al., 2018)

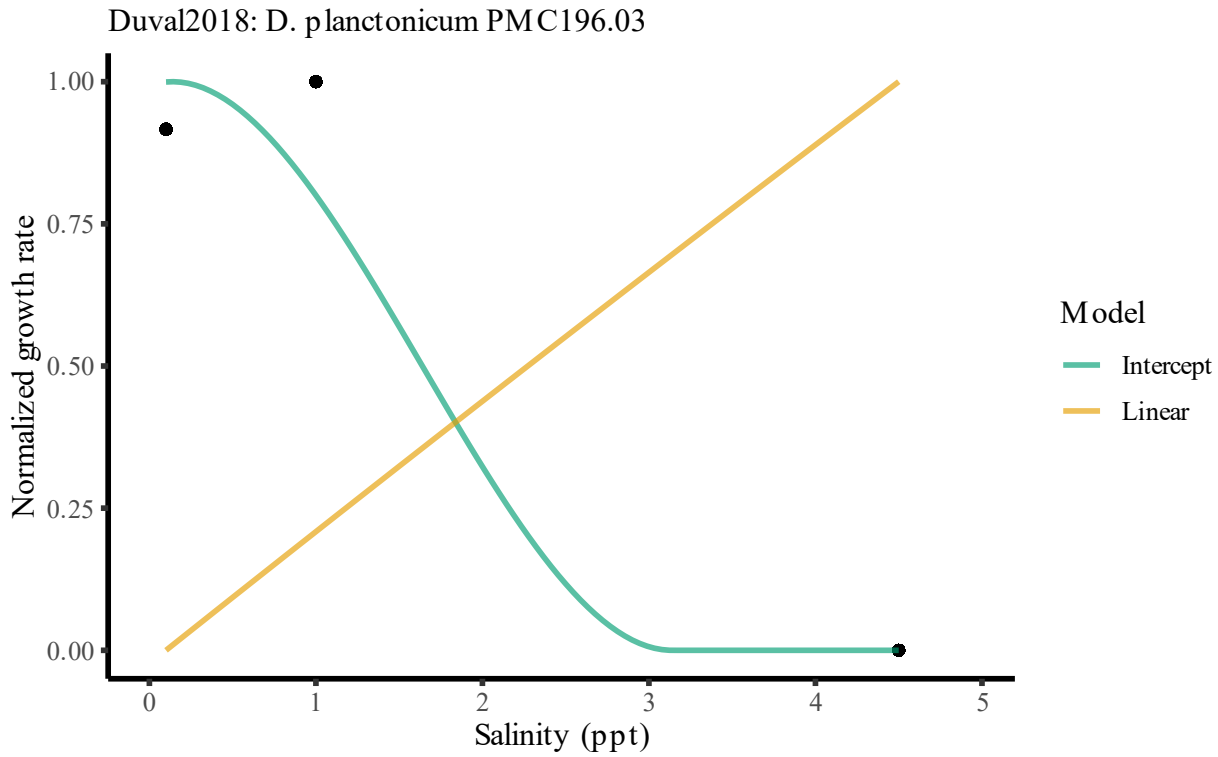

Figure 47: Reaction norm and model fits for Dolichospermum planctonicum PMC196.03 from (Duval et al., 2018)

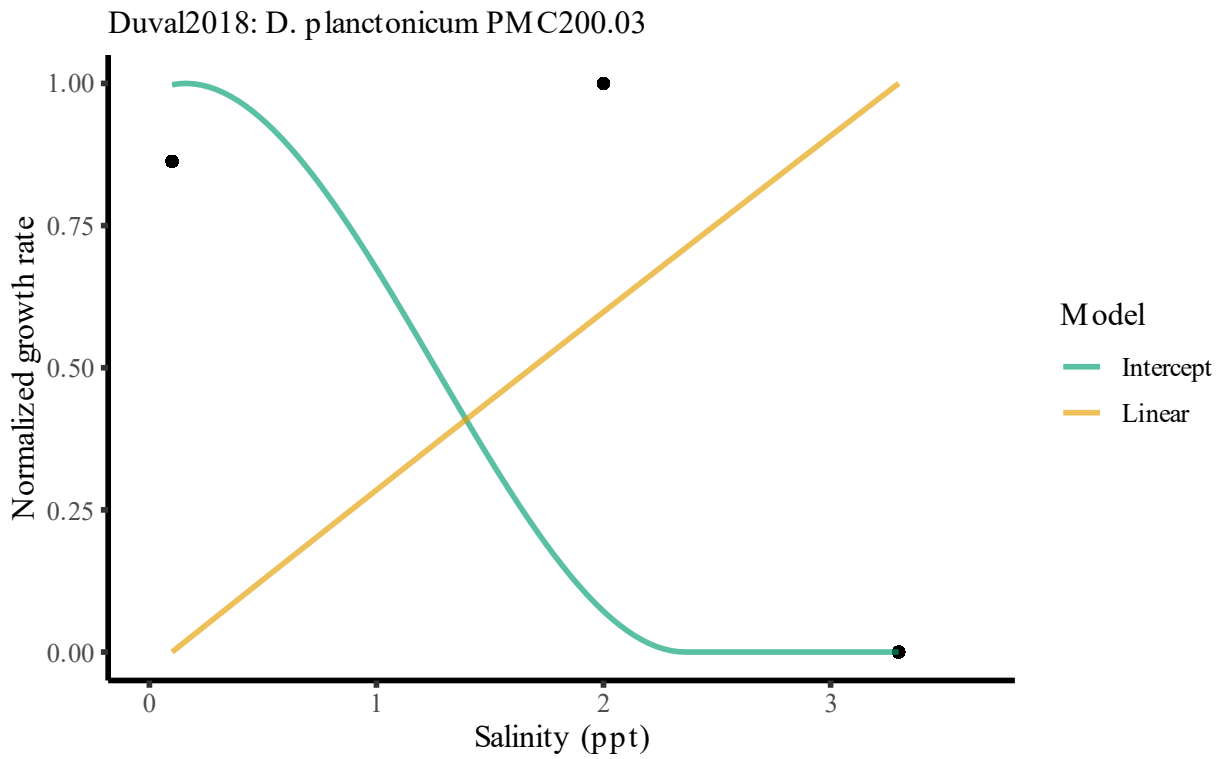

Figure 48: Reaction norm and model fits for Dolichospermum planctonicum PMC200.03 from (Duval et al., 2018)

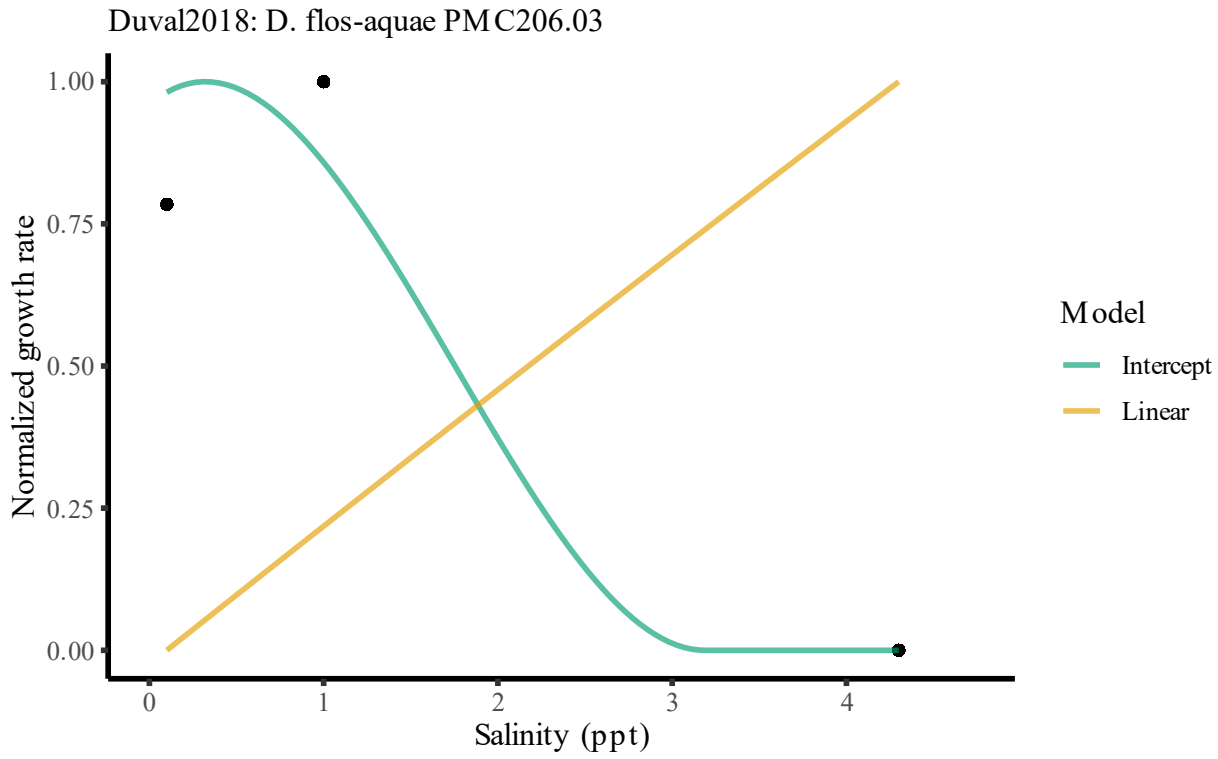

Figure 49: Reaction norm and model fits for Dolichospermum flos-aquae PMC206.03 from (Duval et al., 2018)

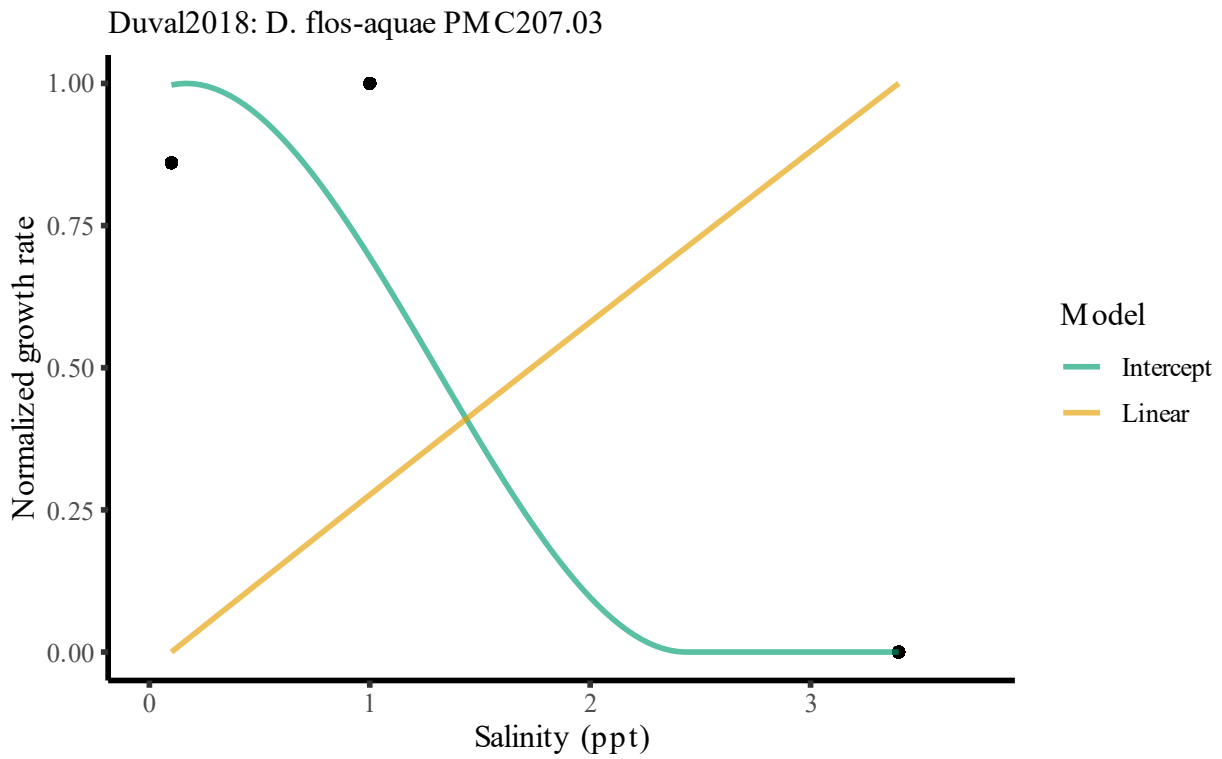

Figure 50: Reaction norm and model fits for Dolichospermum flos-aquae PMC207.03 from (Duval et al., 2018)

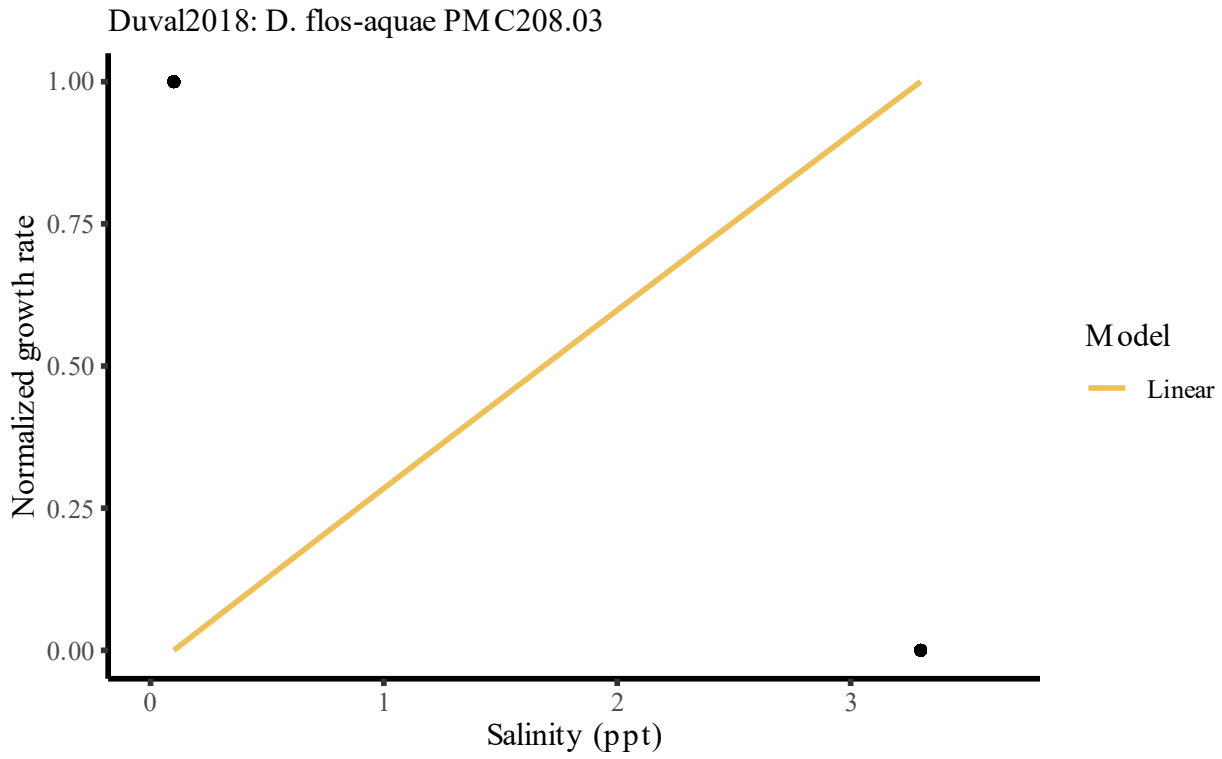

Figure 51: Reaction norm and model fits for Dolichospermum flos-aquae PMC208.03 from (Duval et al., 2018)

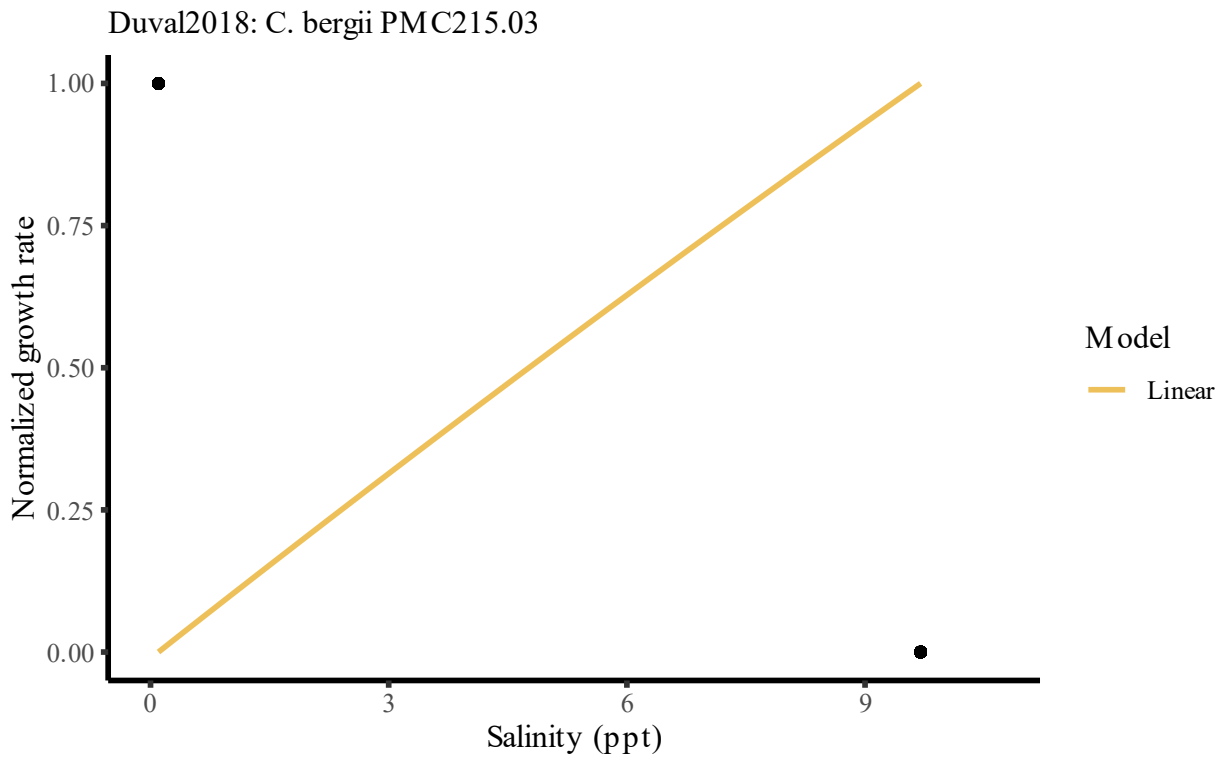

Figure 52: Reaction norm and model fits for Chrysosporum bergii PMC215.03 from (Duval et al., 2018)

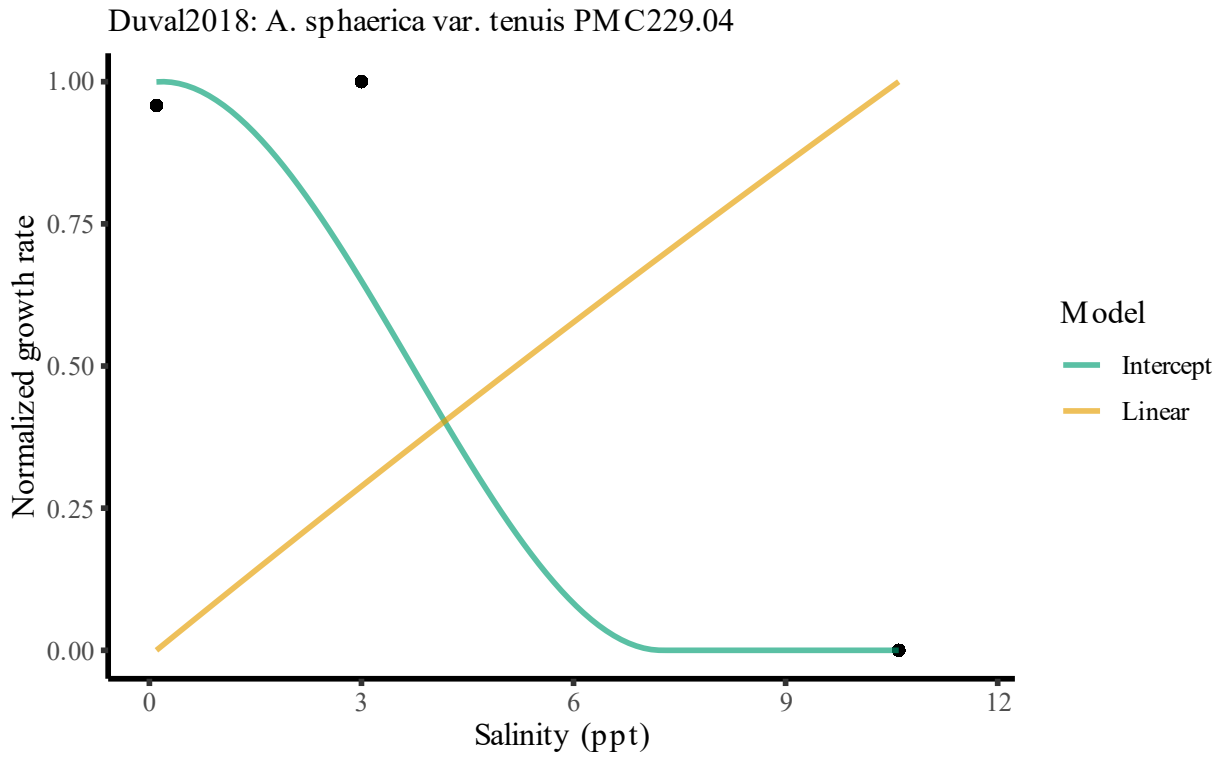

Figure 53: Reaction norm and model fits for Anabaena sphaerica var. tenuis PMC229.04 from (Duval et al., 2018)

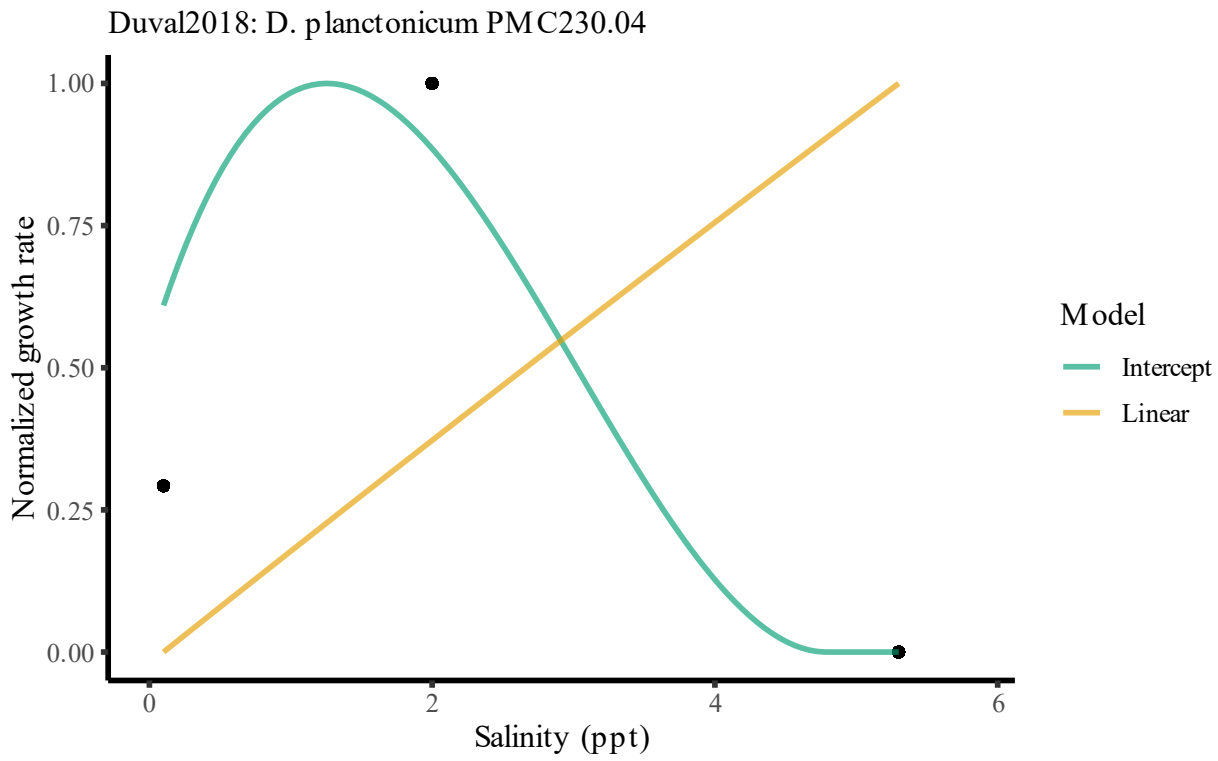

Figure 54: Reaction norm and model fits for Dolichospermum planctonicum PMC230.04 from (Duval et al., 2018)

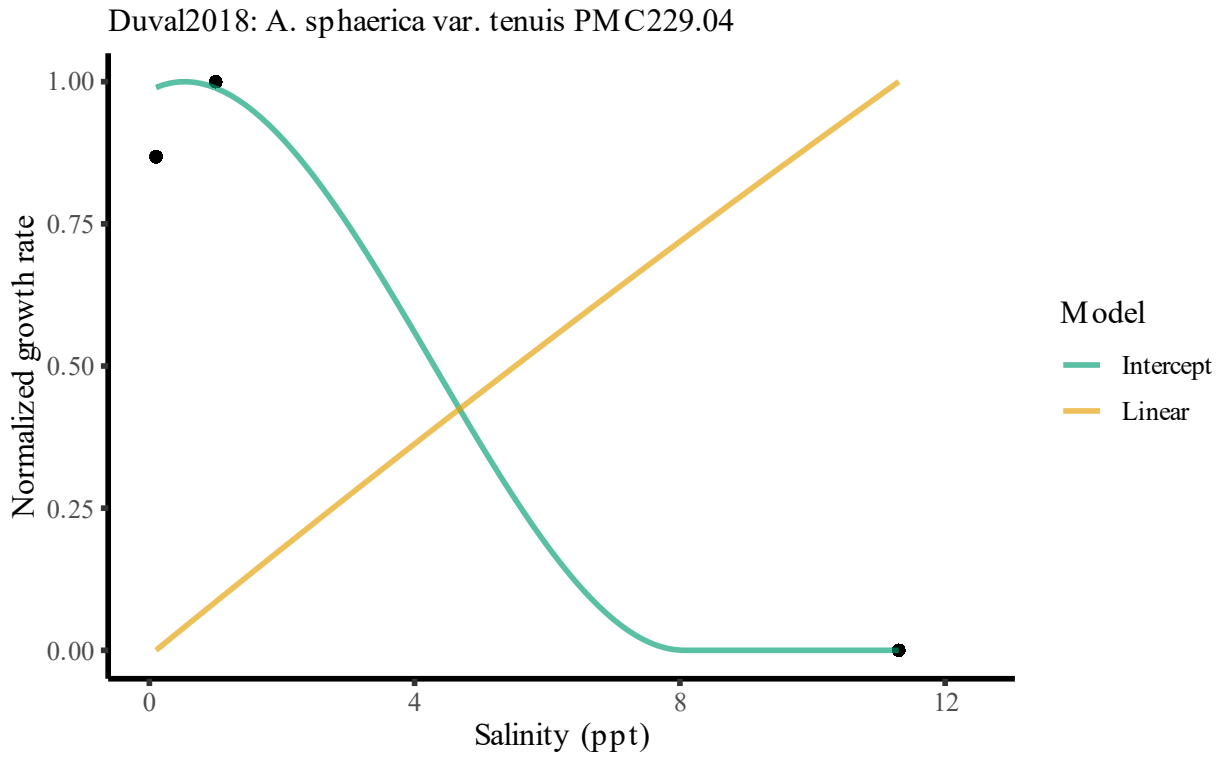

Figure 55: Reaction norm and model fits for Anabaena sphaerica var. tenuis PMC229.04 from (Duval et al., 2018)

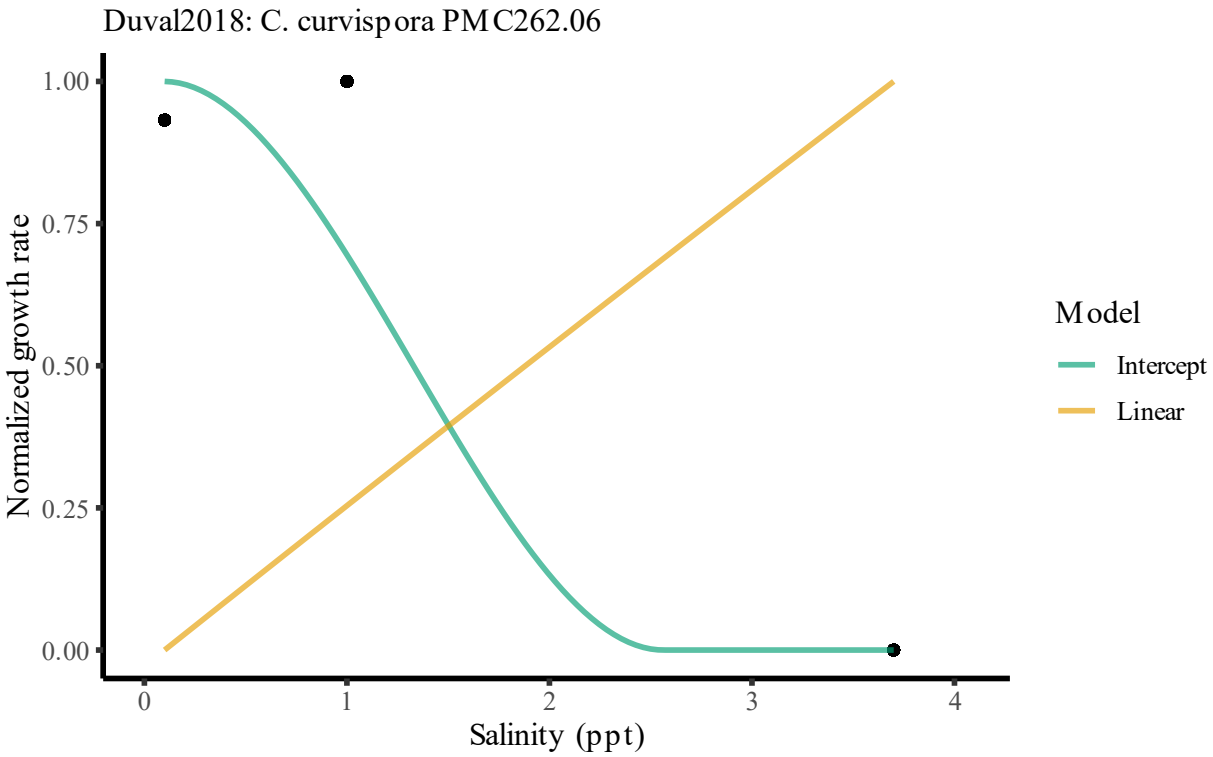

Figure 56: Reaction norm and model fits for Cylindrospermopsis curvispora PMC262.06 from (Duval et al., 2018)

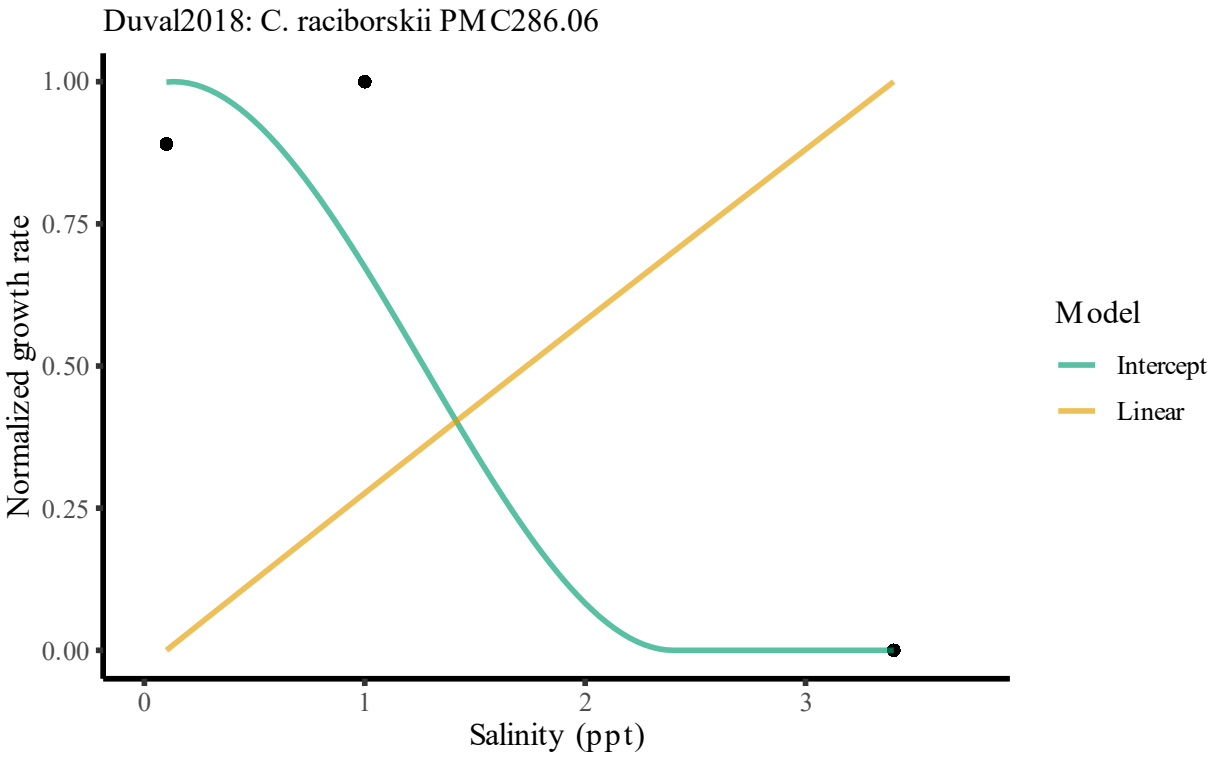

Figure 57: Reaction norm and model fits for Cylindrospermopsis raciborskii PMC286.06 from (Duval et al., 2018)

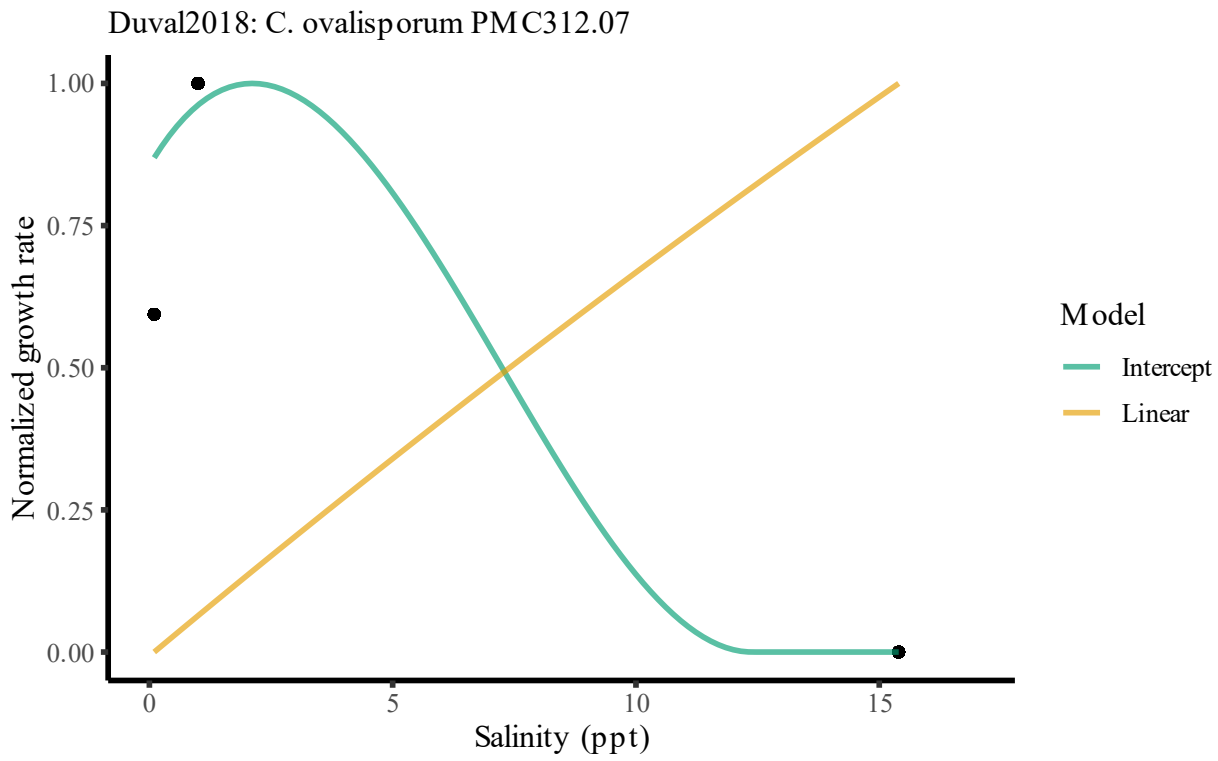

Figure 58: Reaction norm and model fits for Chrysosporum ovalisporum PMC312.07 from (Duval et al., 2018)

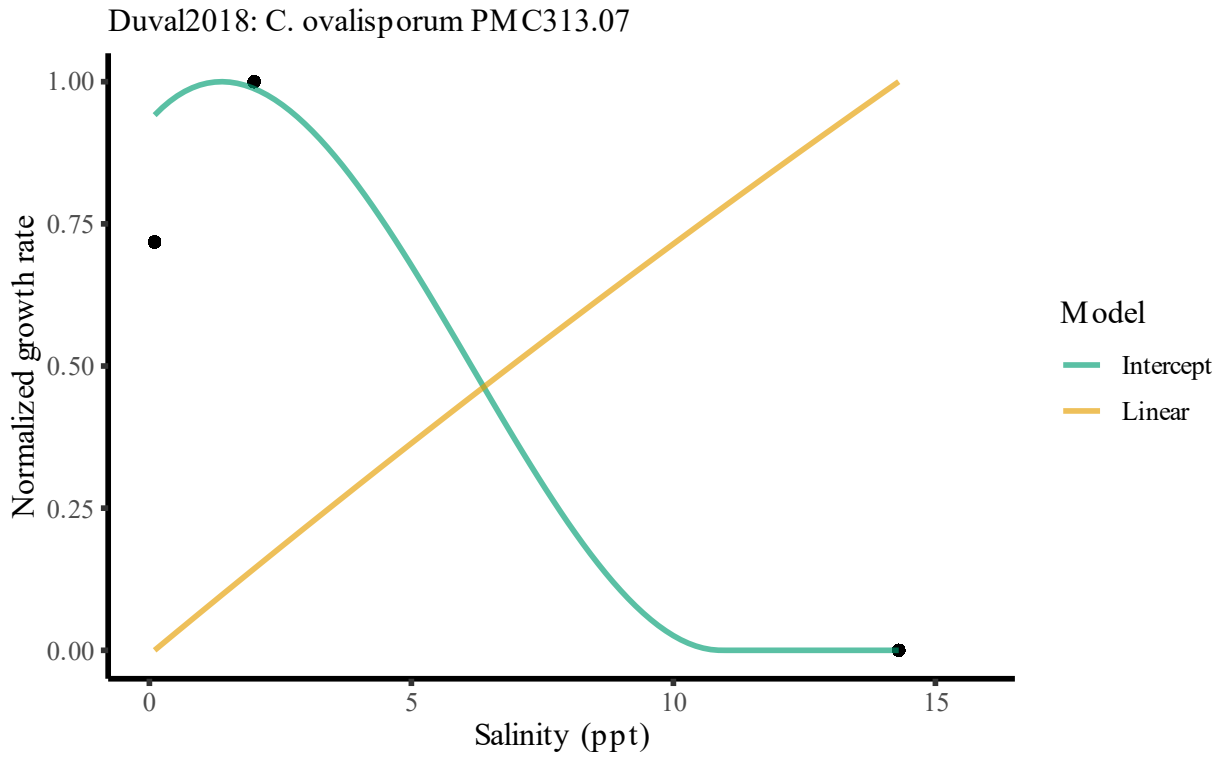

Figure 59: Reaction norm and model fits for Chrysosporum ovalisporum PMC313.07 from (Duval et al., 2018)

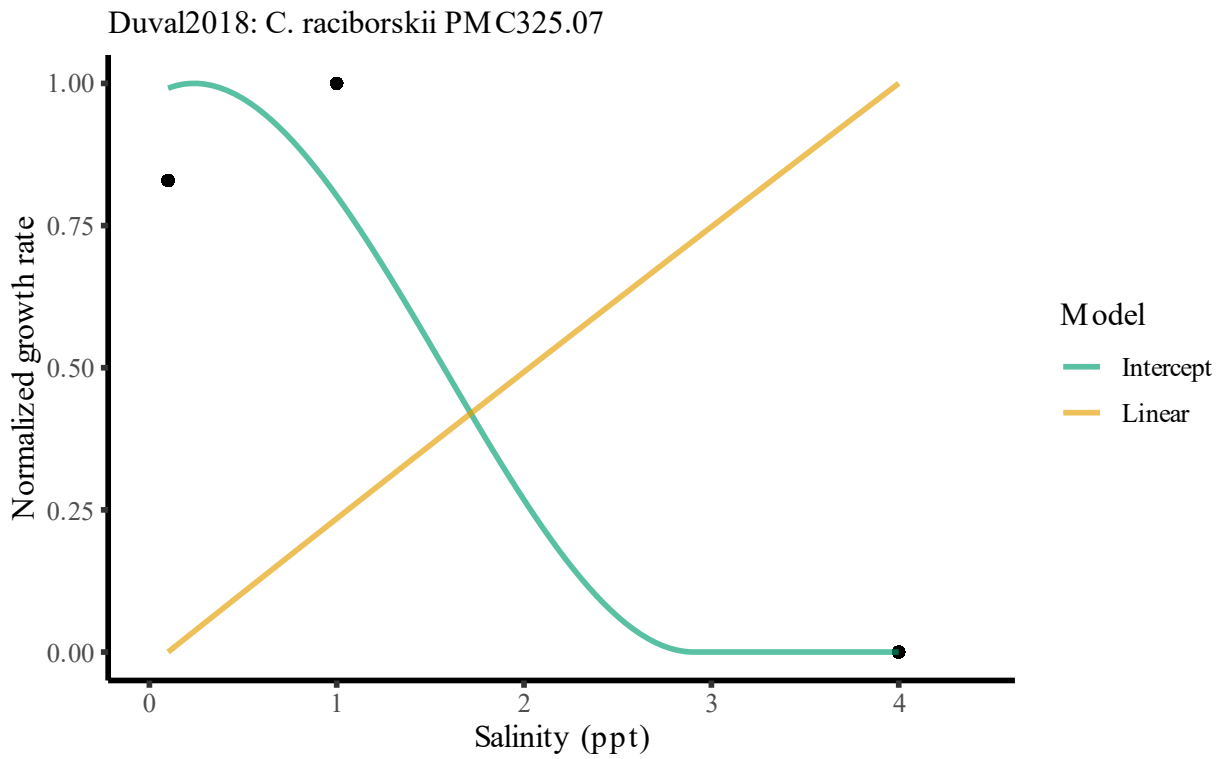

Figure 60: Reaction norm and model fits for Cylindrospermopsis raciborskii PMC325.07 from (Duval et al., 2018)

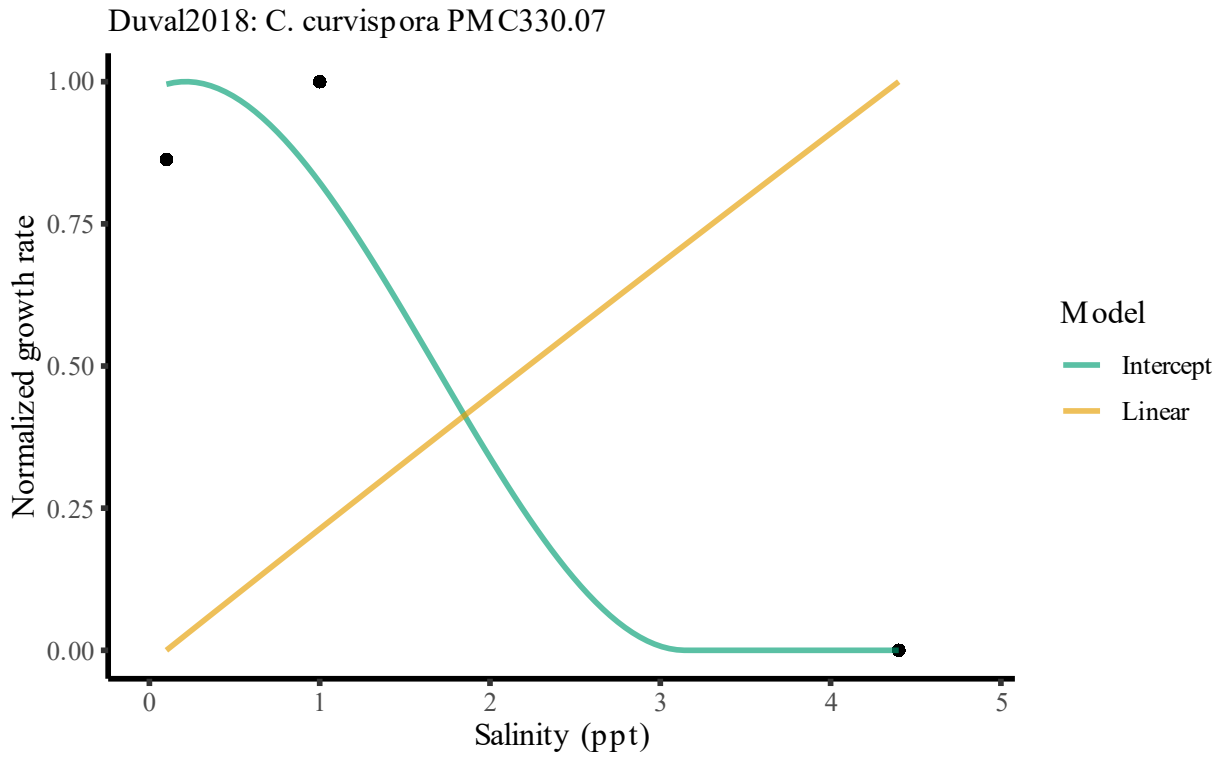

Figure 61: Reaction norm and model fits for Cylindrospermopsis curvispora PMC330.07 from (Duval et al., 2018)

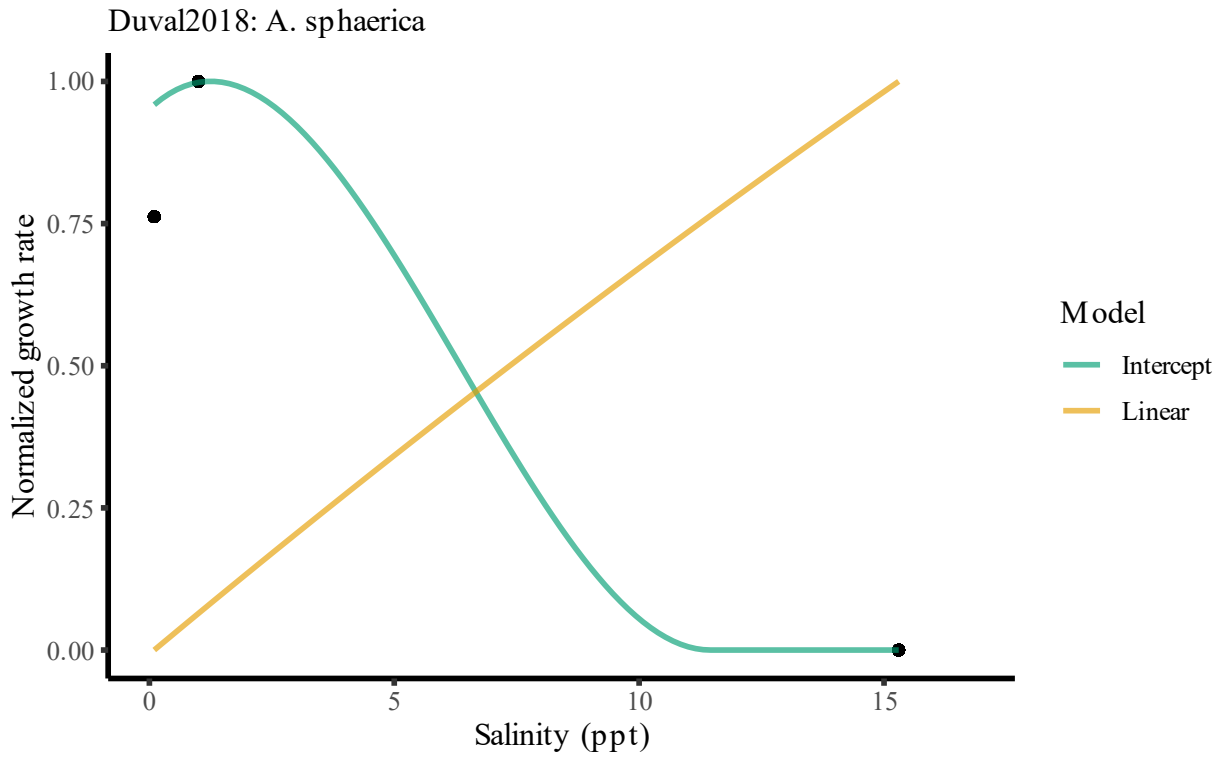

Figure 62: Reaction norm and model fits for Anabaena sphaerica from (Duval et al., 2018)

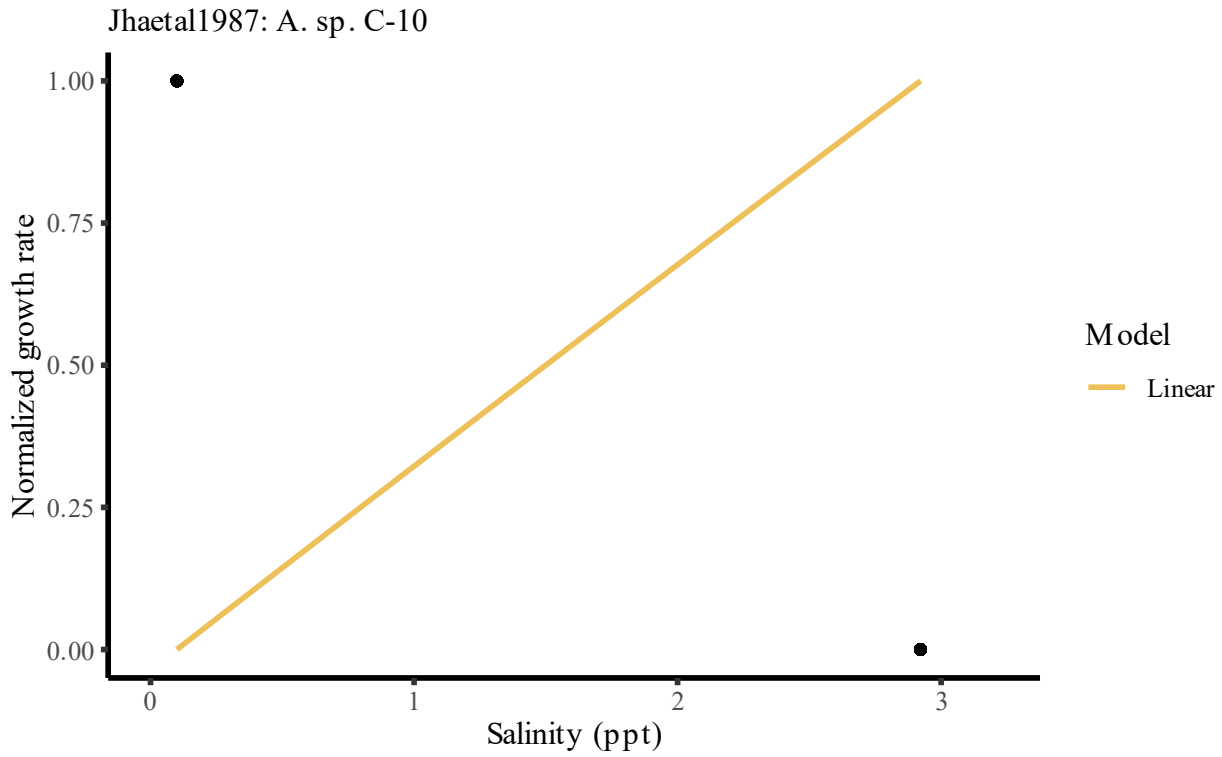

Figure 63: Reaction norm and model fits for Anabaena sp. C-10 from (Jha et al., 1987)

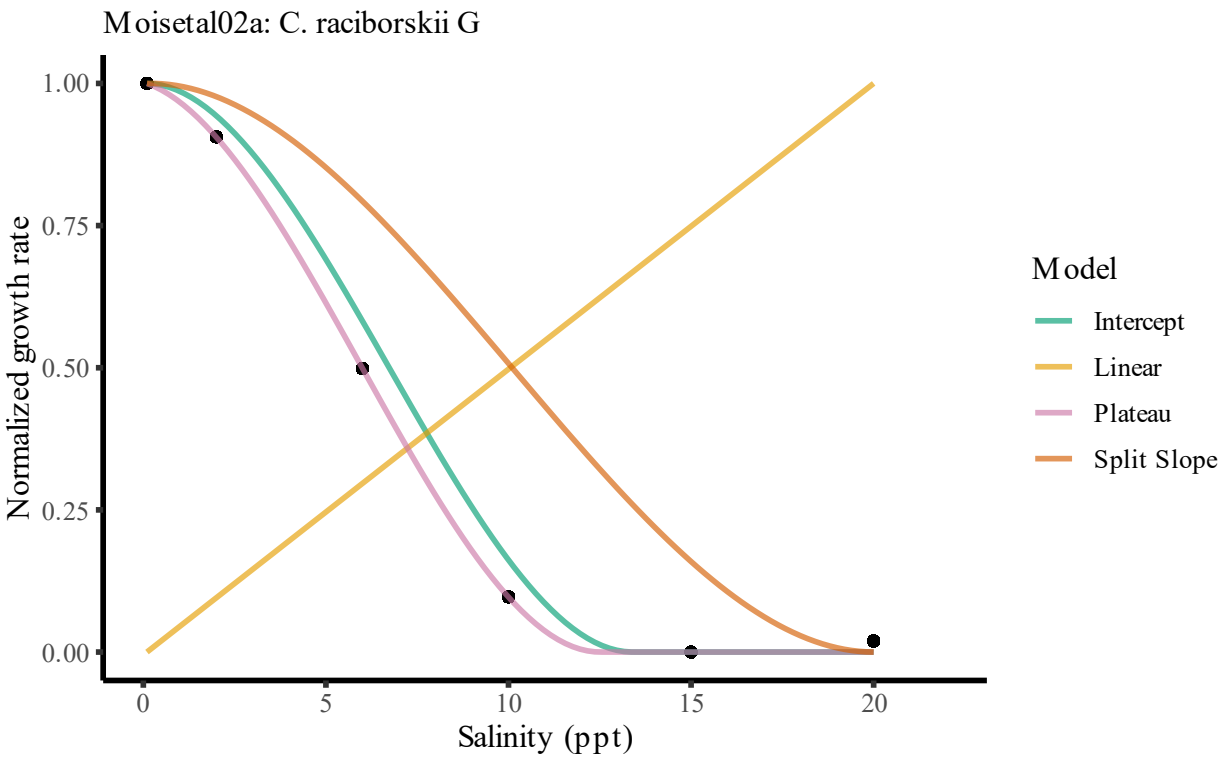

Figure 64: Reaction norm and model fits for Cylindrospermopsis raciborskii G from (Moisander et al., 2002)

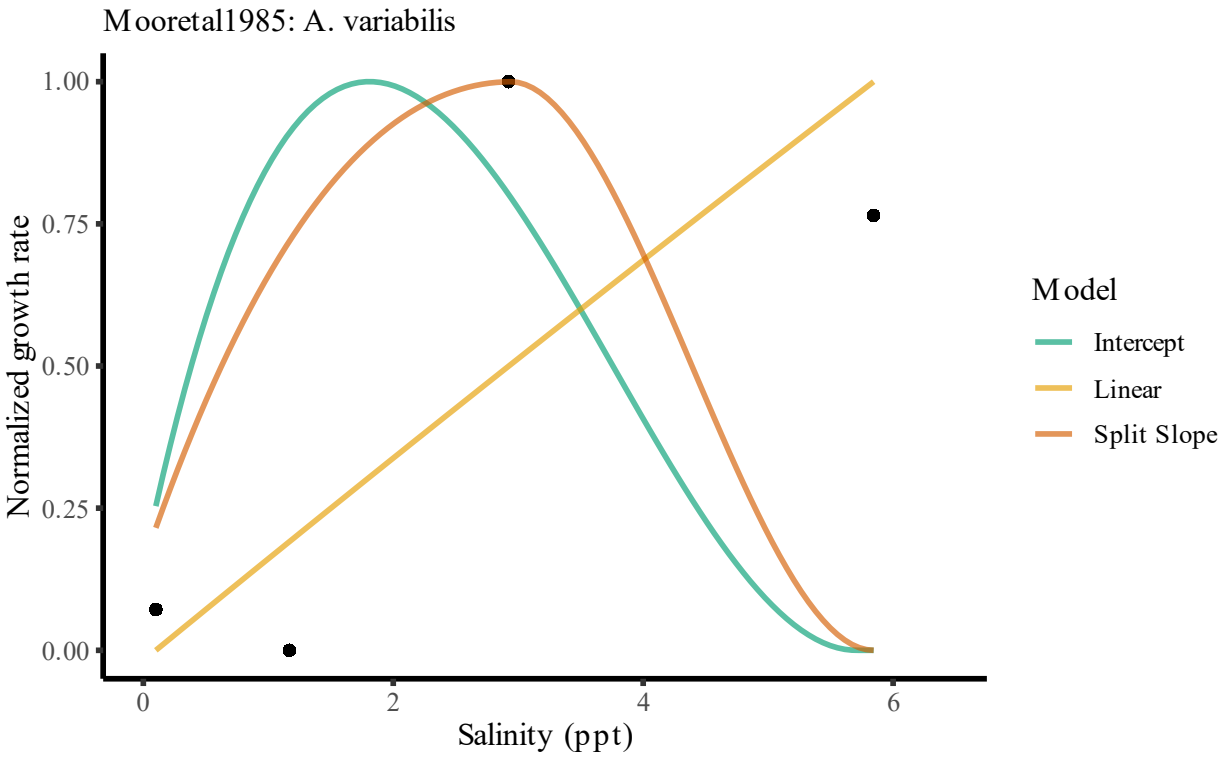

Figure 65: Reaction norm and model fits for Anabaena variabilis from (Moore et al., 1985)

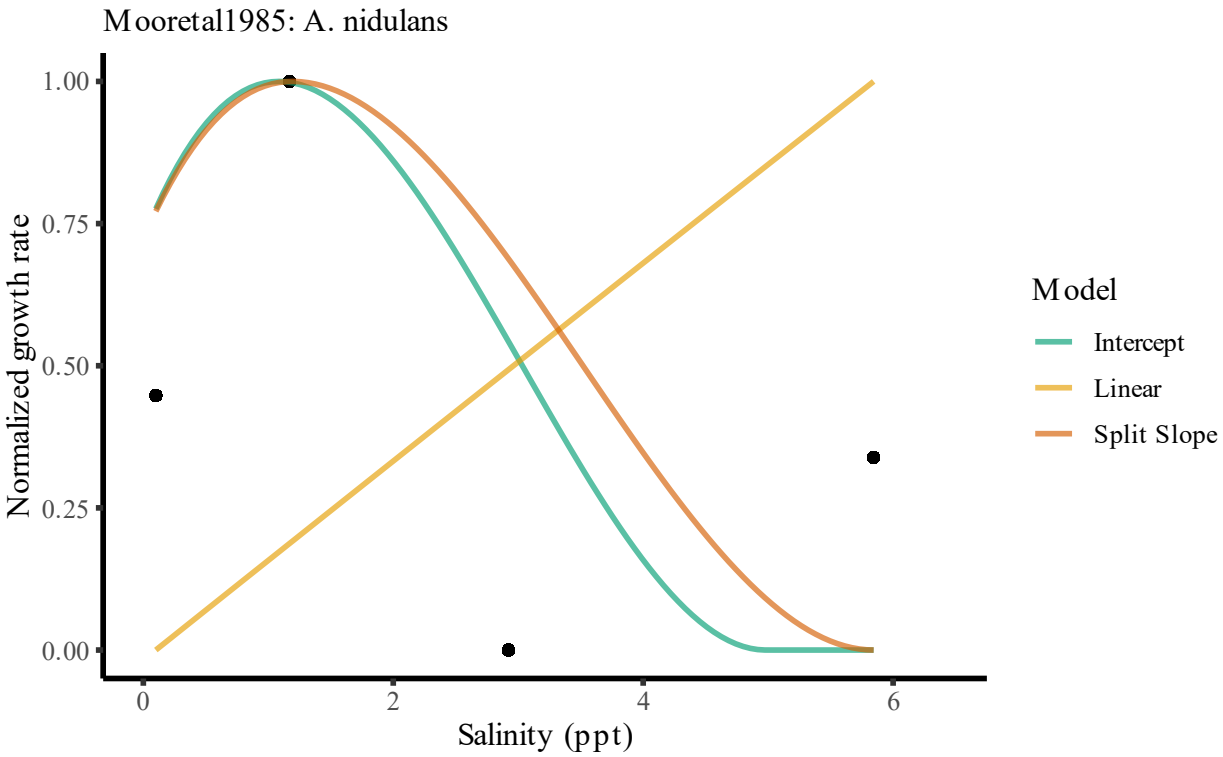

Figure 66: Reaction norm and model fits for Anacystis nidulans from (Moore et al., 1985)

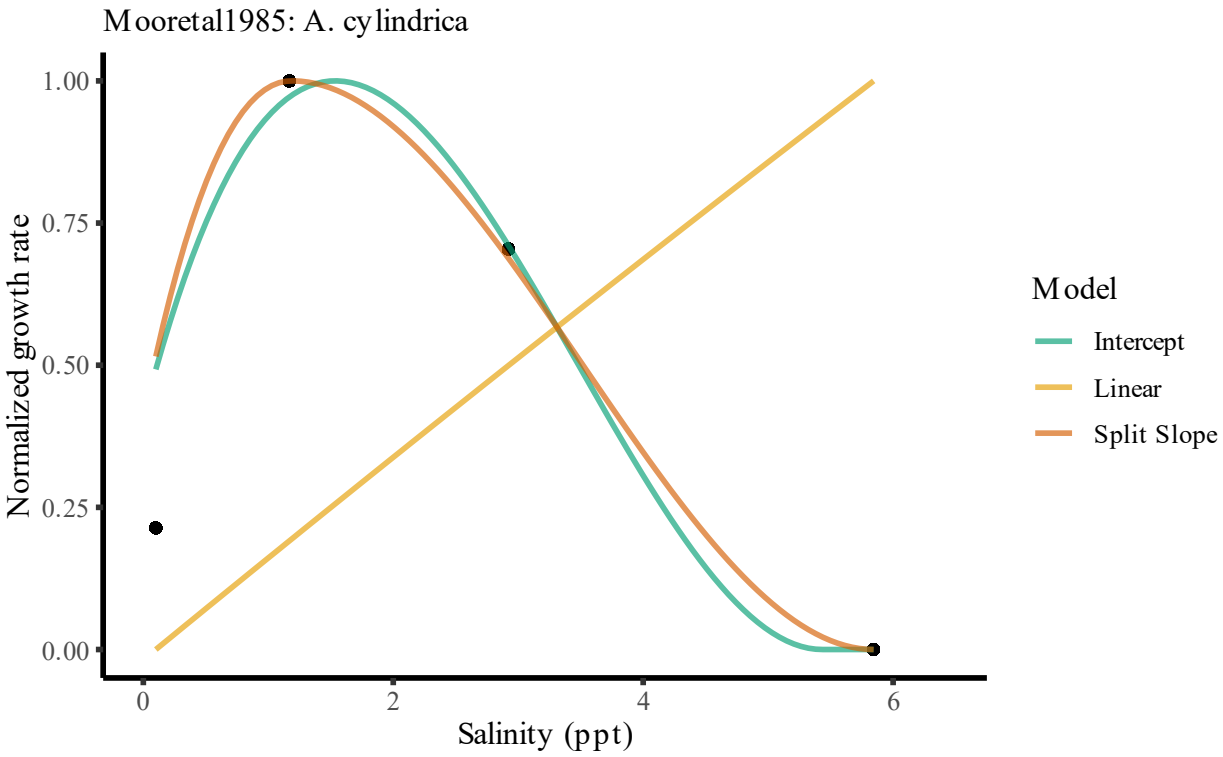

Figure 67: Reaction norm and model fits for Anabaena cylindrica from (Moore et al., 1985)

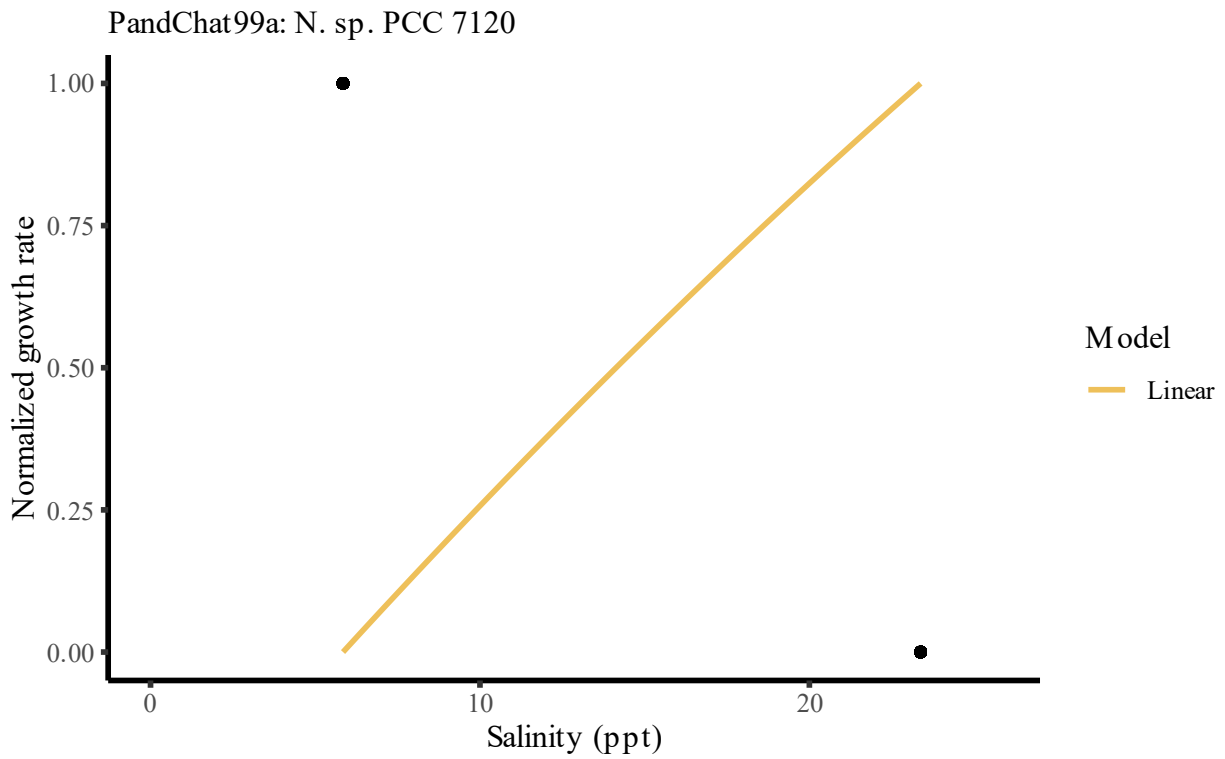

Figure 68: Reaction norm and model fits for Nostoc sp. PCC 7120 from (Pandey and Chatterjee, 1999)

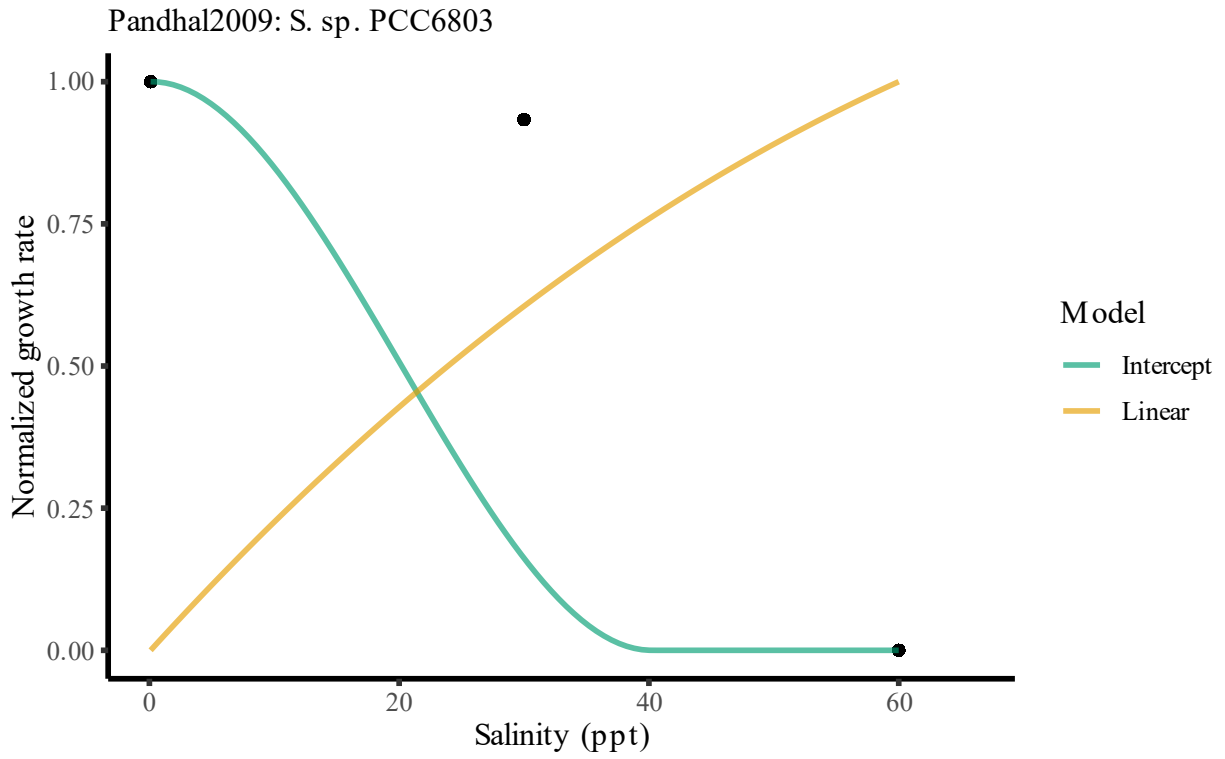

Figure 69: Reaction norm and model fits for Synechocystis sp. PCC 6803 from (Pandhal et al., 2009)

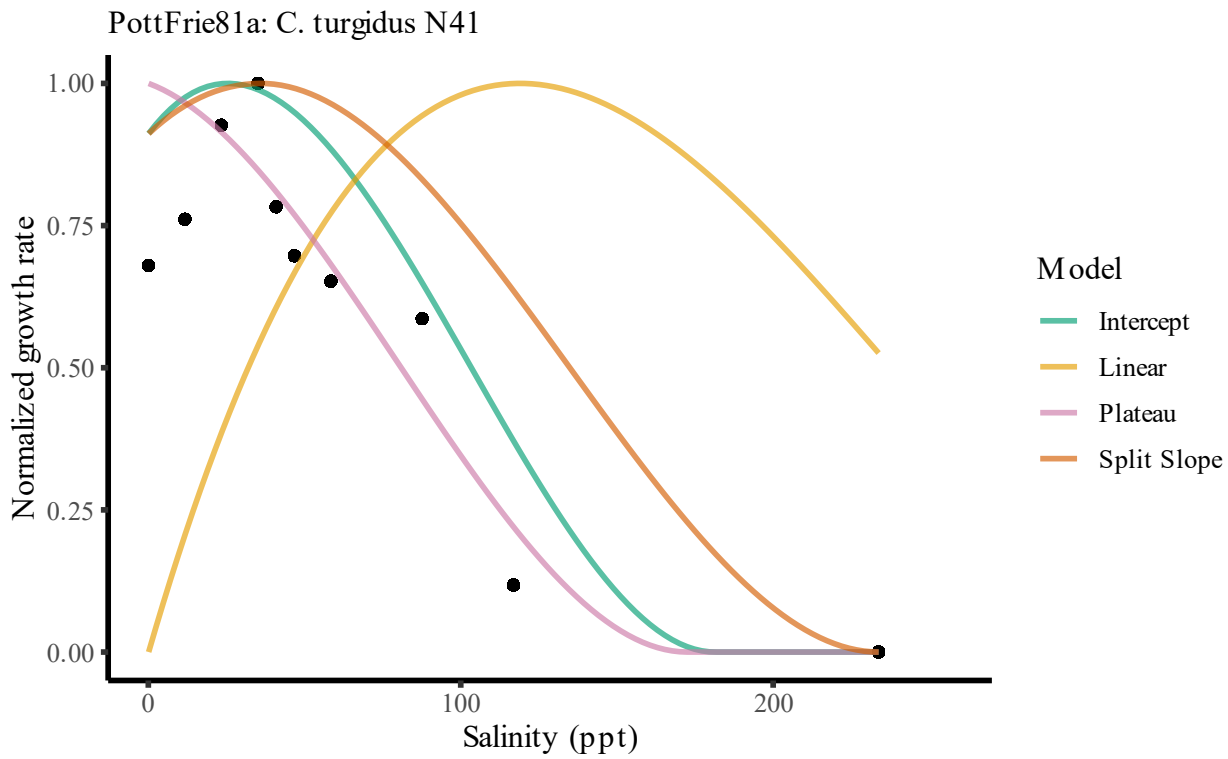

Figure 70: Reaction norm and model fits for Chroococcus turgidus N41 from (Potts and Friedmann, 1981)

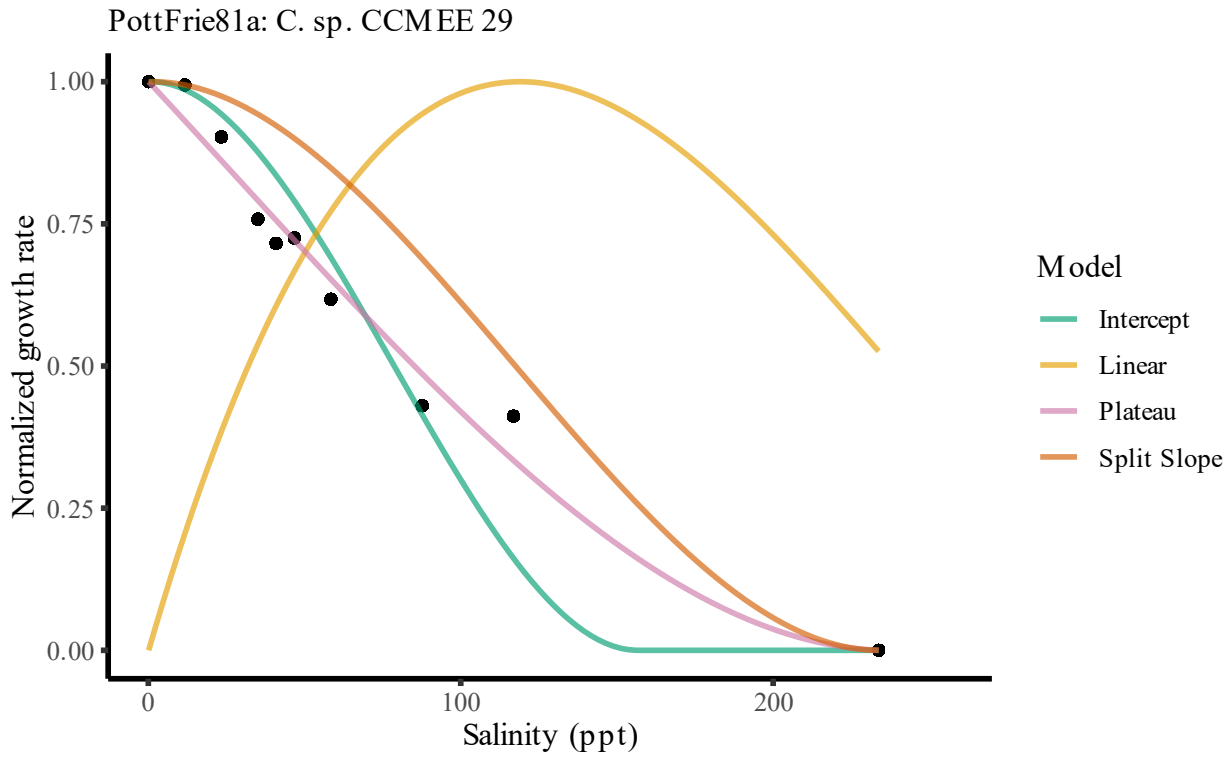

Figure 71: Reaction norm and model fits for Chroococcidiopsis sp. CCMEE 29 from (Potts and Friedmann, 1981)

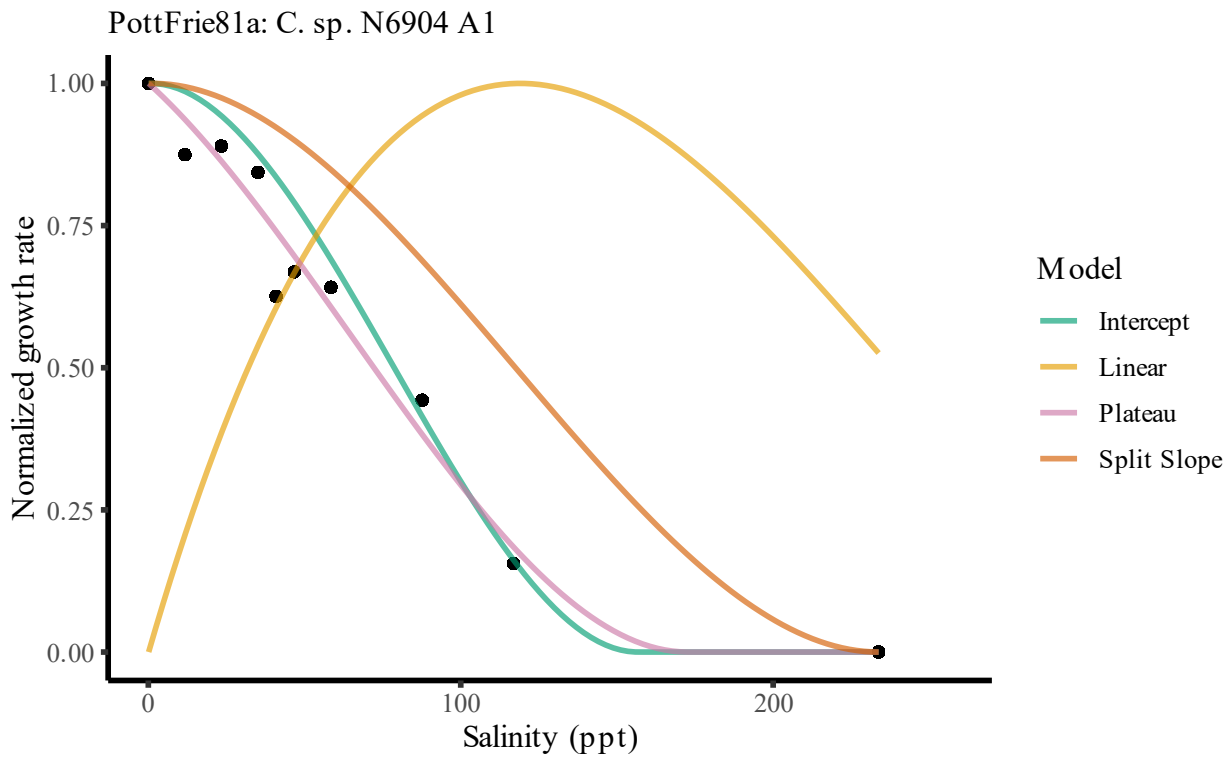

Figure 72: Reaction norm and model fits for Chroococcidiopsis sp. N6904 A1 from (Potts and Friedmann, 1981)

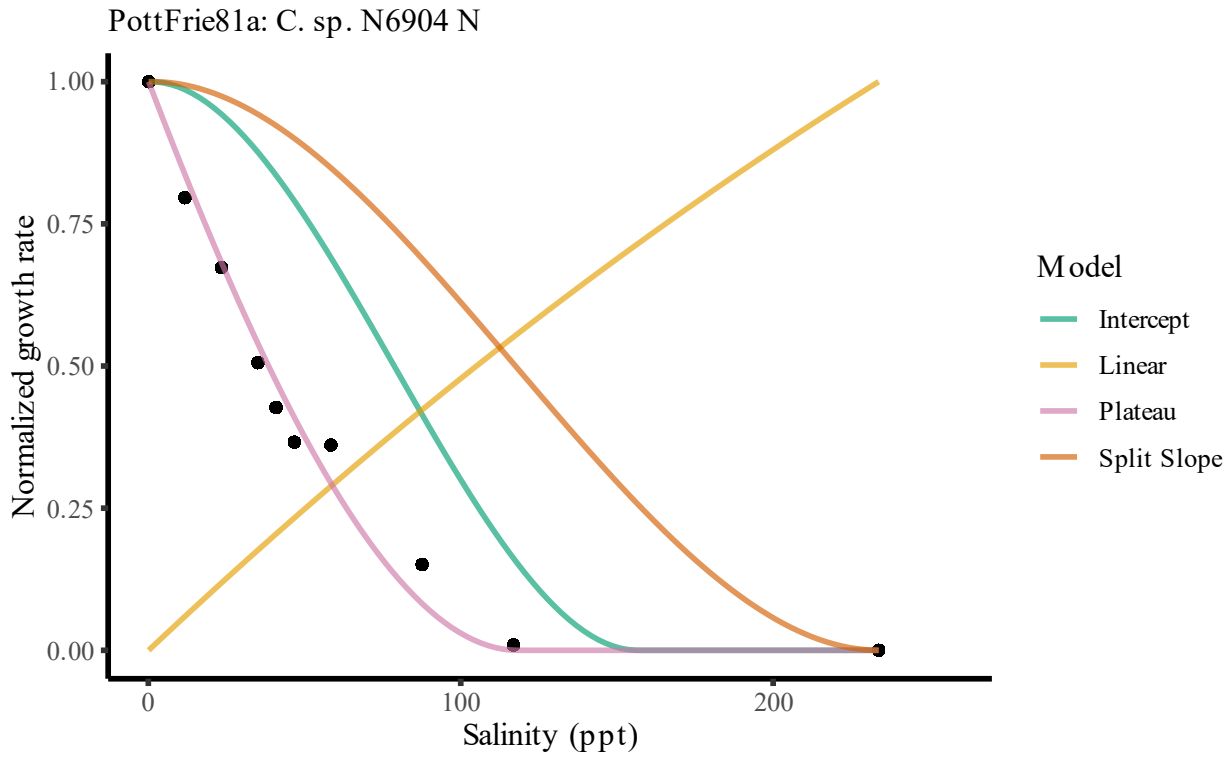

Figure 73: Reaction norm and model fits for Chroococcidiopsis sp. N6904 N from (Potts and Friedmann, 1981)

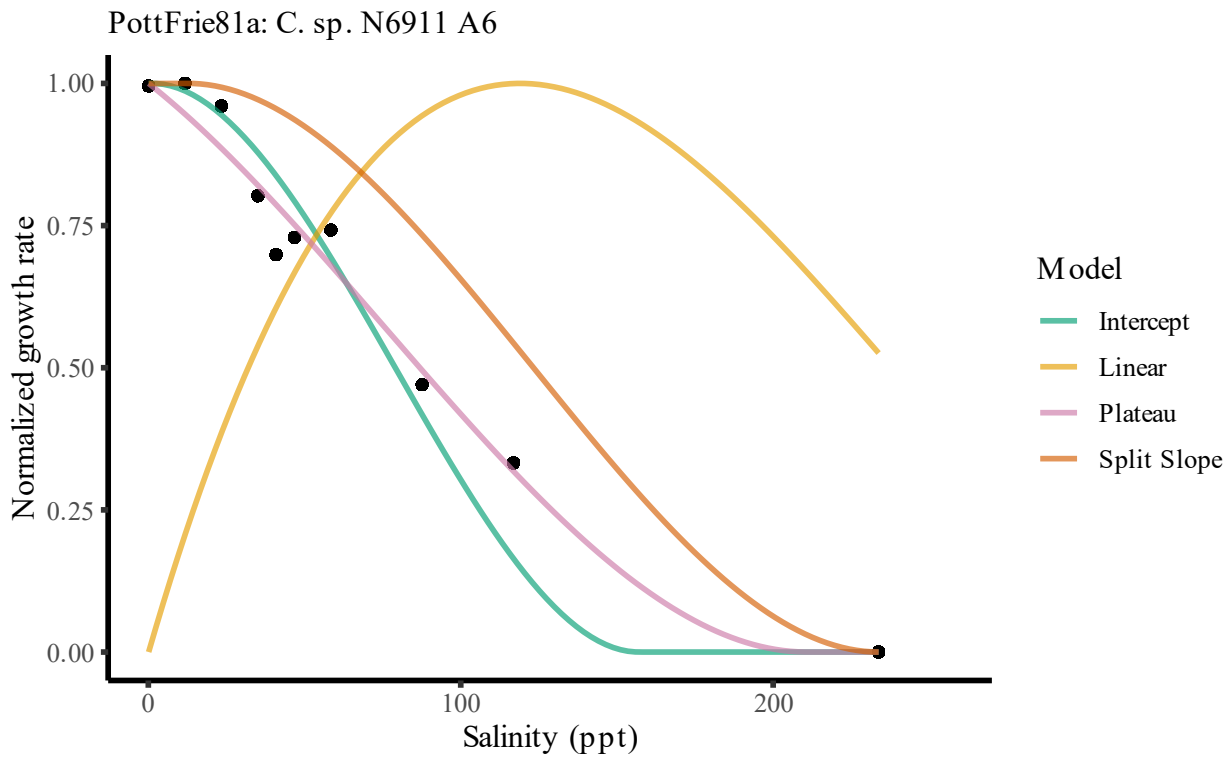

Figure 74: Reaction norm and model fits for Chroococcidiopsis sp. N6911 A6 from (Potts and Friedmann, 1981)

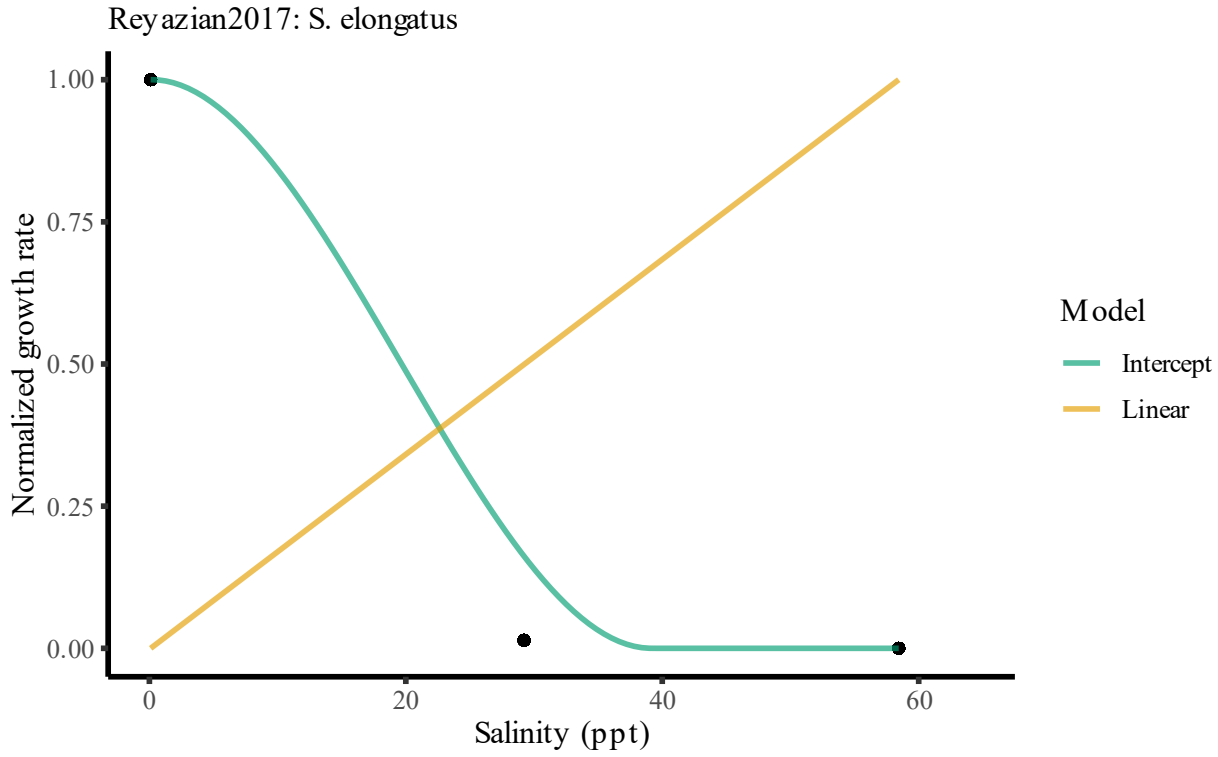

Figure 75: Reaction norm and model fits for Synechococcus elongatus from (Rezayian et al., 2017)

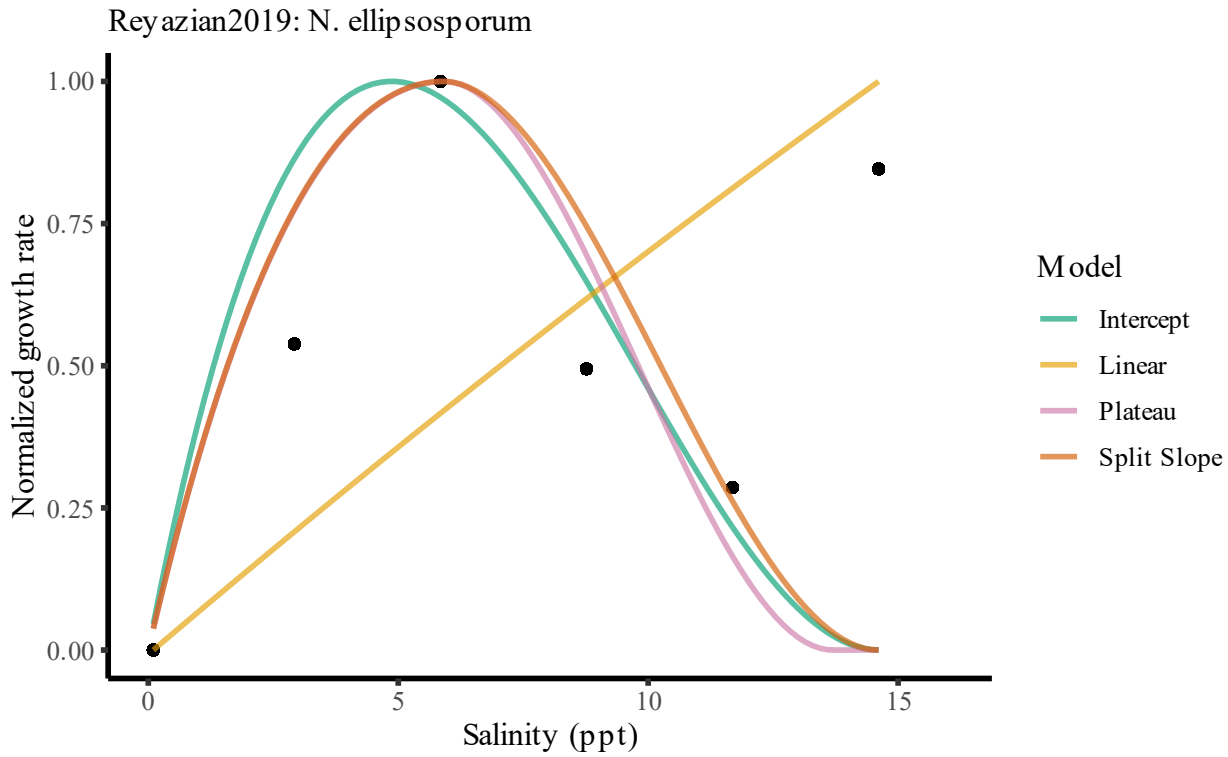

Figure 76: Reaction norm and model fits for Nostoc ellipsosporum from (Rezayian et al., 2019)

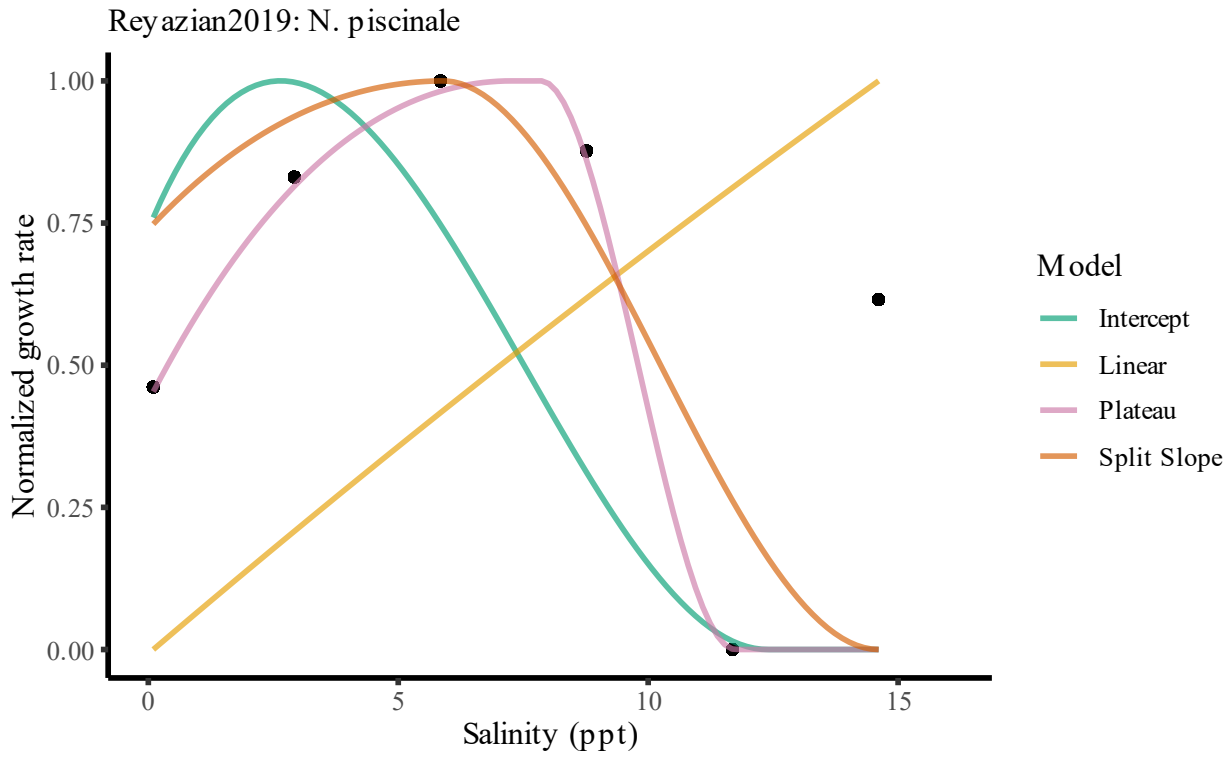

Figure 77: Reaction norm and model fits for Nostoc piscinale from (Rezayian et al., 2019)

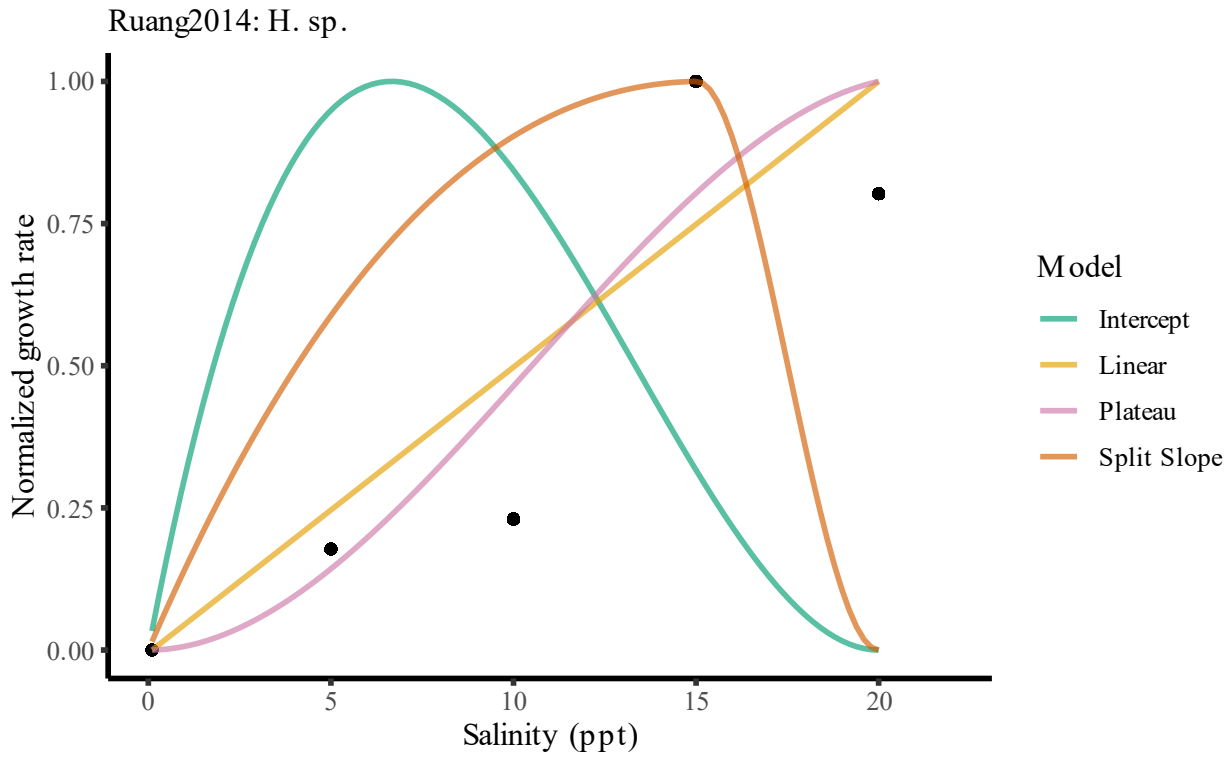

Figure 78: Reaction norm and model fits for Hapalosiphon sp. from (Ruangsomboon, 2014)

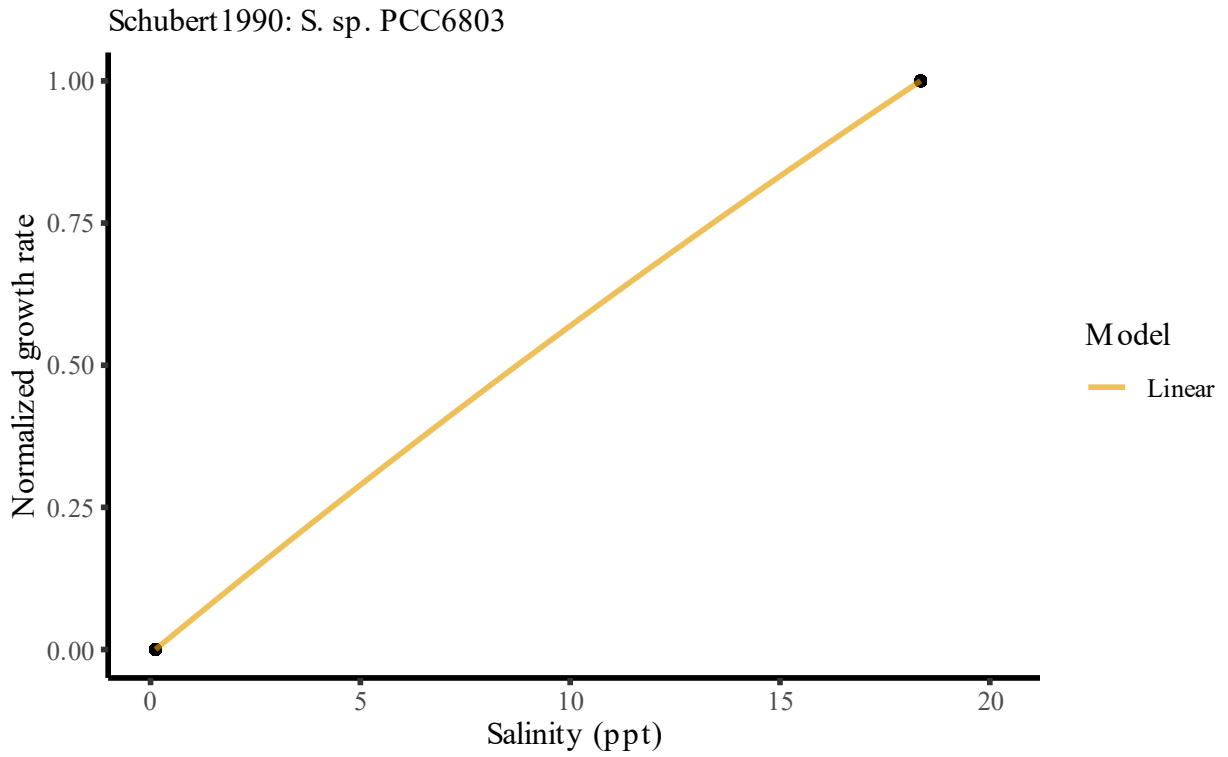

Figure 79: Reaction norm and model fits for Synechocystis sp. PCC 6803 from (Schubert and Hagemann, 1990)

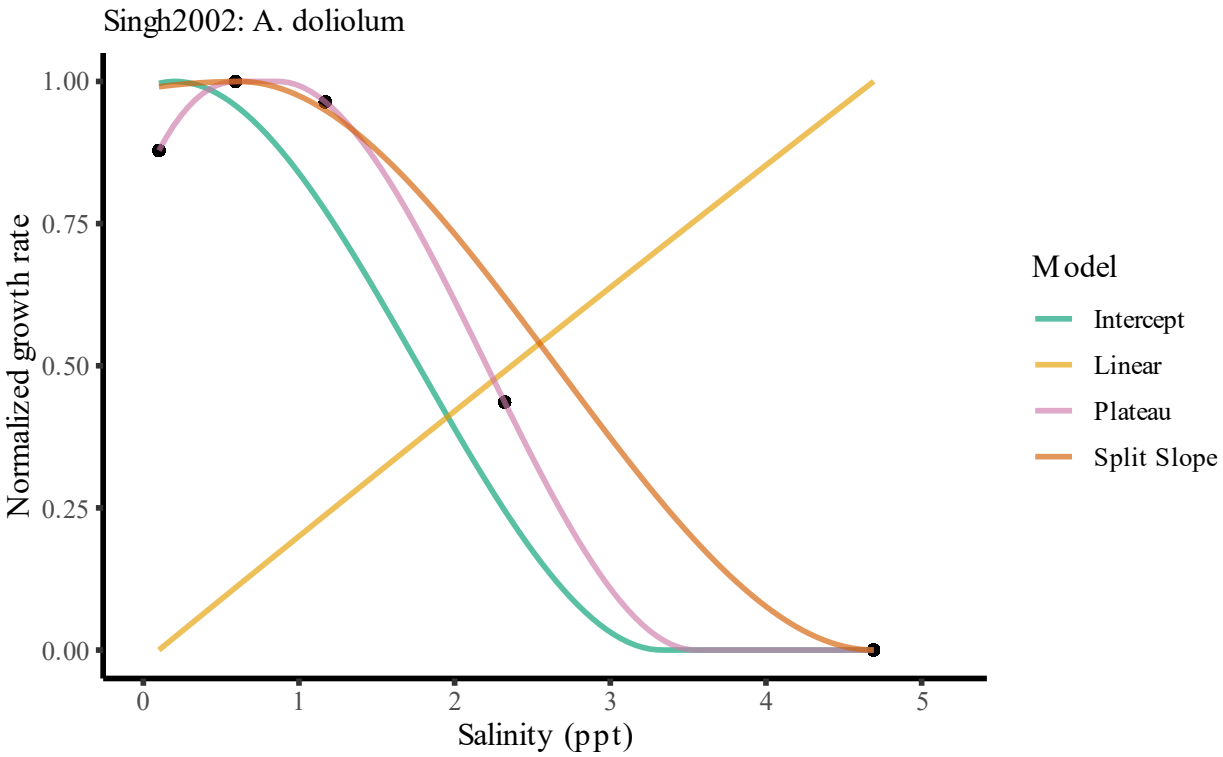

Figure 80: Reaction norm and model fits for Anabaena doliolum from (Singh and Kshatriya, 2002)

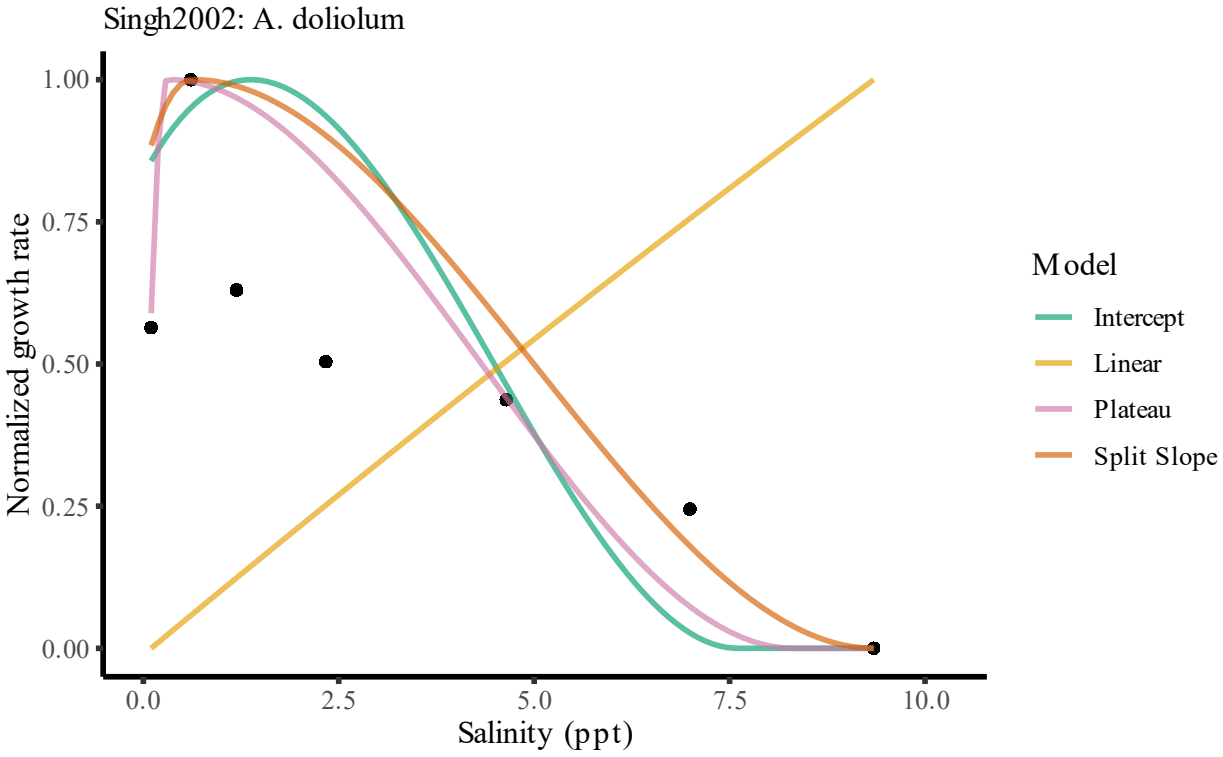

Figure 81: Reaction norm and model fits for Anabaena doliolum from (Singh and Kshatriya, 2002)

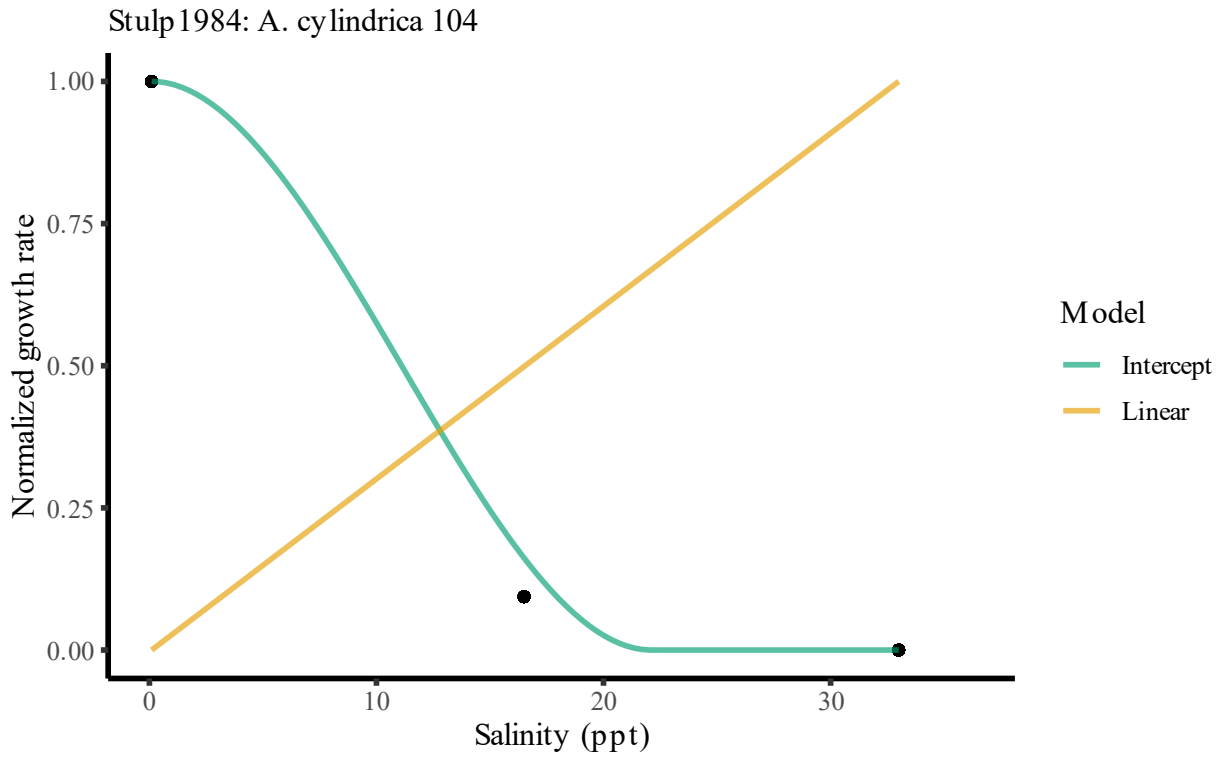

Figure 82: Reaction norm and model fits for Anabaena cylindrica 104 from (Stulp and Stam, 1984)

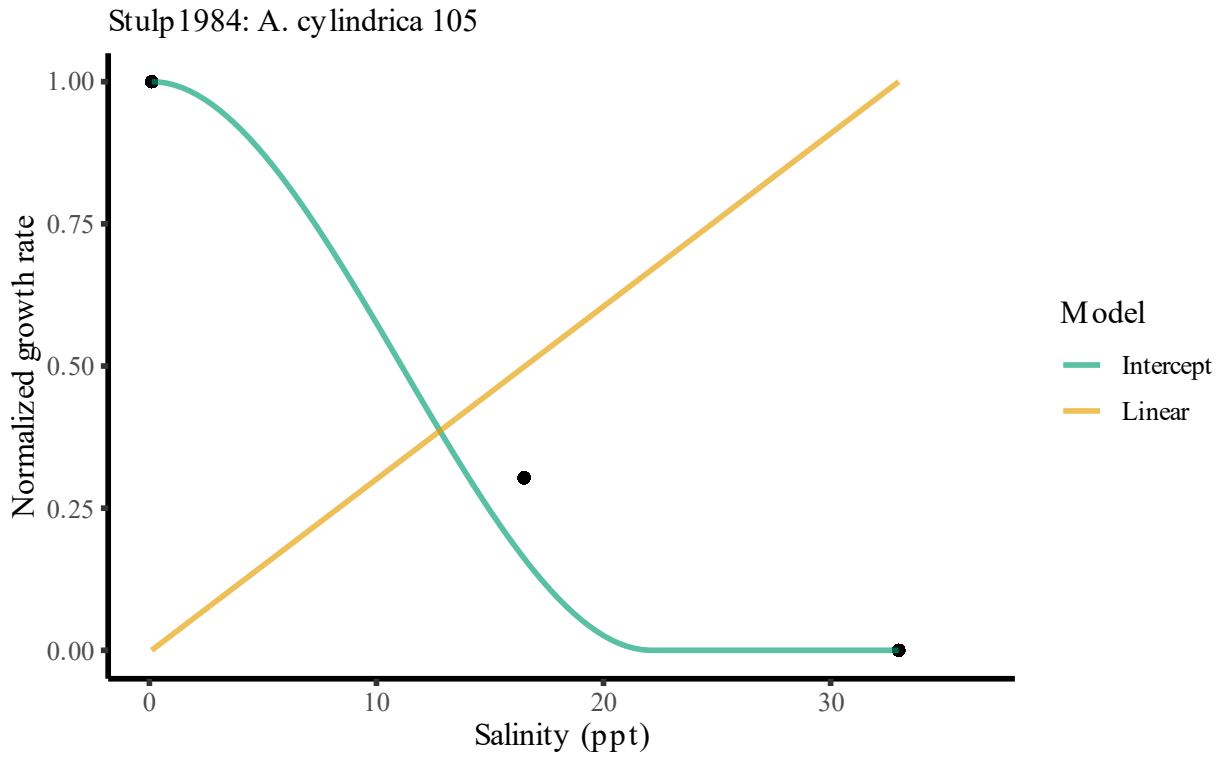

Figure 83: Reaction norm and model fits for Anabaena cylindrica 105 from (Stulp and Stam, 1984)

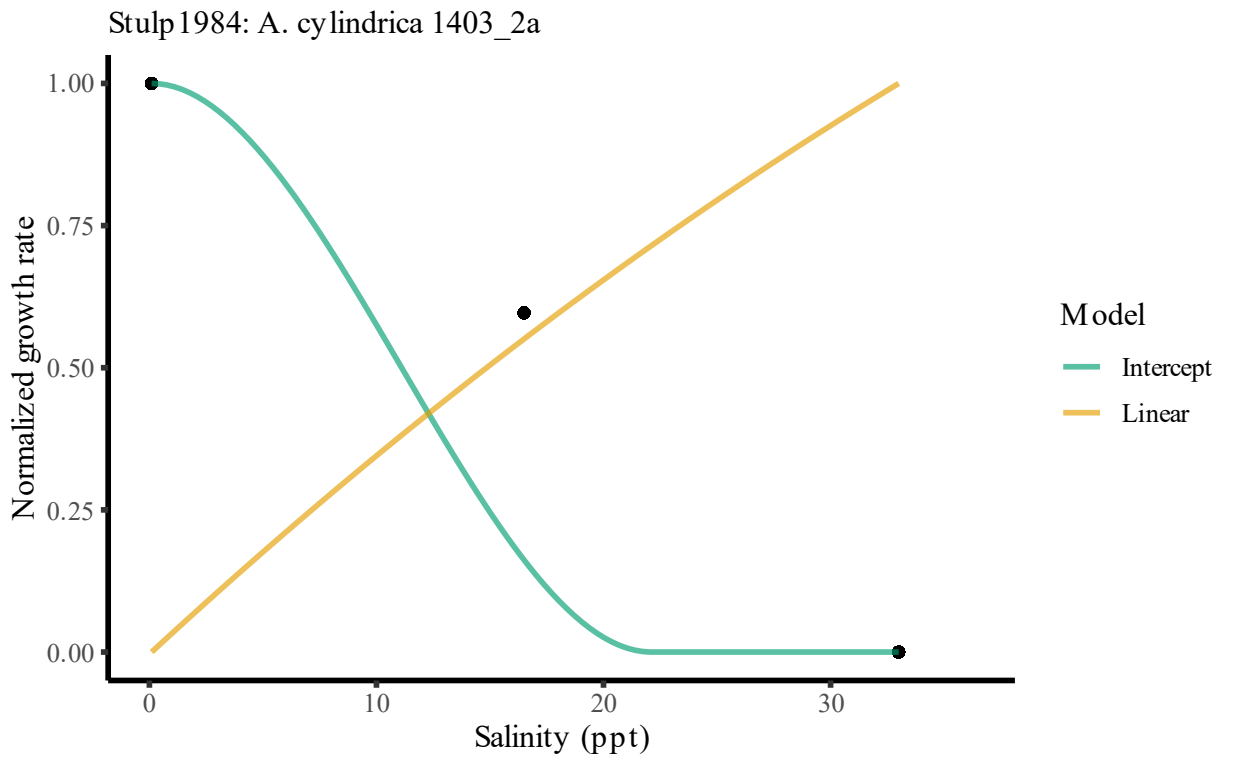

Figure 84: Reaction norm and model fits for Anabaena cylindrica 1403 2a from (Stulp and Stam, 1984)

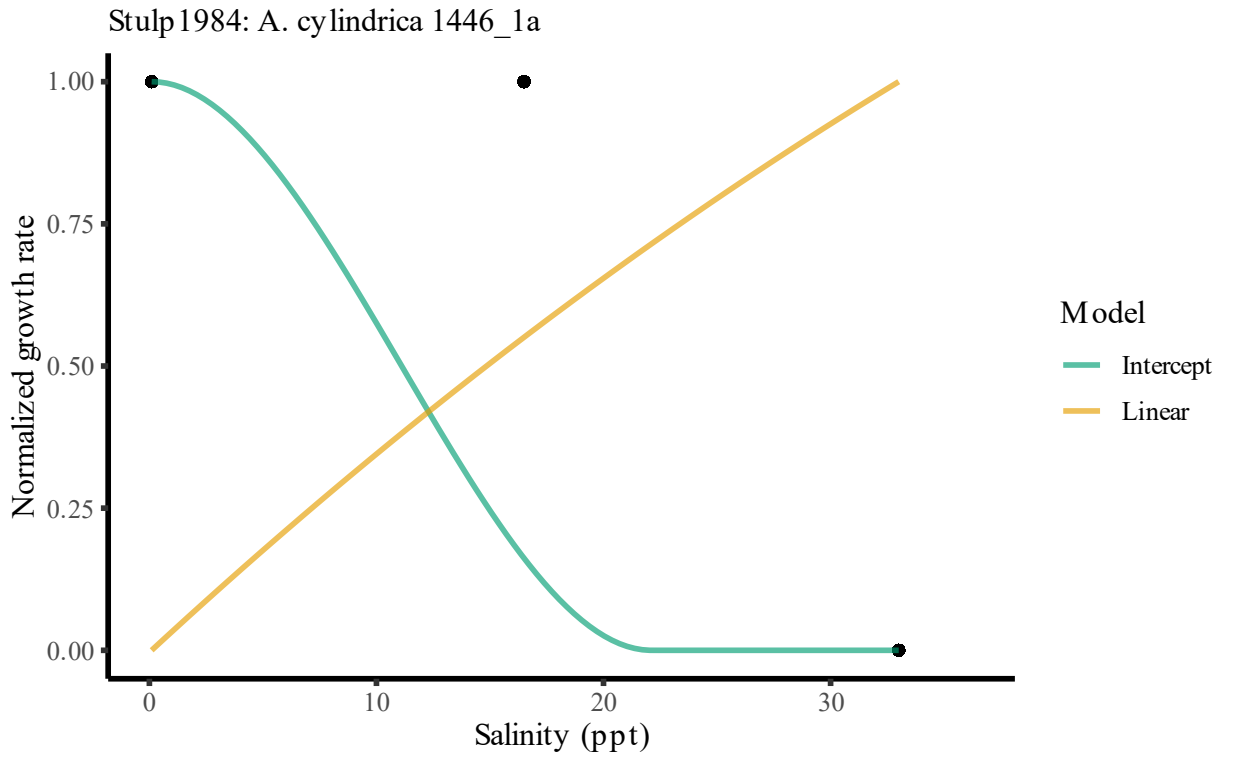

Figure 85: Reaction norm and model fits for Anabaena cylindrica 1446 1a from (Stulp and Stam, 1984)

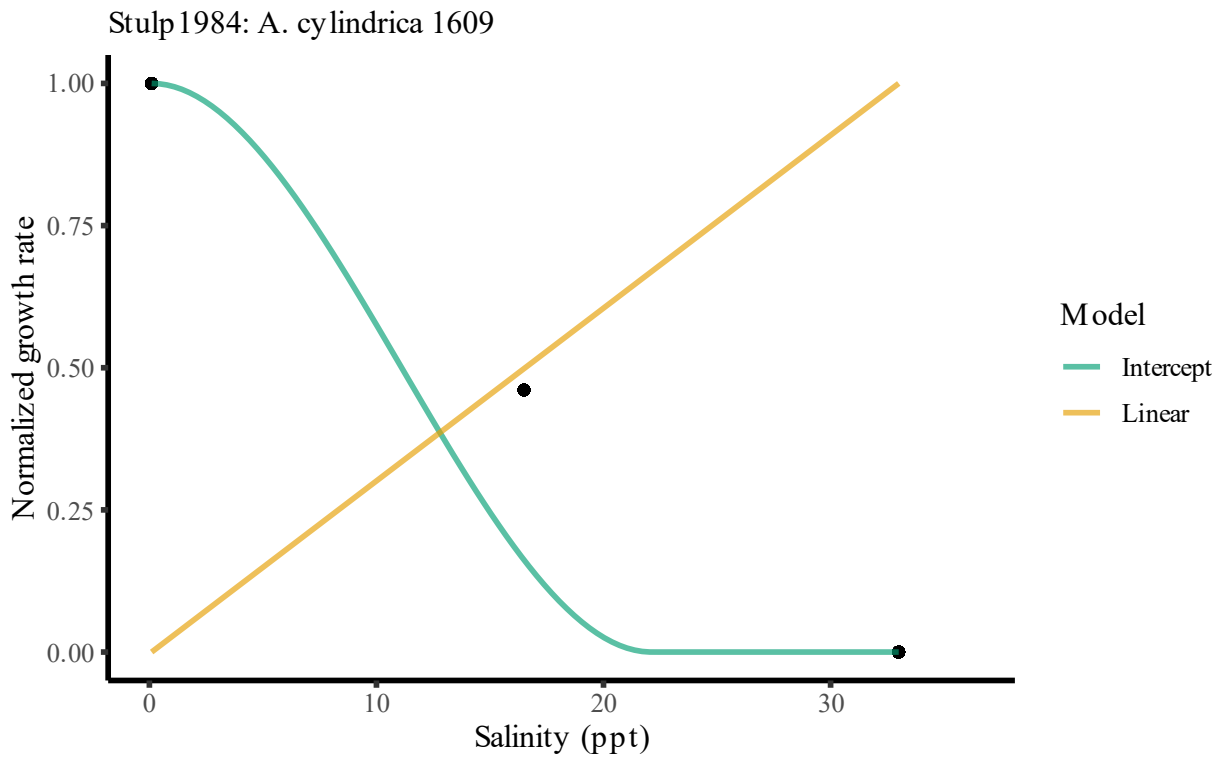

Figure 86: Reaction norm and model fits for Anabaena cylindrica 1609 from (Stulp and Stam, 1984)

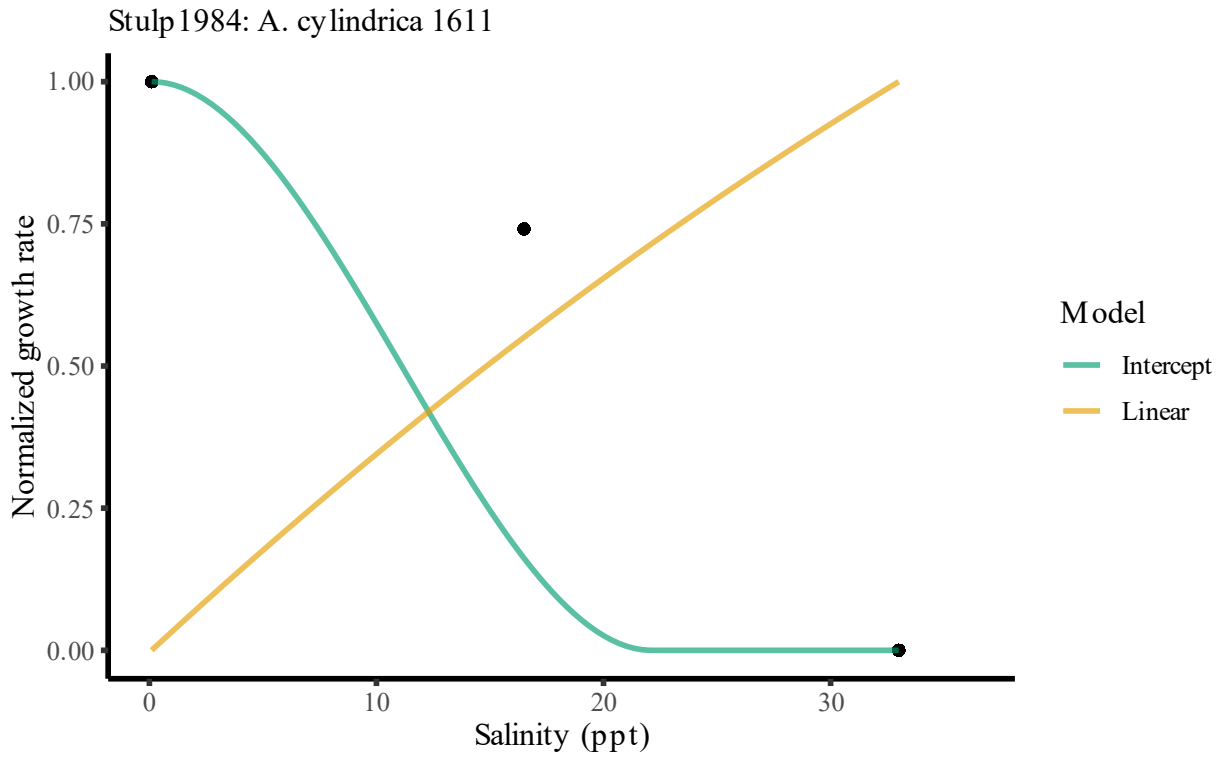

Figure 87: Reaction norm and model fits for Anabaena cylindrica 1611 from (Stulp and Stam, 1984)

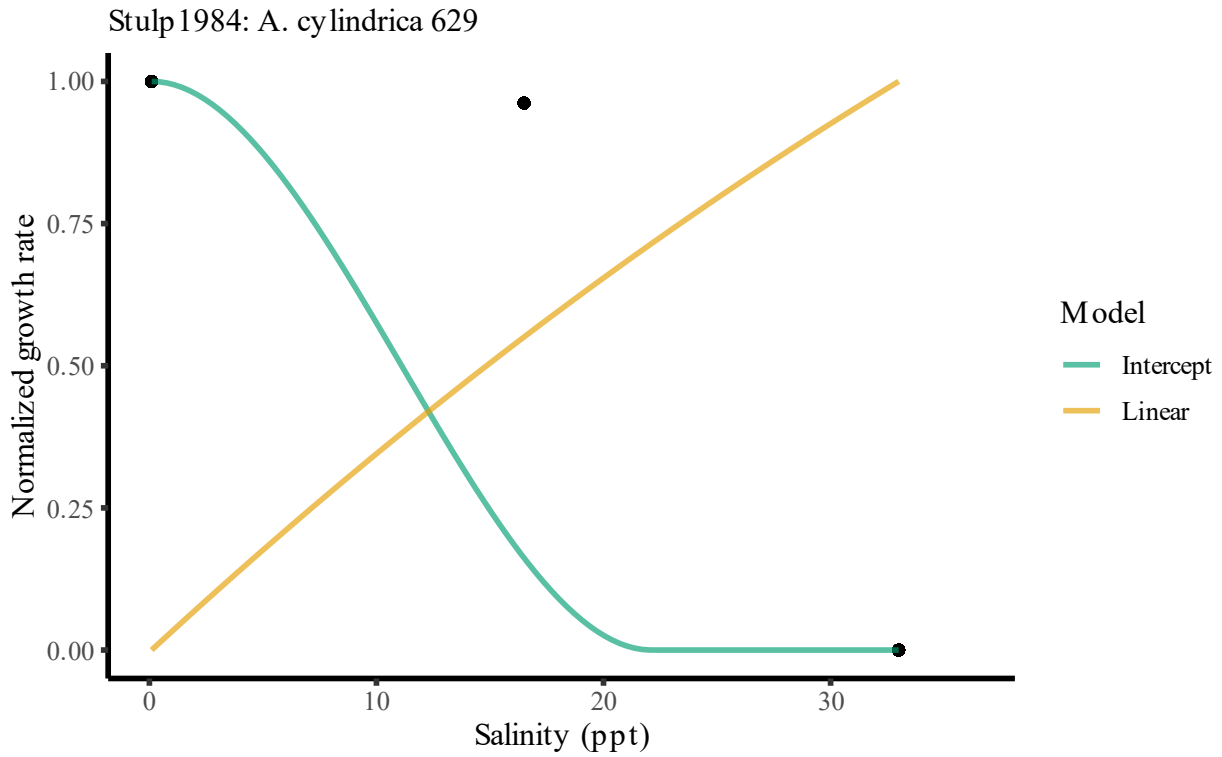

Figure 88: Reaction norm and model fits for Anabaena cylindrica 629 from (Stulp and Stam, 1984)

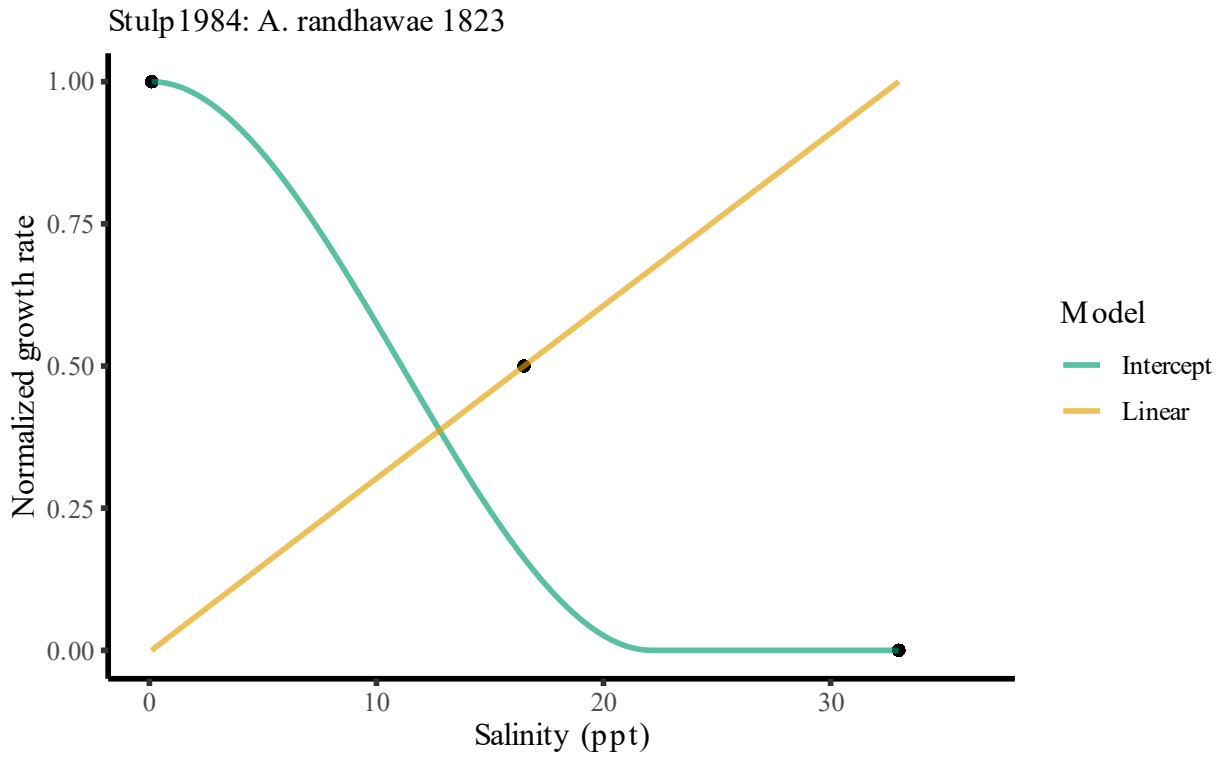

Figure 89: Reaction norm and model fits for Anabaena randhawae 1823 from (Stulp and Stam, 1984)

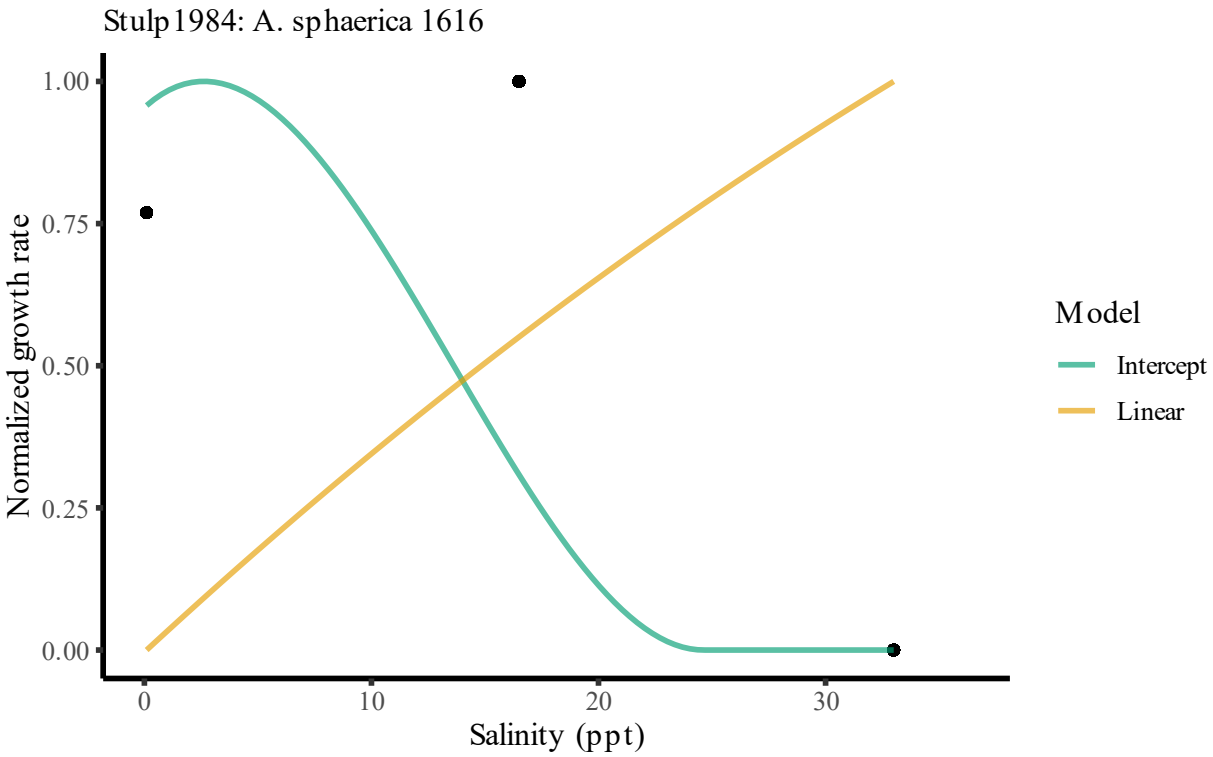

Figure 90: Reaction norm and model fits for Anabaena sphaerica 1616 from (Stulp and Stam, 1984)

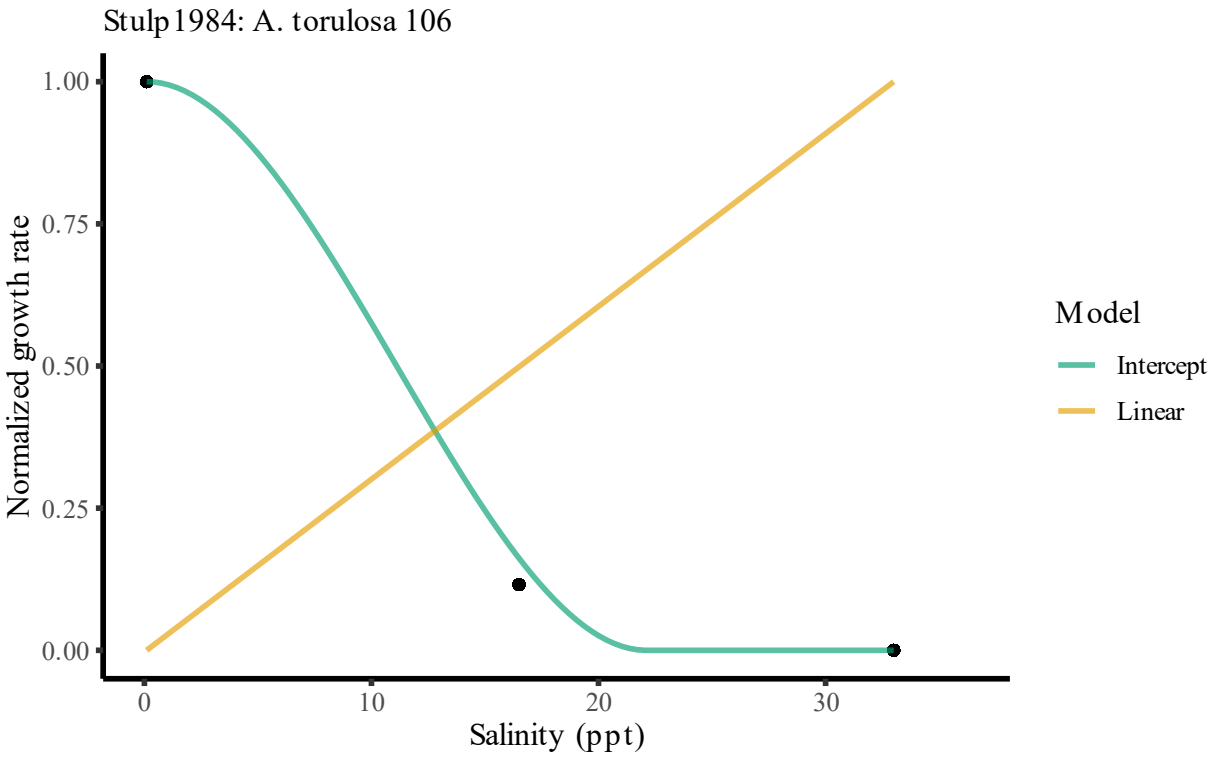

Figure 91: Reaction norm and model fits for Anabaena torulosa 106 from (Stulp and Stam, 1984)

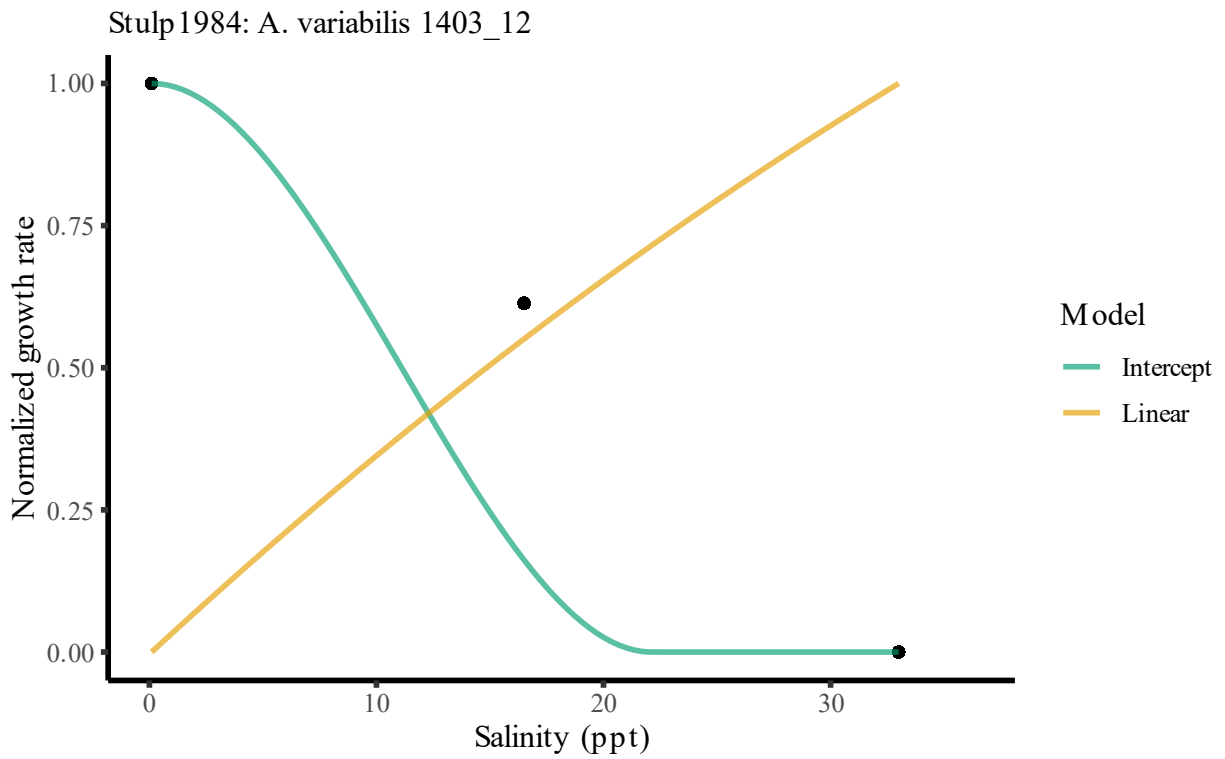

Figure 92: Reaction norm and model fits for Anabaena variabilis 1403 12 from (Stulp and Stam, 1984)

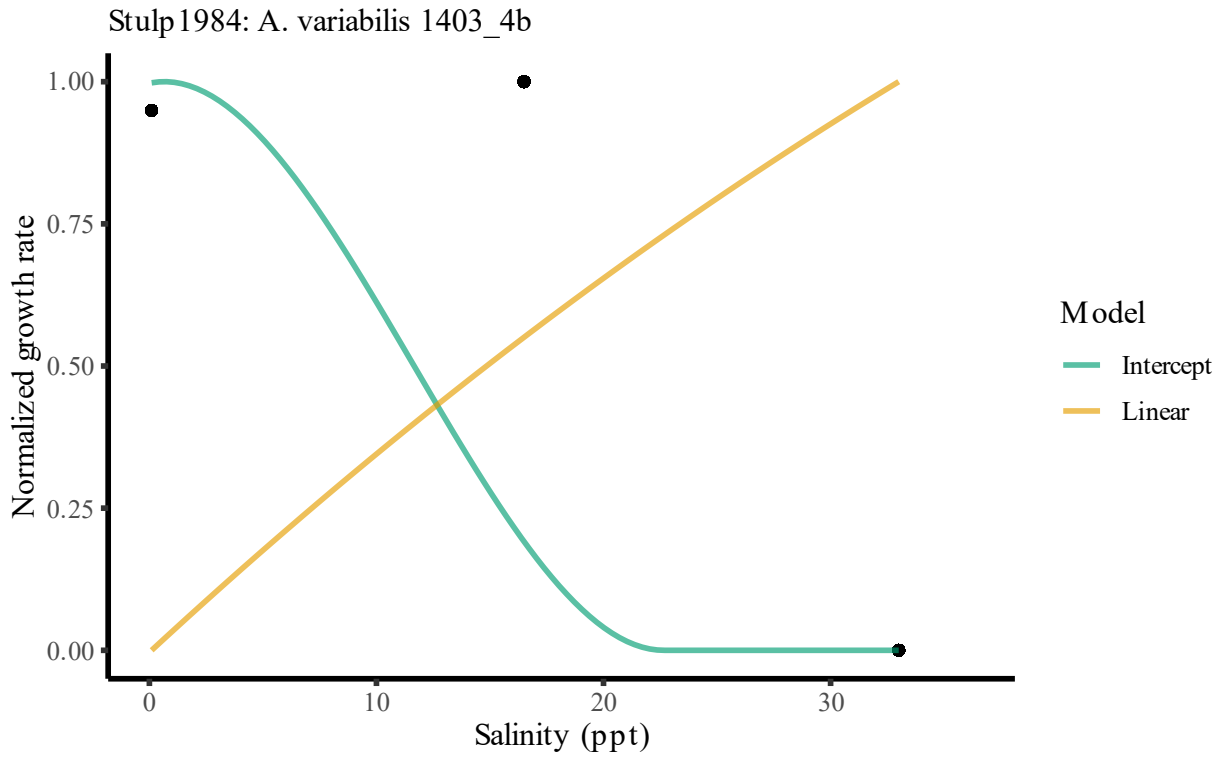

Figure 93: Reaction norm and model fits for Anabaena variabilis 1403 4b from (Stulp and Stam, 1984)

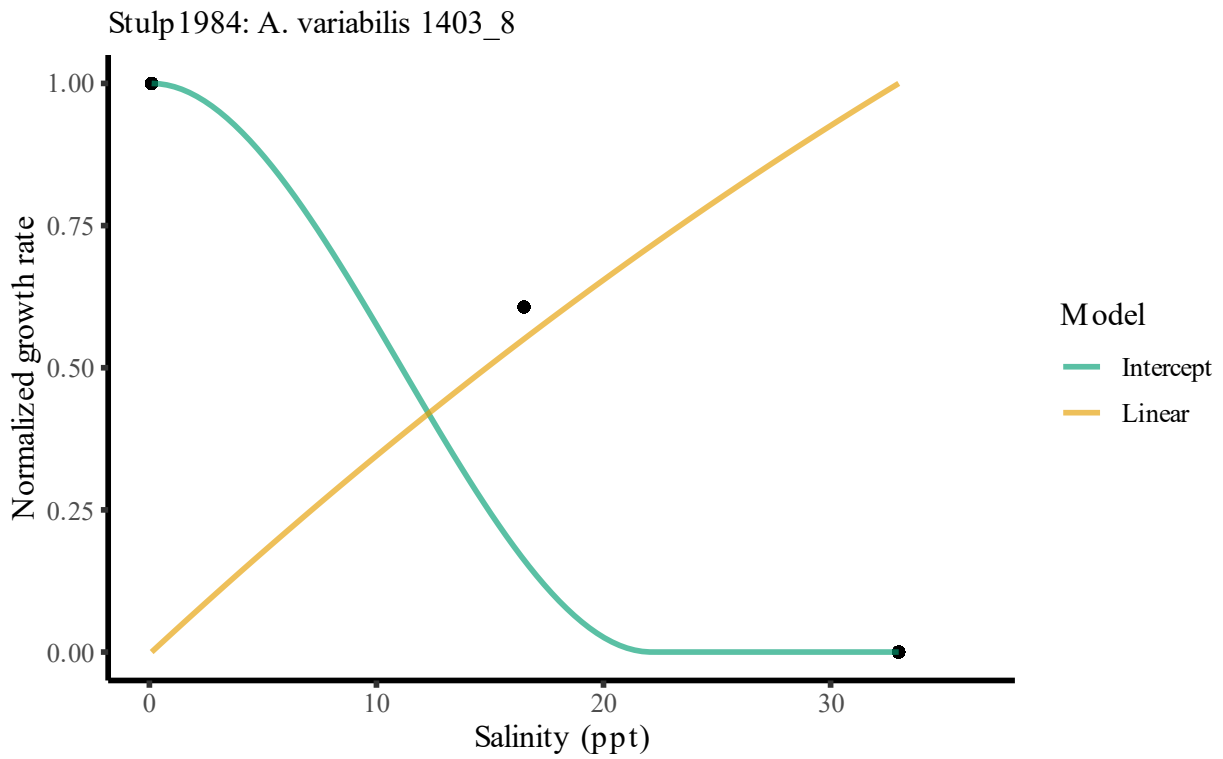

Figure 94: Reaction norm and model fits for Anabaena variabilis 1403 8 from (Stulp and Stam, 1984)

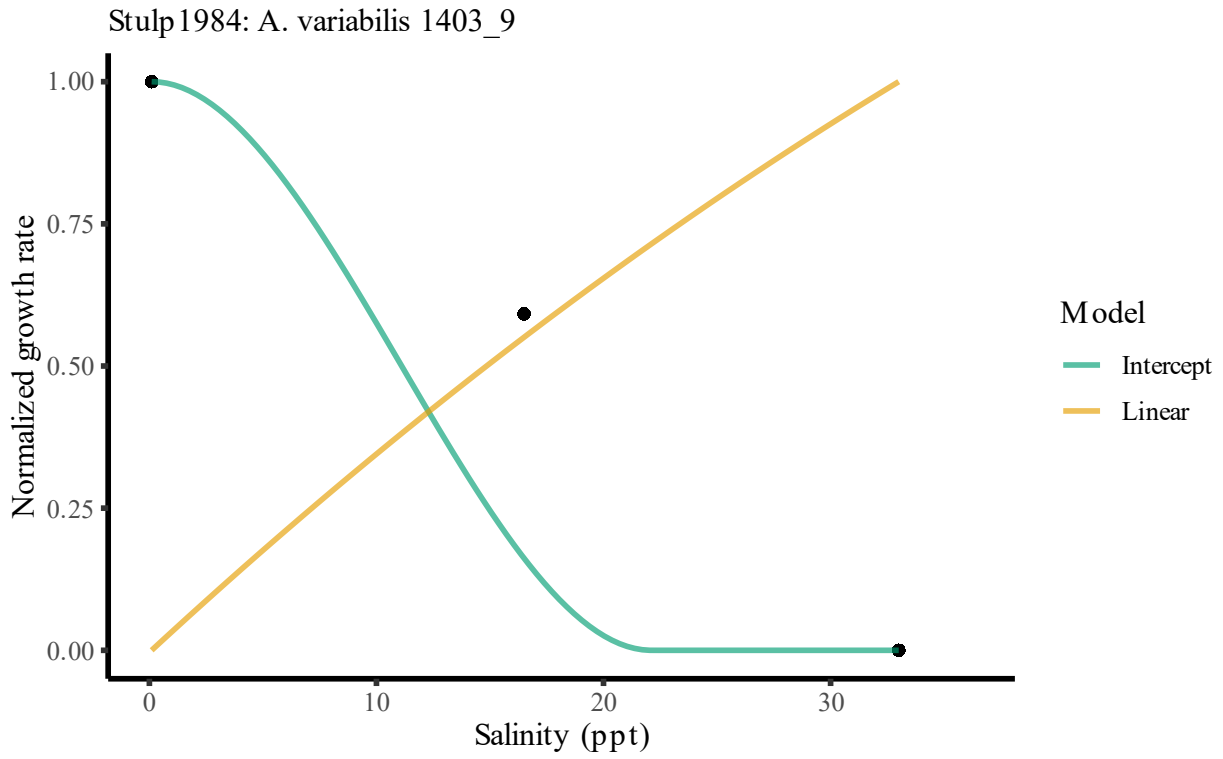

Figure 95: Reaction norm and model fits for Anabaena variabilis 1403 9 from (Stulp and Stam, 1984)

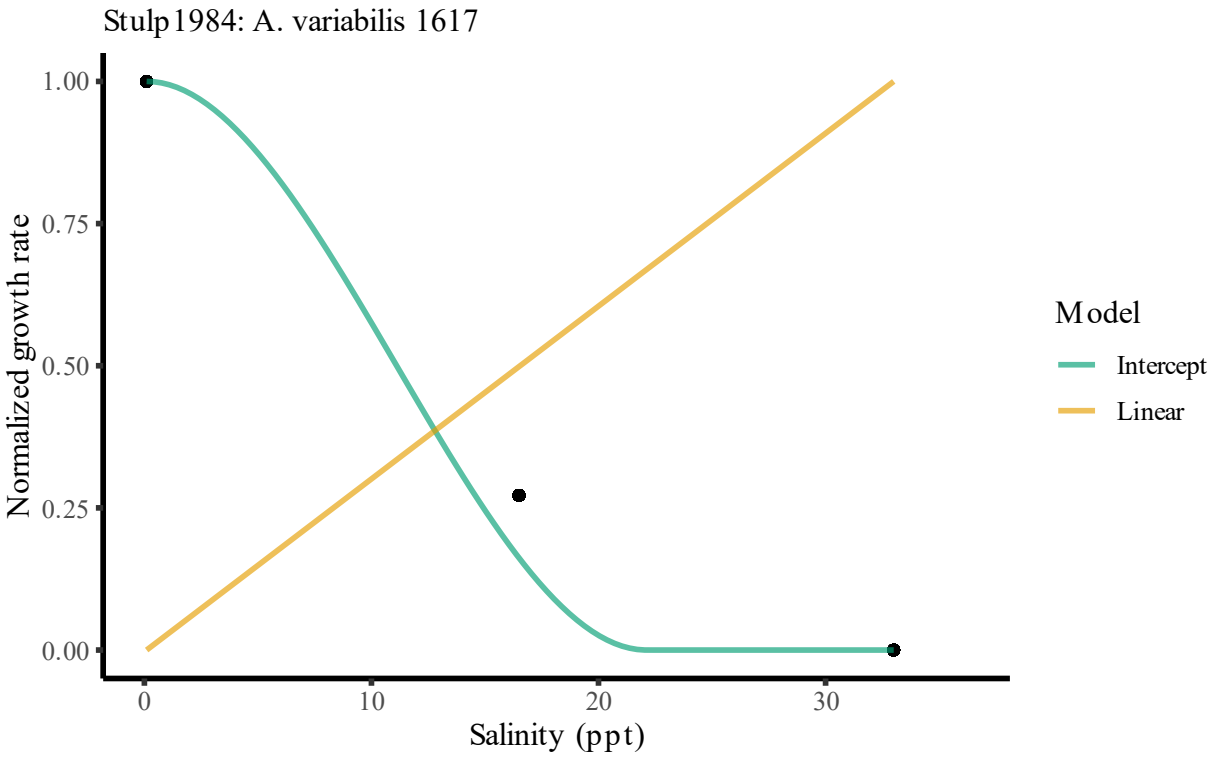

Figure 96: Reaction norm and model fits for Anabaena variabilis 1617 from (Stulp and Stam, 1984)

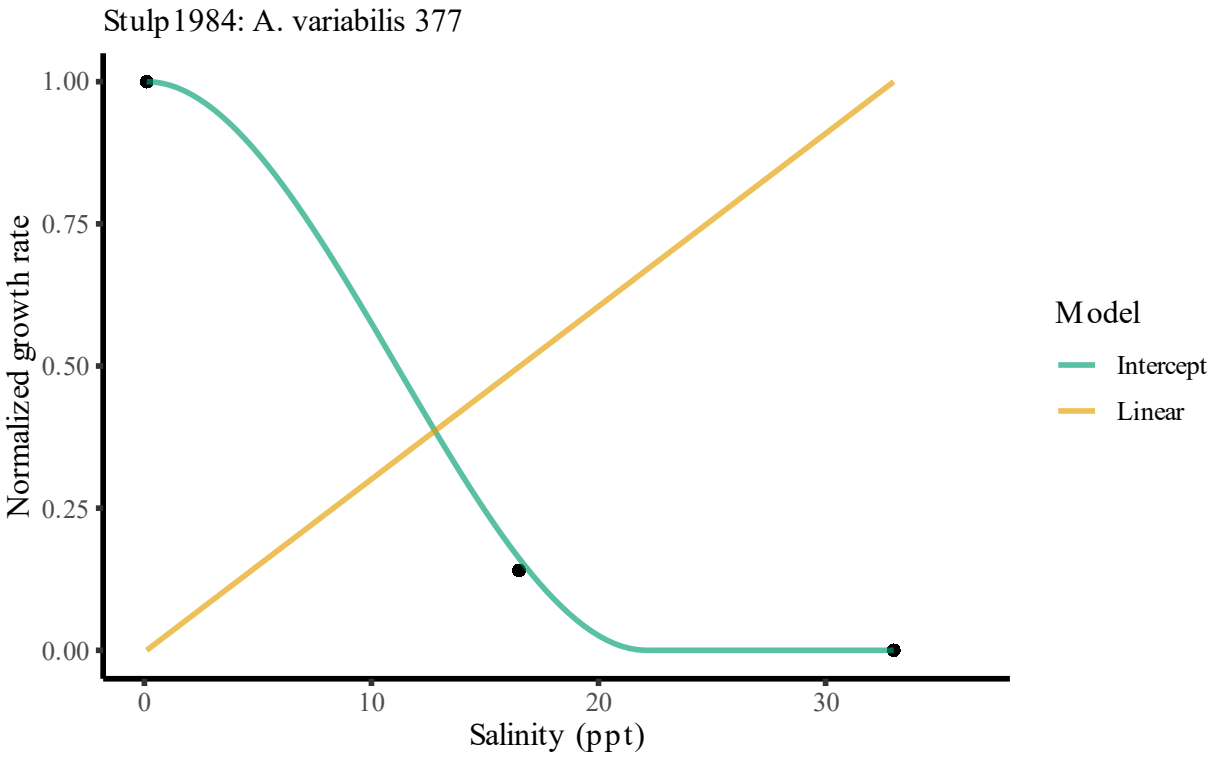

Figure 97: Reaction norm and model fits for Anabaena variabilis 377 from (Stulp and Stam, 1984)

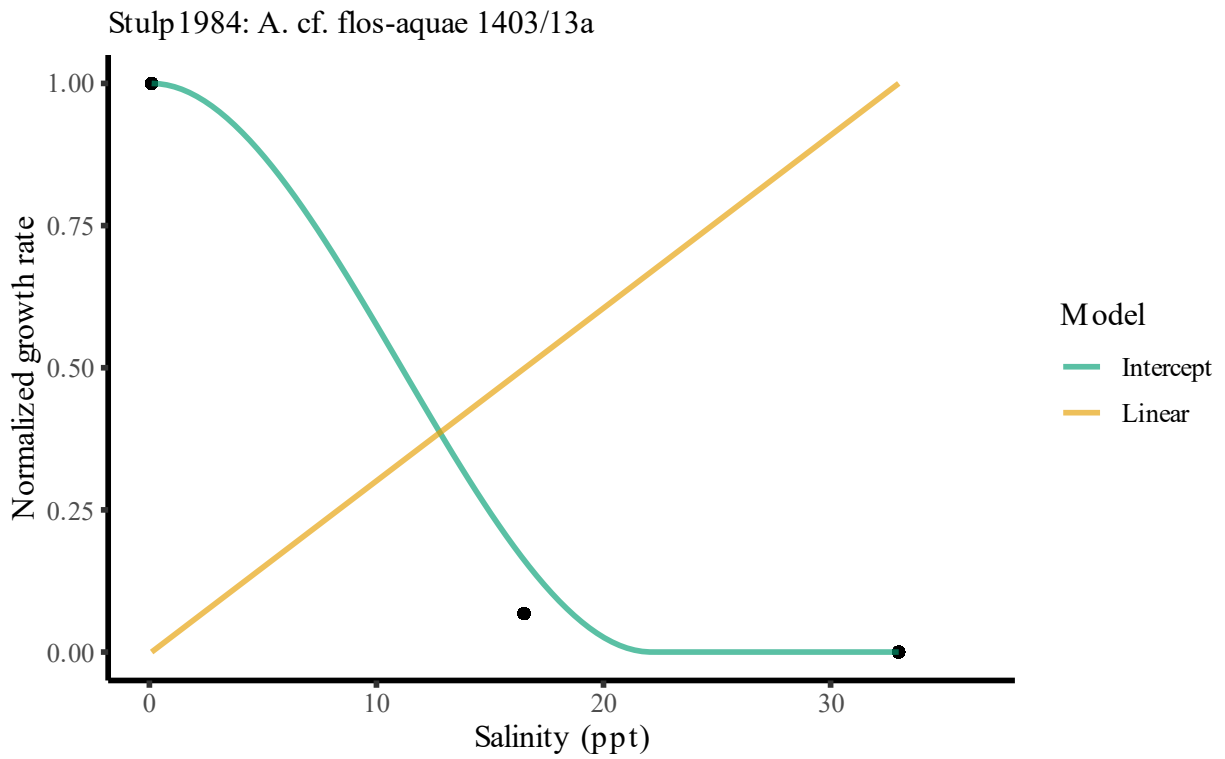

Figure 98: Reaction norm and model fits for Anabaena cf. flos-aquae 1403 13a from (Stulp and Stam, 1984)

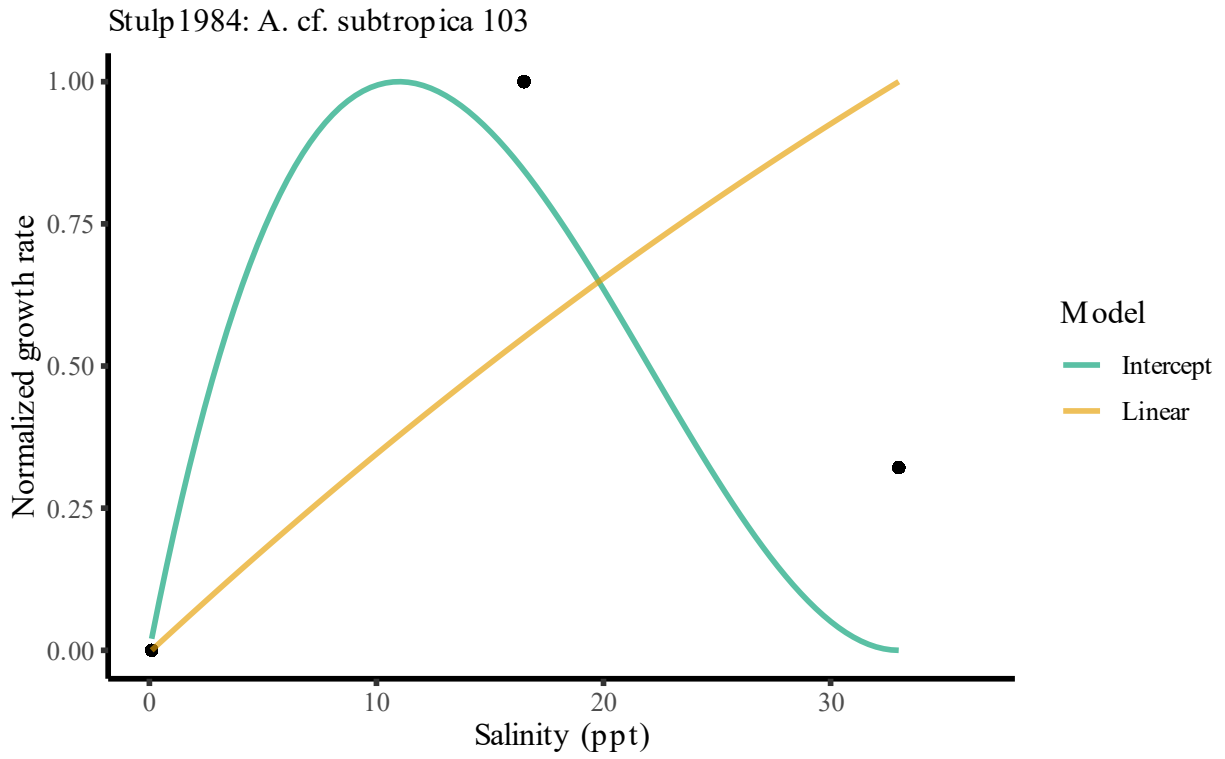

Figure 99: Reaction norm and model fits for Anabaena cf. subtropica 103 from (Stulp and Stam, 1984)

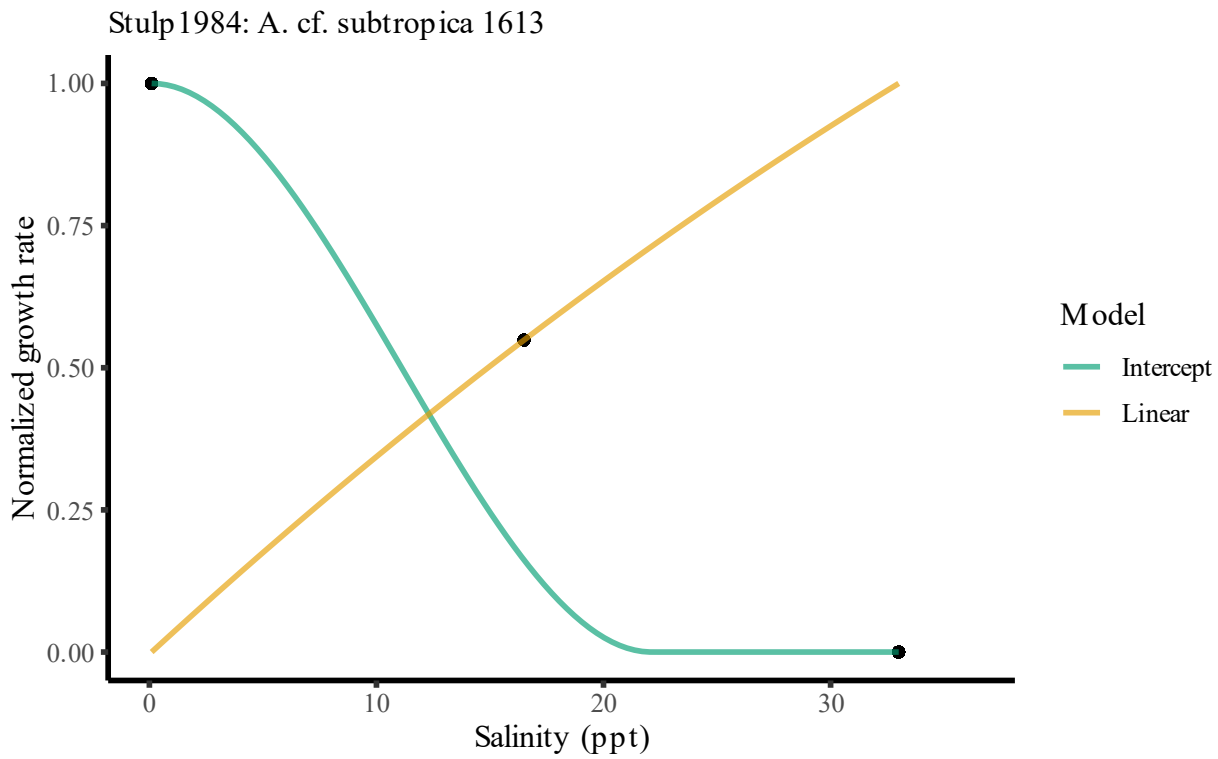

Figure 100: Reaction norm and model fits for Anabaena cf. subtropica 1613 from (Stulp and Stam, 1984)

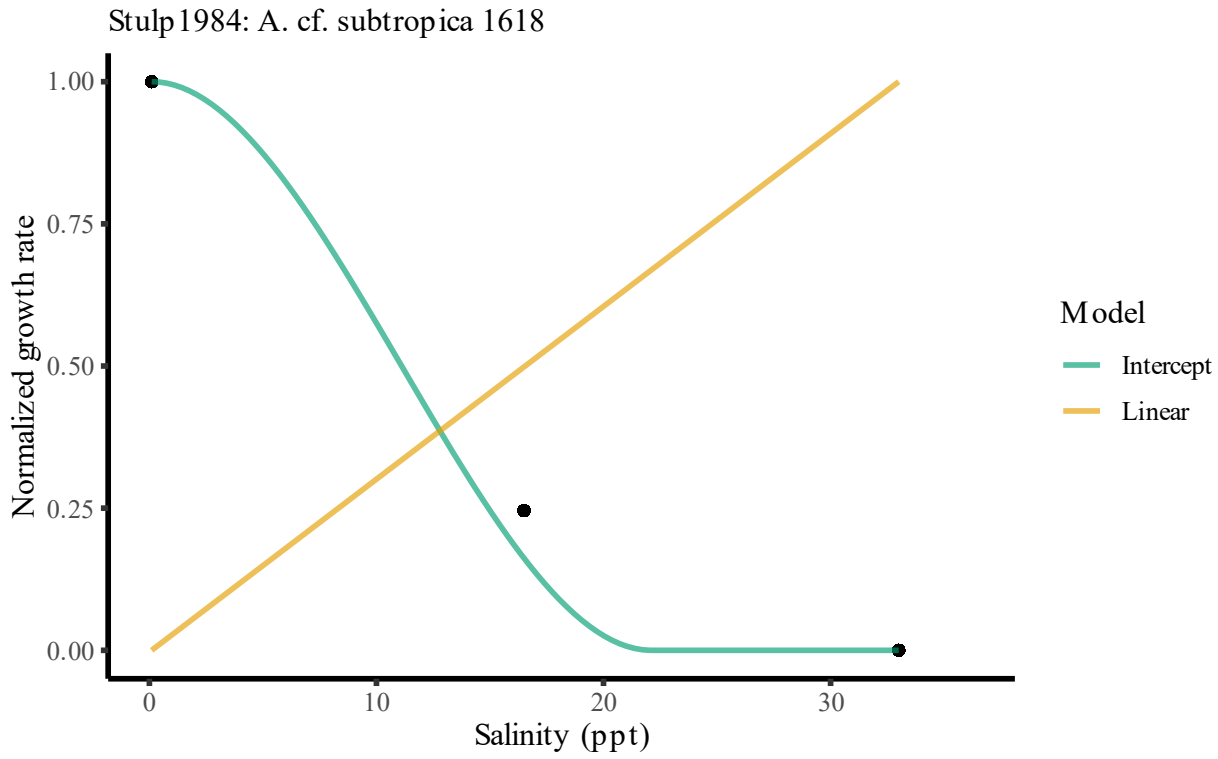

Figure 101: Reaction norm and model fits for Anabaena cf. subtropica 1618 from (Stulp and Stam, 1984)

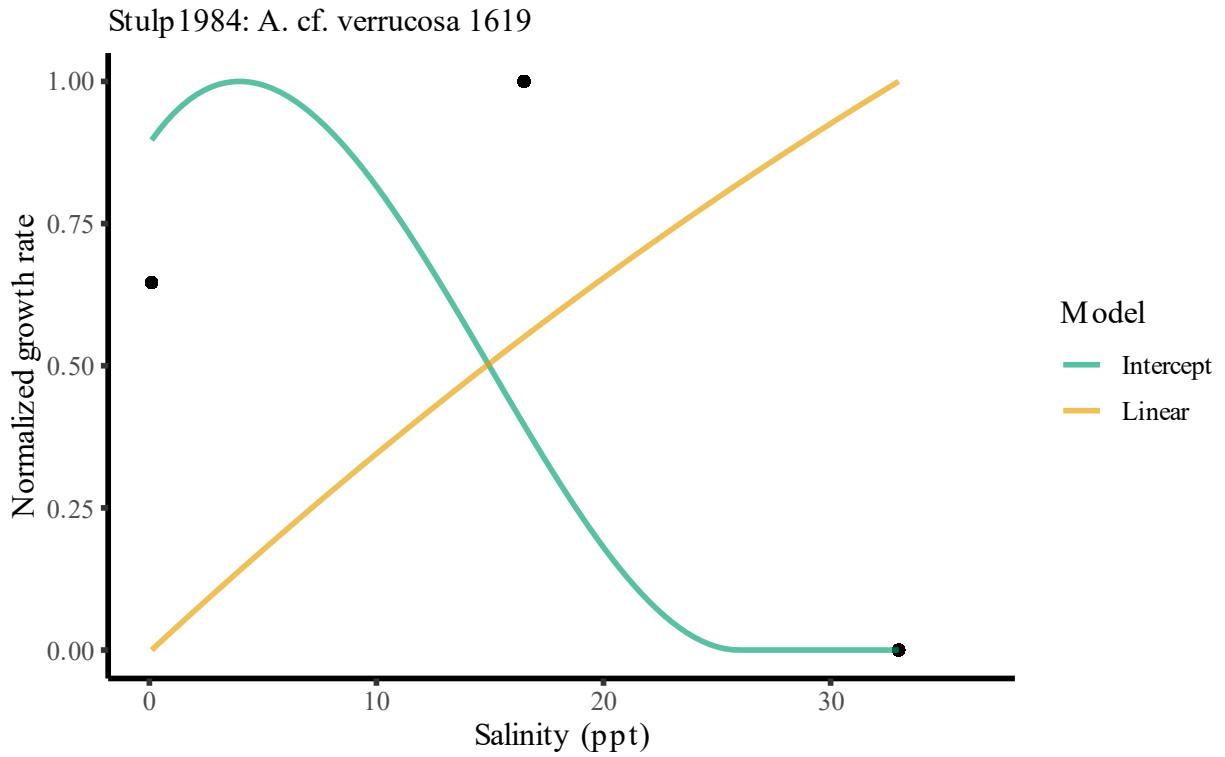

Figure 102: Reaction norm and model fits for Anabaena cf. verrucosa 1619 from (Stulp and Stam, 1984)

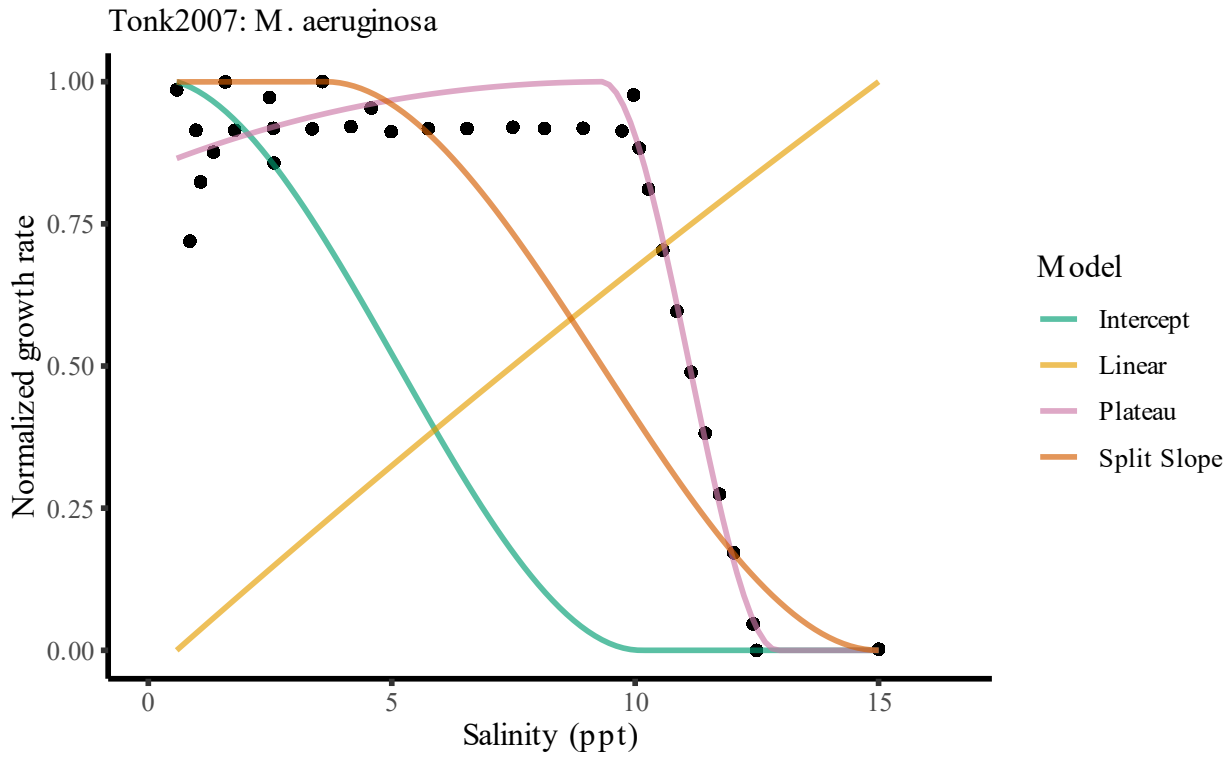

Figure 103: Reaction norm and model fits for Microcystis aeruginosa PCC 7806 from (Tonk et al., 2007)

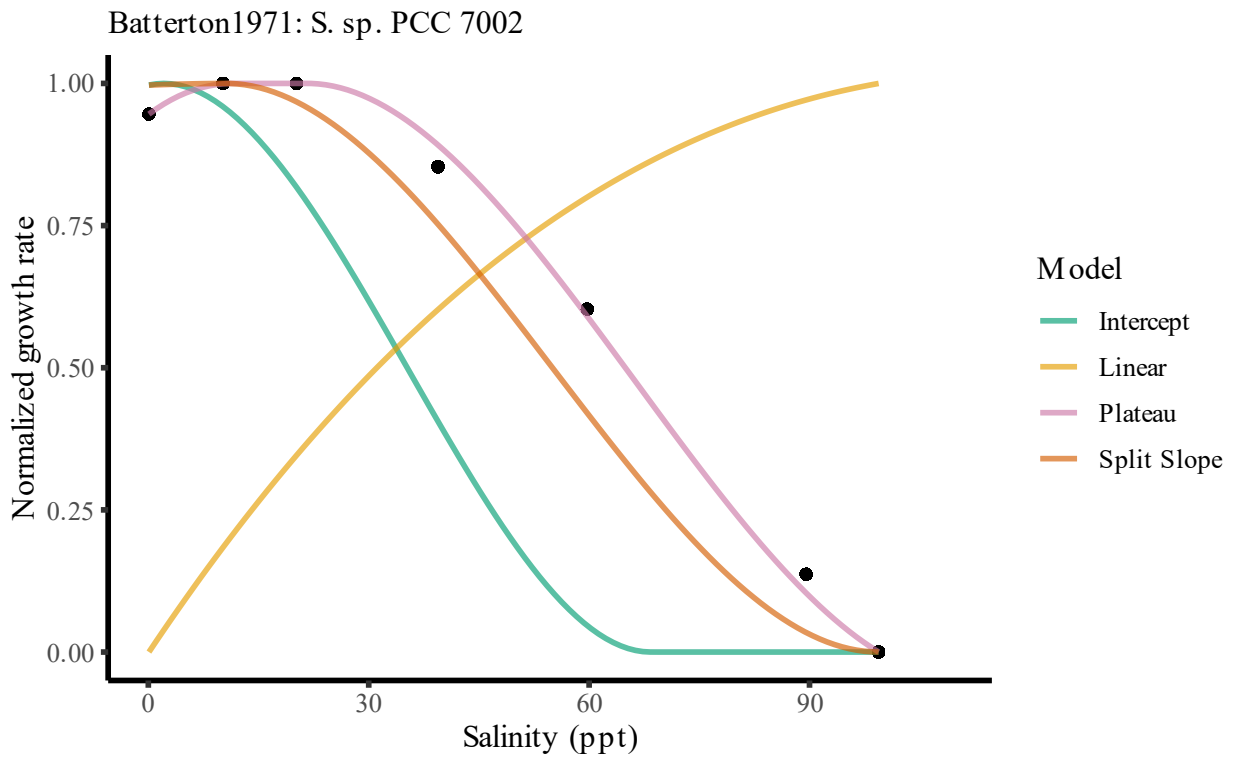

Figure 104: Reaction norm and model fits for Synechococcus sp. PCC 7002 from (Batterton and Van Baalen, 1971)

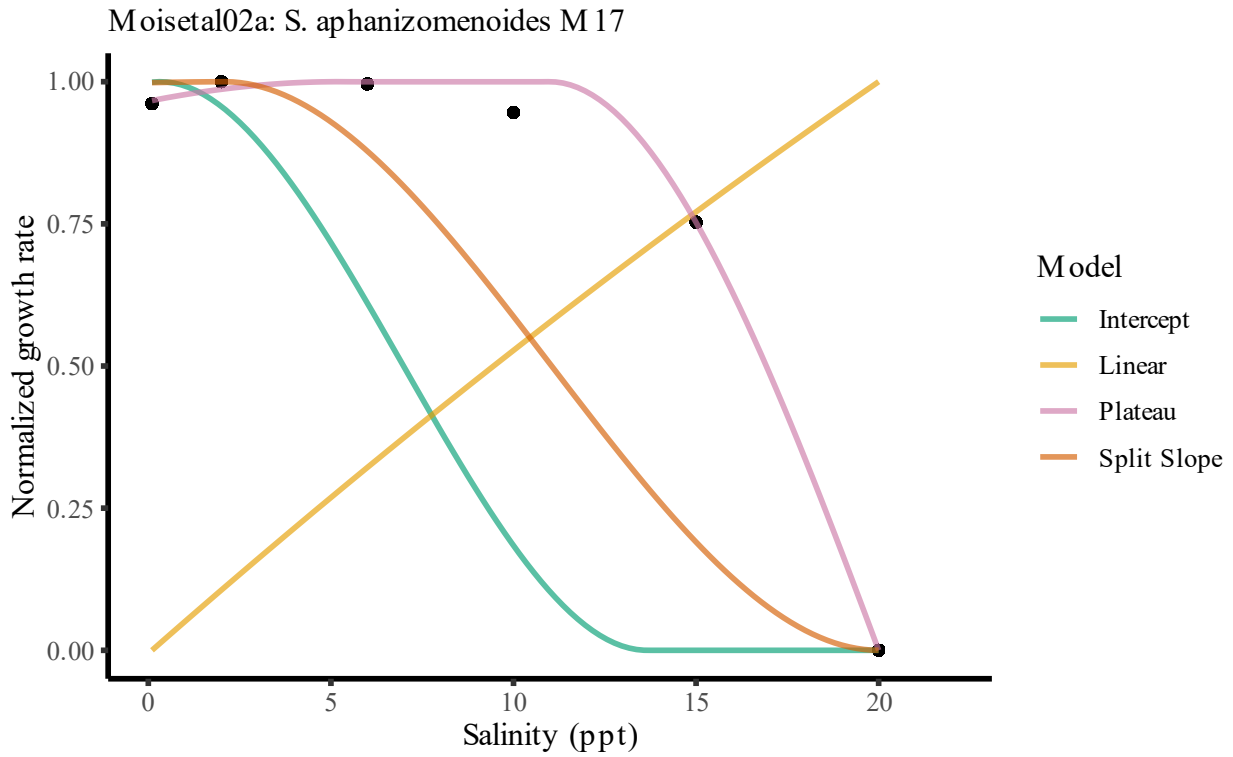

Figure 105: Reaction norm and model fits for Sphaerospermopsis aphanizomenoides M17 from (Moisander et al., 2002)

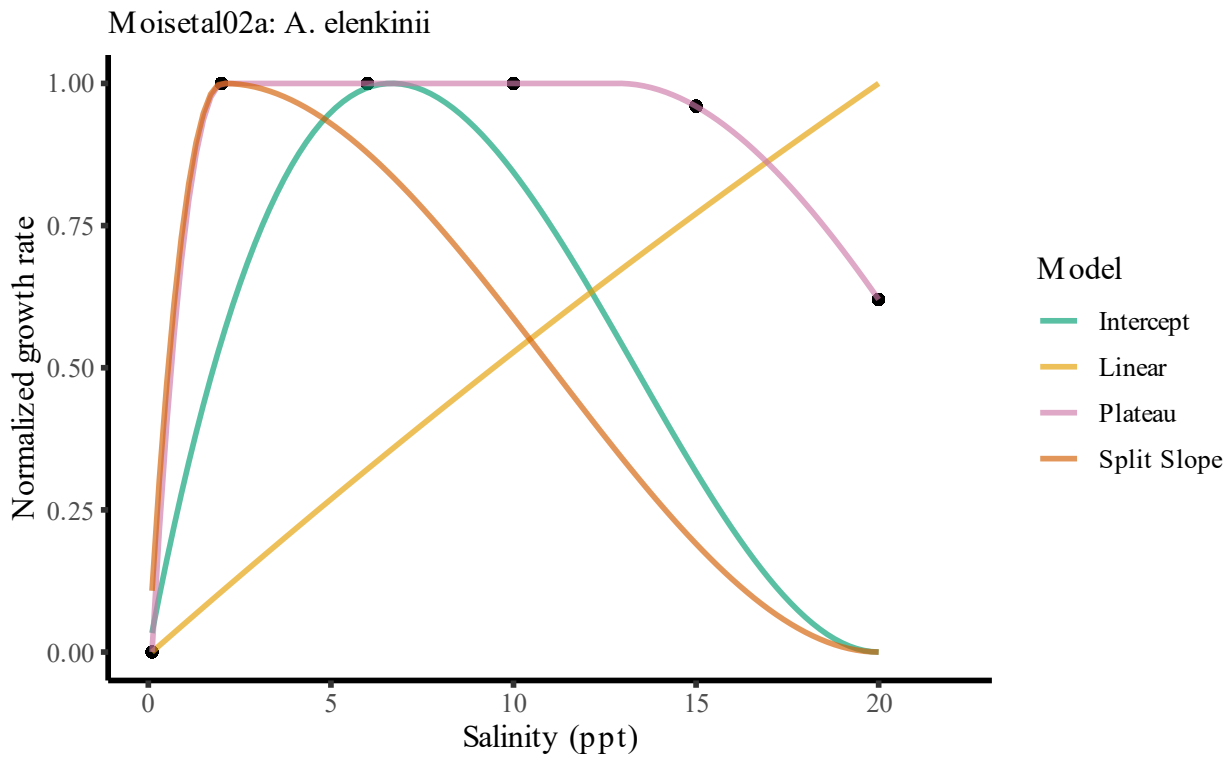

Figure 106: Reaction norm and model fits for Anabaenopsis elenkinii from (Moisander et al., 2002)

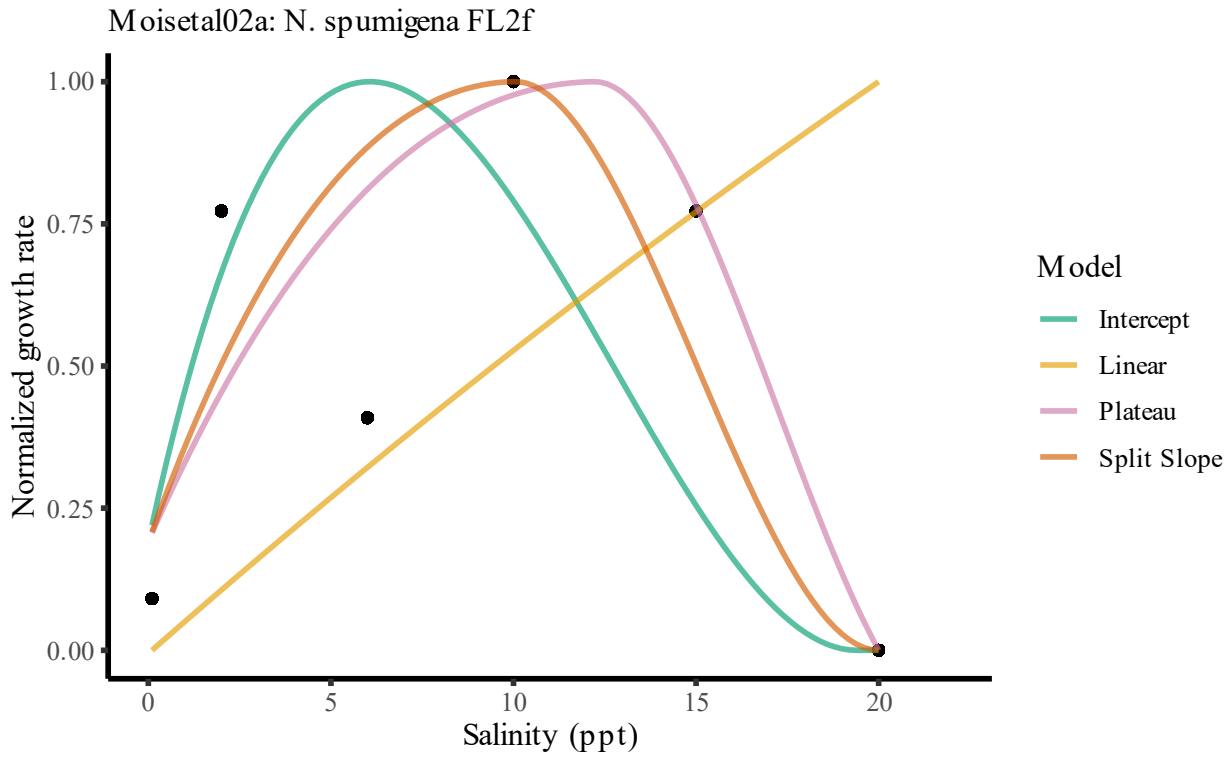

Figure 107: Reaction norm and model fits for Nodularia spumigena FL2f from (Moisander et al., 2002)

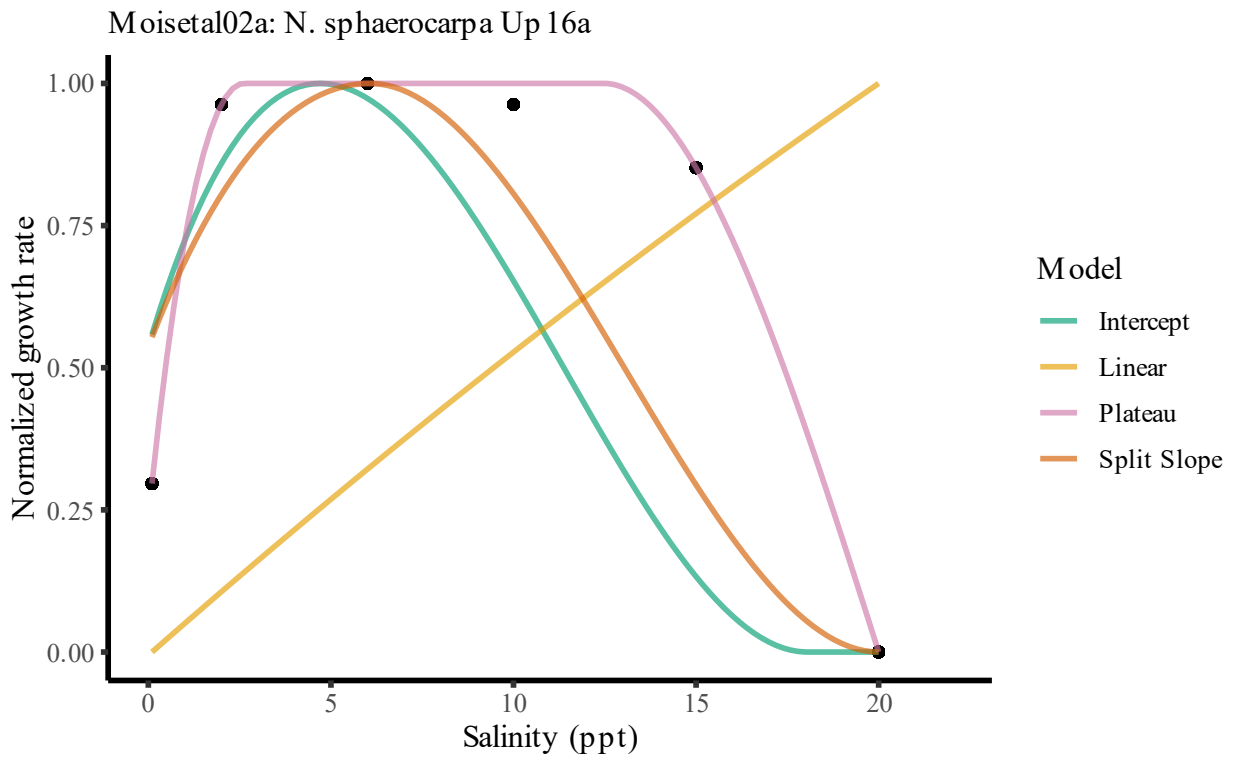

Figure 108: Reaction norm and model fits for Nodularia sphaerocarpa Up16a from (Moisander et al., 2002)

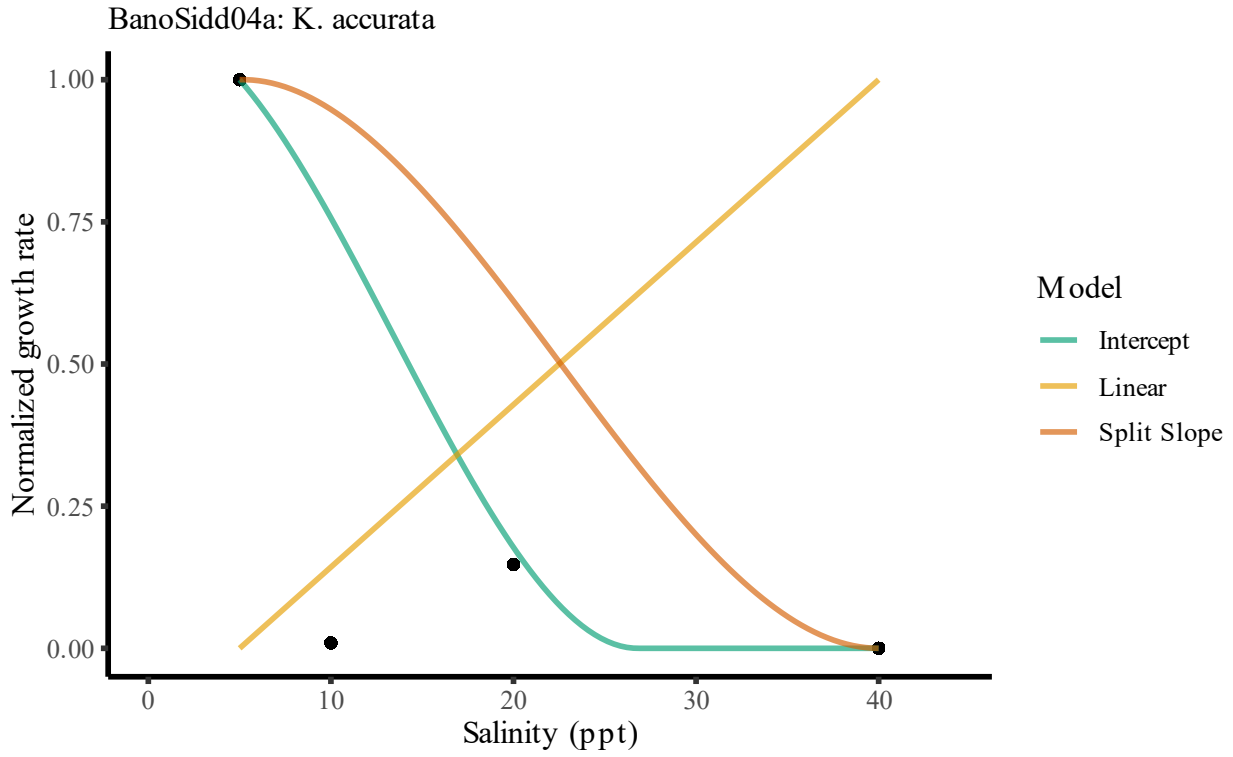

Figure 109: Reaction norm and model fits for Katagnymene accurata from (Bano and Siddiqui, 2004)

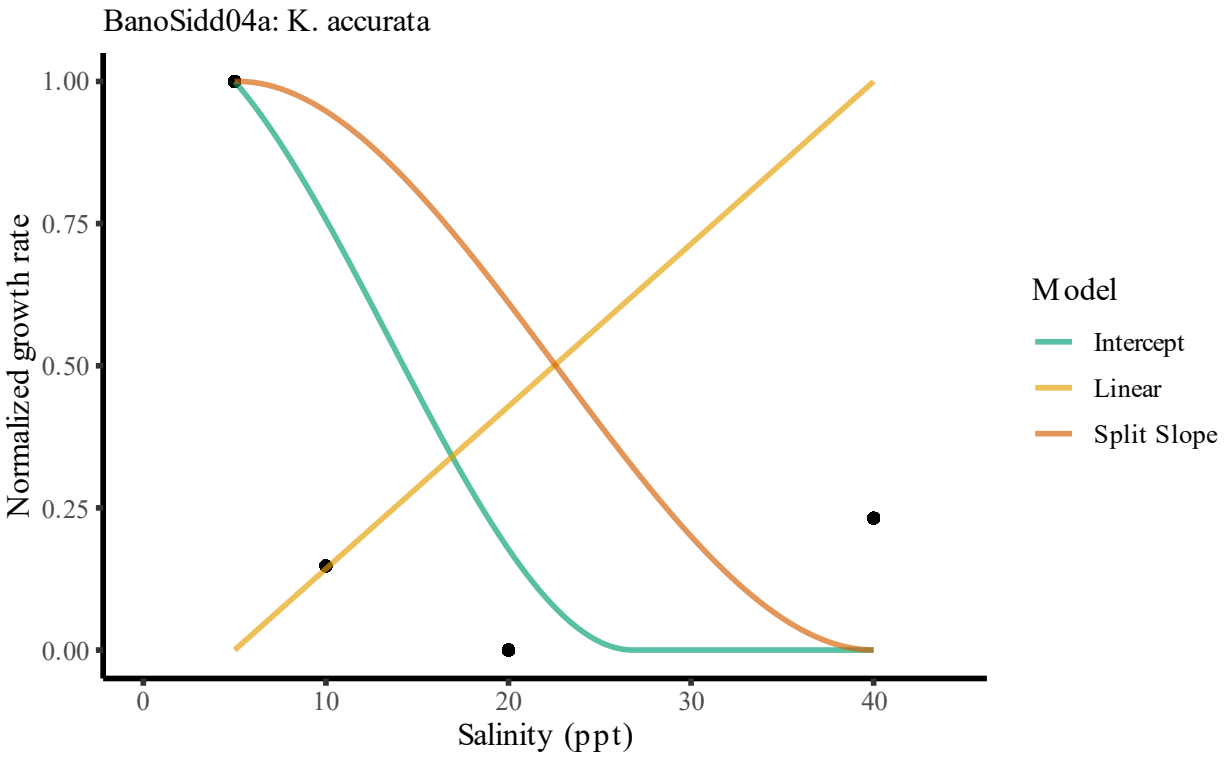

Figure 110: Reaction norm and model fits for Katagnymene accurata from (Bano and Siddiqui, 2004)

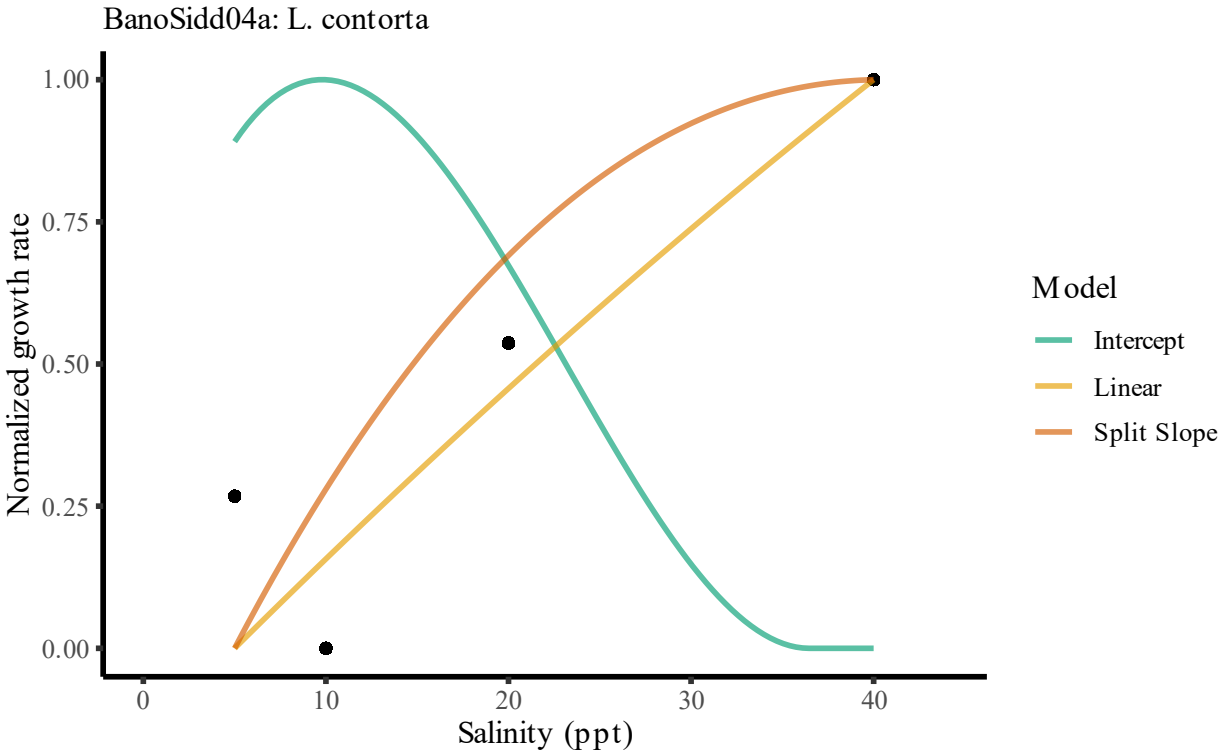

Figure 111: Reaction norm and model fits for Lyngbya contorta from (Bano and Siddiqui, 2004)

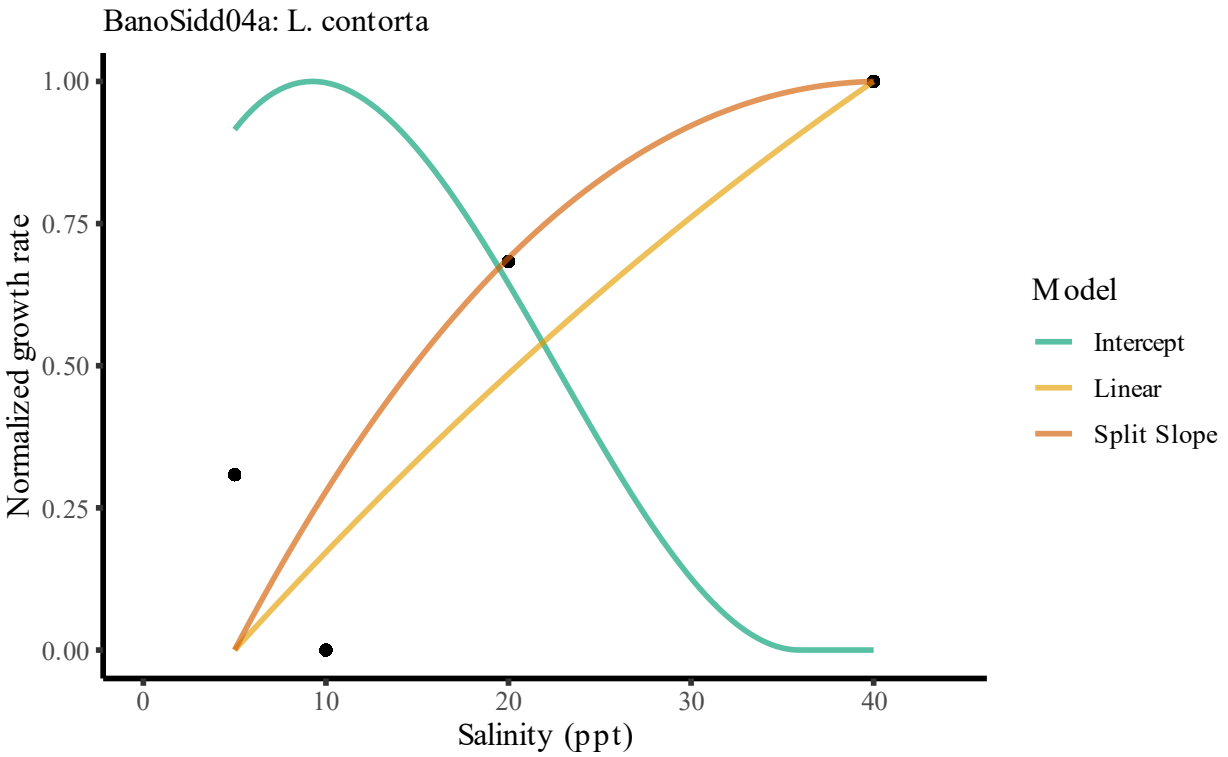

Figure 112: Reaction norm and model fits for Lyngbya contorta from (Bano and Siddiqui, 2004)

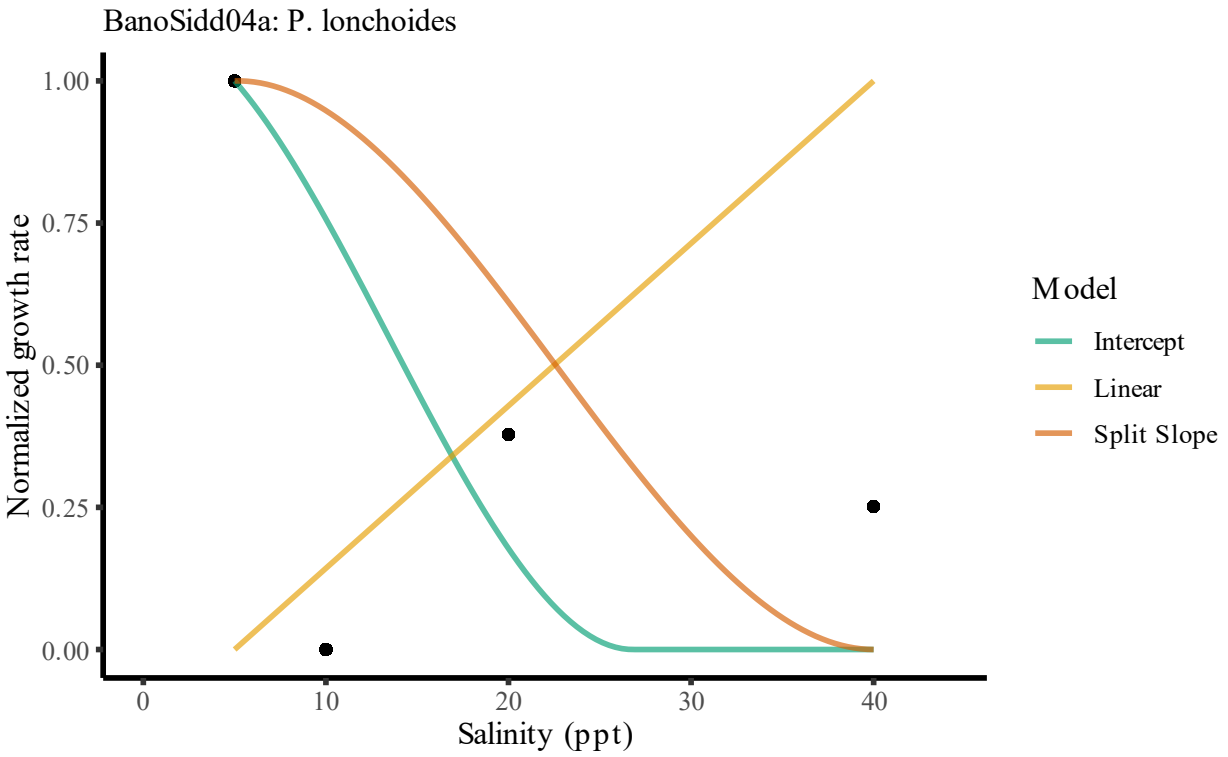

Figure 113: Reaction norm and model fits for Pseudoanabaena lonchoides from (Bano and Siddiqui, 2004)

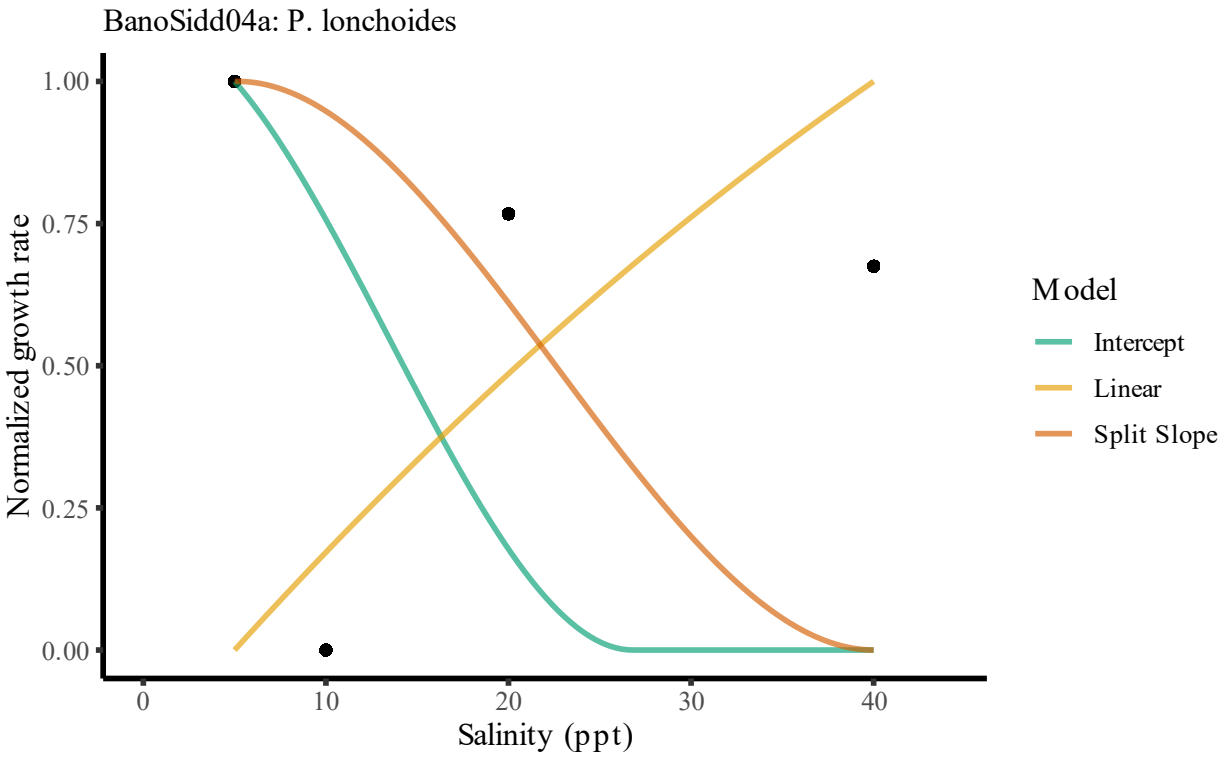

Figure 114: Reaction norm and model fits for Pseudoanabaena lonchoides from (Bano and Siddiqui, 2004)

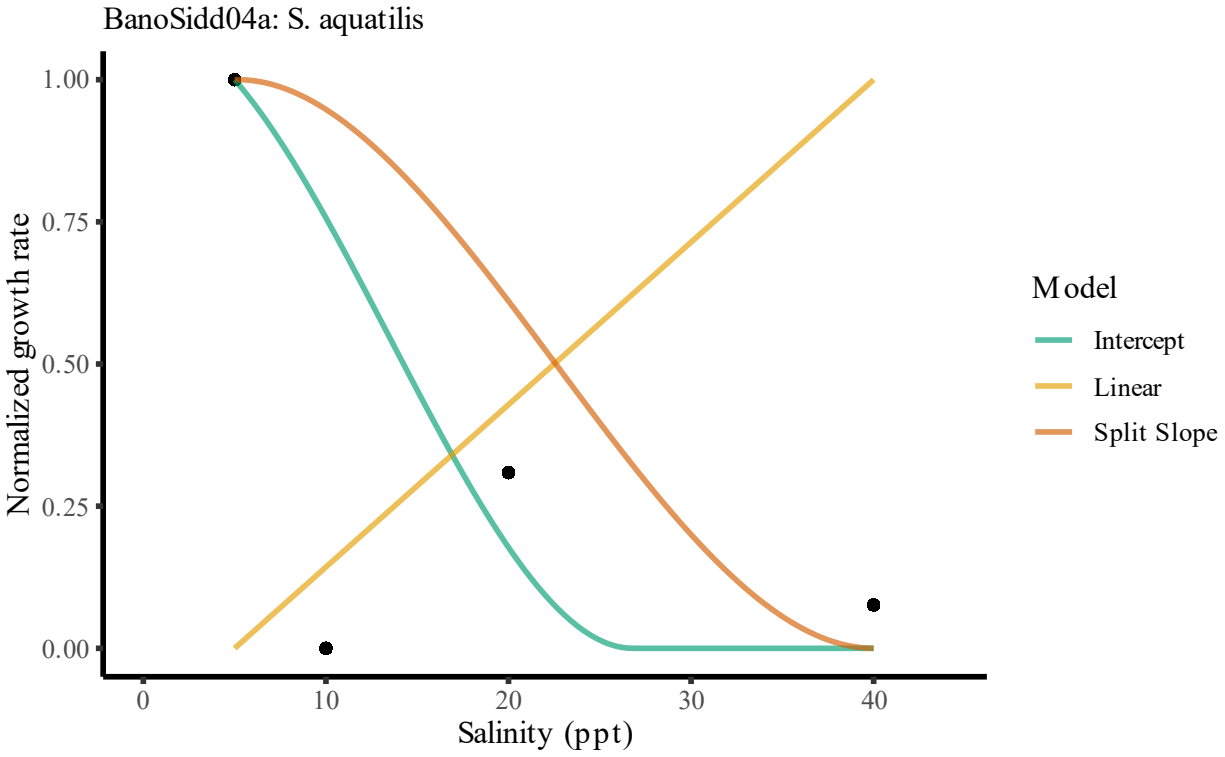

Figure 115: Reaction norm and model fits for Synechocystis aquatilis from (Bano and Siddiqui, 2004)

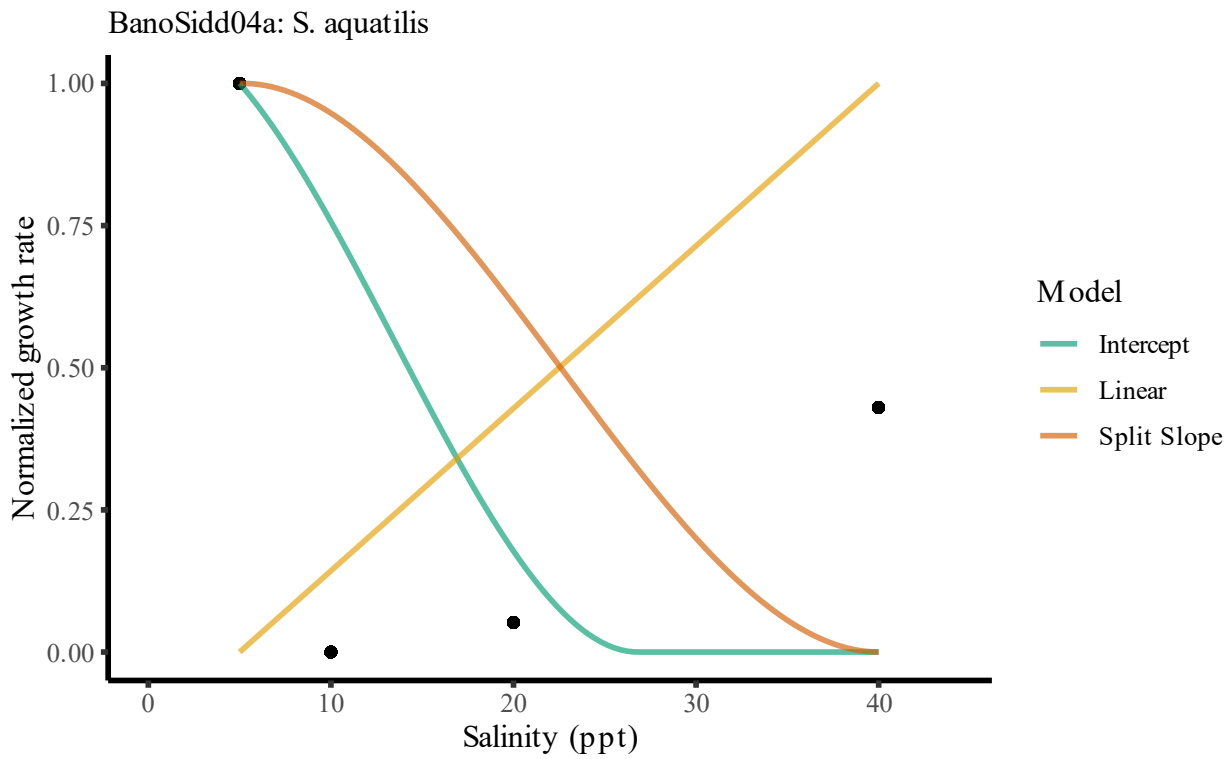

Figure 116: Reaction norm and model fits for Synechocystis aquatilis from (Bano and Siddiqui, 2004)

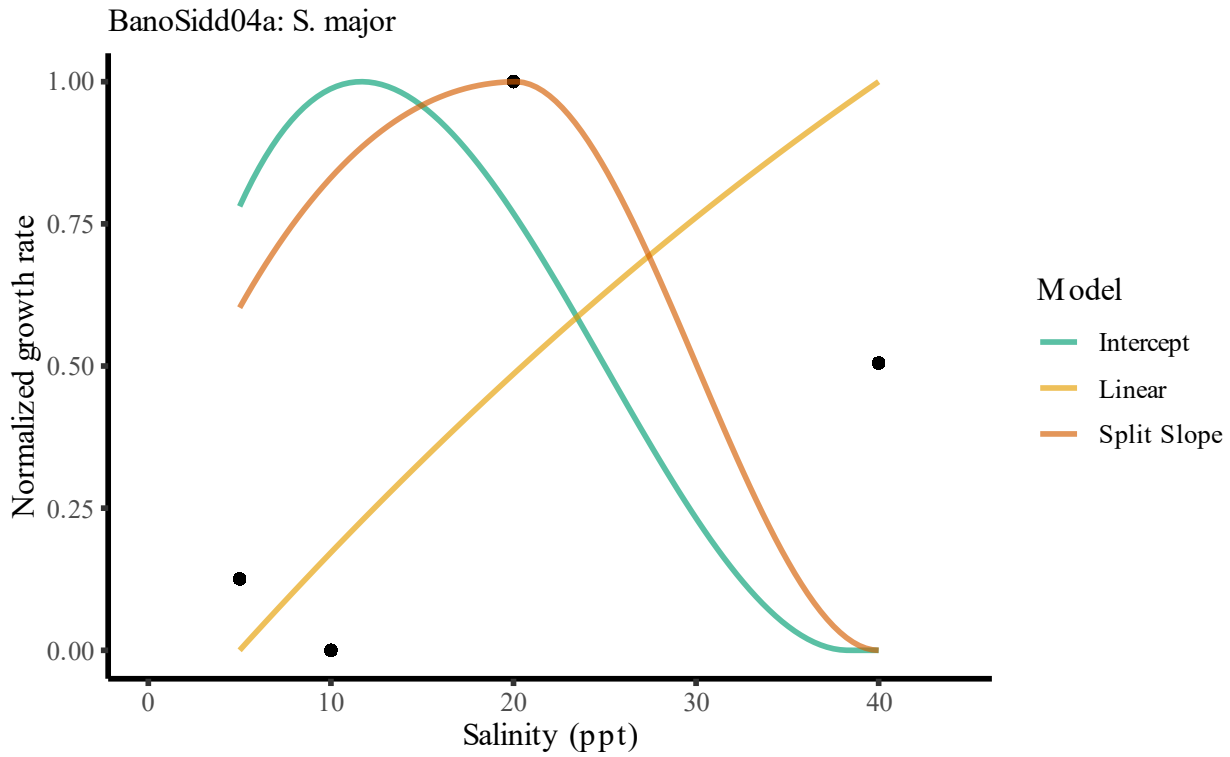

Figure 117: Reaction norm and model fits for Spirulina major from (Bano and Siddiqui, 2004)

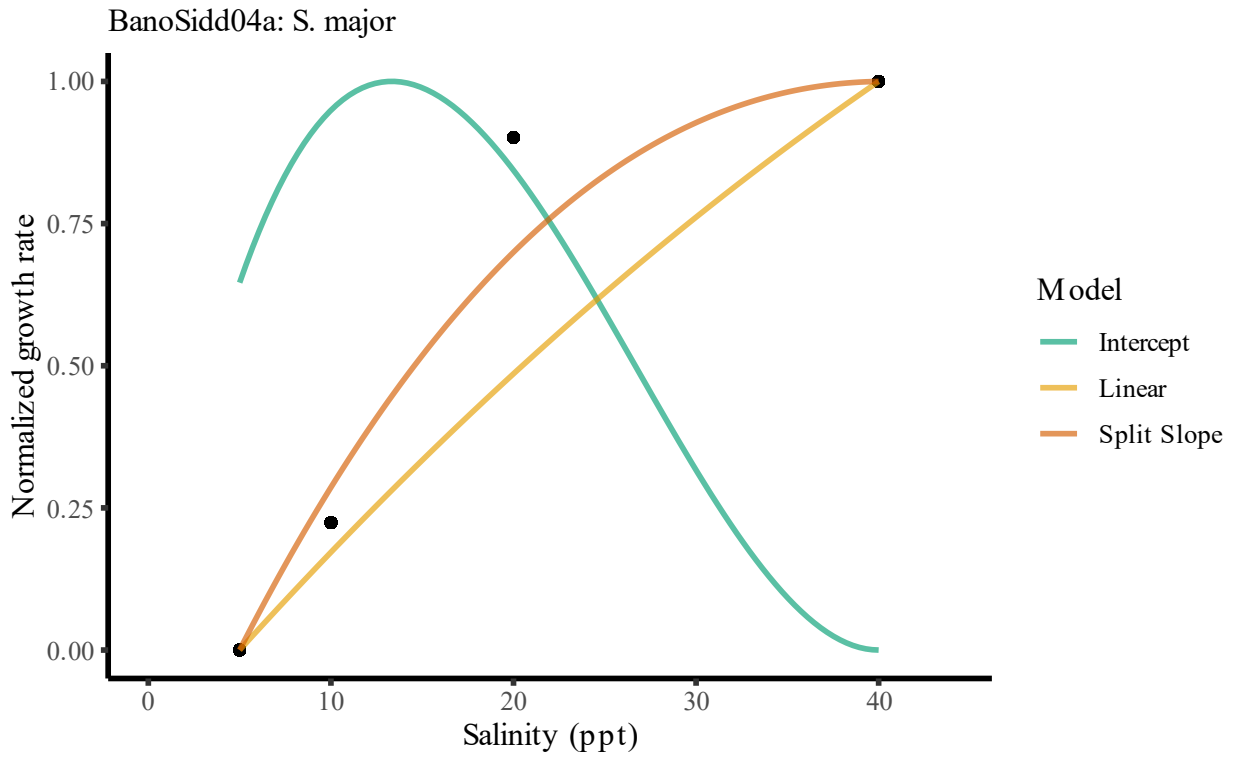

Figure 118: Reaction norm and model fits for Spirulina major from (Bano and Siddiqui, 2004)

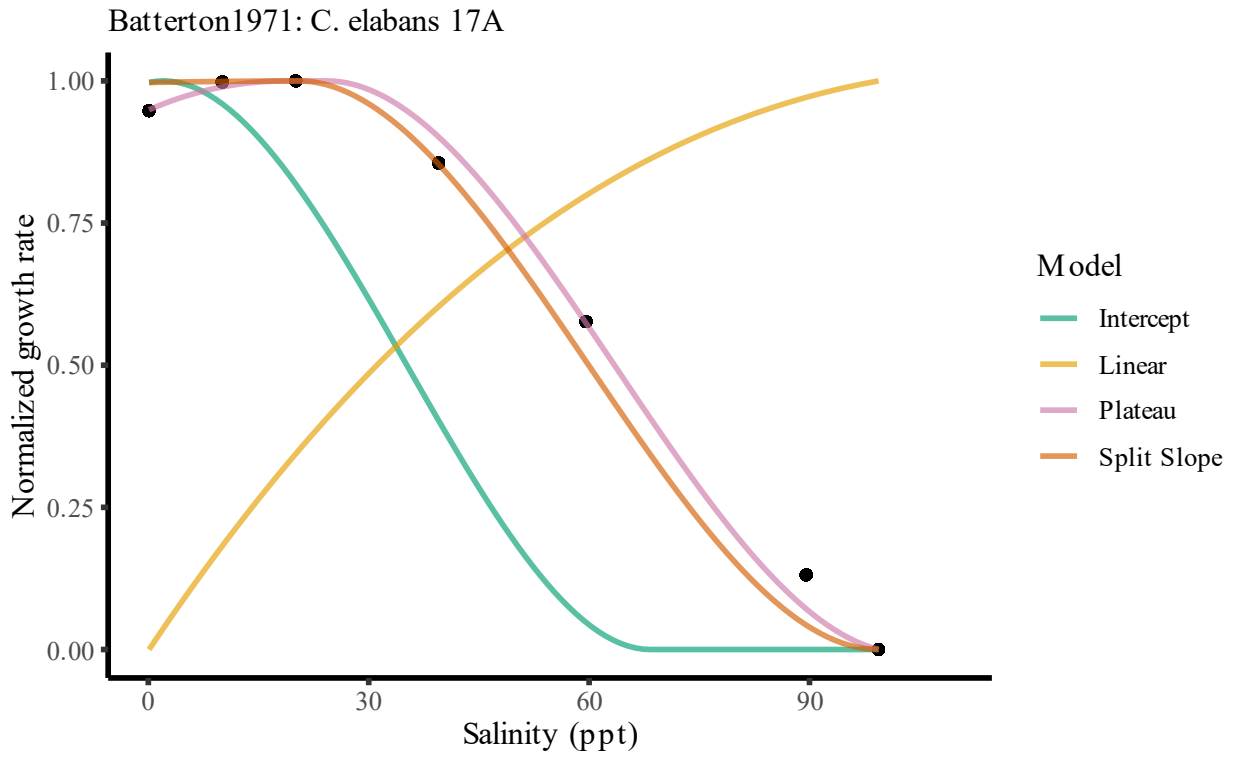

Figure 119: Reaction norm and model fits for Coccochloris elbans 17A from (Batterton and Van Baalen, 1971)

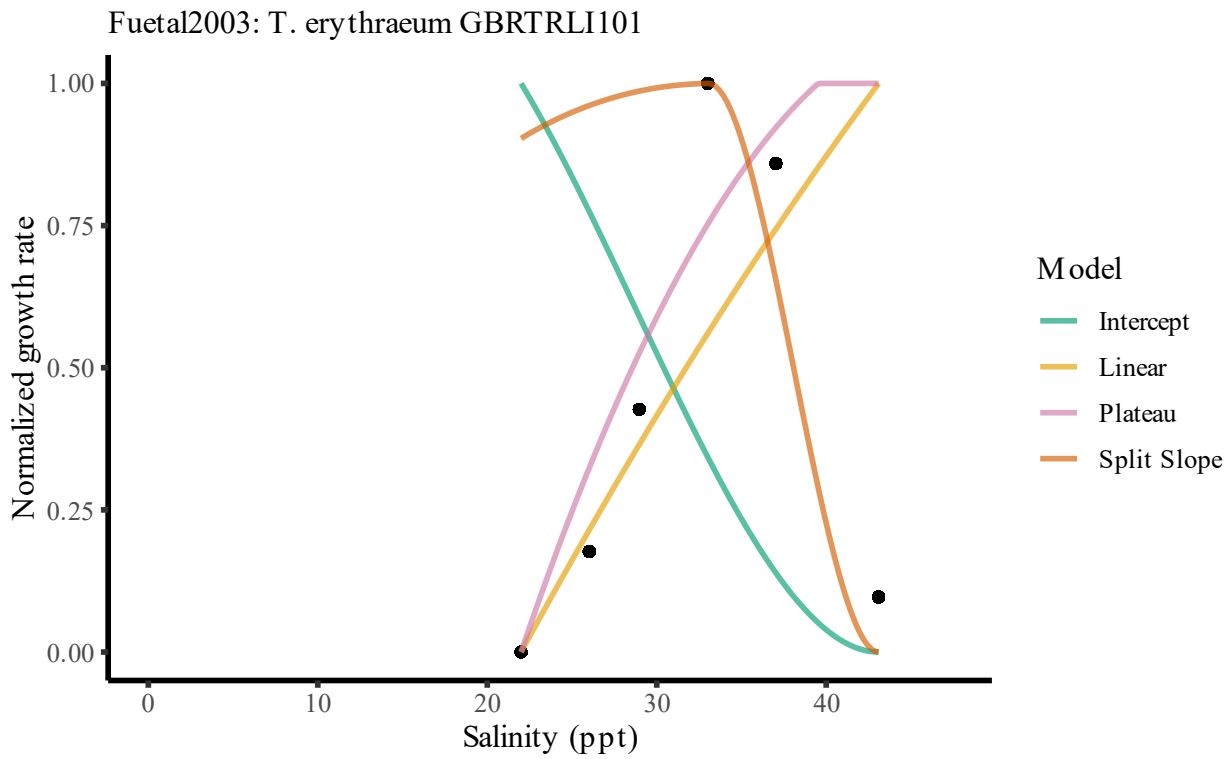

Figure 120: Reaction norms and model fits for Trichodesmium erythraeum GBRTRLI101 from (Fu and Bell, 2003)

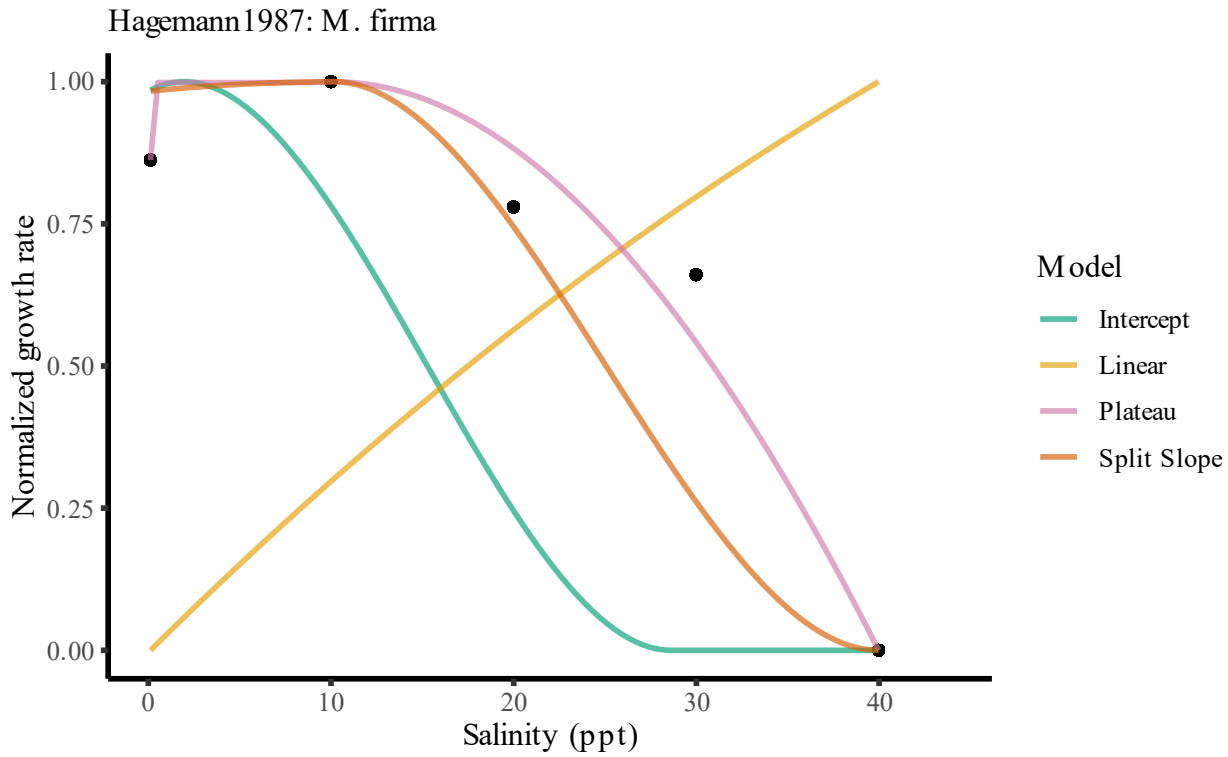

Figure 121: Reaction norm and model fits for Microcystis firma from (Hagemann et al., 1987)

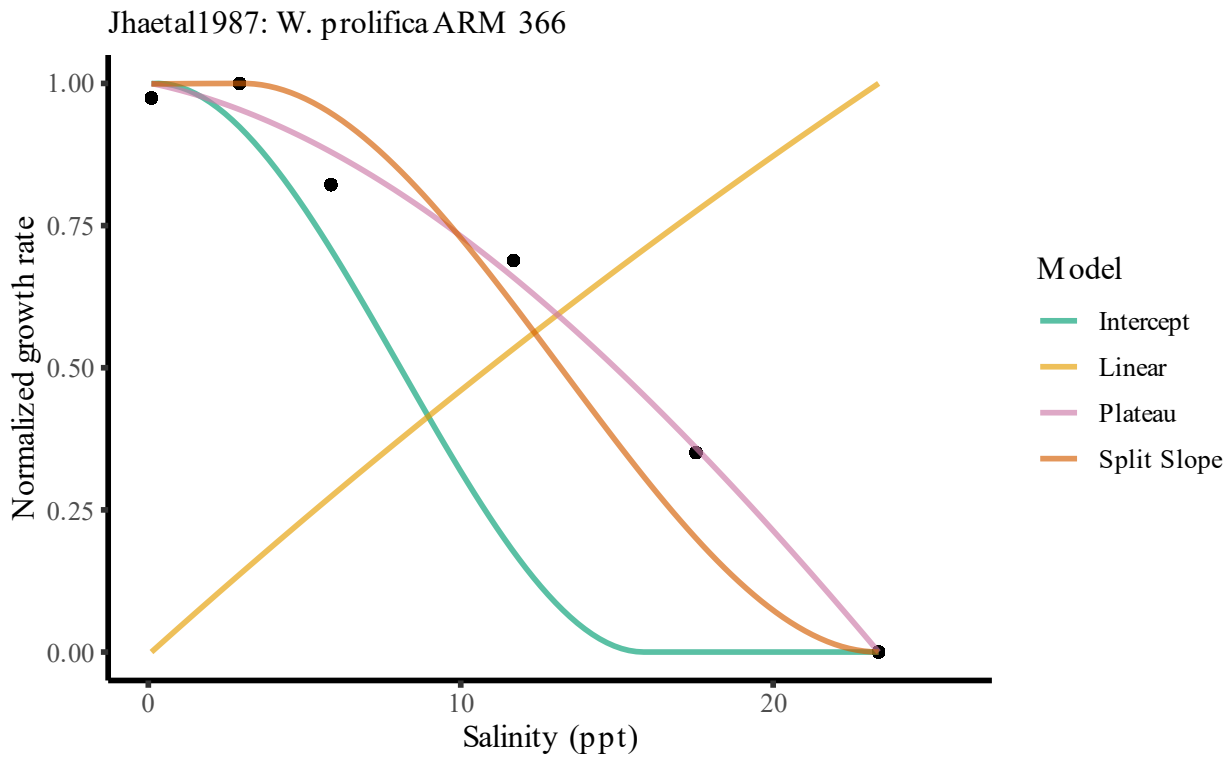

Figure 122: Reaction norm and model fits for Westiellopsis prolifica ARM 366 from (Jha et al., 1987)

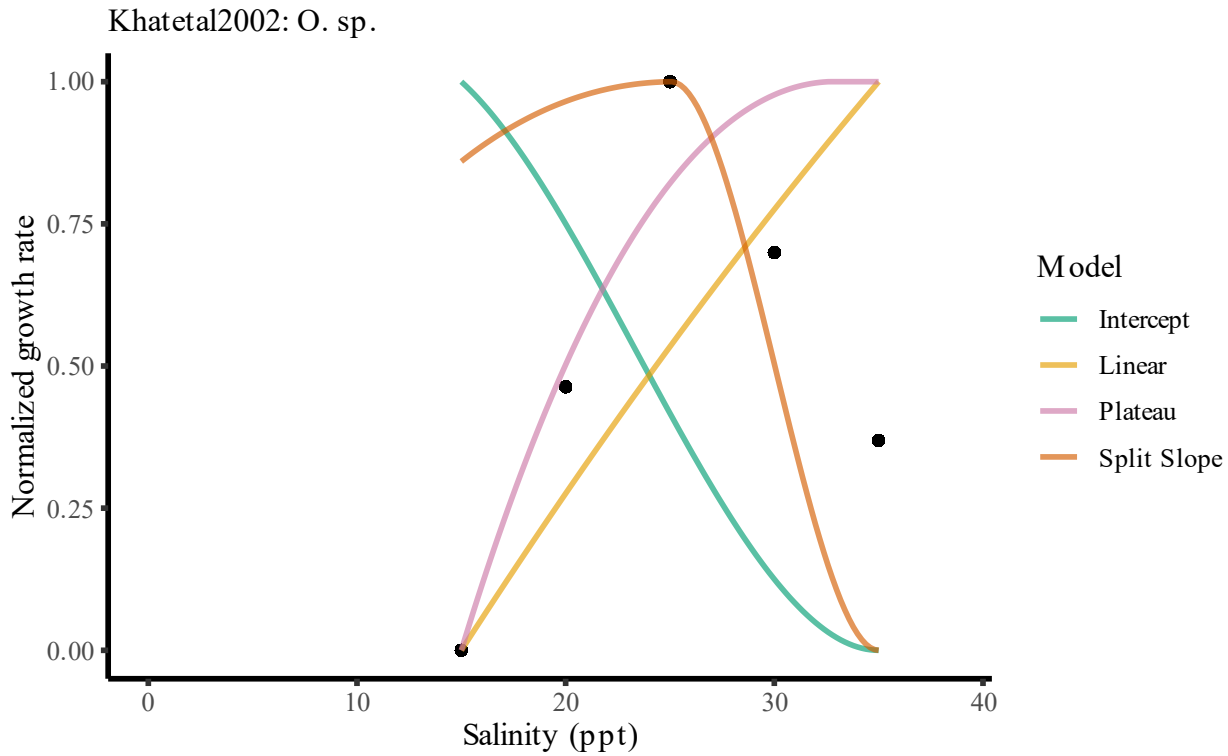

Figure 123: Reaction norm and model fits for Oscillatoria sp. from (Khatoon et al., 2010)

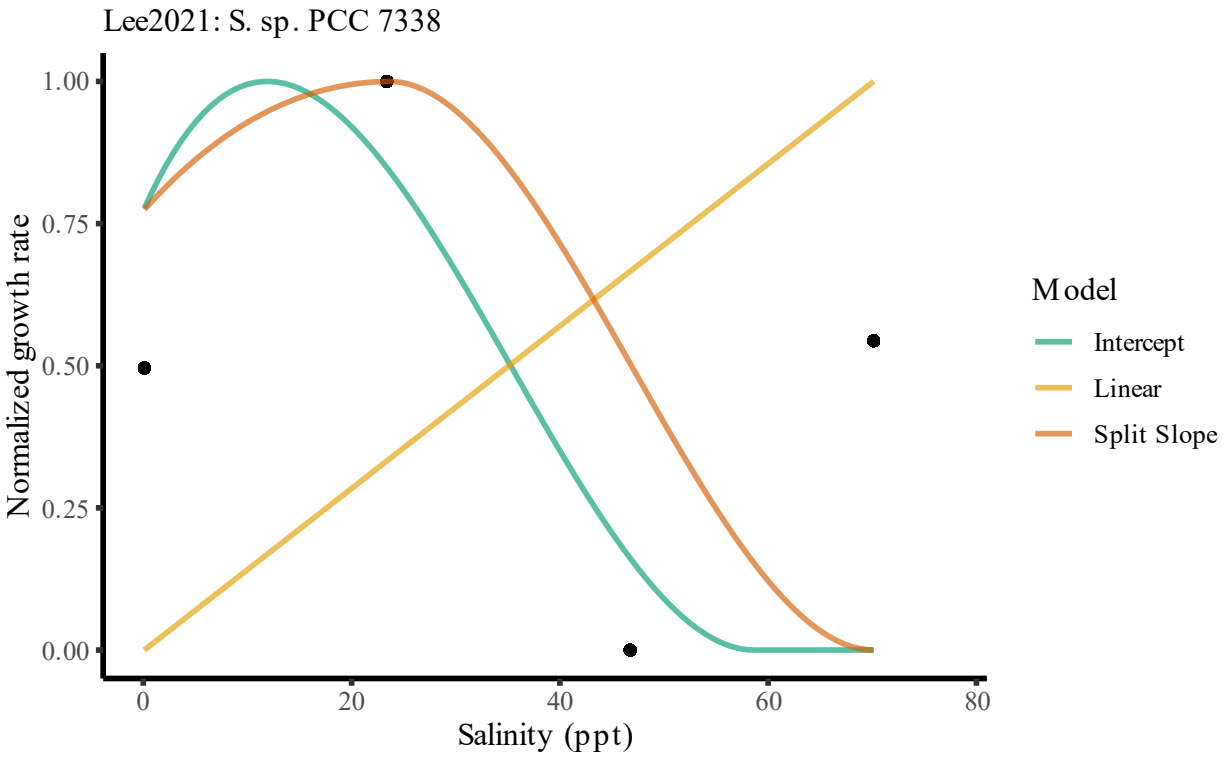

Figure 124: Reaction norm and model fits for Synechocystis sp. PCC 7338 from (Lee et al., 2021)

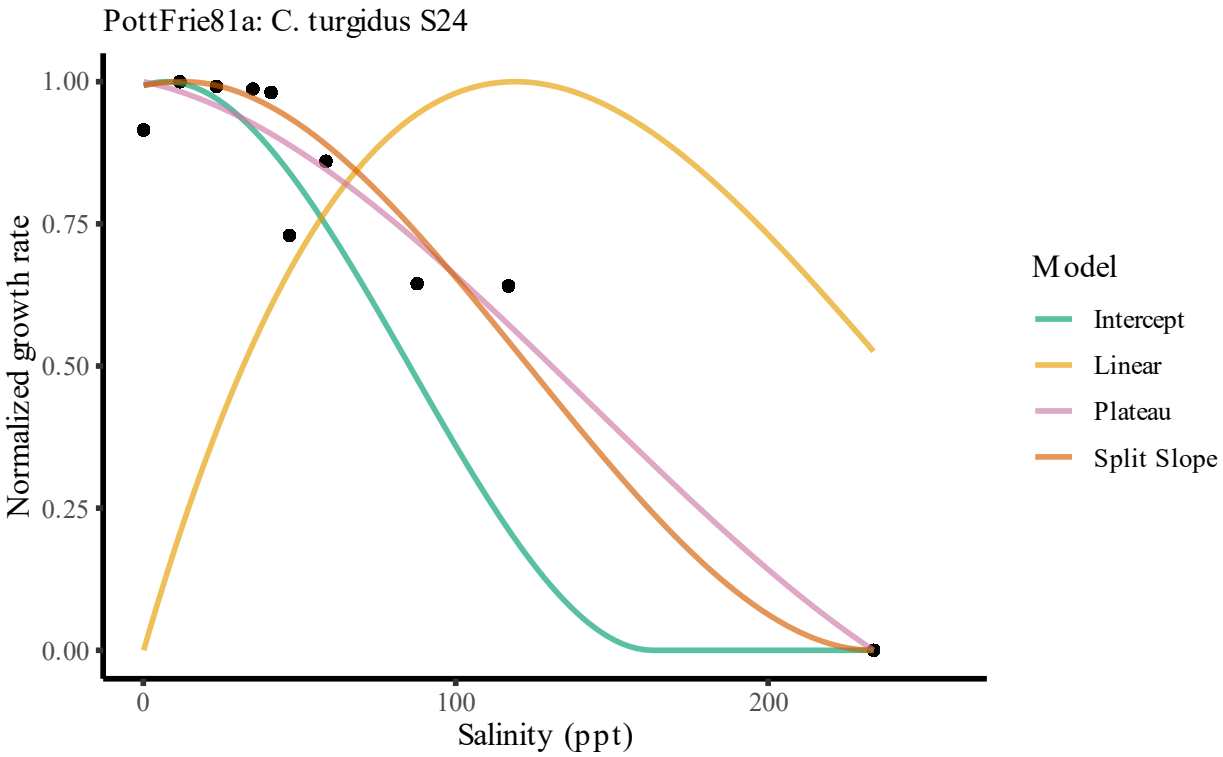

Figure 125: Reaction norm and model fits for Chroococcus turgidus S24 from (Potts and Friedmann, 1981)

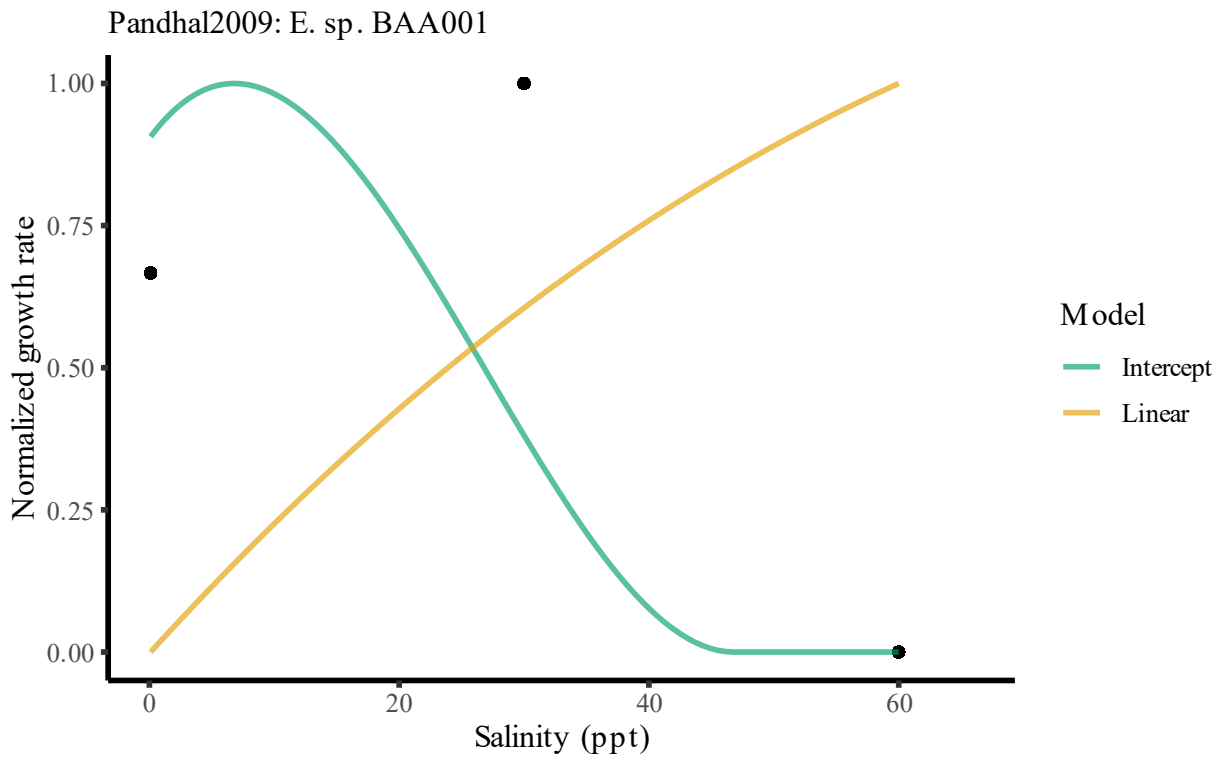

Figure 126: Reaction norm and model fits for Euhalothece sp. BAA001 from (Pandhal et al., 2009)

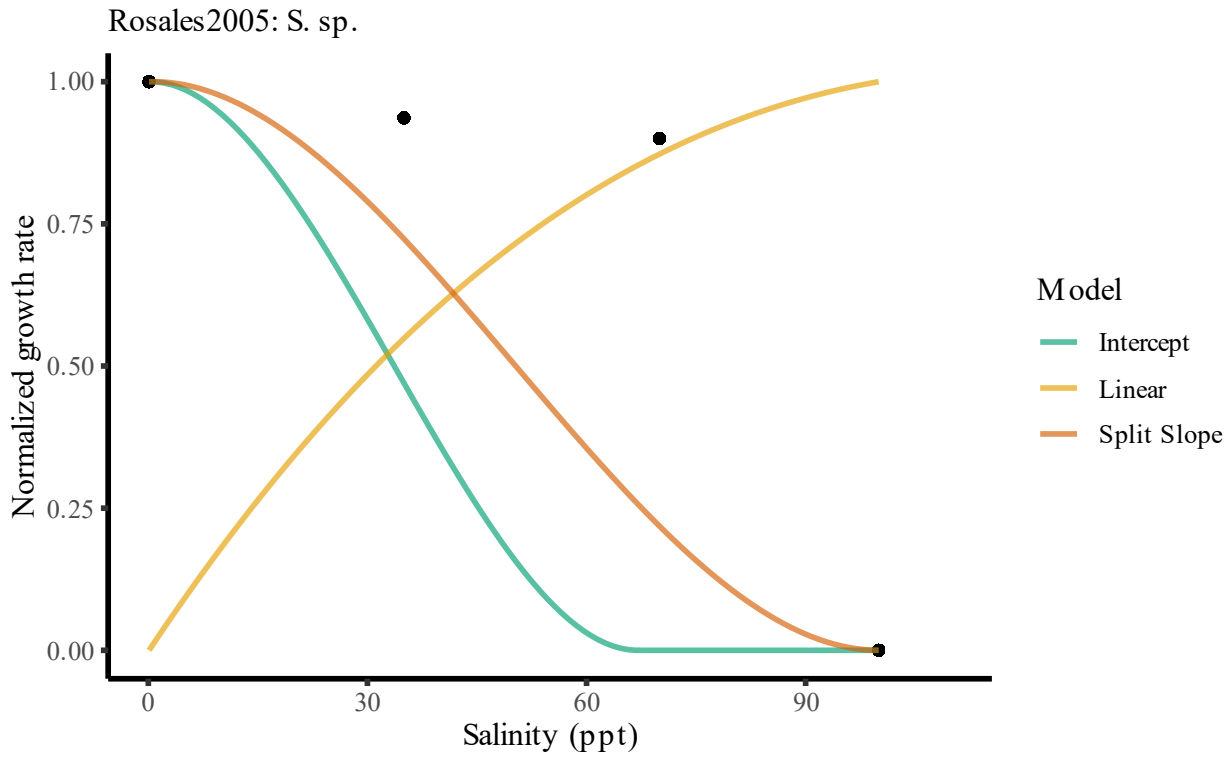

Figure 127: Reaction norm and model fits for Synechococcus sp. from (Rosales et al., 2005)

Appendix C

BG-11 recipe

Stock solution	**Volume (mL)**
100X BG-FPC	10
1000X Fe ammonium citrate	1
1000X Na_2CO_3	1
1000X KH_2PO_4	1
1M HEPES buffer	10

Combine stock solutions in 1L MQ H_2O. pH adjust to pH 7.5. Store in the dark.

Trace minerals (1L recipe)

Chemical	**Mass (g)**
H_3BO_3	2.86
$MnCl_2$ $4H_2O$	1.81
$ZnSO_4$ $7H_2O$	0.222
Na_2MoO_4 2 H_2O	0.39
$CuSO_4$ $5H_2O$	0.079
$Co(NO_3)_2$ $6H_2O$	0.0494

Combine chemicals in 1L MQ H_2O. Store at 4°C.

100X BG-FPC (1L recipe)

Chemical	**Mass (g)**	**Volume (mL)**
$NaNO_3$	149.58	---

$MgSO_4$ $7H_2O$	7.49	---
$CaCl_2$ $2H_2O$	3.6	---
Citric acid	0.596	---
Na-EDTA (119 mM aka 4.43g per 100mL, pH 8.0)	---	2.35
Trace minerals	---	100

Combine chemicals in 1L MQ H_2O. Store at 4°C.

1000X Fe ammonium citrate (50mL recipe)

0.3g Fe ammonium citrate in 50mL MQ H_2O. Store at 4°C.

1000X Na_2CO_3 (50mL recipe)

1g Na_2CO_3 in 50mL MQ H_2O. Store at 4°C.

1000X KH2PO4 (50mL recipe)

1.997g KH2PO4 3H2O in 50mL MQ H_2O. Store at 4°C.

1M HEPES buffer (250mL recipe)

59.575g HEPES in 250mL MQ H_2O. pH adjusted to pH 7.8.

AASW Recipe

For 1L Total

1. To approximately 800mL of MQ H_2O, add each of the components in Table 1 in the order specified (except vitamins) while stirring constantly.
2. Adjust the pH to 8.1
3. Bring the volume to just under 1L with MQ H_2O.

- For 1.5% agar medium: add 15g of agar to the flask; do not mix

4. Cover and autoclave medium

5. Allow to cool and add components in Table 2

- For agar medium: add Table 2 components, mix, and dispense before agar solidifies

6. Store in the dark

Table 1: Components added before autoclaving

Chemical	Amount	Stock Solution Concentration
NaCl*	28.1g	---
KCl*	11.2mL	6g/100mL MQ H_2O
$NaNO_3$*	10mL	10g/100mL MQ H_2O
KH_2PO_4*	10mL	0.5g/100mL MQ H_2O
Tricine (adjust to pH 8)*	20mL	22.4g/100mL MQ H_2O
P-II Metal Solution	10mL	---
Chelated Iron Solution	1mL	---
NH_4Cl*	1mL	2.7g/100mL MQ H_2O

Table 2: Components added after autoclaving

Chemical	Amount	Stock Solution Concentration
$CaCl_2$ $2H_2O$*	10 mL	14.7g/100mL MQ H_2O
$MgSO_4$*	15 mL	46.01g/100mL MQ H_2O
MgCl2 $6H_2O$*	10 mL	54.89g/100mL MQ H_2O
Vitamin B_{12}	1mL	---

All stock solutions in Table 2 should be filter sterilized prior to adding to medium. Vitamin B_{12} should be stored in the refrigerator and wrapped in foil to avoid photodegradation.

P-II trace metal solution

For 100mL Total

1. To approximately 70mL MQ H_2O, add each of the components in the order specified while stirring continuously.
2. Bring total volume to 100 mL with MQ H_2O
3. Store at 4°C

Chemical	Mass (g)
$Na_2EDTA\ 2H_2O$	0.1
H_3BO_3	0.114
$FeCl_3\ 6H_2O$	0.0049
$MnSO_4\ H_2O$	0.0164
$ZnSO_4\ 7H_2O$	0.0022
$CoCl_2\ 6H_2O$	0.00048

Chelated iron solution

Component A

1. Pour approximately 450 mL MQ H_2O into a beaker. Heat the beaker in the microwave to near boiling.
2. Add 10.0g of Na_2EDTA to the stirring beaker.
3. After the EDTA fully dissolves, bring the total volume to 500 mL with MQ H_2O

Component B

1. Pour approximately 450mL 0.1M HCl into a beaker.
2. Add 0.81g of $FeCl_3\ 6H_2O$ to the beaker.
3. Bring the total volume to 500mL with MQ H_2O.

Slowly add Component B to the heated Component A while stirring.

Ingredients

Chemical	Mass (g)	Volume (mL)
$Na_2EDTA\ 2H_2O$	10	---
0.1M HCl	---	450
$FeCl_3\ 6H_2O$	0.81	---

Vitamin B_{12} recipe

For 200mL total

1. Prepare 200 mL of HEPES buffer (50mM)
2. Adjust the pH to 7.8
3. Add Vitamin B_{12} (0.1 mM), wait until fully dissolved
4. Sterilize by 0.45µm Millipore filter. Store in dark at freezer temperature.

Chemical	Mass (g)
HEPES buffer	2.4
Vitamin B_{12} (cyanocobalamin)	0.027

Growth rate comparisons

Table 8: Results from analysis of variance (ANOVA) tests of the growth rate of lineages A, B, C, D and the ancestor in different salinity conditions. Growth media in which statistically significant variance occurred between lineages are bolded.

Growth medium	Statistic	p value
0% AASW	1.92	0.183
10% AASW	**39.9**	**$4.1e^{-6}$**
20% AASW	**64.2**	**$4.3e^{-7}$**
30% AASW	2.98	0.074
40% AASW	**12.5**	**0.00067**
50% AASW	2.94	0.076
60% AASW	**4.02**	**0.034**
70% AASW	1.41	0.30
80% AASW	**9.32**	**0.0021**
90% AASW	**48.9**	**$1.6e^{-6}$**
100% AASW	**10.7**	**0.0012**